The Niemann-Pick C1 Protein Functions in Regulating Lysosome Amine Content

By

Allyn M. Kaufmann

B.S., The University of Kansas, 2003

M.S., The University of Kansas, 2007

Submitted to the graduate degree program in Pharmaceutical Chemistry and the Graduate Faculty of The University of Kansas in partial fulfillment of the requirements for the degree of Doctor of Philosophy

_____
Chairperson

_____

_____

_____

Date defended: _____

The Dissertation Committee for Allyn Kaufmann certifies that this is the approved version of the following dissertation:

The Niemann-Pick C1 Protein Functions in Regulating Lysosome Amine Content

Committee:

_____
Chairperson

_____

_____

_____

Date approved: _____

The Niemann-Pick C1 Protein Functions in Regulating Lysosome Amine Content

Allyn M. Kaufmann

The University of Kansas, 2008

Mutations in the lysosome membrane protein Niemann-Pick C1 (NPC1) are known to cause a generalized block in retrograde vesicle-mediated transport from the lysosome, resulting in the hyper-accumulation of multiple lysosomal cargos. As a result, the true substrate of NPC1 is controversial and not fully understood at the current time. An important, yet often overlooked, category of lysosomal cargo includes the vast array of small molecular weight amine-containing molecules that are substrates for ion trapping in the highly acidic organelle lumen. In this dissertation, we provide experimental evidence to support a novel functional role for NPC1 involving the intracellular trafficking of amine-containing molecules.

In the present study, we show for the first time that lysosomal accumulation of weakly basic amine-containing molecules can significantly stimulate fusion of lysosomes with late endosomes. Subsequently, we observe significant enhancements in the trafficking of lysosomal cargo to the cell periphery. These effects are not observed in NPC1 deficient cells suggesting that NPC1 responds to lysosomal amine build-up and regulates lumenal

concentrations by facilitating their removal. Furthermore, using methods developed to quantitatively evaluate lysosome secretion and late endosome-lysosome fusion, we have identified a number of amine-containing molecules that either stimulate or inhibit NPC1 function. To illustrate the physiological importance of this NPC1-mediated transport pathway we evaluated the toxic effects of an endogenous toxic polyamine metabolite 3-aminopropanal (3-AP). We demonstrate that NPC1-deficient cells are more susceptible to the toxic effects of this metabolite, such as lysosome rupture, due to inefficient efflux of lysosome contents. Moreover, Niemann-Pick Type C (NP-C) fibroblasts are shown to have higher levels and activities of polyamine regulating enzymes including polyamine oxidase, an enzyme involved in the formation of 3-AP. Collectively, these findings provide strong support for a novel functional role for NPC1 and may also provide clues towards understanding NP-C disease progression.

This dissertation is dedicated to my wife, Heather
and our son Jackson

Acknowledgements

Up to this point, there have been an overwhelming number of people that have positively influenced my life. By teaching me invaluable lessons of humility, patience and determination the people mentioned below have made me a better person. Without these influences, this dissertation would not have been possible.

I sincerely acknowledge my research advisor and mentor Jeff Krise. Jeff has been a fantastic advisor and friend over the past four years. I remember the research presentation that Jeff gave to first year graduate students to help us decide which lab we would like to join. Jeff said “If you join my group, I want to you to be thinking about your project every minute of the day; whether you are at the lab, at home in the shower, or whenever you fall asleep at night…you should be thinking about your project and what can be done to solve the problem.” He wasn’t kidding; more than anything Jeff appreciated hard work and motivation to better understand a problem. He has only ever wanted for me and my lab colleagues to succeed in our education and become better thinkers and scientists. Over the past four years, he has stepped up to bat for me more times than I can possibly acknowledge. Just don’t make fun of his oxygen because he can hear you.

The faculty and staff of the Pharmaceutical Chemistry department have been very active and helpful in obtaining my doctorate. In particular, I want to

thank Dr. Valentino J. Stella, Dr. Jennifer S. Laurence, Nancy Helm, Karen Hall and Nicole Brooks for assisting me with various issues over the years. Furthermore, I want to thank the members of my dissertation committee, Dr. C. Russell Middaugh, Dr. Teruna J. Siahaan, Dr. Kenneth L. Audus, and Dr. James A. Orr. I would like to extend particular gratitude to Drs. Middaugh and Orr for critically reading the dissertation and providing me with helpful comments.

During my undergraduate and graduate years at The University of Kansas there were many people that provided key advice or opportunities that led to this doctorate. First, I must acknowledge several people involved with the Office of Diversity in Science Training (ODST) and the Initiative for Minority Student Development (IMSD) program. The IMSD program is the sole reason I began class work at KU and my involvement has led to numerous research and career opportunities. The mission of IMSD is simple: assist minority students that are historically underrepresented in the sciences by exposing them to real research problems in labs on campus. Tutoring for classes, travel to scientific meetings, and other resources were also available in addition to lab placement all of which was tremendously helpful. The director of this office, Dr. James Orr, Molecular Biosciences Professor, has been concerned about my well-being and academic success ever since I stepped foot on KU's campus. He was a great undergraduate advisor and mentor. I must acknowledge Dr. Marigold Linton for assisting me in joining the program when it was still in its infancy and the past and present coordinators of IMSD Claudia Bode, Marian Hukle, and Roberta

Pokphanh for their contributions to my academic advancement over the years. Beginning at KU, Russ Middaugh played an important part in my development as a scientist. When I first moved to Lawrence, I was a green undergraduate with no laboratory research experience. Russ gave me an invaluable opportunity to join his lab and have my own research project, which required trust to use his very expensive instruments to complete. In my graduate years, Russ has been a great career resource and has provided insight for the work presented in this dissertation. I truly respect Russ and value his opinions on just about everything from life to science. The mentor for my undergraduate project while working with Russ was a post-doctoral fellow named LaToya Jones (now Braun). LaToya was very patient in guiding me to independently work on and fully understand why I was performing certain tasks. She has remained a good friend and resource throughout my doctorate work.

I have had the fortune of knowing many interesting, ambitious and intelligent colleagues while completing my doctorate. In particular I want to thank Jo Krise and Murali Duvvuri for taking the time to teach me many of the techniques I used in this research when I initially joined Jeff's lab. Murali dedicated a lot of his free time teaching me how to design relevant experiments so that they had the highest chance of success. Outside of the lab, Murali continues to be a good friend. I will never forget the time he rapped Lil' Jon after a long night of drinking…good stuff. To all of the other Krise lab members past and present, Stephen Goldman, Rosemary Ndolo (Frodo), Ryan Funk, Alana

Toro-Ramos (Pesadilla), Shan Huang (Shan-imal) and Samidha Konkar, thank you for your scientific discussions and all of the good times we had as a lab. I can only hope that I have the pleasure to work with fun and hard-working people such as you in the future. In addition to these fine people, I am extremely grateful to have a network of friends inside and outside of the department to help cope with the rigors of graduate school. Fellow classmates Diana Sperger and Bob Berendt (known together as "Spergbob") were fantastic study companions during our comprehensive exams. Without Spergbob, I might well have bombed all aspects of that exam…which was hell on paper. Furthermore, I want to thank Ben Nelson, Gary Gerstenecker, Dave Fischer, Dr. Dan Mudra, Dr. Bill Marinaro, Andi Skinner, Natalie Ciaccio, Dr. Feng He, Pallabi Mitra, Dr. Tim Kamerzell, and Dr. Kelly Desino for their friendship and help over the years in Pharm Chem. I will definitely miss Fantasy Football, Fall Softball, Cigar Club and nights at the Red Lyon.

Next, I must acknowledge my mother and my father, Carolyn Nott and Mike Kaufmann. When I was growing up my mother made many sacrifices to get me where I am today, both financially and emotionally. My mother has taught me not to take anything for granted because life can change in the blink of an eye. She has always been involved in my education and was always looking for opportunities for my betterment. In fact, my mother is responsible for discovering many of the research opportunities for undergraduate Native Americans at the University of Kansas, which preceded this dissertation. These opportunities

opened doors that allowed me to join the Pharmaceutical Chemistry department and complete this doctorate. I am grateful for my mother's continued support of my goals and for her love.

Overall, my father has been the person that has instilled patience and humility in me. He taught me patience through the game of golf, which he probably regrets now (Me: > 100, Dad: 2). He has also taught me that hard work can result in many things including self respect. Growing up, my father taught me to not do things half-ass: hang your towel up, flush the toilet, turn out lights when leaving a room, and most importantly to always check your car's oil. He has done everything to make sure that I was able to be successful, like maintaining my car while driving to school and helping me find college funding. Aside from life's little lessons, in recent years he has shown me that a well intentioned person will always weather whatever storm life has in store for them. My father has weathered a lot in his life and I am grateful for his continued presence as a role model and friend.

The Quapaw Tribe or the Ugakhpa (down-stream people) have been enormous supporters of my educational endeavors. Specifically, I want to sincerely acknowledge and give thanks for the late Reberta Keyser who was a great help during my undergraduate education years at Pittsburg State University and later at KU. Whether she was directly responsible for the program or not, I could always count on Reberta for help with just about anything the Quapaw tribe

had to offer. After Aunt Bert's passing, the person I counted on the most was her grand-daughter Jennifer Lunsford. Just like Reberta, Jennifer was always interested in my well-being as well as being a tremendous resource within the tribe. I would also like to thank Flossie Matthews and the business committee for realizing the value of a college education and their continued allocation of funds for programs like Higher Education. Although the financial assistance I received was not enough to cover the rising costs of tuition, it was enough to buy books and class materials. Obviously, the successful completion of my bachelor's, master's and doctorate was dependent on these materials. I have been blessed to attend college during a time when the Quapaw tribe was experiencing great financial success through various ventures. Over this time, I have witnessed the tribe expand from one administrative building to owning a multi-million dollar casino and resort. It is my hope that the new-found wealth of the Quapaw people can be invested into programs like the ones that I have used to nurture bright, successful and ambitious Quapaw children.

Last but definitely not least, I want to thank my wife Heather for being the person that supported me the most through this journey. Heather, you have had to endure me talking on and on about my project, my frustrations, and concerns without ever getting tired of hearing the same thing over and over again. You pushed me to apply early for graduate school and helped me finish early by understanding the long hours at the lab that I needed to be successful. In the end, I know that I have accomplished a great thing because of you. I have no

doubts that without you this would not have been possible and that is why this dissertation is dedicated to you because of your love, support and devotion to me. Thank you for everything…..I love you.

The Niemann-Pick C1 Protein Functions in Regulating Lysosome Amine Content

Table of Contents

Content **Page**

Figure Index

Chapter 1

Introduction

1.1. Introduction

Research on Niemann-Pick Type C (NP-C) disease has been ongoing for several decades. Although much research has been performed over this time, a function for the protein responsible for the disease, Niemann-Pick C1 (NPC1), remains elusive.

This introductory chapter provides a review of relevant areas concerning our proposed novel cellular function for the NPC1 protein. First, there will be an introduction to the lysosome compartment and its relevant cellular functions. There will be discussion on the known mechanisms for molecules to enter lysosomes as well as known mechanisms for efflux of lysosome contents. The second section will include a brief introduction to NP-C disease and NPC1. This section will highlight relevant research and conclusions to date. In conclusion, there will be a review on physiologically relevant amine containing molecules and how they could play a role in neurodegenerative diseases like NP-C disease. Specifically, there will be a discussion about endogenous polyamines and their metabolites.

1.2. The lysosome

1.2.1. Overview of the lysosome

Lysosomes were originally discovered in 1949 by Christian de Duve upon the observation of acid-phosphatase activity in sub-cellular fractions of liver [1]. Lysosomes are now known to be an integral part of the endocytic pathway in cells. By definition, lysosomes are membrane bound organelles that possess an array of active acid hydrolase enzymes and a low lumenal pH (typically pH 4-5) which is approximately 2 units below the surrounding cytoplasm [2]. Their membranes are typically laden with glycoproteins (i.e. lysosome associated membrane protein, LAMP and lysosome glycoprotein, LGP) and phospholipids (lysobisphosphatidic acid, LBPA) not found at high concentrations in other locations in the cells except for late endocytic compartments [3; 4]. Lysosomes are further defined and distinguished from endosomes in the endocytic pathway by the absence of mannose-6-phosphate receptors (MPR, late endosomes) and plasma membrane recycling receptors like the transferrin receptor (early endosomes) [5; 6; 7]. Their morphology in cells has been shown to be heterogeneous and electron dense when observed by electron microscopy (EM) [8]. Furthermore, using EM, the inner core of lysosomes has been shown to be multi-vesicular, indicating that more than one membranous structure is present within the organelle and heterogenous with respect to internal osmolarity [8; 9]. Lysosomes have been shown to contribute approximately 6 pL to total cellular volume, which has been proposed to be 0.5-5% of the total depending on cell-type [8; 10; 11].

Since de Duve's discovery, lysosomes have been well-studied and generally regarded as a terminal static degradative compartment within the endocytic pathway [12]. This notion has been challenged by several recent lines of evidence: 1) that lysosomes can interact with other organelles in the endocytic pathway, specifically late endosomes [13; 14] and 2) the discovery that similar to secretory lysosomes, conventional lysosomes can be stimulated to fuse directly with the plasma membrane [15]. These findings are discussed in detail below.

1.2.2. Lysosome dynamics

To put lysosomes into context with other organelles in the endocytic pathway, a general schematic of how macromolecules can localize within lysosomes is shown in Figure 1.1. As seen in Figure 1.1, the pathway for endocytic delivery into lysosomes occurs after endocytosed materials pass through early endosomes and late endosomes. The final step is thought to occur through some type of interaction with late endosomes, although there is much debate on how this is accomplished. The traditional maturation model for endocytic delivery to lysosomes proposes that early endosomes mature into late endosomes which subsequently mature into lysosomes with the resulting organelle phospholipid bilayer being composed of initial plasma membrane [4; 7; 12; 16]. This is unlikely, however, since components common to the plasma membrane are not found in early and late endosomes and that these organelles are biochemically unique [17]. The maturation of late endosomes to lysosomes

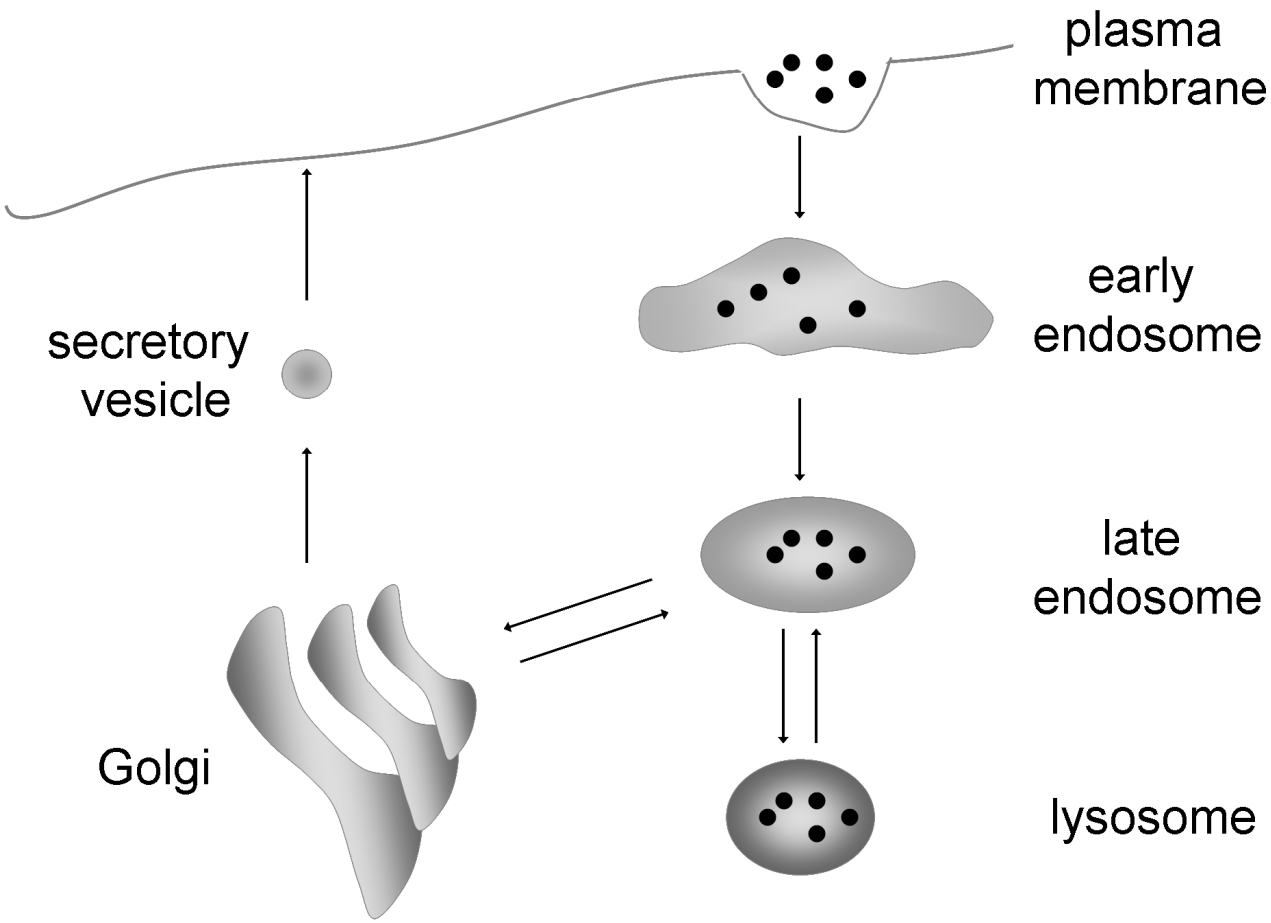

Figure 1.1. General overview of fluid-phase endocytosis and Golgi apparatus secretion. Membrane impermeable molecules (black circles) are engulfed by the plasma membrane and trafficked through early and late endosomes to lysosomes. The Golgi has been proposed to play a role in the indirect exocytosis of lysosome contents (see text).

has not been fully discounted and may contribute to lysosome localization of macromolecules to some degree [8; 18; 19]. A more recent maturation model suggests lysosome biogenesis occurs as a result of continuous organelle-mediated interactions that add and remove components from endosomes to ultimately form the lysosome [16]. For example, late endosomes and their contents can become lysosomes by removal of membrane proteins (such as MPR), further lowering of pH, and increases in density [4; 20]. On the other hand, it has been suggested that cells possess an initial amount of lysosomes following cell division which are maintained and reformed from these types of interactions. Recent mechanisms that address these possibilities include the “kiss and run” and hybrid organelle models (see Figure 1.2) [21; 22; 23].

An essay by Storrie and Desjardins proposed a “kiss and run” theory for macromolecule delivery to lysosomes in response to observations of fluorescence-labeled endosomes transiently bumping into each other and separating [21]. Elegant investigations by Bright et al. using EM and fluorescence microscopy confirmed that this mechanism occurs readily in living cells by observing, in real-time, differentially labeled late endosomes physically making contact with lysosomes, docking, depositing their contents, and then separating [24]. Furthermore, these investigations revealed that complete organelle fusion events (or hybrid organelle formation) between late endosomes

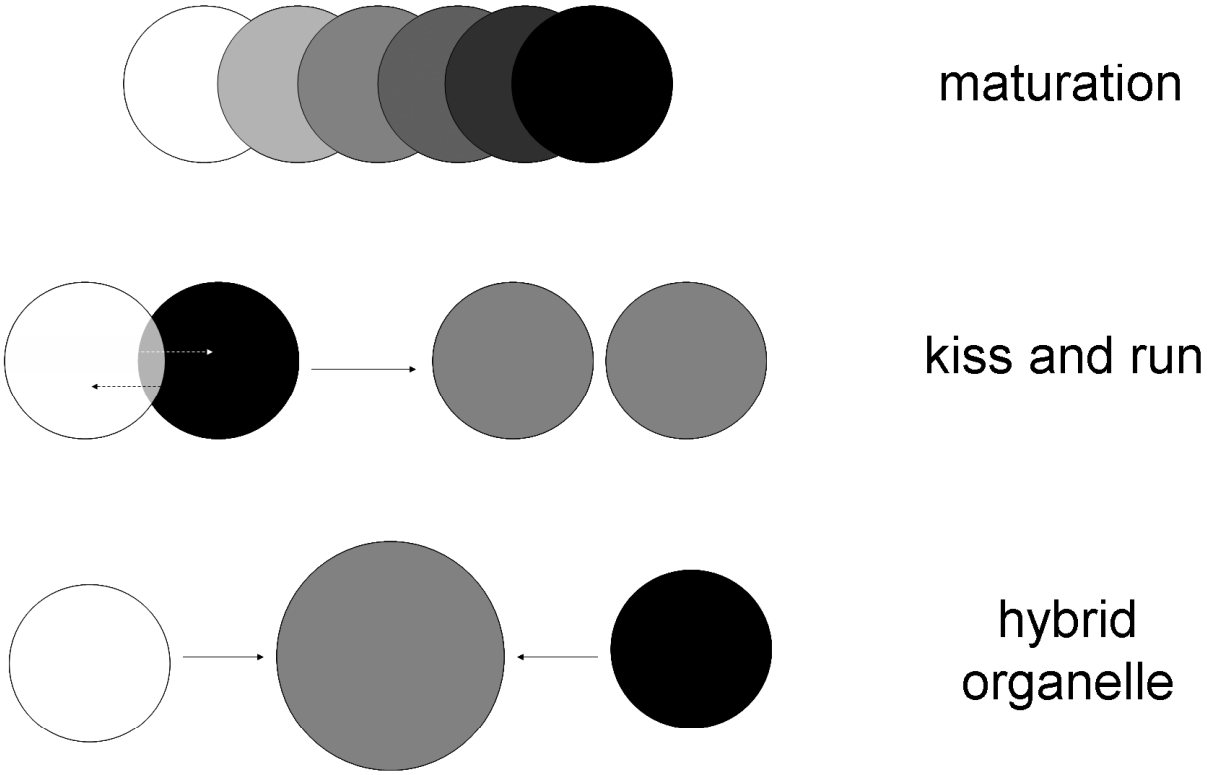

Figure 1.2. Proposed models for delivery of endocytosed cargo from late endosome to lysosomes. Late endosomes (white circles) and lysosomes (black circles) are shown interacting in a representation per Luzio et al. Grey circles represent intermediate organelles with all or some biochemical properties of both late endosomes and lysosomes.

and lysosomes also occur readily in living cells. It was reported by Bright et al. that these two mechanisms (kiss and run, hybrid organelle formation) accounted for all content transfer between late endosomes and lysosomes [24].

In 1989, Mullock et al. reported the use of a cell-free assay for investigating the ability of late endosomes to fuse with lysosomes forming a hybrid organelle of intermediate properties [25]. Hybrid organelle formation events were shown *in vitro* through the mixing of reconstituted fractions of late endosome and lysosomes. Heterotypic fusion events between late endosomes and lysosomes were found to be dependent on the presence of ATP, cytosol, calcium, and temperature [13; 26]. The use of such an assay has shown that all membrane fusion events occurring between late endosomes and lysosomes are doing so with general cytosolic fusion machinery, which requires NSF (N-ethylmaleimide sensitive factor) and SNAPs (soluble NSF attachment proteins) functioning by the SNARE (SNAP receptor) mechanism [27; 28]. According to Rothman and Warren, the SNARE hypothesis (originally discussed by Rothman in 1993 [29]) provides a mechanism for the specific docking and fusion of transport vesicles with their target membrane (in this case late endosomes with lysosomes or vice versa) [30]. This is accomplished through the pairing of specific vesicle (v) and organelle target (t) SNAREs that form a trans-SNARE complex which pull the organelles intimately together [8; 30]. In addition to these components, Mullock et al. further demonstrated that a small GTPase from the Rab family is involved by inhibiting late endosome-lysosome fusion with a Rab

GDP dissociation inhibitor, which maintains the Rab's inactive form [28; 31]. Rabs are organelle specific proteins that are believed to function in the recognition of target membranes as tethers which specifically link organelles together before trans-SNARE formation [32; 33].

Luzio et al. proposes that hybrid organelle formation by fusion of late endosomes and lysosomes follows the traditional steps for membrane fusion: 1) tethering by NSF, SNAP, and Rab proteins, where the two organelles form links with each other, 2) the formation of the trans-SNARE complex between v- and t-SNARES, and 3) membrane fusion [8]. The formation of the intermediate trans-SNARE complex has been shown to be necessary but not sufficient for membrane fusion upon discovery that calcium and calmodulin are required for the late steps of membrane fusion [26; 34]. In addition, optimal lipid composition and asymmetry (curvature) of the phospholipid bilayer are important for successful membrane fusion [35]. The presence of lipid-rich domains such as sphingomyelin and cholesterol in membranes has been shown to favor organelle fusion [36; 37]. In particular, cholesterol facilitates high negative spontaneous curvature of lipid bilayers that has been shown experimentally to drive fusion events in liposomes [35; 38]. Furthermore, it was demonstrated that cholesterol supports the formation and transition of transient fusion intermediates like the trans-SNARE complex [35].

Conventional lysosomes have been shown to fuse with the plasma membrane upon stimulation with high concentrations of cytosolic calcium [15; 39; 40]. The purpose for such events have been demonstrated when cells are injured and are in need of repair since fusion with lysosomes provides immediately available phospholipid membranes for resealing [41; 42]. Similar to fusion with late endosomes, lysosome fusion with the plasma membrane requires the same fusion machinery (tethers, trans-SNARE formation, etc.) [43]. However, the process is regulated by two key components: cytosolic calcium concentrations and synaptotagmin-VII, a calcium sensor that localizes to lysosomes [44; 45]. Cytosolic Ca^{2+} concentrations of approximately 1-5 μM have been shown to stimulate lysosome fusion with the plasma membrane, which according to Pryor et al., is almost 15-fold higher than what is required for late endosome-lysosome fusion [26]. There also exist specialized secretory lysosomes, such as mast-cell secretory granules, basophil granules, and many others that co-exist with conventional lysosomes in certain cell types [46; 47]. Similar to conventional lysosomes, these secretory compartments can be stimulated to fuse with the plasma membrane to release their respective cargos [46]. A more in-depth discussion concerning secretory lysosomes has been omitted here since this review is focused on the dynamics of conventional lysosomes.

The two examples described here, late endosome-lysosome and lysosome-plasma membrane fusion, highlight the emerging identity of the

dynamic lysosome. As described, the lysosome is unlikely to be considered a static or terminal compartment as was previously thought.

1.2.3. Delivery of materials out of the lysosome

The previous section discussed the dynamic trafficking events which result in the localization of endocytosed macromolecules to the lysosome. In this section, I will discuss how the formation of a hybrid organelle compartment can allow trapped molecules to escape from the lysosomal lumen to the extracellular space.

As described above, hybrid organelle formation results from the fusion of late endosomes and lysosomes. It seems intuitive that if late endosomes and lysosomes were to engage in several of these fusion events without being reformed they would essentially be “used up”. Thus, there must be a mechanism for the reformation of these compartments after hybrid organelle formation. Furthermore, this mechanism must take into account the following requirements: 1) lysosomes are much denser than hybrid organelles, so there must be condensing of lumenal components and 2) organelle specific membrane proteins must be segregated. To support the first requirement, there is evidence suggesting that regulated secretory vesicles in neuroendocrine cells undergo condensation by the removal of non-secretory components through the budding of small vesicles from maturing granules [48]. This process was found to be dependent on the low lumenal pH of the granule and calcium concentrations.

Similar to this mechanism, Bright et al. used electron microscopy to show that lysosomes can be reformed from hybrid organelles [49]. To describe this, cells were first labeled with 10 nm BSA-gold particles which were allowed to localize to lysosomes. Next, 15 nm BSA-gold particles were endocytosed and allowed to localize to late endosomes. Initially, the 10 nm BSA-gold particles were in MPR negative lysosomes and the second pulse of 15 nm BSA-gold was in MPR-positive late endosomes. After time, it was observed that lysosomes had both sizes of BSA-gold in their lumen suggesting that lysosomes interacted with late endosomes and were re-usable since they received two different pulses of BSA-gold. In another attempt to describe this mechanism, Pryor et al. used the previously described *in vitro* assay for assessing hybrid organelle formation to describe lysosome reformation by observing organelle density changes by ultracentrifugation on Nycodenz gradients [26]. At various times post-hybrid organelle formation, they observed the movement of lysosomes to different fractions by monitoring *N*-acetyl-β-glucosaminidase activity, a lysosomal enzyme. Over time, as lysosomes reformed, they became denser and were able to separate from the less dense late endosomes and remaining hybrid organelles. Interestingly, similar to the neuroendocrine granules described above, this process was inhibited by raising the lumenal pH using bafilomycin A1 or removing calcium using the chelator EGTA [26].

The next obvious consideration for lysosome reformation is the segregation of membrane or membrane-associated proteins from the hybrid

organelle, with the most obvious candidate being MPR, since lysosomes are defined as MPR-negative organelles (see above) [7]. The MPR recycling pathway from late endosomes to the Golgi apparatus has been well-described by others [5; 32; 50]. The removal of MPR from hybrid organelles and subsequent recycling to the Golgi apparatus has been shown to occur via coated vesicles which at present have unknown lumenal cargo(s) [51]. Retrograde traffic from hybrid organelle to Golgi has been proposed to be a major mechanism for the exocytosis of unwanted lysosome contents since the Golgi is known to secrete continuously to the plasma membrane and conventional lysosomes do not unless stimulated with high calcium concentrations [18; 52]. As mentioned above, however, there is little information to date about the fluid phase cargo that transport vesicles from hybrid organelles to Golgi would contain [51]. It is unlikely that lysosome enzymes, like cathepsin-B, are the primary cargo since the presence of active forms of these enzymes are not present at the cell periphery to a significant degree [53]. Considering this, it seems these vesicles provide a plausible vector for the removal or recycling of non-resident materials and the repackaging of lysosome enzymes.

1.2.4. Lysosome storage disorders

There is no doubt that lysosomes function in the cell to break down endocytosed materials, as well as endogenous components targeted for recycling (i.e. proteins and membranes). Genetic impairment in normal lysosome function (i.e. enzyme metabolism or transport) results in lysosomal storage

disorders, which are characterized by the build-up of a substrate or metabolite in the lysosome lumen. To date there have been many different lysosome storage disorders described in the literature. Typically, these storage disorders are classified into subgroups according to their biochemical deficiency. For example, if lysosomes have dysfunctional sphingomyelinase activity which results in the build-up of sphingomyelin then the disorder is considered a sphingolipidosis. Typically, lysosome storage disorders affect lysosome rich areas of the body such as the spleen or liver, or areas that are rich in lysosomal substrate. For example, as a consequence of being rich in gangliosides, the brain is more affected by gangliosidosis than other areas. The two best examples of this are Tay-Sach's and Sandhoff's disease which are characterized by the build-up of GM2 gangliosides due to defects in lysosomal hexosaminidase A and/or B activity, respectively [54; 55]. Both of these disorders result in severe neurologic impairment and death.

Along with the classification of lysosome storage disorders into subgroups, further classification of these groups can be made by identifying the dysfunctional protein as soluble or insoluble. Soluble protein disorders typically result from deficiencies in enzyme activity as described above for Tay Sach's and Sandhoff's disease. There are cases where disorders result from dysfunctional soluble proteins that are not enzymes, as is the case for Niemann-Pick C2, which has been shown to insert and remove cholesterol from lipid bilayers [56; 57]. Furthermore, soluble protein disorders can be treated with greater success using

enzyme replacement or substrate reduction therapies, except for neurological disorders due to complications with delivery across the blood brain barrier [58; 59]. Insoluble protein disorders result from malfunctioning lysosome membrane proteins. Unlike soluble protein disorders, insoluble proteins typically function in the transport of a substrate from the lumen to other parts of the cell. The two best examples are mucolipidosis type IV (MLIV) and Niemann-Pick Type C (NP-C) disease. Mucolipin-1, the lysosome membrane protein defective in MLIV, has been shown to be involved in the sub-cellular transport of sphingolipids, phospholipids, and acid mucopolysaccharides [60]. Similar to MLIV, NP-C disease is characterized by the build-up of cholesterol, sphingolipids, phospholipids and gangliosides [61].

Interestingly, there are many lysosome storage disorders that are inefficient at secreting lysosome contents to the cell periphery. Chediak-Higashi, Griscelli and Hermansky-Pudlak syndromes all result from defects in normal secretion of lysosomal contents [46; 62; 63]. In addition, NP-C disease has been shown to have inefficient egress of lysosome contents [64; 65]. This disease and the protein responsible, Niemann-Pick C1, are discussed in greater detail in the next section.

1.3. Niemann-Pick Type C disease and the Niemann-Pick C1 protein

1.3.1. Niemann-Pick Type C disease

Niemann-Pick Type C (NP-C) disease is an extremely rare childhood disorder that results in severe neurodegeneration, hepatosplenomegaly, and ultimately death [66; 67]. Unlike Niemann-Pick Types A and B, which result from deficient sphingomyelinase activity [68], NP-C is hallmarked by a hyperaccumulation of free unesterified low-density lipoprotein (LDL) derived cholesterol in lysosomes and late endosomes of affected cells. This hypreaccumulation phenotype can be visualized by staining cellular cholesterol with the polyene antibiotic filipin (Fig. 1.3) [67; 69; 70]. The inability of affected cells to efficiently transfer unesterified cholesterol from endosomes/lysosomes results in the inability to down-regulate key components of endogenous cholesterol synthesis and uptake. These components include 3-hydroxy-3-methyl-glutaryl coenzyme A (HMG-CoA) reductase (a key enzyme necessary for endogenous cholesterol synthesis), and the LDL-receptor (necessary for the endocytosis of cholesterol-laden LDL particles) [71]. Thus, NP-C disease is classified as a lysosomal storage disorder and the uptake of LDL-derived cholesterol in affected cells remains continuous [72].

NP-C disease is autosomal recessive and is caused by mutations in the *npc1* gene, which results in a mutated non-functional form of the encoded protein

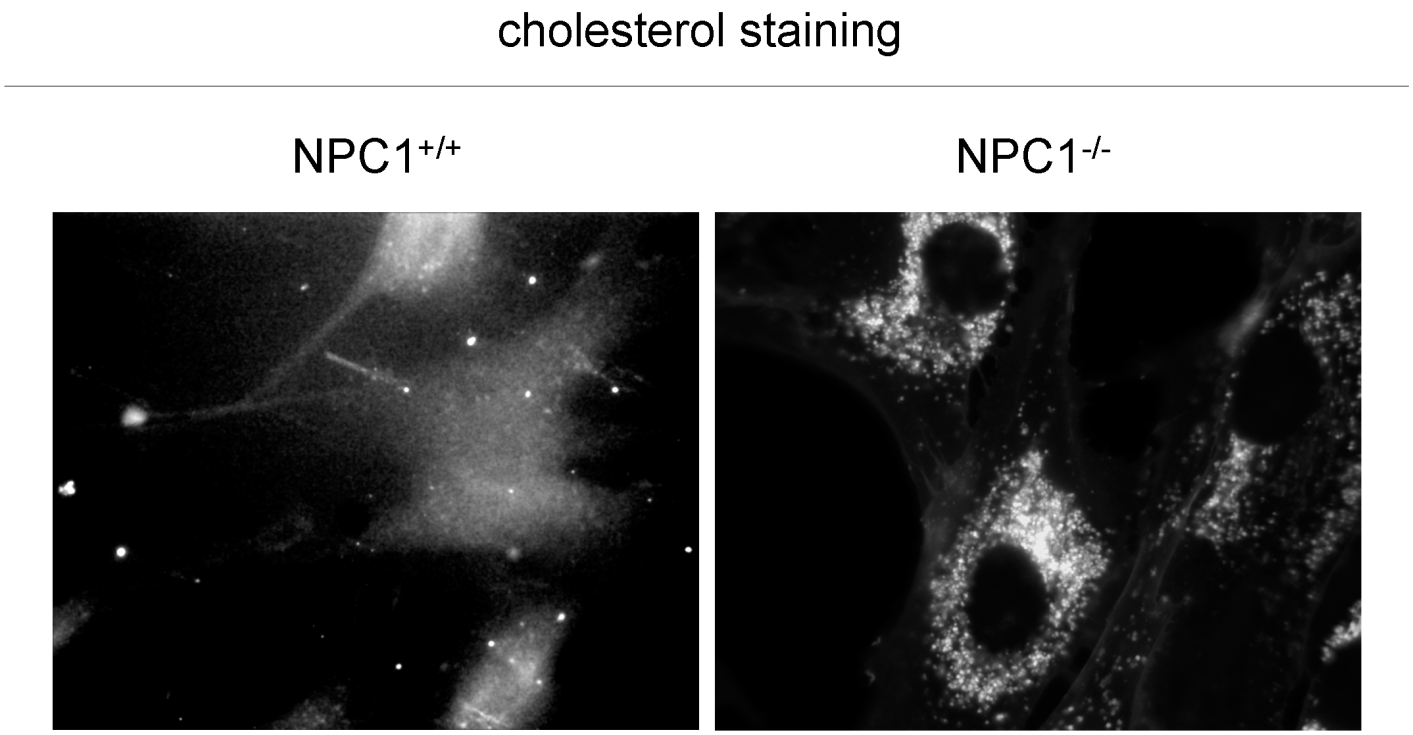

Figure 1.3. Lysosome cholesterol accumulation phenotype associated with NP-C disease. Free cholesterol was specifically stained with the polyene antibiotic filipin (white). Consistent with NPC1 malfunction, NP-C disease cells ($NPC1^{-/-}$) have a punctate perinuclear staining pattern due to cholesterol build-up in lysosomes. Normal cells ($NPC1^{+/+}$), with functional NPC1, have diffuse staining patterns.

Niemann-Pick C1 (NPC1) [73]. At the time of this thesis, there have been over 200 different reports of NP-C disease causing mutations [74]. In 2004, further analysis revealed that 23% are non-sense mutations which result in a truncated form of NPC1. The other 77% of these mutations are point mutations and result in amino acid substitutions [75]. These substitutions are found in all areas of the protein and have no significant trend with regards to amino acids, (i.e. hydrophobic residue for a charged residue) or location (i.e. lumenal vs. transmembrane) [75].

The neurodegeneration prevalent in NP-C disease has been shown to manifest itself in the form of impaired motor movement and tremors. In some cases, heterozygous NP-C carriers experience these symptoms later in life [76]. To this end, researchers have identified that neurodegeneration occurs primarily in the cerebellum by observations of increased Purkinje cell death [77; 78; 79; 80]. The cerebellum is an area of the brain that contributes heavily to sensory perception, coordination and motor function which correlates with disease pathology. Apart from these observations, significant loss of neurons in other loci of the brain has not been reported, although there is generalized atrophy of the central nervous system.

1.3.2. Niemann-Pick C1 protein

NPC1 is a large transmembrane protein that resides on the membranes of lysosomes and late endosomes. The protein comprises of 1278 amino acids and

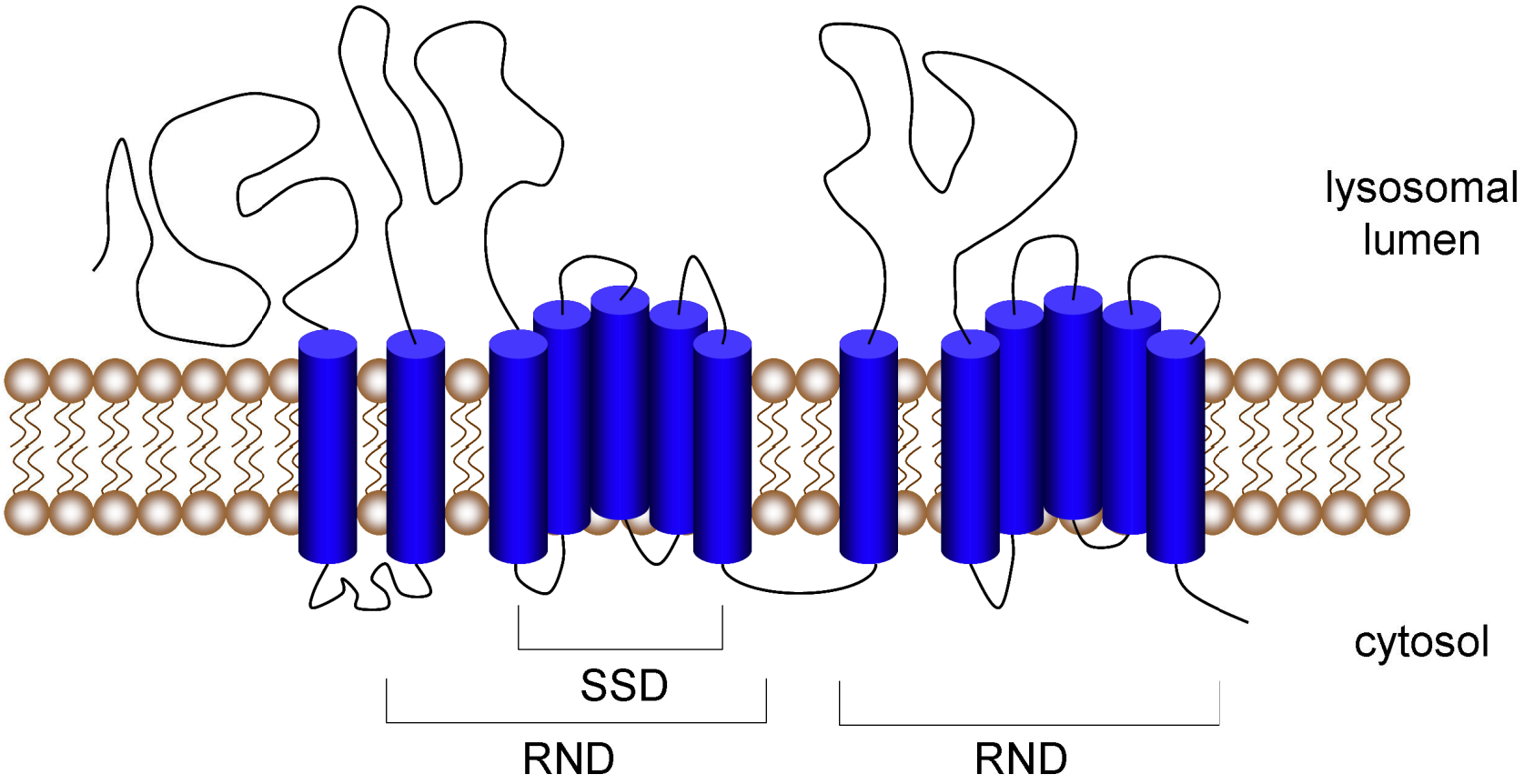

Figure 1.4. Topology of the Niemann-Pick C1 (NPC1) protein. NPC1 is a lysosome membrane protein that possesses 13 transmembrane domains (blue), 3 large lumenal loops, and multiple cytosolic loops. Regions of structural homology include a predicted sterol sensing domain (SSD) similar to cholesterol regulators HMG-CoA reductase and SCAP and two transmembrane configurations consistent with the resistance nodulation division (RND) family of prokaryotic permeases.

has a predicted molecular weight of 142 kDa, though the protein is glycosylated resulting in increased mass [73; 81]. The protein consists of 13 transmembrane domains, 3 large lumenal loops, multiple cytosolic loops and a cytosolic C-terminal tail (see Figure 1.4 for protein topology) [75; 82]. The C-terminal tail possesses a lysosome targeting sequence in the form a dileucine motif [83], which has been shown to target other membrane proteins to the lysosome [84]. This sequence is not needed for targeting membrane proteins to late endosomes, which suggests the protein resides in lysosomes more than late endosomes, although both localizations have been observed to varying degrees [85].

1.3.3. Function of Niemann-Pick C1

Structural comparisons between NPC1 and other proteins have been performed in an attempt to discover NPC1 function (i.e. structure implying function). A particular transmembrane amino acid sequence was shown to have similarity with the sterol sensing regions of the morphogen receptor PATCHED, SREBP cleavage-activating protein (SCAP) and HMG-CoA reductase proteins [75; 82; 86; 87]. These proteins are necessary for cholesterol homeostasis and all have putative sterol sensing domains which were identified by Carstea et al. for NPC1 [73; 88]. These findings suggest that NPC1 plays an important role in trafficking lysosome cholesterol. A unique lipoprotein-attachment site, similar to that found in prokaryotic transmembrane proteins, is found multiple times in NPC1's protein sequence [89]. These sites have been shown to be prevalent in

the resistance-nodulation-division (RND) family of prokaryotic permeases [90]. Further research revealed that NPC1 and members of the RND family share the same RND signature repeated twice: six transmembrane domains separated by a large hydrophilic loop [89]. RND-permeases have been shown to transport a variety of cargos which include lipophilic drugs and fatty acids [91; 92]. These results suggest that NPC1 is functioning as a membrane transporter of cholesterol.

Traditionally, NPC1 has been implicated as a cholesterol transporter due to the cholesterol hyperaccumulation phenotype associated with NP-C disease and the presence of structural elements associated with cholesterol trafficking (see above). However, functional studies with regards to NPC1 transporting cholesterol have been disappointing. In NPC1-expressing E. coli, NPC1 was shown to transport fatty acids, but not cholesterol or cholesterol esters [89]. If cholesterol was indeed NPC1's primary substrate, then binding of cholesterol to NPC1 should occur with great affinity. To test this, investigators used a photoactivatible crosslinker attached to cholesterol (azo-cholesterol) and showed that NPC1 could bind low levels of cholesterol in cell culture models [93]. Most recently, Infante et al. reported that purified NPC1 could bind both cholesterol and oxysterols, with oxysterols such as 25-hydroxycholesterol having much higher affinity for NPC1 [94]. This supports previous observations using azo-deriviatives of cholesterol that showed NPC1 binds cholesterol with low affinity and suggests that LDL-derived cholesterol is not NPC1's primary substrate.

There is no question that malfunctioning NPC1 negatively affects cholesterol traffic from lysosomes; however, is this due to NPC1's true functional role? Interestingly, investigations have revealed that cholesterol is not the only molecule that hyperaccumulates in NP-C diseases lysosomes. Gangliosides, sphingoid bases, phospholipids, and glycolipids have all been shown to accumulate in lysosomes of NP-C cells [65; 95]. Thus, the possibility exists that NPC1 may not function solely as a cholesterol transporter but may play a more general role in the egress of lysosome contents resulting in indirect cholesterol accumulation. In support of this, we and others have observed that a generalized block in secretion of lysosome contents occurs in NP-C disease cells [64; 65]. In our lab, we showed that multi-drug resistant HL-60 cancer cells with a dysfunctional form of NPC1 were able to sequester weak bases without subsequent egress to the plasma membrane, unlike normal cells [64]. Studies by Neufeld et al. demonstrated that fluid phase endocytosis markers, such as sucrose, could be localized to NPC1 containing lysosomes but were inefficiently trafficked elsewhere in NP-C cells [65]. Furthermore, NP-C cells have an inability to correctly sort MPR, suggesting transport between late endosomes and the Golgi apparatus is defective [65]. Accordingly, the true functional role of the NPC1 protein remains controversial and is, perhaps, best described as unknown.

1.3.4. Therapies for NP-C disease

As discussed above, the function of NPC1 is unclear at present. Thus, therapeutic endeavors aimed at increasing the lifespan of affected individuals or delaying onset of disease have been met with limited success.

The notion of NPC1 as a cholesterol transporter has dominated therapeutic research for many years. The early work of Pentchev and others showed that NPC-diseased cells were laden with LDL-derived free unesterified cholesterol, which was thought to be the direct cause of NP-C disease pathology [67]. To address this possibility, researchers examined the effects of reducing cholesterol build-up in lysosomes on longevity and disease progression. To accomplish this, three approaches have been taken: 1) dietary limitations on cholesterol, 2) cholesterol lowering drugs, 3) genetic manipulation of cholesterol uptake. First, feline models of NP-C disease were observed with or without cholesterol in their daily diet. The onset of disease progression, as determined by appearance of tremors, dysmetria, and atrophy, did not change with restrictions in dietary cholesterol [96]. Second, the lowering of cholesterol levels in NP-C murine models was accomplished through the use of pharmacological agents, such as the cholesterol lowering drug probucol. Administration to NP-C mice resulted in a significant decrease in liver cholesterol levels (up to ~50%) when compared to control NP-C mice [97]. However, the onset of ataxia and tremor was not statistically significant with untreated NP-C mice. In the same study, genetic manipulations were performed to address the source of cholesterol build-up in lysosomes of NP-C mice, the LDL-receptor. Double

knockout mice were bred that had deficiencies in both NPC1 protein and LDL-receptor. Interestingly, cholesterol levels were similar in LDL-receptor negative NP-C mice and showed the same disease progression time-line as the single knockout NP-C murine model [97].

It is becoming increasingly apparent that in order to effectively treat NP-C disease there must be a functional understanding of NPC1 in the cell. The treatments described above are meant to alleviate disease phenotypes but are lacking with regards to rationally developing a strategy to address NPC1 dysfunction. In the next sections there will be a discussion concerning other molecules, besides lipids, that may contribute to NP-C disease pathology. In particular, the accumulation of weakly basic amines will be examined.

1.4. Significance of lysosomal amine sequestration and NP-C disease

1.4.1. Overview of pH-partitioning

Typically, there are two ways that weakly basic amines can localize within the lysosome lumen to a significant degree: 1) passive-diffusion and 2) fluid phase endocytosis as described above in Section 1.2. This section will concentrate on passive diffusion mechanisms for weakly basic amine accumulation in lysosomes. Of the indicated pathways, this mechanism has the highest sequestration capacity if conditions associated with the cell and the amine are optimal, as will be discussed. Endocytosis is a very dynamic process; however, its ability to concentrate amines into lysosomes is minimal when compared to passive mechanisms.

Most researchers agree that the accumulation of amines in lysosomes occurs by a passive pH-partitioning mechanism [10; 98; 99; 100; 101]. A basic overview of this process is depicted in Figure 1.5; however, for a more in-depth quantitative perspective Christian de Duve, the discoverer of lysosomes, has reviewed weak base sequestration in detail [102]. Briefly, a weak base in its unionized and membrane permeable form (B, Fig. 1.5) can diffuse through the lysosome membrane after traversing the plasma membrane and cytosol. The cytosol has been shown to have a pH around neutrality and thus weak bases that have pKa values near this will exist to a significant degree in the free base form.

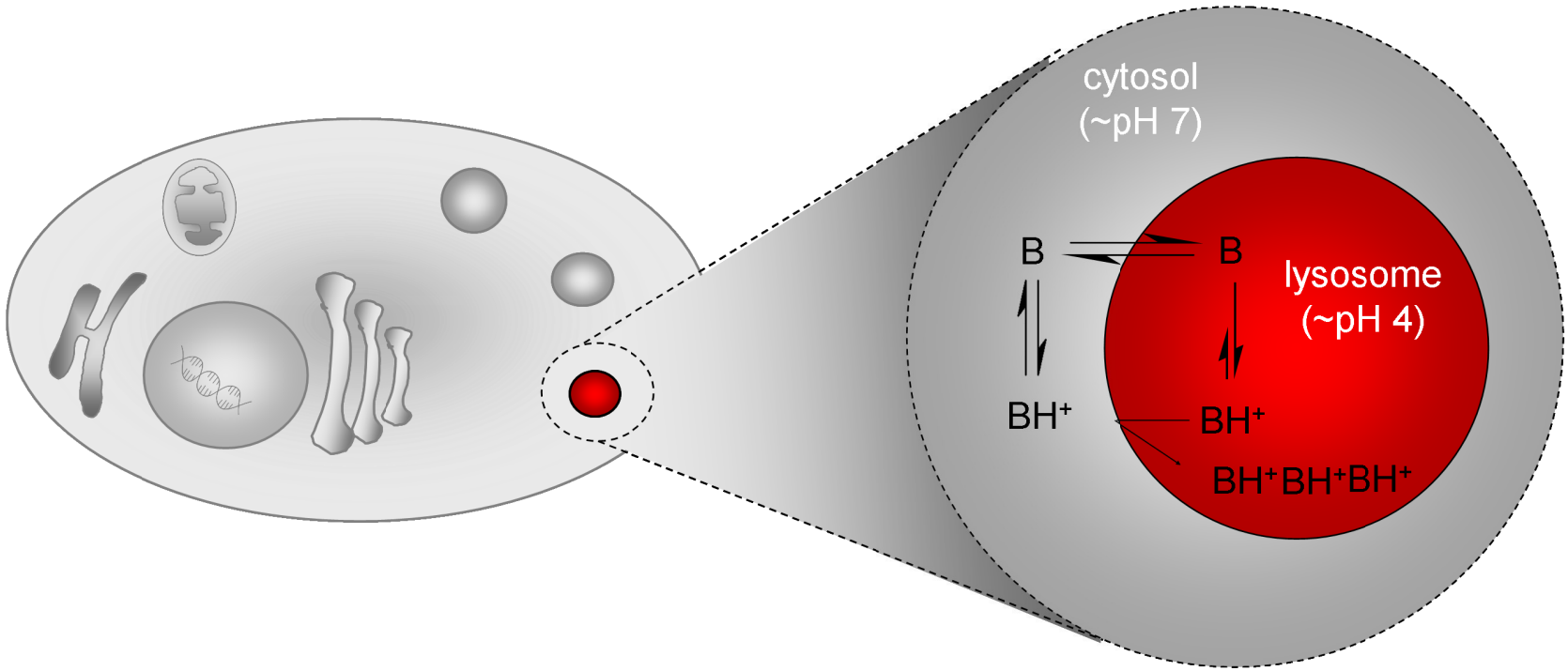

Figure 1.5. Weak base accumulation in lysosomes occurs via a pH-partitioning type mechanism.

Once inside the acidic lysosome lumen, weak bases experience a shift in ionization equilibrium to favor the protonated form (BH^+) and will sequester here due to the inability of the base in its charged form to permeate back across the membrane. It is important to note that the charged species must not be membrane permeable in order for sequestration, otherwise accumulation will not occur [103]. In addition, the low pH of the lysosome must be maintained in order for significant accumulation of weak bases to occur [101; 104]. If these requirements are met, at steady state there will be a dramatically increased concentration of weak bases in lysosomes as compared to the cytoplasm. The pKa value of the weak base has been correlated with the capacity for sequestration, in which higher values result in higher lumenal concentrations [105]. Evaluations with weakly basic vital stains such as neutral red provided some of the first evidence supporting the extreme concentrative capacity of lysosomes for basic molecules [106].

1.4.2. Endogenous molecules that substrates for pH-partitioning

Cells are known to be continuously exposed to high concentrations of endogenous biogenic amines, polyamines, and their metabolites [107; 108]. Despite the fact that these molecules are not fluorescent, making it difficult to analyze their intracellular localization, a number of reports have suggested that these molecules and their metabolites can become extensively compartmentalized in lysosomes [109; 110; 111].

The polyamines; spermine, spermidine, and their di-amine precursor putrescine, are positively charged aliphatic amines that have been shown to be essential for the normal growth of cells. Using polyamine biosynthesis inhibitors, cells in culture can be deprived of polyamines which results in marked decreases in growth and proliferation [112]. Polyamines are proposed to function by preserving and increasing the stability of DNA structure *in vivo* through electrostatic interactions [113; 114]. These molecules are found in cells at high concentrations (millimolar for spermine and spermidine, while putrescine is slightly lower) [115]. Polyamine concentrations are highly regulated as evidenced by a complex network of enzymes, antizymes, and transporters which are used for intracellular synthesis, degradation, uptake and efflux of these molecules *in vivo* [116]. Deviations in homeostatic concentrations of polyamines have been shown to lead to cell death and have been described in several neurological disorders as discussed below.

1.4.3. Altered polyamine levels *in vivo*

In contrast to being necessary for cell growth, polyamines are also known to participate in programmed cell death or apoptosis which has been recognized for many years [117]. In somewhat of a paradox, it appears that polyamines act as protectors, modulators or even promoters of apoptosis [118]. Abnormally high polyamine levels in cells have been shown to cause apoptotic cell death [119; 120]. Exposure to high concentrations of spermine and spermidine results in upregulation of polyamine oxidase (PAO), the enzyme responsible for

degradation of these polyamines. Degradation results in the formation of aminoaldehyde metabolites from polyamines, which are known to be strong inducers of apoptosis [121]. One of these metabolites in particular, 3-aminopropanal, has been shown to exert its toxic effects specifically on lysosomes by facilitating membrane rupture and leakage [122]. Interestingly, these effects are greatly enhanced in neuronal cells [123; 124]. Decreased levels of polyamines have been shown to induce apoptosis by a variety of mechanisms. First, very low levels of polyamines available to DNA have been shown to lead to cell cycle arrest due to stoppage of DNA replication [125]. Second, since polyamines bind to DNA, low levels result in destabilization of important cellular structures, like chromatin, which can become sensitized to nucleases and ultimately lead to cell death [126]. Thus, it appears that a delicate balance exists in cells between too little and too much intracellular polyamine concentration.

In the case of polyamines, it is vitally important for the efficient regulation of homeostatic concentrations to avoid deleterious effects of increased or decreased cellular levels. Since polyamines and their metabolites have been shown to localize within lysosomes, the inefficient release of lysosome contents, as observed in NP-C disease, may result in concentration imbalances and neurological dysfunction. Investigations concerning NP-C disease pathology and polyamines have been lacking; however, there have been significant investigations of multiple neurodegenerative disorders similar to NP-C disease

[127]. These disorders include Alzheimer's disease and multiple sclerosis, both of which have altered polyamine pools and/or deviant enzyme activities [128; 129; 130].

1.5. Objectives of dissertation

The objectives of this work were to identify and characterize differences in lysosome trafficking of weakly basic amines between NPC1-deficient and competent cells with the overall goal of elucidating a novel function for this intriguing protein. The following studies were carried out to address this goal and are discussed in detail in the following chapters:

1. Elucidate the NPC1-mediated molecular events that are occurring in normal cells, but not in NP-C cells, which could permit efficient clearance of amines from lysosomes.

2. Determine the role of NPC1 in the secretion of amines from lysosomes.

3. Develop and employ methods to determine the influence of weakly basic amines on NPC1-mediated secretion of lysosome contents.

4. Link NPC1-defective amine-trafficking to NP-C disease pathology using a physiologically relevant example of amine-induced toxicity in cells.

1.6. References

[1]C. de Duve, J. Berthet, H.G. Hers, and L. Dupret, The hexose-phosphatase system. I. Existence of a specific glucose-6-phosphatase in liver. Bull. Soc. Chim. Biol. 31 (1949) 1242-1253.

[2]J.B. Lloyd, The Taxonomy of Lysosomes. in: J.B. Lloyd, (Ed.), Subcellular Biochemistry: Biology of the Lysosome, Plenum Press, New York, 1996.

[3]T. Kobayashi, M.H. Beuchat, M. Lindsay, S. Frias, R.D. Palmiter, H. Sakuraba, R.G. Parton, and J. Gruenberg, Late endosomal membranes rich in lysobisphosphatidic acid regulate cholesterol transport. Nat Cell Biol 1 (1999) 113-8.

[4]S. Kornfeld, and I. Mellman, The biogenesis of lysosomes. Annu Rev Cell Biol 5 (1989) 483-525.

[5]S.M. Dintzis, V.E. Velculescu, and S.R. Pfeffer, Receptor extracellular domains may contain trafficking information. Studies of the 300-kDa mannose 6-phosphate receptor. J Biol Chem 269 (1994) 12159-66.

[6]W. Stoorvogel, H.J. Geuze, J.M. Griffith, and G.J. Strous, The pathways of endocytosed transferrin and secretory protein are connected in the trans-Golgi reticulum. J Cell Biol 106 (1988) 1821-9.

[7]S. Mukherjee, R.N. Ghosh, and F.R. Maxfield, Endocytosis. Physiol Rev 77 (1997) 759-803.

[8]J.P. Luzio, P.R. Pryor, and N.A. Bright, Lysosomes: fusion and function. Nat Rev Mol Cell Biol 8 (2007) 622-32.

[9]F. Applemans, and C. de Duve, Tissue fractionation studies. 3. Further observations on the binding of acid phosphatase by rat-liver particles. Biochem J. 59 (1955) 426-433.

[10]M. Duvvuri, and J.P. Krise, A novel assay reveals that weakly basic model compounds concentrate in lysosomes to an extent greater than pH-partitioning theory would predict. Mol Pharm 2 (2005) 440-8.

[11]G. Griffiths, R. Back, and M. Marsh, A quantitative analysis of the endocytic pathway in baby hamster kidney cells. J Cell Biol 109 (1989) 2703-20.

[12]I. Mellman, Endocytosis and molecular sorting. Annu Rev Cell Dev Biol 12 (1996) 575-625.

[13]B.M. Mullock, J.H. Perez, T. Kuwana, S.R. Gray, and J.P. Luzio, Lysosomes can fuse with a late endosomal compartment in a cell-free system from rat liver. J Cell Biol 126 (1994) 1173-82.

[14]A. Jahraus, B. Storrie, G. Griffiths, and M. Desjardins, Evidence for retrograde traffic between terminal lysosomes and the prelysosomal/late endosome compartment. J Cell Sci 107 (Pt 1) (1994) 145-57.

[15]A. Rodriguez, P. Webster, J. Ortego, and N.W. Andrews, Lysosomes behave as Ca2+-regulated exocytic vesicles in fibroblasts and epithelial cells. J Cell Biol 137 (1997) 93-104.

[16]R.F. Murphy, Maturation models for endosome and lysosome biogenesis. Trends Cell Biol 1 (1991) 77-82.

[17]S.L. Schmid, R. Fuchs, P. Male, and I. Mellman, Two distinct subpopulations of endosomes involved in membrane recycling and transport to lysosomes. Cell 52 (1988) 73-83.

[18]G. Griffiths, On vesicles and membrane compartments. Protoplasma 195 (1996) 37-58.

[19]J.P. Luzio, V. Poupon, M.R. Lindsay, B.M. Mullock, R.C. Piper, and P.R. Pryor, Membrane dynamics and the biogenesis of lysosomes. Mol Membr Biol 20 (2003) 141-54.

[20]E. Smythe, Endocytosis. in: J.B. Lloyd, (Ed.), Subcellular Biochemistry: Biology of the Lysosome, Plenum Press, New York, 1996.

[21]B. Storrie, and M. Desjardins, The biogenesis of lysosomes: is it a kiss and run, continuous fusion and fission process? Bioessays 18 (1996) 895-903.

[22]T.E. Tjelle, A. Brech, L.K. Juvet, G. Griffiths, and T. Berg, Isolation and characterization of early endosomes, late endosomes and terminal lysosomes: their role in protein degradation. J Cell Sci 109 (Pt 12) (1996) 2905-14.

[23]J.P. Luzio, B.A. Rous, N.A. Bright, P.R. Pryor, B.M. Mullock, and R.C. Piper, Lysosome-endosome fusion and lysosome biogenesis. J Cell Sci 113 (Pt 9) (2000) 1515-24.

[24]N.A. Bright, M.J. Gratian, and J.P. Luzio, Endocytic delivery to lysosomes mediated by concurrent fusion and kissing events in living cells. Curr Biol 15 (2005) 360-5.

[25]B.M. Mullock, W.J. Branch, M. van Schaik, L.K. Gilbert, and J.P. Luzio, Reconstitution of an endosome-lysosome interaction in a cell-free system. J Cell Biol 108 (1989) 2093-9.

[26]P.R. Pryor, B.M. Mullock, N.A. Bright, S.R. Gray, and J.P. Luzio, The role of intraorganellar Ca(2+) in late endosome-lysosome heterotypic fusion and in the reformation of lysosomes from hybrid organelles. J Cell Biol 149 (2000) 1053-62.

[27]B.M. Mullock, N.A. Bright, C.W. Fearon, S.R. Gray, and J.P. Luzio, Fusion of lysosomes with late endosomes produces a hybrid organelle of intermediate density and is NSF dependent. J Cell Biol 140 (1998) 591-601.

[28]B.M. Mullock, C.W. Smith, G. Ihrke, N.A. Bright, M. Lindsay, E.J. Parkinson, D.A. Brooks, R.G. Parton, D.E. James, J.P. Luzio, and R.C. Piper, Syntaxin 7 is localized to late endosome compartments, associates with Vamp 8, and Is required for late endosome-lysosome fusion. Mol Biol Cell 11 (2000) 3137-53.

[29]T. Sollner, M.K. Bennett, S.W. Whiteheart, R.H. Scheller, and J.E. Rothman, A protein assembly-disassembly pathway in vitro that may correspond to sequential steps of synaptic vesicle docking, activation, and fusion. Cell 75 (1993) 409-18.

[30]J.E. Rothman, and G. Warren, Implications of the SNARE hypothesis for intracellular membrane topology and dynamics. Curr Biol 4 (1994) 220-33.

[31]T. Soldati, M.A. Riederer, and S.R. Pfeffer, Rab GDI: a solubilizing and recycling factor for rab9 protein. Mol Biol Cell 4 (1993) 425-34.

[32]D. Lombardi, T. Soldati, M.A. Riederer, Y. Goda, M. Zerial, and S.R. Pfeffer, Rab9 functions in transport between late endosomes and the trans Golgi network. EMBO J 12 (1993) 677-82.

[33]M. Zerial, and H. McBride, Rab proteins as membrane organizers. Nat Rev Mol Cell Biol 2 (2001) 107-17.

[34]C. Peters, and A. Mayer, Ca2+/calmodulin signals the completion of docking and triggers a late step of vacuole fusion. Nature 396 (1998) 575-80.

[35]M.A. Churchward, T. Rogasevskaia, D.M. Brandman, H. Khosravani, P. Nava, J.K. Atkinson, and J.R. Coorssen, Specific lipids supply critical negative spontaneous curvature--an essential component of native Ca2+-triggered membrane fusion. Biophys J 94 (2008) 3976-86.

[36]T. Rogasevskaia, and J.R. Coorssen, Sphingomyelin-enriched microdomains define the efficiency of native Ca(2+)-triggered membrane fusion. J Cell Sci 119 (2006) 2688-94.

[37]M.A. Churchward, T. Rogasevskaia, J. Hofgen, J. Bau, and J.R. Coorssen, Cholesterol facilitates the native mechanism of Ca2+-triggered membrane fusion. J Cell Sci 118 (2005) 4833-48.

[38]T. Shemesh, A. Luini, V. Malhotra, K.N. Burger, and M.M. Kozlov, Prefission constriction of Golgi tubular carriers driven by local lipid metabolism: a theoretical model. Biophys J 85 (2003) 3813-27.

[39]N.W. Andrews, Regulated secretion of conventional lysosomes. Trends Cell Biol 10 (2000) 316-21.

[40]J.K. Jaiswal, N.W. Andrews, and S.M. Simon, Membrane proximal lysosomes are the major vesicles responsible for calcium-dependent exocytosis in nonsecretory cells. J Cell Biol 159 (2002) 625-35.

[41]A. Reddy, E.V. Caler, and N.W. Andrews, Plasma membrane repair is mediated by Ca(2+)-regulated exocytosis of lysosomes. Cell 106 (2001) 157-69.

[42]P.L. McNeil, Repairing a torn cell surface: make way, lysosomes to the rescue. J Cell Sci 115 (2002) 873-9.

[43]S.K. Rao, C. Huynh, V. Proux-Gillardeaux, T. Galli, and N.W. Andrews, Identification of SNAREs involved in synaptotagmin VII-regulated lysosomal exocytosis. J Biol Chem 279 (2004) 20471-9.

[44]N.W. Andrews, Membrane resealing: synaptotagmin VII keeps running the show. Sci STKE 2005 (2005) pe19.

[45]I. Martinez, S. Chakrabarti, T. Hellevik, J. Morehead, K. Fowler, and N.W. Andrews, Synaptotagmin VII regulates Ca(2+)-dependent exocytosis of lysosomes in fibroblasts. J Cell Biol 148 (2000) 1141-49.

[46]E.J. Blott, and G.M. Griffiths, Secretory lysosomes. Nat Rev Mol Cell Biol 3 (2002) 122-31.

[47]T. Kawakami, and S.J. Galli, Regulation of mast-cell and basophil function and survival by IgE. Nat Rev Immunol 2 (2002) 773-86.

[48]S.A. Tooze, Biogenesis of secretory granules in the trans-Golgi network of neuroendocrine and endocrine cells. Biochim Biophys Acta 1404 (1998) 231-44.

[49]N.A. Bright, B.J. Reaves, B.M. Mullock, and J.P. Luzio, Dense core lysosomes can fuse with late endosomes and are re-formed from the resultant hybrid organelles. J Cell Sci 110 (Pt 17) (1997) 2027-40.

[50]K.S. Carroll, J. Hanna, I. Simon, J. Krise, P. Barbero, and S.R. Pfeffer, Role of Rab9 GTPase in facilitating receptor recruitment by TIP47. Science 292 (2001) 1373-6.

[51]S.R. Pfeffer, Membrane transport: retromer to the rescue. Curr Biol 11 (2001) R109-11.

[52]A.M. Kaufmann, A.J. Toro-Ramos, and J.P. Krise, Assessment of Golgi Apparatus versus Plasma Membrane-Localized Multi-Drug Resistance-Associated Protein 1. Mol Pharm (2008).

[53]B.E. Linebaugh, M. Sameni, N.A. Day, B.F. Sloane, and D. Keppler, Exocytosis of active cathepsin B enzyme activity at pH 7.0, inhibition and molecular mass. Eur J Biochem 264 (1999) 100-9.

[54]T. Yuasa, M. Fukuma, S. Takashima, and R. Takaki, Cultured skin fibroblasts in lipidoses. Enzymatic, histochemical, and ultrastructural relationship in Fabry's Tay-Sachs, and Sandhoff's diseases. Arch Pathol Lab Med 104 (1980) 321-7.

[55]P.A. Bolhuis, J.G. Oonk, P.E. Kamp, A.J. Ris, J.C. Michalski, B. Overdijk, and A.J. Reuser, Ganglioside storage, hexosaminidase lability, and urinary oligosaccharides in adult Sandhoff's disease. Neurology 37 (1987) 75-81.

[56]S.R. Cheruku, Z. Xu, R. Dutia, P. Lobel, and J. Storch, Mechanism of cholesterol transfer from the Niemann-Pick type C2 protein to model membranes supports a role in lysosomal cholesterol transport. J Biol Chem 281 (2006) 31594-604.

[57]M.T. Vanier, and G. Millat, Structure and function of the NPC2 protein. Biochim Biophys Acta 1685 (2004) 14-21.

[58]F.M. Platt, and M. Jeyakumar, Substrate reduction therapy. Acta Paediatr Suppl 97 (2008) 88-93.

[59]D.J. Begley, C.C. Pontikis, and M. Scarpa, Lysosomal storage diseases and the blood-brain barrier. Curr Pharm Des 14 (2008) 1566-80.

[60]C.S. Chen, G. Bach, and R.E. Pagano, Abnormal transport along the lysosomal pathway in mucolipidosis, type IV disease. Proc Natl Acad Sci U S A 95 (1998) 6373-8.

[61]L. Liscum, Niemann-Pick type C mutations cause lipid traffic jam. Traffic 1 (2000) 218-25.

[62]C. Huynh, D. Roth, D.M. Ward, J. Kaplan, and N.W. Andrews, Defective lysosomal exocytosis and plasma membrane repair in Chediak-Higashi/beige cells. Proc Natl Acad Sci U S A 101 (2004) 16795-800.

[63]R. Clark, and G.M. Griffiths, Lytic granules, secretory lysosomes and disease. Curr Opin Immunol 15 (2003) 516-21.

[64]Y. Gong, M. Duvvuri, M.B. Duncan, J. Liu, and J.P. Krise, Niemann-Pick C1 protein facilitates the efflux of the anticancer drug daunorubicin from cells according to a novel vesicle-mediated pathway. J Pharmacol Exp Ther 316 (2006) 242-7.

[65]E.B. Neufeld, M. Wastney, S. Patel, S. Suresh, A.M. Cooney, N.K. Dwyer, C.F. Roff, K. Ohno, J.A. Morris, E.D. Carstea, J.P. Incardona, J.F. Strauss, 3rd, M.T. Vanier, M.C. Patterson, R.O. Brady, P.G. Pentchev, and E.J. Blanchette-Mackie, The Niemann-Pick C1 protein resides in a vesicular compartment linked to retrograde transport of multiple lysosomal cargo. J Biol Chem 274 (1999) 9627-35.

[66]S.L. Sturley, M.C. Patterson, W. Balch, and L. Liscum, The pathophysiology and mechanisms of NP-C disease. Biochim Biophys Acta 1685 (2004) 83-7.

[67]P.G. Pentchev, Niemann-Pick C research from mouse to gene. Biochim Biophys Acta 1685 (2004) 3-7.

[68]J. Sarna, S.R. Miranda, E.H. Schuchman, and R. Hawkes, Patterned cerebellar Purkinje cell death in a transgenic mouse model of Niemann Pick type A/B disease. Eur J Neurosci 13 (2001) 1873-80.

[69]W.S. Garver, and R.A. Heidenreich, The Niemann-Pick C proteins and trafficking of cholesterol through the late endosomal/lysosomal system. Curr Mol Med 2 (2002) 485-505.

[70]S. Mukherjee, and F.R. Maxfield, Lipid and cholesterol trafficking in NPC. Biochim Biophys Acta 1685 (2004) 28-37.

[71]P.G. Pentchev, H.S. Kruth, M.E. Comly, J.D. Butler, M.T. Vanier, D.A. Wenger, and S. Patel, Type C Niemann-Pick disease. A parallel loss of regulatory responses in both the uptake and esterification of low density lipoprotein-derived cholesterol in cultured fibroblasts. J Biol Chem 261 (1986) 16775-80.

[72]L. Liscum, and J.J. Klansek, Niemann-Pick disease type C. Curr Opin Lipidol 9 (1998) 131-5.

[73]E.D. Carstea, J.A. Morris, K.G. Coleman, S.K. Loftus, D. Zhang, C. Cummings, J. Gu, M.A. Rosenfeld, W.J. Pavan, D.B. Krizman, J. Nagle, M.H. Polymeropoulos, S.L. Sturley, Y.A. Ioannou, M.E. Higgins, M. Comly, A. Cooney, A. Brown, C.R. Kaneski, E.J. Blanchette-Mackie, N.K. Dwyer, E.B. Neufeld, T.Y. Chang, L. Liscum, J.F. Strauss, 3rd, K. Ohno, M. Zeigler, R. Carmi, J. Sokol, D. Markie, R.R. O'Neill, O.P. van Diggelen, M. Elleder, M.C. Patterson, R.O. Brady, M.T. Vanier, P.G. Pentchev, and D.A. Tagle, Niemann-Pick C1 disease gene: homology to mediators of cholesterol homeostasis. Science 277 (1997) 228-31.

[74]M.E. Gelsthorpe, N. Baumann, E. Millard, S.E. Gale, S.J. Langmade, J.E. Schaffer, and D.S. Ory, Niemann-Pick type C1 I1061T mutant encodes a functional protein that is selected for endoplasmic reticulum-associated degradation due to protein misfolding. J Biol Chem 283 (2008) 8229-36.

[75]C. Scott, and Y.A. Ioannou, The NPC1 protein: structure implies function. Biochim Biophys Acta 1685 (2004) 8-13.

[76]K.A. Josephs, J.Y. Matsumoto, and N.M. Lindor, Heterozygous Niemann-Pick disease type C presenting with tremor. Neurology 63 (2004) 2189-90.

[77]D.C. Ko, L. Milenkovic, S.M. Beier, H. Manuel, J. Buchanan, and M.P. Scott, Cell-autonomous death of cerebellar purkinje neurons with autophagy in Niemann-Pick type C disease. PLoS Genet 1 (2005) 81-95.

[78]J.R. Sarna, M. Larouche, H. Marzban, R.V. Sillitoe, D.E. Rancourt, and R. Hawkes, Patterned Purkinje cell degeneration in mouse models of Niemann-Pick type C disease. J Comp Neurol 456 (2003) 279-91.

[79]G. Yadid, I. Sotnik-Barkai, C. Tornatore, B. Baker-Cairns, J. Harvey-White, P.G. Pentchev, and E. Goldin, Neurochemical alterations in the cerebellum of a murine model of Niemann-Pick type C disease. Brain Res 799 (1998) 250-6.

[80]P.A. March, M.A. Thrall, D.E. Brown, T.W. Mitchell, A.C. Lowenthal, and S.U. Walkley, GABAergic neuroaxonal dystrophy and other cytopathological alterations in feline Niemann-Pick disease type C. Acta Neuropathologica 94 (1997) 164-172.

[81]H. Watari, E.J. Blanchette-Mackie, N.K. Dwyer, M. Watari, E.B. Neufeld, S. Patel, P.G. Pentchev, and J.F. Strauss, 3rd, Mutations in the leucine zipper motif and sterol-sensing domain inactivate the Niemann-Pick C1 glycoprotein. J Biol Chem 274 (1999) 21861-6.

[82]J.P. Davies, and Y.A. Ioannou, Topological analysis of Niemann-Pick C1 protein reveals that the membrane orientation of the putative sterol-sensing domain is identical to those of 3-hydroxy-3-methylglutaryl-CoA

reductase and sterol regulatory element binding protein cleavage-activating protein. J Biol Chem 275 (2000) 24367-74.

[83]C. Scott, M.E. Higgins, J.P. Davies, and Y.A. Ioannou, Targeting of NPC1 to late endosomes involves multiple signals, including one residing within the putative sterol-sensing domain. J Biol Chem 279 (2004) 48214-23.

[84]M. Boonen, R. RezendeÂ deÂ castro, G.I. Cuvelier, I. Hamer, and M. Jadot, A dileucine signal situated in the C-terminal tail of the lysosomal membrane protein p40 is responsible for its targeting to lysosomes. Biochem J 414 (2008) 431-440.

[85]W.S. Garver, R.A. Heidenreich, R.P. Erickson, M.A. Thomas, and J.M. Wilson, Localization of the murine Niemann-Pick C1 protein to two distinct intracellular compartments. J Lipid Res 41 (2000) 673-87.

[86]X. Hua, A. Nohturfft, J.L. Goldstein, and M.S. Brown, Sterol resistance in CHO cells traced to point mutation in SREBP cleavage-activating protein. Cell 87 (1996) 415-26.

[87]Y.A. Ioannou, The structure and function of the Niemann-Pick C1 protein. Mol Genet Metab 71 (2000) 175-81.

[88]E.E. Millard, S.E. Gale, N. Dudley, J. Zhang, J.E. Schaffer, and D.S. Ory, The sterol-sensing domain of the Niemann-Pick C1 (NPC1) protein regulates trafficking of low density lipoprotein cholesterol. J Biol Chem 280 (2005) 28581-90.

[89]J.P. Davies, F.W. Chen, and Y.A. Ioannou, Transmembrane molecular pump activity of Niemann-Pick C1 protein. Science 290 (2000) 2295-8.

[90]N. Gotoh, T. Kusumi, H. Tsujimoto, T. Wada, and T. Nishino, Topological analysis of an RND family transporter, MexD of Pseudomonas aeruginosa. FEBS Lett 458 (1999) 32-36.

[91]H. Nikaido, M. Basina, V. Nguyen, and E.Y. Rosenberg, Multidrug efflux pump AcrAB of Salmonella typhimurium excretes only those beta-lactam antibiotics containing lipophilic side chains. J Bacteriol 180 (1998) 4686-92.

[92]D.G. Thanassi, L.W. Cheng, and H. Nikaido, Active efflux of bile salts by Escherichia coli. J Bacteriol 179 (1997) 2512-8.

[93]N. Ohgami, D.C. Ko, M. Thomas, M.P. Scott, C.C. Chang, and T.Y. Chang, Binding between the Niemann-Pick C1 protein and a photoactivatable cholesterol analog requires a functional sterol-sensing domain. Proc Natl Acad Sci U S A 101 (2004) 12473-8.

[94]R.E. Infante, L. Abi-Mosleh, A. Radhakrishnan, J.D. Dale, M.S. Brown, and J.L. Goldstein, Purified NPC1 Protein: I. BINDING OF CHOLESTEROL AND OXYSTEROLS TO A 1278-AMINO ACID MEMBRANE PROTEIN. J. Biol. Chem. 283 (2008) 1052-1063.

[95]Y. Liu, Y.P. Wu, R. Wada, E.B. Neufeld, K.A. Mullin, A.C. Howard, P.G. Pentchev, M.T. Vanier, K. Suzuki, and R.L. Proia, Alleviation of neuronal ganglioside storage does not improve the clinical course of the Niemann-Pick C disease mouse. Hum Mol Genet 9 (2000) 1087-92.

[96]K.L. Somers, D.E. Brown, R. Fulton, P.C. Schultheiss, D. Hamar, M.O. Smith, R. Allison, H.E. Connally, C. Just, T.W. Mitchell, D.A. Wenger, and M.A.

Thrall, Effects of dietary cholesterol restriction in a feline model of Niemann-Pick type C disease. J Inherit Metab Dis 24 (2001) 427-36.

[97]R.P. Erickson, W.S. Garver, F. Camargo, G.S. Hossain, and R.A. Heidenreich, Pharmacological and genetic modifications of somatic cholesterol do not substantially alter the course of CNS disease in Niemann-Pick C mice. J Inherit Metab Dis 23 (2000) 54-62.

[98]Y. Chen, M. Schindler, and S.M. Simon, A mechanism for tamoxifen-mediated inhibition of acidification. J Biol Chem 274 (1999) 18364-73.

[99]A.M. Kaufmann, and J.P. Krise, Lysosomal sequestration of amine-containing drugs: Analysis and therapeutic implications. J Pharm Sci 96 (2007) 729-46.

[100]S. Ohkuma, and B. Poole, Cytoplasmic vacuolation of mouse peritoneal macrophages and the uptake into lysosomes of weakly basic substances. J Cell Biol 90 (1981) 656-64.

[101]G. Morissette, E. Moreau, C.G. R, and F. Marceau, Massive cell vacuolization induced by organic amines such as procainamide. J Pharmacol Exp Ther 310 (2004) 395-406.

[102]C. de Duve, T. de Barsy, B. Poole, A. Trouet, P. Tulkens, and F. Van Hoof, Commentary. Lysosomotropic agents. Biochem Pharmacol 23 (1974) 2495-531.

[103]Y. Gong, M. Duvvuri, and J.P. Krise, Separate roles for the Golgi apparatus and lysosomes in the sequestration of drugs in the multidrug-resistant human leukemic cell line HL-60. J Biol Chem 278 (2003) 50234-9.

[104]B. Poole, and S. Ohkuma, Effect of weak bases on the intralysosomal pH in mouse peritoneal macrophages. J Cell Biol 90 (1981) 665-9.

[105]M. Duvvuri, S. Konkar, R.S. Funk, J.M. Krise, and J.P. Krise, A chemical strategy to manipulate the intracellular localization of drugs in resistant cancer cells. Biochemistry 44 (2005) 15743-9.

[106]A. Bulychev, A. Trouet, and P. Tulkens, Uptake and intracellular distribution of neutral red in cultured fibroblasts. Exp Cell Res 115 (1978) 343-55.

[107]B.A. Davis, Biogenic amines and their metabolites in body fluids of normal, psychiatric and neurological subjects. J Chromatogr 466 (1989) 89-218.

[108]T. Masuko, K. Kusama-Eguchi, K. Sakata, T. Kusama, S. Chaki, S. Okuyama, K. Williams, K. Kashiwagi, and K. Igarashi, Polyamine transport, accumulation, and release in brain. J Neurochem 84 (2003) 610-7.

[109]H. Dai, D.L. Kramer, C. Yang, K.G. Murti, C.W. Porter, and J.L. Cleveland, The polyamine oxidase inhibitor MDL-72,527 selectively induces apoptosis of transformed hematopoietic cells through lysosomotropic effects. Cancer Res 59 (1999) 4944-54.

[110]D. Soulet, B. Gagnon, S. Rivest, M. Audette, and R. Poulin, A fluorescent probe of polyamine transport accumulates into intracellular acidic vesicles via a two-step mechanism. J Biol Chem 279 (2004) 49355-66.

[111]P.M. Cullis, R.E. Green, L. Merson-Davies, and N. Travis, Probing the mechanism of transport and compartmentalisation of polyamines in mammalian cells. Chem Biol 6 (1999) 717-29.

[112]D. Balasundaram, and A.K. Tyagi, Polyamine--DNA nexus: structural ramifications and biological implications. Mol Cell Biochem 100 (1991) 129-40.

[113]A.U. Khan, P. Di Mascio, M.H. Medeiros, and T. Wilson, Spermine and spermidine protection of plasmid DNA against single-strand breaks induced by singlet oxygen. Proc Natl Acad Sci U S A 89 (1992) 11428-30.

[114]A.U. Khan, Y.H. Mei, and T. Wilson, A proposed function for spermine and spermidine: protection of replicating DNA against damage by singlet oxygen. Proc Natl Acad Sci U S A 89 (1992) 11426-7.

[115]K. Igarashi, and K. Kashiwagi, Polyamines: mysterious modulators of cellular functions. Biochem Biophys Res Commun 271 (2000) 559-64.

[116]E.W. Gerner, and F.L. Meyskens, Jr., Polyamines and cancer: old molecules, new understanding. Nat Rev Cancer 4 (2004) 781-92.

[117]J.C. Allen, C.J. Smith, J.I. Hussain, J.M. Thomas, and J.M. Gaugas, Inhibition of lymphocyte proliferation by polyamines requires ruminant-plasma polyamine oxidase. Eur J Biochem 102 (1979) 153-8.

[118]R.G. Schipper, L.C. Penning, and A.A. Verhofstad, Involvement of polyamines in apoptosis. Facts and controversies: effectors or protectors? Semin Cancer Biol 10 (2000) 55-68.

[119]X. Xie, M.E. Tome, and E.W. Gerner, Loss of intracellular putrescine pool-size regulation induces apoptosis. Exp Cell Res 230 (1997) 386-92.

[120]R. Poulin, G. Pelletier, and A.E. Pegg, Induction of apoptosis by excessive polyamine accumulation in ornithine decarboxylase-overproducing L1210 cells. Biochem J 311 (Pt 3) (1995) 723-7.

[121]R.E. Parchment, and G.B. Pierce, Polyamine oxidation, programmed cell death, and regulation of melanoma in the murine embryonic limb. Cancer Res 49 (1989) 6680-6.

[122]Z. Yu, W. Li, and U.T. Brunk, 3-Aminopropanal is a lysosomotropic aldehyde that causes oxidative stress and apoptosis by rupturing lysosomes. Apmis 111 (2003) 643-52.

[123]Z. Yu, W. Li, J. Hillman, and U.T. Brunk, Human neuroblastoma (SH-SY5Y) cells are highly sensitive to the lysosomotropic aldehyde 3-aminopropanal. Brain Res 1016 (2004) 163-9.

[124]P.L. Wood, M.A. Khan, and J.R. Moskal, The concept of "aldehyde load" in neurodegenerative mechanisms: cytotoxicity of the polyamine degradation products hydrogen peroxide, acrolein, 3-aminopropanal, 3-acetamidopropanal and 4-aminobutanal in a retinal ganglion cell line. Brain Res 1145 (2007) 150-6.

[125]J.O. Fredlund, and S.M. Oredsson, Impairment of DNA replication within one cell cycle after seeding of cells in the presence of a polyamine-biosynthesis inhibitor. Eur J Biochem 237 (1996) 539-44.

[126]H.S. Basu, M.C. Sturkenboom, J.G. Delcros, P.P. Csokan, J. Szollosi, B.G. Feuerstein, and L.J. Marton, Effect of polyamine depletion on chromatin

structure in U-87 MG human brain tumour cells. Biochem J 282 (Pt 3) (1992) 723-7.

[127]T.G. Ohm, S. Treiber-Held, R. Distl, F. Glockner, B. Schonheit, M. Tamanai, and V. Meske, Cholesterol and tau protein--findings in Alzheimer's and Niemann Pick C's disease. Pharmacopsychiatry 36 Suppl 2 (2003) S120-6.

[128]H.G. Bernstein, and M. Muller, The cellular localization of the L-ornithine decarboxylase/polyamine system in normal and diseased central nervous systems. Prog Neurobiol 57 (1999) 485-505.

[129]L.D. Morrison, and S.J. Kish, Brain polyamine levels are altered in Alzheimer's disease. Neurosci Lett 197 (1995) 5-8.

[130]M. Virgili, C. Crochemore, E. Pena-Altamira, and A. Contestabile, Regional and temporal alterations of ODC/polyamine system during ALS-like neurodegenerative motor syndrome in G93A transgenic mice. Neurochem Int 48 (2006) 201-7.

Chapter 2

Evaluating the role of NPC1 in amine-induced vacuolization of lysosomes

2.1. Introduction

It has been demonstrated repeatedly that the administration of certain weakly basic compounds to cells in culture results in the formation of large vacuoles of lysosomal origin that are visible by conventional light microscopy. These vacuoles are known to form due to the hyperaccumulation of weak bases, also known as lysosomotropics, in the lysosomal lumen. The pH-partitioning type mechanism by which these weakly basic molecules enter lysosomes has been described elsewhere [1; 2] (Chapter 1). Briefly, the accumulation of weakly basic compounds in lysosomes is based on the following assumptions: 1) neutral forms of weakly basic compounds can passively diffuse through lipid bilayers such as the plasma membrane and the limiting lysosomal membrane. 2) The ionized forms of these compounds cannot, to a significant degree, diffuse back through the membranes. 3) There exists a pH gradient between the cytosol and lysosome, in which the pH of the lysosome is considerably lower [3; 4; 5]. As a consequence, the formation of a weak base concentration gradient between lysosomes and the cytosol will occur.

In 1981, Okhuma and Poole suggested that the presence of a weak base concentration gradient between lysosomes and cytosol would result in osmotic stress being applied to the lysosome membrane [6]. Ultimately, they proposed that an influx of water into the lysosome occurs to dissipate the concentration imbalance leading to increased organelle volume and the formation of a large cytoplasmic vacuole. However, several lines of evidence have suggested that

osmotic stretching of lysosome membranes to facilitate organelle expansion is not a probable mechanism of amine-induced vacuolization [7; 8; 9]. Experiments using agents which inhibited microtubule networks in cells showed that vacuoles did not form after weak base administration [9]. The dependence of an intact microtubule network on the formation of amine-induced vacuoles suggests that lysosomes are recruiting membrane components (i.e. from other organelles) to facilitate organelle size increase. Furthermore, Solheim et al., compared the rates of amine clearance from cells with the time it took for the vacuolized lysosomes to return to normal size [7]. The authors argued that if vacuolization was caused by osmotic stretching, then the rate of amine depletion from lysosomes should parallel the rate of reduction in organelle size. This work had shown that complete amine depletion from cells significantly preceded the reduction in organelle size and therefore provided strong evidence supporting the requirement for membrane recruitment in the vacuolization process.

Although the basis for accumulation of weak bases has been thoroughly described, the cellular components that allow vacuolization to occur are poorly understood. Previous research in our laboratory suggested that the lysosome membrane protein Niemann-Pick C1 (NPC1) played a critical role in the uptake and clearance of weakly basic amines [10]. To expand on this area and evaluate if NPC1 was necessary for the amine-induced vacuolization of lysosomes we have evaluated the uptake and distribution of model weakly basic amines in

normal fibroblasts and fibroblasts that possess a mutated and dysfunctional form of the NPC1 protein.

2.2. Materials and methods

2.2.1. Antibodies and reagents

Anti-EEA1 (early endosomes), anti-golgin-84, and anti-GM130 (Golgi apparatus) mouse monoclonal antibodies were obtained from BD Biosciences (San Jose, CA). Mouse monoclonal anti-mannose 6-phosphate receptor (MPR, late endosomes) and β-actin antibodies were obtained from Abcam (Cambridge, MA). Mouse monoclonal anti-LAMP-1 (lysosomes) antibody was purchased from Developmental Studies Hybridoma (Iowa City, IA). Rabbit polyclonal anti-NPC1 antibody was obtained from Novus Biologicals (Littleton, CO). Alexa Fluor 647 dextran and goat anti-mouse and anti-rabbit secondary antibodies, biotinylated dextran amine, and Alexa Fluor 555 and 647 succinimidyl esters were obtained from Invitrogen (Eugene, OR). Carboxylate-modified polystyrene beads were purchased from Polysciences (Warrington, PA). siRNA specific to NPC1 was custom synthesized by Ambion (Austin, TX). NPC1-GFP and Rab9-YFP plasmid DNA were kindly provided by Dr. Matthew Scott and Dr. Suzanne Pfeffer of Stanford University School of Medicine (Stanford, CA). Transfection reagents for siRNA (siPORT-amine) and plasmid DNA (FuGene6) were purchased from Ambion and Roche (La Jolla, CA) respectively. All other materials, unless otherwise stated, were acquired from Sigma-Aldrich.

2.2.2. Cell culture and conditions

Normal human fibroblasts (CRL-2076, designated $NPC1^{+/+}$) were cultured according to Coriell Cell Repository's (Camden, NJ) suggestions. Niemann-Pick

Type C disease (NP-C) fibroblasts were obtained through ATCC. These fibroblasts possess a mutated *npc1* gene coding for two amino acid substitutions (P237S and I1061T) which results in a dysfunctional NPC1 protein (GM-03123, designated $NPC1^{-/-}$) [11]. $NPC1^{-/-}$, mucolipidosis type IV (GM-02408, designated MLIV), and Sandhoff's disease (GM-11707) fibroblasts were all cultured according to ATCC (Manassas, VA) instructions. All media was supplemented with 10% FBS and 1% penicillin/streptomycin. Cultures were maintained at 37°C in a humidified 5% carbon dioxide atmosphere. For all experiments, cells were used before passage 5 and plated 24 hrs prior to evaluations to permit adherence.

2.2.3. Western blot analysis and densitometry

Western blots were performed as previously described in our laboratory [12]. First, post-nuclear supernatant (PNS) proteins were separated by SDS-PAGE using 7.5% bis-acrylamide gels. Proteins were then transferred to 0.45 μm nitrocellulose membranes for 2 hrs at 100V for every sample except those identifying MPR expression which were transferred for 3 hrs. Membranes were blocked overnight at 4°C with 5% milk in Tris-buffered saline (TBS) supplemented with 0.5% Tween-20 at pH 7.4. Primary antibodies specific to proteins of interest were incubated in 5% milk in TBS for 2 hrs. β-actin primary antibodies were included to control for protein loading (all primary antibodies were diluted 1:250 in 5% milk-in-TBS). Secondary HRP-conjugated antibodies at 1:1000 dilutions in 5% milk in TBS were subsequently incubated for 2 hrs.

Enhanced chemiluminescence (ECL) reagents were used to illuminate protein bands which were visualized by exposure to Kodak Biomax film. All steps were performed at room temperature unless otherwise stated.

For densitometry, exposed films were scanned and converted into greyscale JPEG images. Using ImageJ software, images were corrected for background (Analyze>Calibrate>Function>Uncalibrated OD). Next, bands were selected by drawing a rectangle encompassing the band and selected as the first band (Analyze>Gels>Select First Lane). These bands were then plotted (Analyze>Gels>Plot lanes) and the area under the curve measured. This procedure was then repeated for each band of interest. For comparison between samples, band areas were normalized to their respective actin band for each lane and expressed as a percentage.

2.2.4. Amine-induced vacuole size determinations

A confocal microscopy method was developed to obtain average diameters of NR-containing compartments. Briefly, cells were treated with 50 μM nocodazole (NOC) for 1 h, washed with PBS (3X) and then exposed to 70 μM neutral red (NR) in culture medium for 6 hrs. Cells without NOC pretreatment were included as positive controls for NR-induced vacuolization. Fibroblast monolayers were viewed with a Zeiss Meta 510 confocal microscope equipped with an argon laser set at 458 nm for transmission. Images were captured with a Hamamatsu Orca ER camera using identical magnification settings for each

image. For size determination, NR-containing compartments were measured using the line and measure area functions in MetaMorph software version 7.0 from Universal Imaging Corporation (Downington, PA). The diameters of 150 NR-containing vesicles from 3 separate experiments were averaged.

2.2.5. Silencing of NPC1 protein expression using siRNA

An siRNA construct was utilized to silence NPC1 expression as previously reported [13]. NPC1 was targeted using siRNA against the following mRNA sequence: CCAGGTTCTTGACTTACAA. Non-specific scrambled siRNA (Ambion Austin, TX) was used as a negative control under identical transfection conditions per the manufacturer's suggestions. All siRNA transfections were performed using the siPORT-amine transfection reagent (Ambion) for 72 hrs. To confirm NPC1 knockdown, cells were harvested post-transfection and lysates subjected to Western blot analysis. Relative band intensities of NPC1 were determined using densitometry with ImageJ software. For siRNA experiments requiring subsequent amine exposure, transfections were performed as described, at which point cells were exposed to 70 μM NR or 100 μM chloroquine for 6 hrs.

2.2.6. Immunofluorescence

Cells were seeded in 8-well culture slides at 50,000 cells per well the day before experimentation to allow for adherence. Fibroblasts were fixed using freshly prepared 4% paraformaldehyde in PBS for 20 mins and washed 1X with

PBS. Cells were then permeabilized using a solution of PBS containing 0.1% saponin and 10% FBS for 30 mins. Primary and secondary antibody solutions were made in 0.05% saponin and 10% FBS in PBS. Cells were incubated with primary antibodies for 2 h using the following dilutions: EEA1 (1:50); MPR (1:50); LAMP-1 (1:100); NPC1 (1:100); and GM130 (1:100). Cells were subsequently washed with PBS (3X) and secondary antibodies (Alexa Fluor 647 conjugated anti-mouse or rabbit IgG, 1:1000) were applied for 2 h. Cells were washed again with PBS (4X) prior to microscopy (Nikon Eclipse 80i). Images were acquired with a Nikon Eclipse 80i equipped with standard PlanFluor 60X epifluorescence optics and a Hamammatsu Orca ER camera. Cy5 filter sets (Nikon Cy5-HyQ, Brattleboro, VT) were employed for visualization of Alexa Fluor 647. All steps were carried out at room temperature unless otherwise noted.

2.2.7. DNA transfections

Functional NPC1-GFP and Rab9-YFP plasmid DNA [14; 15] were amplified using Novablue gigacompetent E. coli cells (Novagen-EMD Biosciences, San Diego, CA) and selected using 30 ug/mL kanamycin in lysogeny broth (0.5% yeast extract, 1.0% peptone, 1.0% sodium chloride). DNA was subsequently purified using the Midipreps system from Promega (Madison, WI). DNA was quantified by measuring absorbance at 260 nm using a Cary 100 Bio spectrophotometer. DNA to protein ratios (A_{260}/A_{280}) for purified plasmid stocks were approximately 1.8-2.0.

Transfections were performed using FuGene6 (Roche, Indianapolis, IN) per the manufacturer's suggestions. This included FuGene6 to DNA ratios of 8:2 and 3:1 for NPC1-GFP and Rab9-YFP respectively. For dual transfected cells, DNA was mixed to give appropriate ratios. Transfections were carried out for 48 hrs to allow adequate protein expression in fibroblasts. To assess the effects of amine exposure on single and dual transfected cells, 100 μM chloroquine was added post-transfection to the culture medium for 6 hrs. Microscopy was then performed using standard epifluorescence optics (Nikon) as described above. For fluorescent imaging of GFP/YFP in dually transfected cells, filter sets specific to GFP and YFP were employed (Chroma, GFP-31019 and Semrock Brightline YFP-2427A).

2.2.8. Isolation and characterization of amine-containing vacuoles

Lysosomes were isolated using a previously described magnetic chromatography approach [12; 16]. The isolation procedure, as well as control experiments, was performed as previously described with minor modifications to allow for localization of the superparamagnetic iron dextran (FeDex) in lysosomes of amine treated adherent cells. FeDex was prepared as described [16]. Briefly, fibroblasts (5×10^7) were grown to 80% confluence before incubation with 2 mg/mL FeDex for 2 hrs at 37^{o}C. Cells were then washed with warm PBS (4X) and chased in FeDex free media for 20 hrs at 37^{o}C to permit FeDex localization to lysosomes. Subsequently, FeDex containing cells were washed with ice-cold PBS (2X) and homogenized in 0.75 mL of a hypotonic

buffer containing 15 mM potassium chloride, 1.5 mM magnesium acetate, 1 mM dithiothreitol and 10 mM Hepes (pH = 7.4). This buffer was supplemented with protease inhibitors (0.1 mM phenyl-methyl sulfonyl fluoride and 1 μg/mL of aprotin, leupeptin and pepstatin) on the day of isolation. Cells were homogenized using a glass dounce homogenizer with 20 strokes to permit at least 80% cell breakage. Immediately after homogenization, 0.25 mL of a hypertonic buffer containing 375 mM potassium chloride, 22.5 mM magnesium acetate, 1 mM dithiothreitol and 220 mM Hepes (pH = 7.4) was added. The homogenate was then centrifuged at 2,000 rpm for 10 min to pellet nuclei and intact cells. The resulting post-nuclear supernatant (PNS) was then applied to a magnetic column (25-MS miniMACS, Miltenyi Biotec, Auburn, CA). The column had been previously equilibrated with a solution of bovine serum albumin (0.5%) for 10 min to discourage non-specific protein binding. After the PNS was passed through the column (flow through was kept for later analysis), 1 mL of 0.5 mg/mL DNase I was incubated in the column for 10 min. The column was then washed with 1 mL of PBS and eluted with 0.7 mL of 0.5% Triton X-100 that was incubated in the column for 10 min. To characterize the isolated fraction for purity and protein content, Western blot analysis was performed.

To confirm that FeDex was localizing in amine containing compartments, cells were incubated with 2 mg/ml Alexa Fluor 647 dextran in PBS for 2 hrs, washed with PBS (4X), and subsequently given chase in complete dextran-free medium for 20 hrs at 37^{o}C. Cells were then exposed to 100 μM CQ for 6 hrs.

Phase contrast and fluorescence images were taken and merged using MetaMorph software.

2.2.9. Sucrosome formation

Sucrosomes were formed by culturing cells in complete medium containing 0.1% sucrose for 48 hrs.

2.2.10. Late endosome-lysosome fusion assay

The fusion between late endosomes and lysosomes was evaluated in fibroblasts using a method described by Jahraus *et al*. [17] with modifications to allow quantitative assessments based on fluorescence resonance energy transfer (FRET) of late endosome/lysosome contents upon fusion. To accomplish this, biotinylated dextran, fluorescently labeled with Alexa Fluor 647 (FRET acceptor), was localized to lysosomes using the above optimized pulse/chase scheme for dextran (Section 2.2.8). Next, streptavidin-conjugated latex beads (0.792 ± 0.037 μm), fluorescently labeled with Alexa Fluor 555 (FRET donor), were localized to late endosomes for 2 hrs per Jahraus *et al.* [17]. To detect fusion, FRET measurements were made using a Photon Technologies International (Birmingham, NJ) Ratiomaster microscope-mounted spectrofluorimeter with PMT detection. Complete details on experimental design, tracer construction, control measurements and analysis can be found in Appendix I.

2.3. Results

2.3.1. Amine-induced vacuolization of lysosomes requires functional NPC1

We examined if NPC1 was involved in the amine-induced vacuolization of lysosomes. Human foreskin fibroblasts (normal or with a mutated and dysfunctional NPC1, represented by $NPC1^{+/+}$ and $NPC1^{-/-}$, respectively) were incubated with the lysosomotropic amine neutral red (NR) and high resolution images of cells were taken with a confocal microscope to examine the average diameter of NR-containing compartments. Normal cells exposed to NR had an approximate vacuole size of 1.5 μm (Fig. 2.1A, B). Exposed $NPC1^{-/-}$ cells had NR-containing compartments approximately one half the size of those from $NPC1^{+/+}$ cells. $NPC1^{+/+}$ cells treated with nocodazole also had small NR-containing vacuoles. This illustrates the involvement of microtubules in vacuolization, suggesting that the membrane is not obtained, at least significantly, from internal sources such as multi-vesicular bodies.

To more specifically illustrate that amine-induced vacuolization was NPC1-dependent, we utilized a small interfering RNA (siRNA) designed to transiently suppress the expression of NPC1 in normal cells. This was confirmed experimentally in $NPC1^{+/+}$ cells by Western blot analysis (Fig. 2.2A). When performing the siRNA transfections, we were sometimes able to view, on a single image, cells that were not efficiently transfected (i.e. normal NPC1 expression) alongside those that were efficiently transfected and had depleted NPC1. Immunofluorescence staining of NPC1 allowed us to demonstrate that only cells

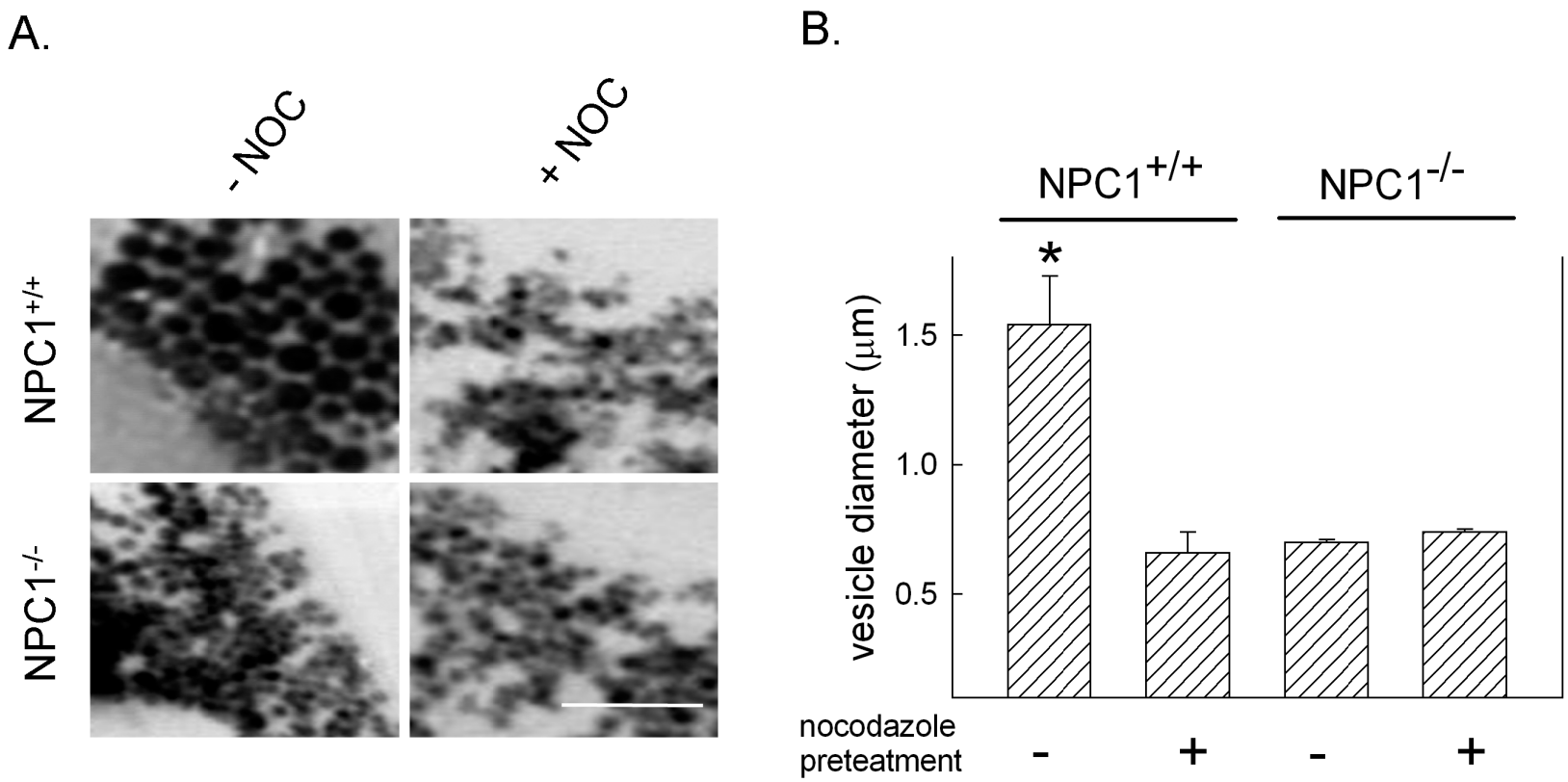

Figure 2.1. Amine-induced vacuolization requires functional NPC1 and an intact microtubule network. (A) NPC1$^{+/+}$ and NPC1$^{-/-}$ fibroblasts were treated with neutral red (NR) and imaged using confocal microscopy. NR induces vacuolization in NPC1$^{+/+}$ fibroblasts but not in NPC1$^{-/-}$ cells. Nocodazole (NOC) pre-treatment disrupts the vacuolization process in NPC1$^{+/+}$ cells. Scale bars represent 5 μm. (B) Average amine-induced vacuole diameters. NR-containing vacuoles in normal cells are approximate twice the size of NR-compartments in NPC1$^{-/-}$ fibroblasts or from fibroblasts pre-treated with NOC (*, $p < 0.01$ by unpaired t-test).

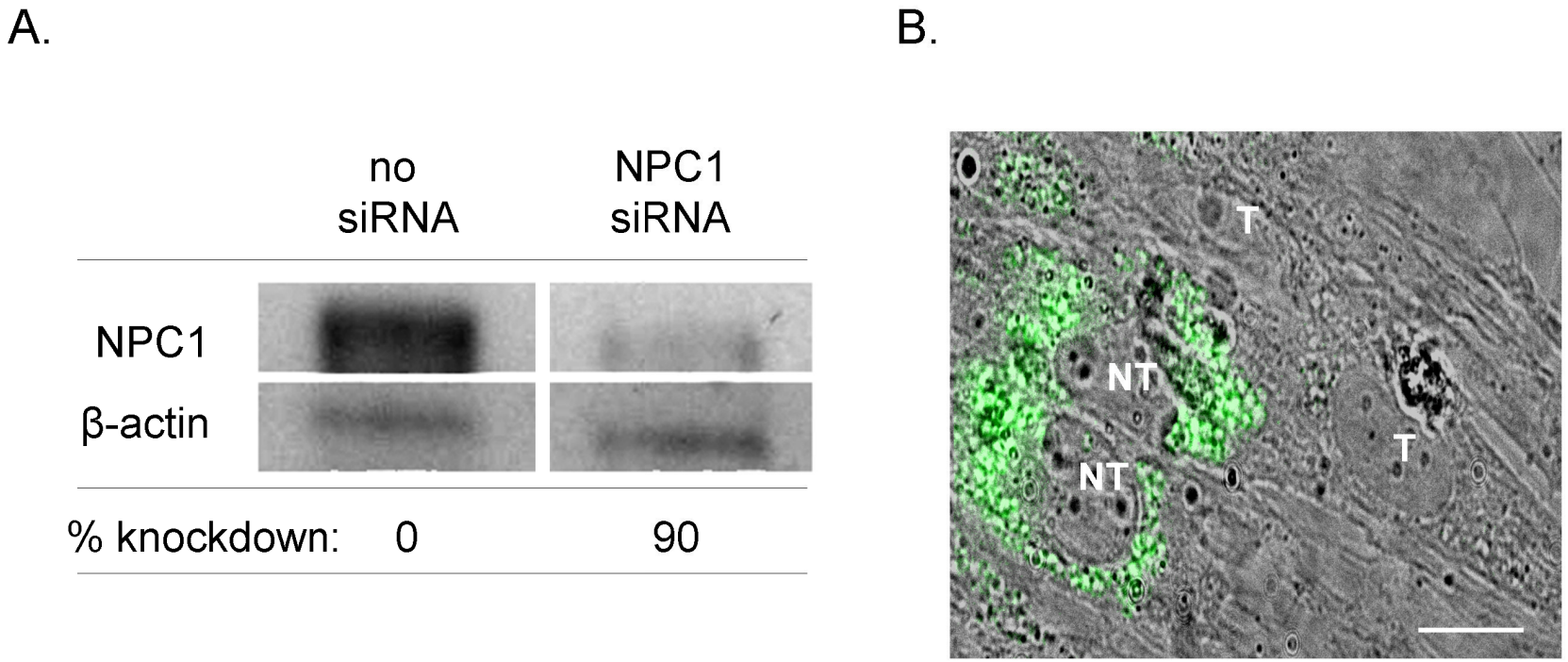

Figure 2.2. NPC1 siRNA inhibits the formation of amine induced vacuoles(A) Western blot analysis of cellular NPC1 protein levels after transfection with NPC1 specific siRNA in NPC1$^{+/+}$ cells. (B) Combined phase contrast and NPC1 immunofluorescence (green) images of NPC1$^{+/+}$ fibroblasts transfected with NPC1 siRNA and subsequently incubated with 100 μM chloroquine to induce vacuolization. Cells that did not contain NPC1 (i.e., efficiently transfected, T) did not form visible vacuoles. Cells inefficiently transfected (NT) contained NPC1 and were able to form amine-induced vacuoles. Scale bars represent 10 μm.

expressing NPC1 formed amine-induced vacuoles (Fig. 2.2B). Conversely, cells that did not have visible amounts of NPC1 did not form the amine-induced vacuoles. We were also able to rescue the amine-induced vacuolization phenotype in NPC1$^{-/-}$ fibroblasts by transfection with a functional NPC1-GFP construct (Fig. 2.3). To control for the possibility that cholesterol accumulation could be affecting the ability of lysosomes to vacuolize when exposed to NR, we utilized two more cell lines with lysosomal storage disorders, Sandhoff's disease and mucolipidosis type IV (MLIV). Both of these lysosome storage disorders result in the accumulation of multiple lipids, including cholesterol, in the lysosomal lumen as shown by cholesterol staining with filipin (Fig. 2.4A). However, both of these cell lines exhibited a normal lysosome vacuolization phenotype when compared to normal cells exposed to NR (Fig. 2.4B). Collectively, these results illustrate the requirement for NPC1 in the amine-induced vacuolization of lysosomes.

2.3.2. Amine-induced vacuoles are formed through a heterotypic fusion of lysosomes with late endosomes.

It is important to realize that amine-induced vacuolization requires the recruitment of membranes to allow lipid bilayers to expand [7]. This is consistent with our previous results that illustrated the requirement of intact microtubules in this process (Fig. 2.1). Accordingly, we sought to characterize the properties of the vacuole. Initially, we examined if amines facilitated the fusion of lysosomes with other organelles or vesicles. Immunofluorescence analysis of

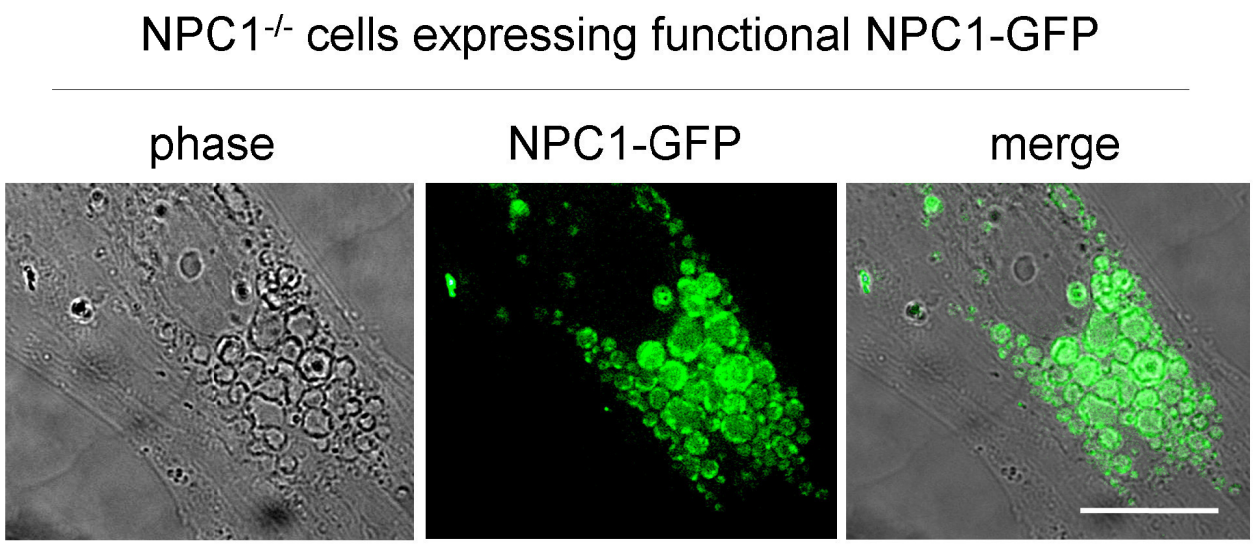

Figure 2.3. Amine-induced vacuolization phenotype can be rescued in NPC1 deficient cells. NPC1$^{-/-}$ cells were transfected with a functional NPC1-GFP plasmid and subsequently exposed to 100 μM CQ to form vacuoles. NPC1-GFP is shown in green and the scale bar represents 10 μm.

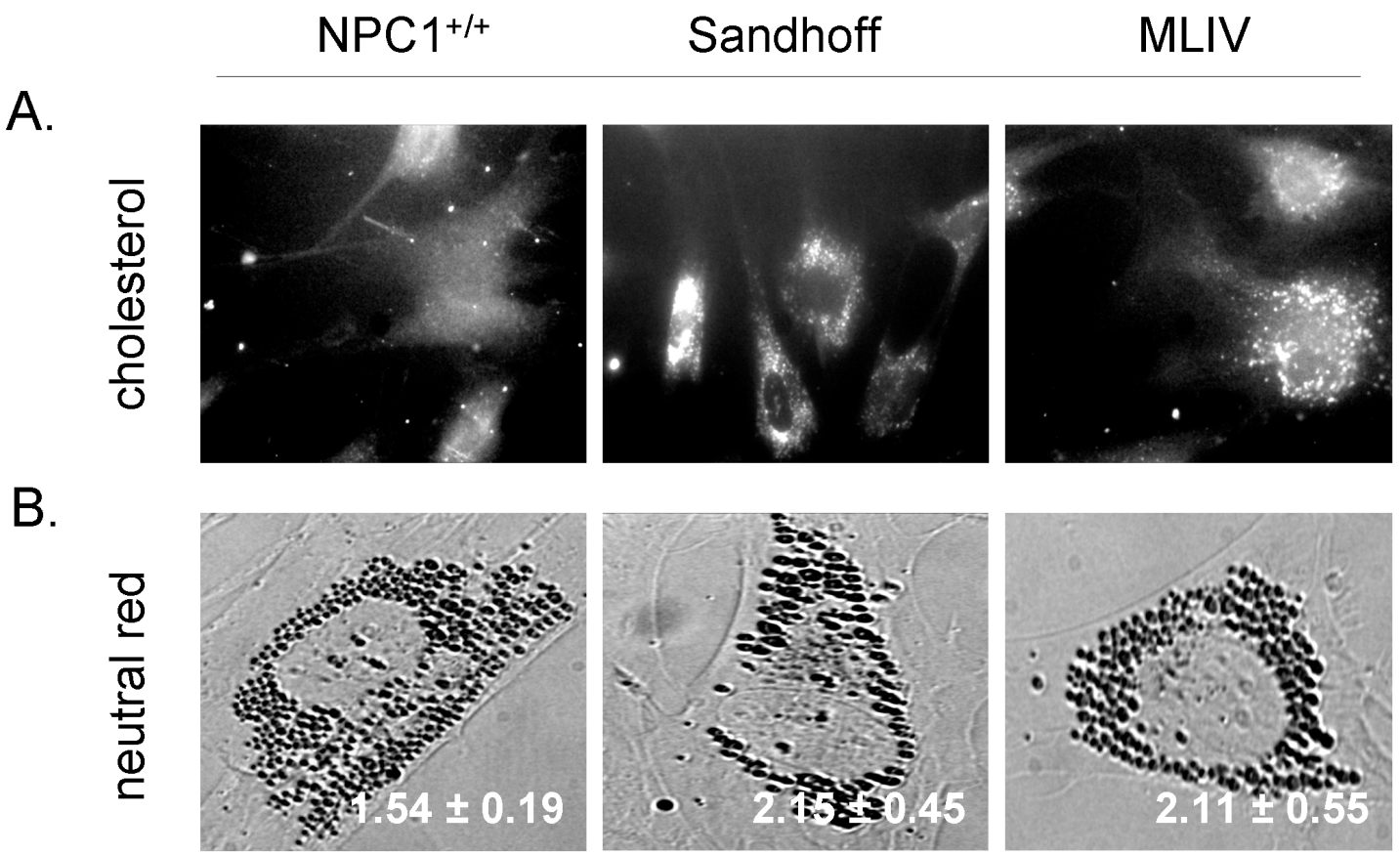

Figure 2.4. Vacuolization occurs regardless of lysosomal cholesterol accumulation. (A) Normal NPC1$^{+/+}$, Sandhoff's disease and mucolipidosis type IV (MLIV) fibroblasts were stained for free cholesterol (white) using filipin. Sandhoff and MLIV cells exhibit lysosomal staining of cholesterol. (B) NR-induced vacuolization occurs in Sandhoff's disease and MLIV fibroblasts to the same extent as in normal cells. The average diameter ± s.d. of amine-containing compartments are shown in the inset.

NPC1$^{+/+}$ fibroblasts demonstrated that without amine treatment NPC1 is shown to reside predominantly on a subset of LAMP-1 (a lysosome-specific membrane protein) positive lysosomes and not to a significant extent on late endosomes containing the cation-independent mannose 6-phosphate receptor (MPR) (Fig. 2.5). However, when NPC1$^{+/+}$ cells were treated with NR the resultant vacuoles contained LAMP-1, MPR, and the NPC1 protein (Fig. 2.6). The vacuoles did not colocalize with a Golgi-specific protein GM130 or with the early endosome antigen-1 (EEA1) an early endosome specific protein (Fig. 2.6). Importantly, the exposure of NPC1$^{-/-}$ cells to NR had no effect on LAMP-1 or MPR distribution. The two markers were found in distinct organelles pre and post-amine treatments (Fig. 2.7).

To further confirm the colocalization of late endosome markers with lysosome markers observed with immunofluorescence microscopy, organelle isolations and Western blot analysis was performed. Terminal endocytic compartments (native lysosomes and vacuoles) were purified from fibroblasts using a previously described magnetic chromatographic approach that utilizes endocytosed iron-coated dextran (FeDex, 10,000 MW) [12]. To ensure FeDex was localizing with amine-induced vacuoles using optimized pulse-chase parameters, a fluorescence-labelled dextran of the same size was incubated with cells (Fig. 2.8A). Significant fluorescence was observed in chloroquine-induced vacuoles suggesting similar behavior by FeDex. Western blot analysis revealed that in the absence of amines, the isolated compartment was highly enriched in

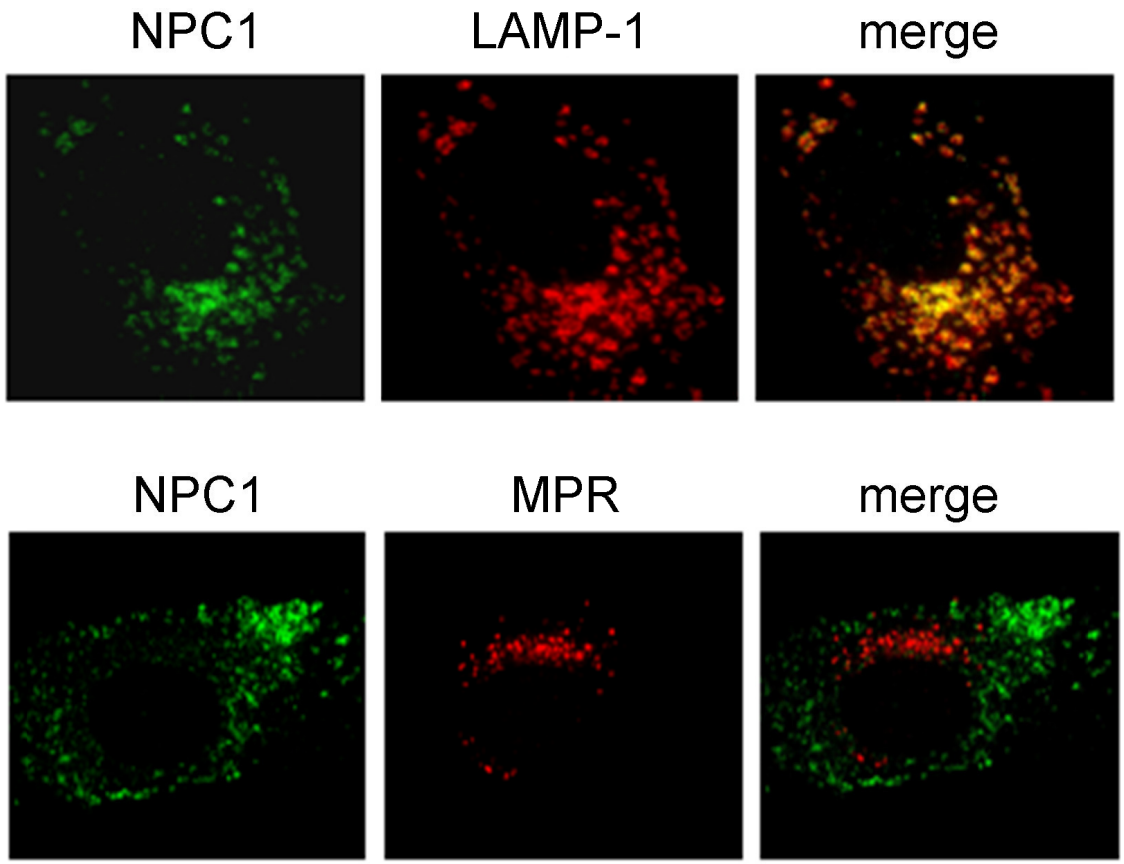

Figure 2.5. In normal cells, NPC1 localizes to lysosomes in the absence of amine treatments. Immunofluorescence images of NPC1$^{+/+}$ cells showing the intracellular localization of NPC1. NPC1 (green) does not colocalize with the late endosome-specific mannose-6-phosphate receptor (MPR, red) but does colocalize with the lysosome-associated membrane protein-1 (LAMP-1, red).

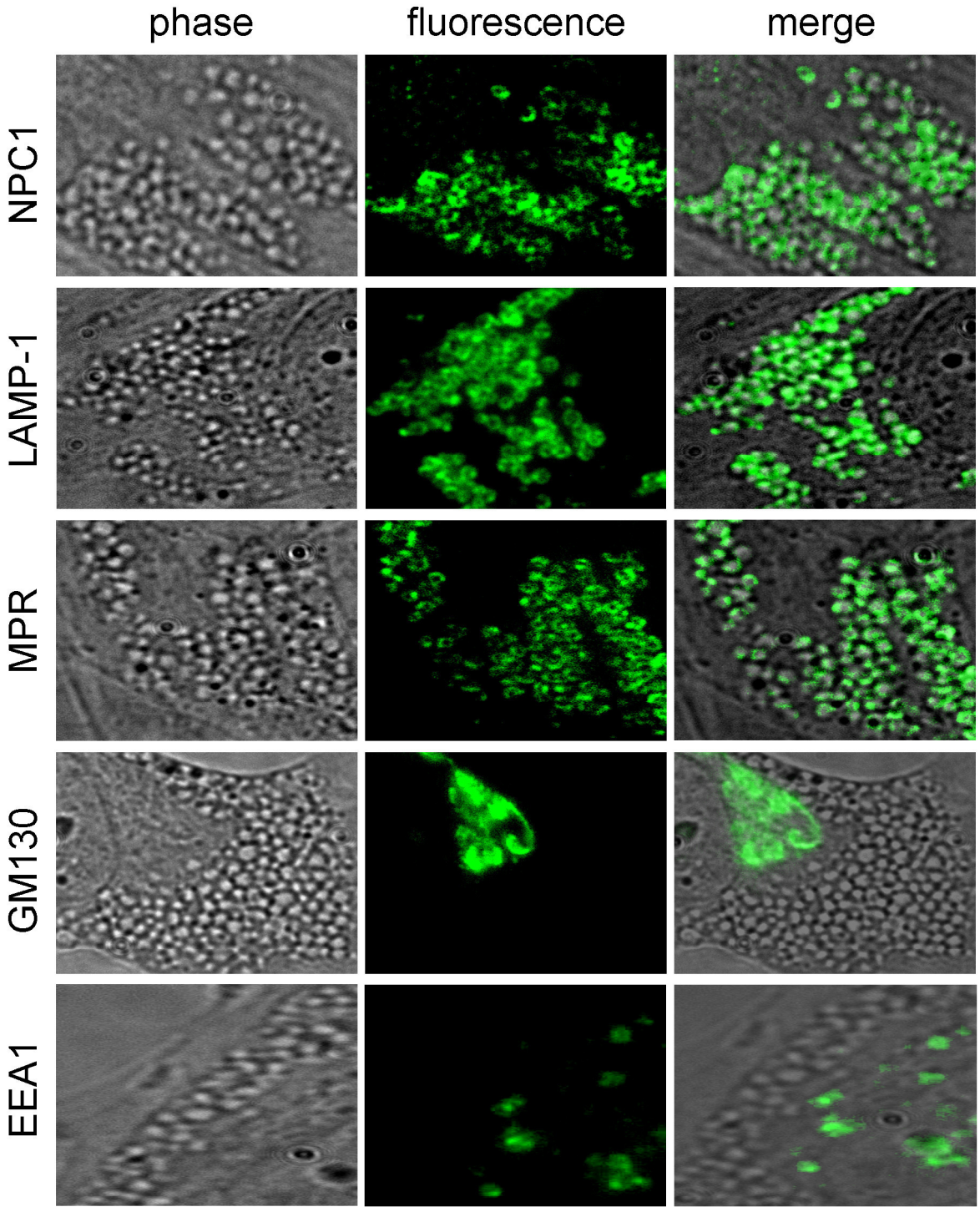

Figure 2.6. Vacuole membranes contain late endosome and lysosome proteins. Immunofluorescence and phase contrast images of NPC1$^{+/+}$ cells incubated with NR to induce vacuolization. NPC1, LAMP-1, and MPR are all localized to the membrane of the newly formed vacuoles.

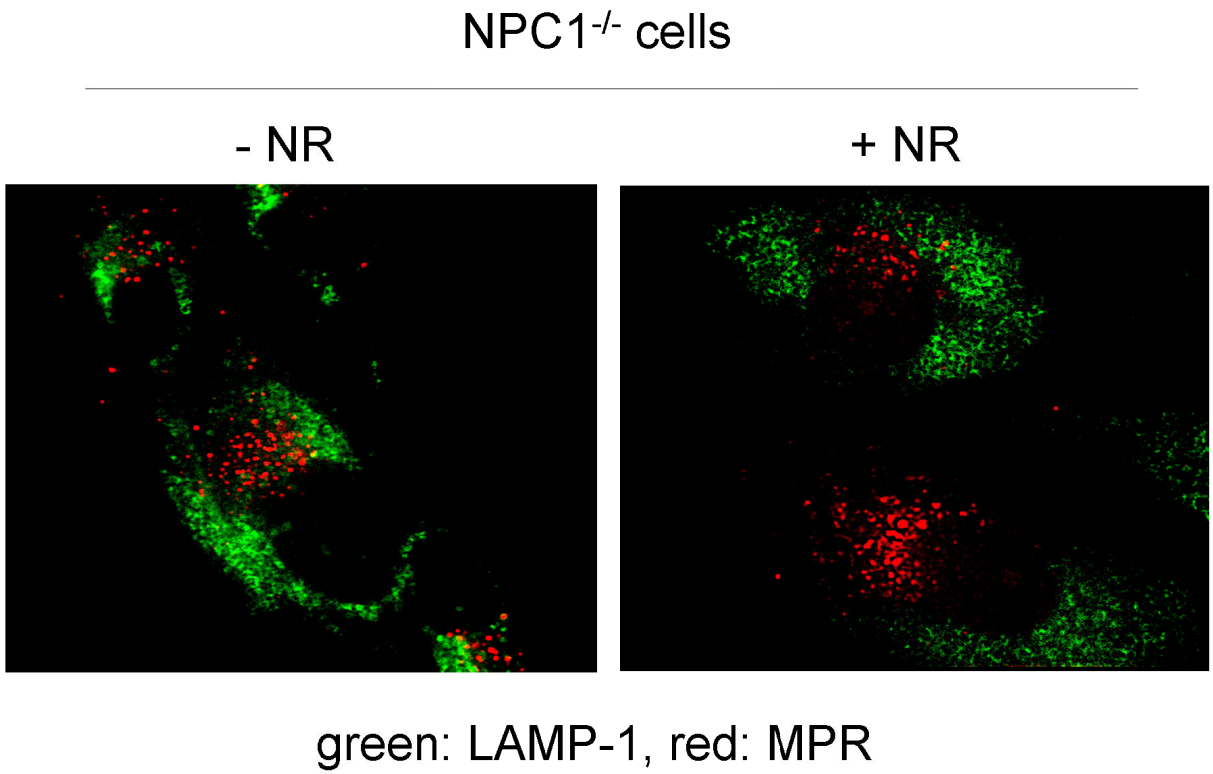

Figure 2.7. Lysosomes and late endosomes do not colocalize in NPC1$^{-/-}$ cells upon NR treatment. Merged immunofluorescence images of LAMP-1 containing lysosomes (green) and MPR containing late endosomes (red) with or without 70 μM neutral red (NR) treatment for 6 hrs in NP-C disease fibroblasts.

the lysosomal protein LAMP-1 and was not significantly contaminated with other compartments such as the Golgi (Golgin-84) or early endosomes (EEA1) (Fig. 2.8B). These protein bands were observed in post nuclear supernatant (PNS) and column flow through fractions. The isolated compartment was analyzed for the presence of MPR, which was shown to become enriched only in $NPC1^{+/+}$ and not in $NPC1^{-/-}$ fibroblasts that were treated with amines prior to the isolation (Fig. 2.8C). These results confirm previous observations using immunofluorescence microscopy (Fig. 2.6).

MPR has been shown to redistribute to other organelles in response to exogenous treatments, which might lead to the false observation of late endosome colocalization with lysosomes [18; 19]. To confirm that late endosomes were involved with vacuolization and membrane recruitment in living cells, $NPC1^{+/+}$ fibroblasts were co-transfected with Rab9-YFP, another late endosome specific protein, and with NPC1-GFP for lysosomes. Consistent with prior results, colocalization of these proteins occurred extensively on amine-induced vacuoles, although a much smaller degree of colocalization was observed in cells not incubated with the amine chloroquine (Fig. 2.9). Collectively, these findings provide strong evidence that amine-induced vacuoles are the result of lysosome and late endosome fusion.

We next evaluated whether NPC1 was required for any vacuolization event involving lysosomes or if it was specific to vacuolization induced by

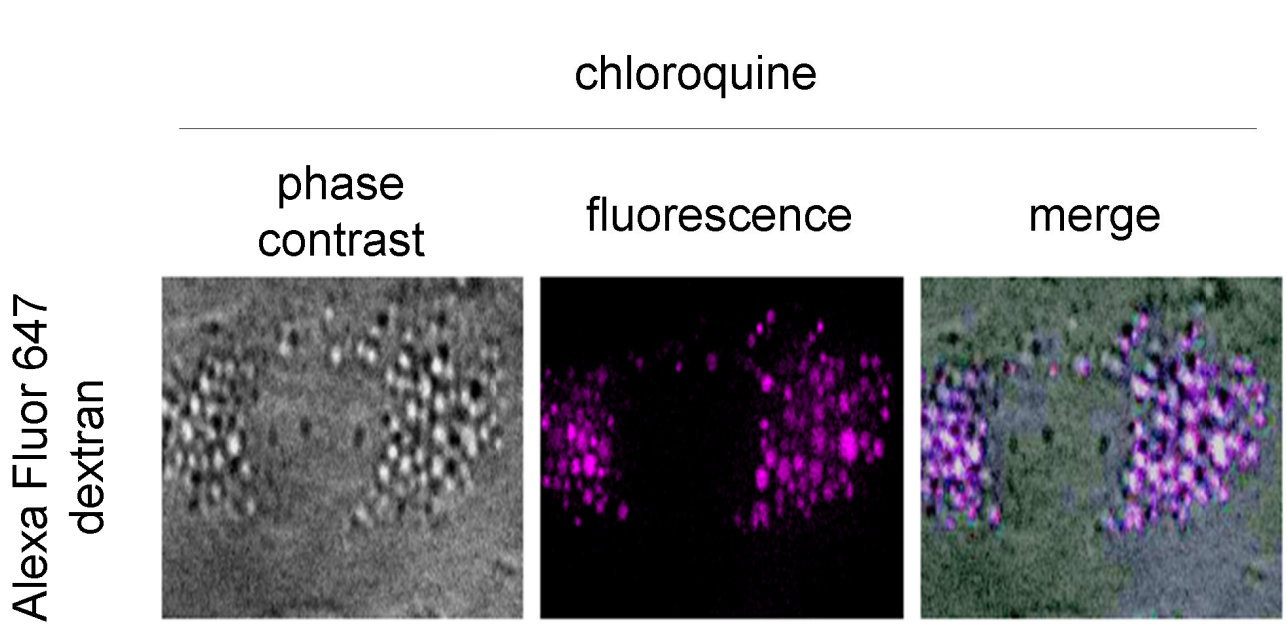

Figure 2.8. Western blot analysis reveals isolated vacuoles contain lysosome and late endosome markers. (A) Alexa Fluor 647 dextran was incubated in NPC1$^{+/+}$ cells to optimize pulse/chase conditions for isolating amine-induced vacuoles using iron dextran. To form the vacuoles, 100 μM chloroquine was added to culture medium for 6 hrs.

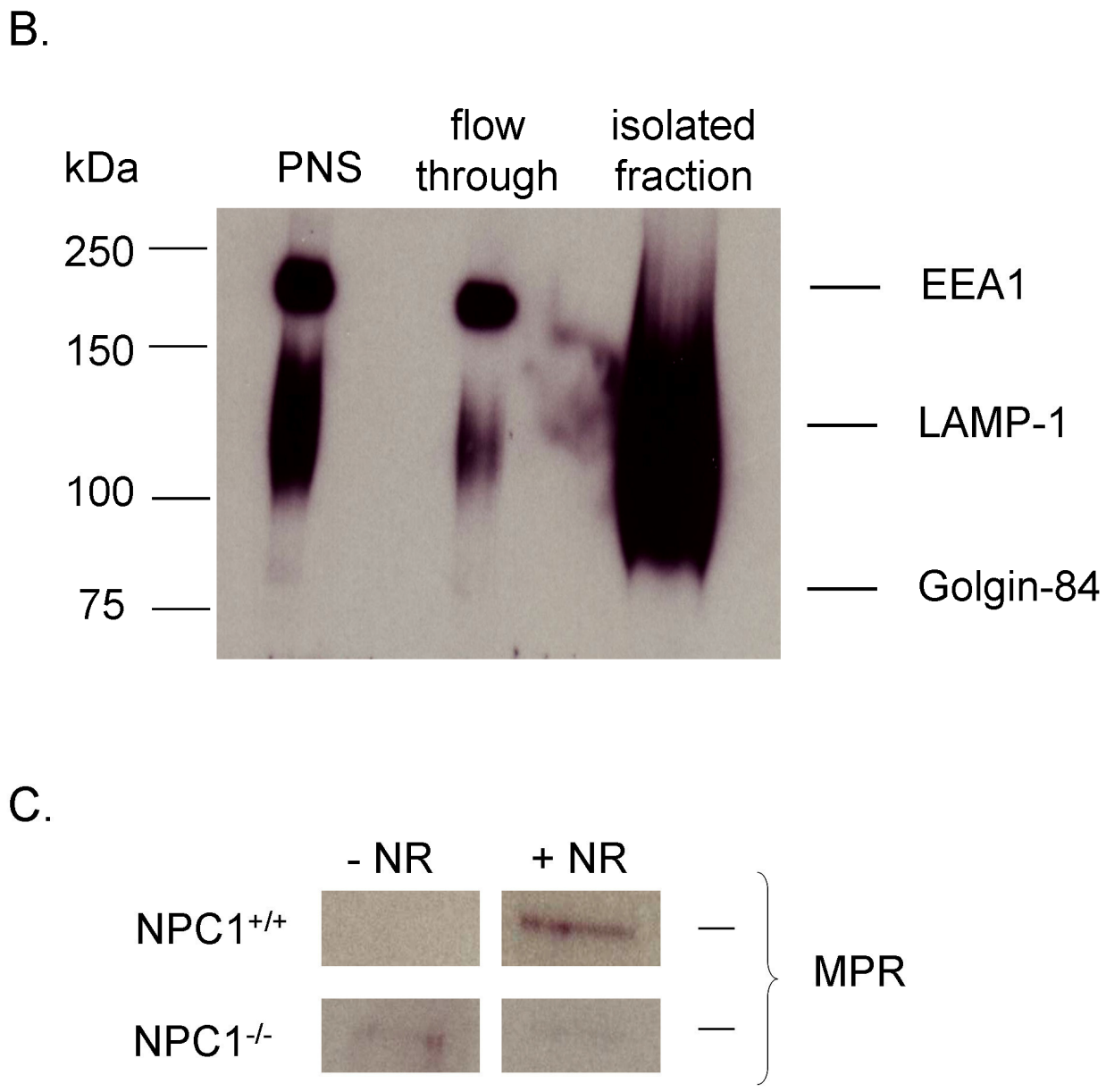

***(cont.)* Figure 2.8. Western blot analysis reveals isolated vacuoles contain lysosome and late endosome markers.** (B) Isolated terminal endocytic compartment fractions in the absence of NR treatment were devoid of Golgi (Golgin-84) and early endosome (EEA1) markers, but enriched in lysosome (LAMP-1) proteins in $NPC1^{+/+}$ cells. (C) Western blot analysis of late endosomal MPR in purified terminal endocytic-compartments before and after amine (NR) treatments. $NPC1^{+/+}$ fibroblasts become enriched in MPR after amine treatment, which does not occur with $NPC1^{-/-}$ fibroblasts.

amines. It is well known that lysosomes can be vacuolated by incubating cells in high concentrations of sucrose [20]. The resultant vacuoles are referred to as sucrosomes. Interestingly, the formation of sucrosomes occurred regardless of NPC1 functional status (Fig. 2.10). This result suggests that sucrose-induced vacuolization occurs by a different mechanism, independent of NPC1. Moreover, formation of sucrosomes did not appear to involve fusion of late endosomes with lysosomes since MPR and LAMP-1 did not significantly colocalize when observed with immunofluorescence (Fig. 2.10). This is consistent with previous findings which stated that sucrose-induced vacuoles were primarily formed from homotypic lysosome-lysosome interactions and not heterotypic fusion events [21].

Late endosomes and lysosomes have been shown to interact in normal cells without amine treatments [17; 22; 23]. Previously we had shown that amine-induced vacuoles were formed from the fusion of late endosomes with lysosomes and this phenomenon did not occur in NPC1 deficient cells (Figs. 2.7 and 2.9). Next, we investigated if NPC1 was involved in the fusion of lysosomes and late endosomes without amine treatments. To evaluate this possibility, a method for quantitatively determining these events in our NPC1 fibroblast model was developed and is described in Appendix I. Briefly, using optimized pulse-chase conditions (see Appendix I) we localized biotin-dextran into lysosomes and streptavidin-coated latex beads into late endosomes. Each of these probes was labelled with a different fluorophore that could be used for fluorescence

resonance energy transfer (FRET)-based evaluations if the two organelles were to interact and mix contents. We observed, through the appearance of FRET signal over time, that lysosomes and late endosomes were interacting in NPC1 competent cells without amine treatments (Fig. 2.11). Furthermore, NPC1$^{-/-}$ cells showed no increase in FRET signal over time which indicated little to no late endosome-lysosome interactions was occurring in these cells.

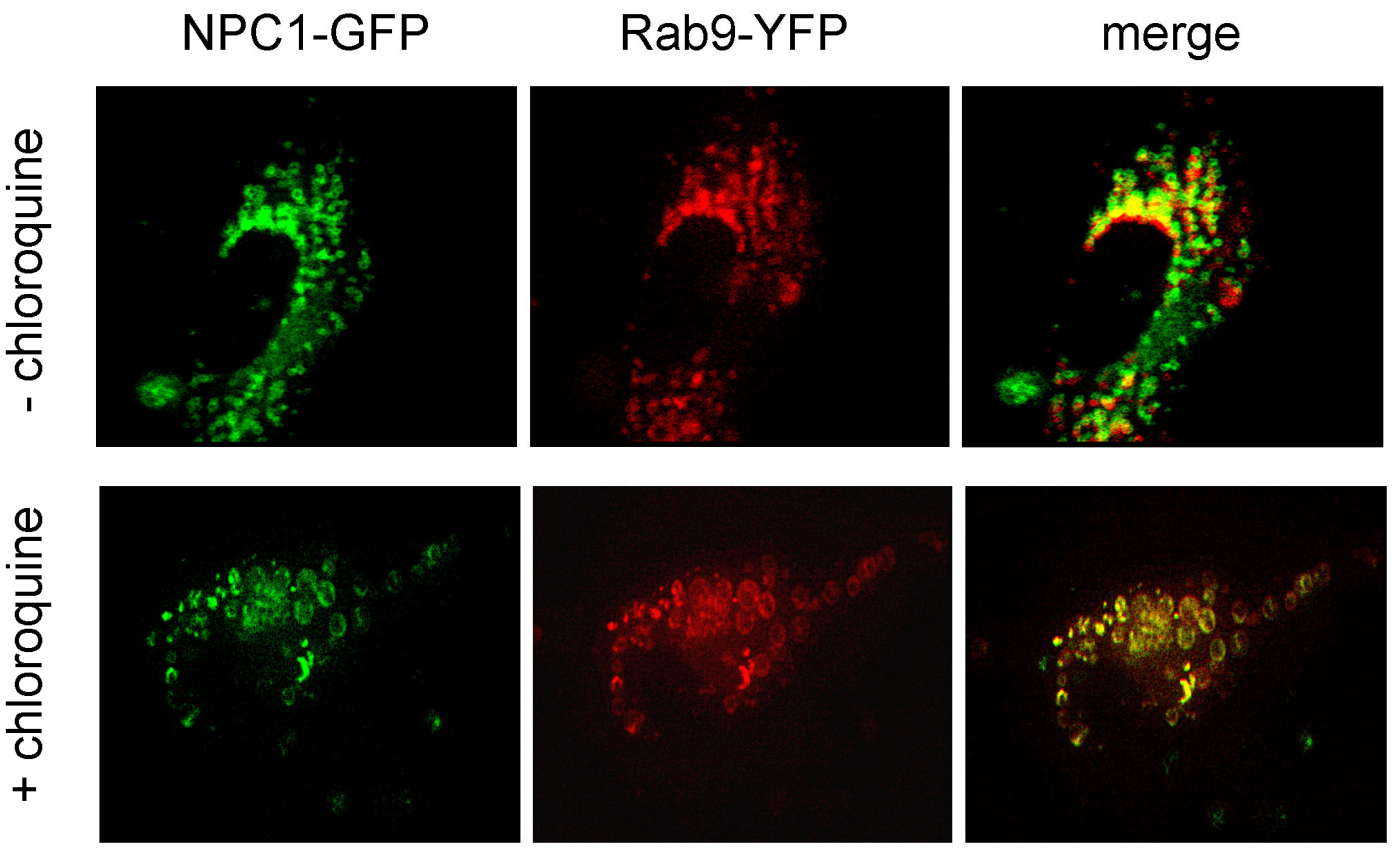

Figure 2.9. NPC1-GFP and Rab9-YFP colocalize in normal cells upon amine treatment. Fluorescence images of NPC1$^{+/+}$ fibroblasts expressing NPC1-GFP (green) and late endosome-specific Rab9-YFP (red). An increase in NPC1/Rab9 colocalization is observed following treatment with 100 μM CQ for 6 hrs.

2.4. Discussion

Since the discovery of the lysosome by Christian De Duve, there has been a significant amount of research done to understand weak base sequestration in lysosomes and how this accumulation contributes to vacuolization. The basis for weak base accumulation in lysosomes has long been theoretically accepted, although the mechanism for vacuolization is still poorly understood. Previously, it was thought that vacuolization occurred due to an osmotic expansion, whereby an influx of water into the organelle would help to dissipate the weak base concentration gradient [6]. Such a mechanism would justify the increase in organelle volume and has been observed for hyper-osmotic molecules such as sucrose [21]. Since lysosomes and late endosomes are multi-vesicular, meaning they have multiple membranous structures within one organelle; the osmotic stress would induce these vesicular structures to fuse with the limiting lysosome membrane resulting in a larger organelle. Although osmotic stress is not precluded from weak base accumulation in lysosomes, the formation of large vacuoles has been shown to be microtubule dependent, which suggests that the recruitment of membrane to the lysosome from other sources is necessary for organelle expansion (Fig. 2.1).

In this chapter, we have provided evidence that the amine-induced vacuolization of lysosomes observed in human fibroblasts is facilitated by the heterotypic fusion of lysosomes with late endosomes in an NPC1-dependent manner. In support of this, Arai et al. have described a cell-free system that

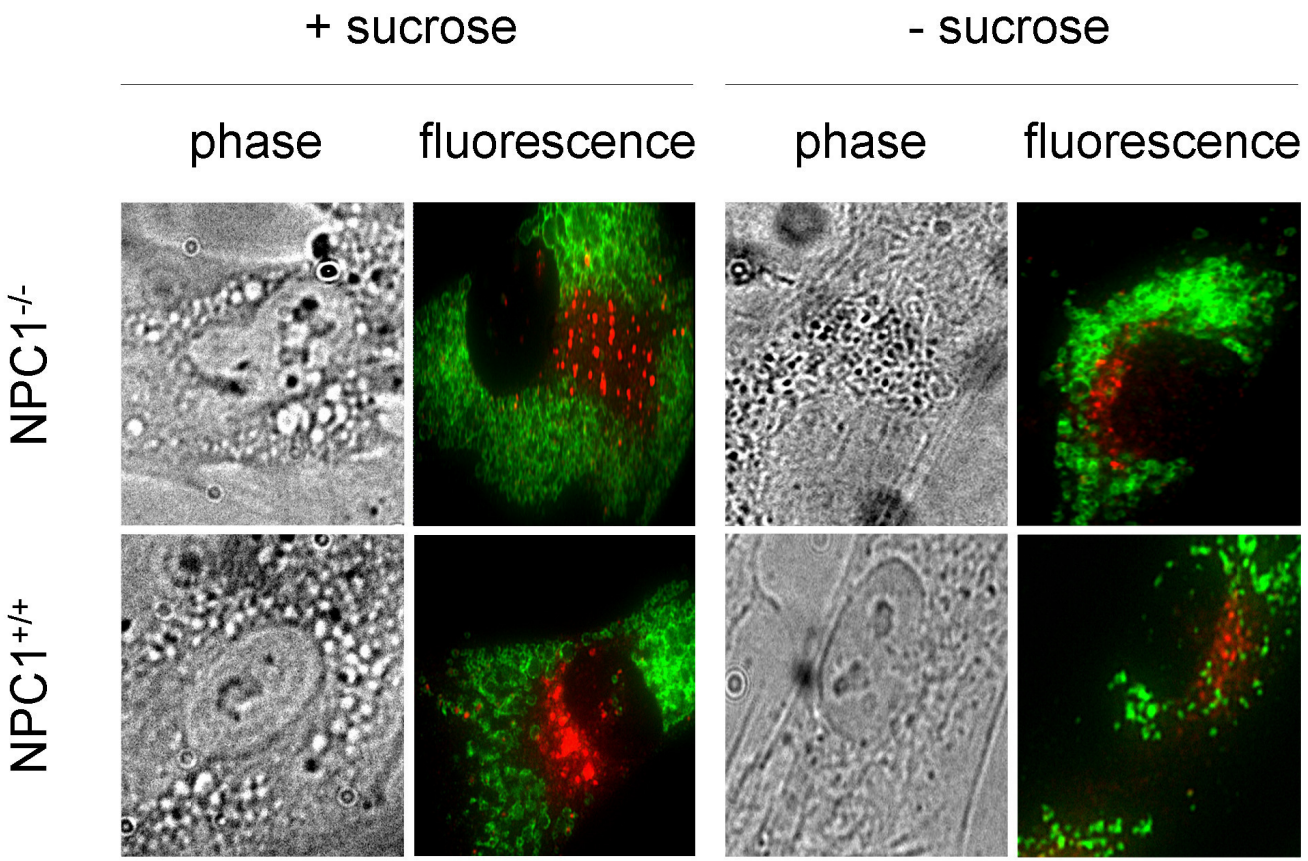

Figure 2.10. Vacuolization of lysosomes with sucrose occurs regardless of NPC1 functional status and does not involve fusion with late endosomes. Phase contrast images show the addition of 0.1% sucrose induced vacuolization in both $NPC1^{+/+}$ and $NPC1^{-/-}$ fibroblasts. Immunofluorescence analysis of LAMP-1 (green) and MPR (red) reveals that lysosomes and late endosomes do not colocalize with or without sucrose.

shows lysosomes resuspended in isotonic buffer can osmotically rupture when exposed to weakly basic amines if not incubated with cell cytosol containing intact organelles [8]. The authors argue that the presence of cytosol provides the re-suspended lysosome solution with more lysosomes or possibly late endosomes for interaction. These interactions would help to dissipate the amine concentration gradient in lysosomes since the recruitment of late endosomes would increase the volume of the organelle. Although Arai et al. speculated that these events were occurring; the interaction of lysosomes with late endosomes has been well documented in the literature. Bright et al. has observed transient interactions between the two organelles in living cells using fluorescence and electron microscopy [22; 24]. Mullock et al. has described in great detail the ability of lysosomes to fuse with late endosomes *in vivo* and *in vitro* [25; 26]. They have observed, using transmission electron microscopy, these interactions occurring and have used a cell-free system to describe necessary protein components. In a similar fashion, we have used a FRET-based method to show that NPC1 is required for the interaction of lysosomes with late endosomes (Fig. 2.11).

At present, there is limited information on the proteins required for the amine-induced vacuolization process to occur. It has been reported that the function of the vacuolar-ATPase (V-ATPase) is necessary for vacuolization [27]. This seems reasonable since disruption of the pH gradient between the cytosol and the lysosome should not permit increased weak base accumulation. Experiments using purified VacA, a non-amine toxin excreted from

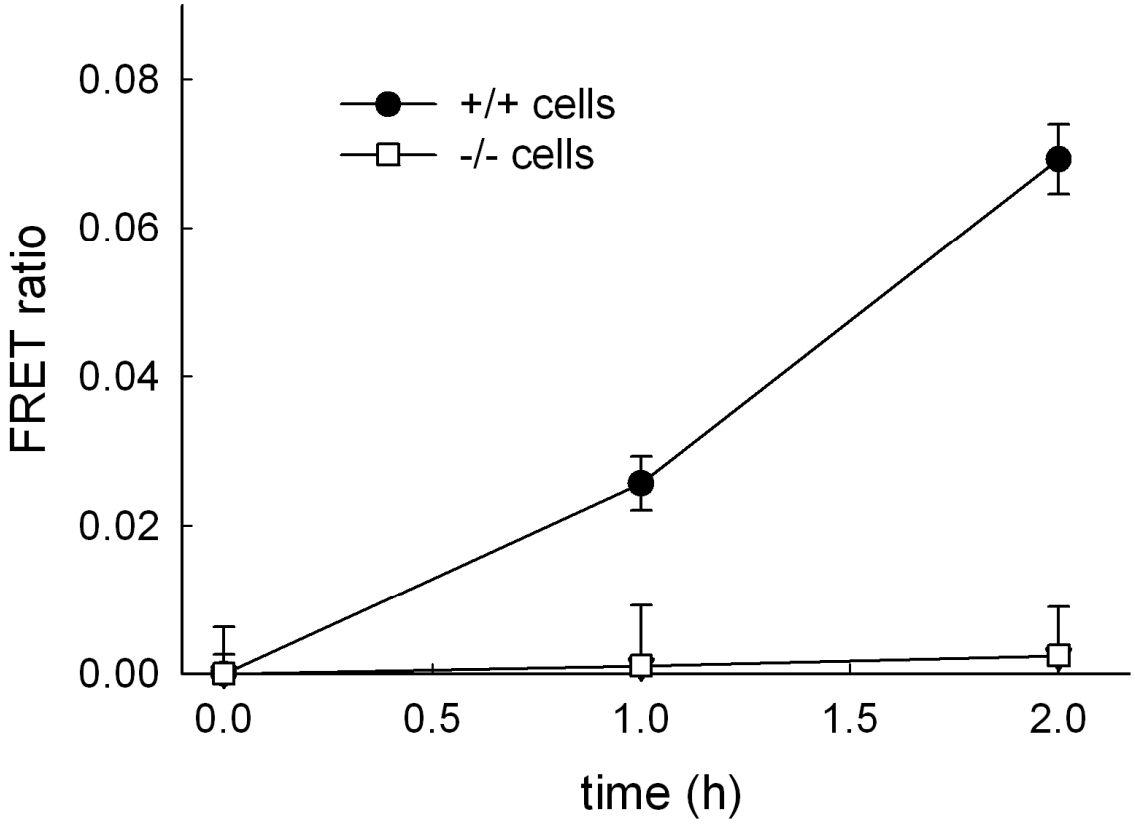

Figure 2.11. Profiles for late endosome/lysosome fusion assay in NPC1$^{+/+}$ and NPC1$^{-/-}$ cells. Cells were observed over a period of 2 hrs after the final chase of the late endosome FRET tracer as described in Appendix I. NPC1$^{-/-}$ lysosomes were unable to fuse with late endosomes as demonstrated by the lack of FRET signal appearance.

pylori, which vacuolizes lysosomes via late endosome fusion, have provided insight into vacuolization mechanisms. Using VacA it was shown that Rab7 (GTPase tether) and VAMP-7 (a SNARE protein) are necessary for vacuolization to occur [28; 29]. By transfecting cells with plasmid DNA encoding for mutated Rab7 or siRNA specific to syntaxin-7 (another SNARE protein), vacuolization was inhibited upon administration of VacA. Since the function of both of these proteins is to aid in organelle fusion *in vivo* [30; 31], these findings support membrane recruitment to facilitate vacuolization of lysosomes.

The lysosome is now understood to be a dynamic organelle capable of interacting with other compartments of the cell. The findings presented here provide evidence in support of these observations and suggest that without a functional NPC1 protein amine-induced vacuolization cannot occur. NPC1 appears to be mediating lysosome expansion by facilitating the fusion of late endosomes with lysosomes.

2.5. References

[1]A. Martin, Physical Pharmacy. In: Diffusion and dissolution., Lippincott Williams and Wilkins, MD., 2001.

[2]A.M. Kaufmann, and J.P. Krise, Lysosomal sequestration of amine-containing drugs: Analysis and therapeutic implications. J Pharm Sci 96 (2007) 729-46.

[3]M. Duvvuri, Y. Gong, D. Chatterji, and J.P. Krise, Weak base permeability characteristics influence the intracellular sequestration site in the multidrug-resistant human leukemic cell line HL-60. J Biol Chem 279 (2004) 32367-72.

[4]M. Duvvuri, S. Konkar, R.S. Funk, J.M. Krise, and J.P. Krise, A chemical strategy to manipulate the intracellular localization of drugs in resistant cancer cells. Biochemistry 44 (2005) 15743-9.

[5]M. Duvvuri, S. Konkar, K.H. Hong, B.S. Blagg, and J.P. Krise, A new approach for enhancing differential selectivity of drugs to cancer cells. ACS Chem Biol 1 (2006) 309-15.

[6]S. Ohkuma, and B. Poole, Cytoplasmic vacuolation of mouse peritoneal macrophages and the uptake into lysosomes of weakly basic substances. J Cell Biol 90 (1981) 656-64.

[7]A.E. Solheim, and P.O. Seglen, Structural and physical changes in lysosomes from isolated rat hepatocytes treated with methylamine. Biochim Biophys Acta 763 (1983) 284-91.

[8]K. Arai, N. Yasuda, F. Isohashi, K. Okamoto, and S. Ohkuma, Inhibition of weak-base amine-induced lysis of lysosomes by cytosol. J Biochem (Tokyo) 132 (2002) 529-34.

[9]A.M. Kaufmann, and J.P. Krise, Niemann-pick c1 functions in regulating lysosomal amine content. J Biol Chem 283 (2008) 24584-93.

[10]Y. Gong, M. Duvvuri, M.B. Duncan, J. Liu, and J.P. Krise, Niemann-Pick C1 protein facilitates the efflux of the anticancer drug daunorubicin from cells according to a novel vesicle-mediated pathway. J Pharmacol Exp Ther 316 (2006) 242-7.

[11]T. Yamamoto, E. Nanba, H. Ninomiya, K. Higaki, M. Taniguchi, H. Zhang, S. Akaboshi, Y. Watanabe, T. Takeshima, K. Inui, S. Okada, A. Tanaka, N. Sakuragawa, G. Millat, M.T. Vanier, J.A. Morris, P.G. Pentchev, and K. Ohno, NPC1 gene mutations in Japanese patients with Niemann-Pick disease type C. Hum Genet 105 (1999) 10-6.

[12]M. Duvvuri, and J.P. Krise, A novel assay reveals that weakly basic model compounds concentrate in lysosomes to an extent greater than pH-partitioning theory would predict. Mol Pharm 2 (2005) 440-8.

[13]I.G. Ganley, and S.R. Pfeffer, Cholesterol accumulation sequesters Rab9 and disrupts late endosome function in NPC1-deficient cells. J Biol Chem (2006).

[14]D.C. Ko, M.D. Gordon, J.Y. Jin, and M.P. Scott, Dynamic movements of organelles containing Niemann-Pick C1 protein: NPC1 involvement in late endocytic events. Mol Biol Cell 12 (2001) 601-14.

[15]P. Barbero, L. Bittova, and S.R. Pfeffer, Visualization of Rab9-mediated vesicle transport from endosomes to the trans-Golgi in living cells. J Cell Biol 156 (2002) 511-8.

[16]O. Diettrich, K. Mills, A.W. Johnson, A. Hasilik, and B.G. Winchester, Application of magnetic chromatography to the isolation of lysosomes from fibroblasts of patients with lysosomal storage disorders. FEBS Lett 441 (1998) 369-72.

[17]A. Jahraus, B. Storrie, G. Griffiths, and M. Desjardins, Evidence for retrograde traffic between terminal lysosomes and the prelysosomal/late endosome compartment. J Cell Sci 107 (Pt 1) (1994) 145-57.

[18]A. Umeda, H. Fujita, T. Kuronita, K. Hirosako, M. Himeno, and Y. Tanaka, Distribution and trafficking of MPR300 is normal in cells with cholesterol accumulated in late endocytic compartments: evidence for early endosome-to-TGN trafficking of MPR300. J Lipid Res 44 (2003) 1821-32.

[19]T. Kobayashi, M.H. Beuchat, M. Lindsay, S. Frias, R.D. Palmiter, H. Sakuraba, R.G. Parton, and J. Gruenberg, Late endosomal membranes rich in lysobisphosphatidic acid regulate cholesterol transport. Nat Cell Biol 1 (1999) 113-8.

[20]N.A. Bright, M.R. Lindsay, A. Stewart, and J.P. Luzio, The relationship between lumenal and limiting membranes in swollen late endocytic compartments formed after wortmannin treatment or sucrose accumulation. Traffic 2 (2001) 631-42.

[21]K. DeCourcy, and B. Storrie, Osmotic swelling of endocytic compartments induced by internalized sucrose is restricted to mature lysosomes in cultured mammalian cells. Exp Cell Res 192 (1991) 52-60.

[22]N.A. Bright, M.J. Gratian, and J.P. Luzio, Endocytic delivery to lysosomes mediated by concurrent fusion and kissing events in living cells. Curr Biol 15 (2005) 360-5.

[23]B.M. Mullock, N.A. Bright, C.W. Fearon, S.R. Gray, and J.P. Luzio, Fusion of lysosomes with late endosomes produces a hybrid organelle of intermediate density and is NSF dependent. J Cell Biol 140 (1998) 591-601.

[24]N.A. Bright, B.J. Reaves, B.M. Mullock, and J.P. Luzio, Dense core lysosomes can fuse with late endosomes and are re-formed from the resultant hybrid organelles. J Cell Sci 110 (Pt 17) (1997) 2027-40.

[25]B.M. Mullock, J.H. Perez, T. Kuwana, S.R. Gray, and J.P. Luzio, Lysosomes can fuse with a late endosomal compartment in a cell-free system from rat liver. J Cell Biol 126 (1994) 1173-82.

[26]B.M. Mullock, C.W. Smith, G. Ihrke, N.A. Bright, M. Lindsay, E.J. Parkinson, D.A. Brooks, R.G. Parton, D.E. James, J.P. Luzio, and R.C. Piper, Syntaxin 7 is localized to late endosome compartments, associates with Vamp 8, and Is required for late endosome-lysosome fusion. Mol Biol Cell 11 (2000) 3137-53.

[27]G. Morissette, E. Moreau, C.G. R, and F. Marceau, Massive cell vacuolization induced by organic amines such as procainamide. J Pharmacol Exp Ther 310 (2004) 395-406.

[28]E. Papini, B. Satin, C. Bucci, M. de Bernard, J.L. Telford, R. Manetti, R. Rappuoli, M. Zerial, and C. Montecucco, The small GTP binding protein rab7 is essential for cellular vacuolation induced by Helicobacter pylori cytotoxin. EMBO J 16 (1997) 15-24.

[29]H. Mashima, J. Suzuki, T. Hirayama, Y. Yoshikumi, H. Ohno, H. Ohnishi, H. Yasuda, T. Fujita, and M. Omata, Involvement of vesicle-associated membrane protein 7 in human gastric epithelial cell vacuolation induced by Helicobacter pylori-produced VacA. Infect Immun 76 (2008) 2296-303.

[30]R.J. Advani, B. Yang, R. Prekeris, K.C. Lee, J. Klumperman, and R.H. Scheller, VAMP-7 mediates vesicular transport from endosomes to lysosomes. J Cell Biol 146 (1999) 765-76.

[31]D.M. Ward, J. Pevsner, M.A. Scullion, M. Vaughn, and J. Kaplan, Syntaxin 7 and VAMP-7 are soluble N-ethylmaleimide-sensitive factor attachment protein receptors required for late endosome-lysosome and homotypic lysosome fusion in alveolar macrophages. Mol Biol Cell 11 (2000) 2327-33.

Chapter 3

Evaluating the role of NPC1 in vesicle-mediated amine clearance from lysosomes

3.1. Introduction

Traditionally, the lysosome has been considered the terminal compartment for materials endocytosed into cells [1]. However, research has shown that materials either endocytosed into lysosomes or ion-trapped by pH-partitioning can be efficiently released to the cell periphery [2]. Although the mechanism of fluid phase endocytosis and weakly basic amine sequestration in lysosomes has been well-described by our lab and others [3; 4; 5], the mechanism for the efflux of lysosome contents is poorly understood. Considering the high concentrations of amines that can sequester into lysosomes, mechanisms must exist for their removal to avoid toxic effects such as lysosome rupture.

In this chapter, we attempt to identify Niemann-Pick C1 as a necessary protein for the trafficking of amines from the lysosome. Previous research has shown that defects in Niemann-Pick C1 (NPC1) activity result in the inefficient secretion of multiple lysosome cargos. To date, LDL-derived unesterified cholesterol, sphingomyelin, glycolipids and phospholipids have been shown to accumulate in the lysosomal lumen of NP-C disease cells *in vivo* [6; 7; 8; 9]. The clearance of endocytosed lysosome probes, such as radioactive sucrose, is also been impeded by NPC1 dysfunction [10]. Although defects in the clearance of membrane impermeable molecules in NP-C disease cells have been described, research investigating the proteins required for efficient efflux of amines from lysosomes is lacking.

In an attempt to describe NPC1 involvement in small molecule amine transport, it was recently reported that NPC1 shares significant structural homology with a family of prokaryotic permeases [11]. From this homology, Davies et al. proposed that NPC1 may function in intracellular drug transport as a membrane transporter, similar to P-glycoprotein. To test this hypothesis, the authors monitored the efflux of acriflavine, a fluorescent small molecule amine that localizes to lysosomes. The authors concluded that acriflavine was cleared from lysosomes by NPC1-mediated translocation from the lumen to the cytosol. However, the implication of NPC1 acting as a molecular transporter (i.e. a P-gp like pump or flippase) of acriflavine has since been discredited [12]. Our laboratory has shown that the functional status of NPC1 could influence the release of trapped weakly basic drugs from lysosomes to the extracellular space by a novel vesicle mediated microtubule-dependent pathway [2]. In this study, we observe that cells with mutated and dysfunctional NPC1, such as the multi-drug resistant human leukemic cell line 60 (HL-60/MDR), are inefficient at clearing the weakly basic anti-cancer agent daunorubicin from lysosomes when compared to cells with functional NPC1. Furthermore, when normal cells are treated with the microtubule destabilizer nocodazole, amine clearance is diminished [2]. These findings are in agreement with NPC1 facilitating removal of amines from lysosomes by a vesicle pathway and not by direct translocation across lipid membranes.

The work described in this section serves to specifically confirm the dependence on functional NPC1 for the efficient trafficking of lysosomal contents from lysosomes, in particular, trapped weakly basic amines. Previous evaluations in HL-60/MDR cells were important for identifying NPC1 involvement in amine transport from the lysosome; however, in comparative evaluations using diseased cells, such as HL-60 or NP-C cells, there can be factors influencing clearance behavior that may not be due to protein malfunction. For example, the clearance defects observed in NP-C cells could be due to the hyperaccumulation of lipids in the lysosome lumen. To address these questions, we have sought to specifically silence NPC1 in normal cells, as well as evaluate lipid accumulation effects on the clearance of lysosome contents.

3.2. Materials and methods

3.2.1. Reagents

[^{3}H]-dextran (70,000MW; 125 μCi/mg) was purchased through American Radiolabeled Chemicals (St. Louis, MO). Scintiverse-BD liquid scintillation cocktail was obtained from Fisher Scientific (Pittsburgh, PA) and neutral red (NR) from Sigma-Aldrich (St. Louis, MO). Alexa Fluor 488 dextran and Lysotracker Red DND-99 (LTR) was obtained from Invitrogen (Eugene, OR). siRNA specific to NPC1 was custom synthesized by Ambion (Austin, TX). All other reagents unless otherwise specified were purchased through Sigma-Aldrich.

3.2.2. Cell culture and conditions

Normal human fibroblasts (CRL-2076, designated NPC1$^{+/+}$) were cultured according to Coriell Cell Repository's (Camden, NJ) suggestions. Niemann-Pick Type C disease (NP-C) fibroblasts (NPC1$^{-/-}$) were obtained through the ATCC. NPC1$^{-/-}$, mucolipidosis type IV (GM-02408, designated MLIV), and Sandhoff's disease (GM-11707) fibroblasts were all cultured according to the ATCC (Manassas, VA) instructions. All media was supplemented with 10% FBS and 1% penicillin/streptomycin. Cultures were maintained at 37^{o}C in a humidified 5% carbon dioxide atmosphere. For all experiments, cells were used before passage 5 and plated 24 hrs prior to evaluations to allow for adherence.

3.2.3. Dextran secretion assay

3.2.3.1. Fluorescent dextran release

To qualitatively assess the clearance of endocytosed dextran, fibroblasts were plated in 8-well chamber slides at 3 x 10^4 cells per well and allowed to adhere overnight prior to incubating with 2 mg/mL Alexa Fluor 488 dextran for 2 hrs (in complete phenol red free DMEM). Cells were washed with warm PBS (2X) and medium replaced. Dextran was allowed to localize to lysosomes for 20 hrs at which point fluorescence images were acquired at different time points using standard epifluorescence optics (Nikon).

3.2.3.2. Radioactive dextran release

Fibroblasts were plated at 3 x 10^5 cells per well in 6-well culture plates and allowed to adhere overnight. Cells were incubated with 50 µCi/mL of [^{3}H]-dextran in addition to 0.9 mg/mL cold dextran of the same molecular weight in complete medium at 37^{o}C for 3 hrs and washed with warm media (4X). Cells were then chased in dextran free media and the amount of [^{3}H]-dextran secreted into the media was analyzed at indicated time points. At the end of the assay, the fibroblast monolayer was dissolved using a solution of 50 mM Tris, 150 mM NaCl, and 1.0% NP-40 to determine total dextran uptake of each well. To address the non-specific association of radioactive dextran with the cell monolayer on total amounts released, experiments were repeated at 4^{o}C for 4 hrs (after the initial dextran incubation)and curve fit to obtain later data points. These data points were subtracted from the same points from experiments

carried out at 37^{o}C. The cumulative amount of dextran released into the media is given as a percentage of the total amount of dextran endocytosed. Quantitation of [^{3}H]-dextran at each time point was performed using a liquid scintillation counter (Beckman LS5000; Beckman Coulter, Fullerton, CA) and Scintiverse-BD liquid scintillation cocktail.

3.2.4. Silencing of NPC1 expression using siRNA.

An siRNA construct was utilized to silence NPC1 expression as previously reported [13]. All siRNA transfections were performed using siPORT-Amine (Ambion) transfection reagent for 72 hrs as described previously (Section 2.2.5). For siRNA experiments requiring subsequent amine exposure, transfections were performed as described, at which point cells were exposed to 70 μM NR.

3.2.5. Evaluating amine clearance from lysosomes

3.2.5.1. Qualitative evaluations of amine clearance

To qualitatively assess the clearance of sequestered model amines, cells were plated in 24-well plates (5 x 10^{4} cells per well) and allowed to adhere overnight prior to incubation with either 70 μM NR for 6 hrs or 2 μM LTR for 1 h. After the incubation, cells were washed with PBS (3X) and chased with complete amine-free culture medium. Images were then taken at various time-points using a Nikon TE-2000U inverted microscope for NR and an upright epifluorescent microscope (Nikon Eclipse 80i) with a Texas Red filter set (Nikon, HQ:TR) for LTR. For

quantitatively evaluating the secretion of model amines, methods were developed as described below:

3.2.5.2. Neutral red release assay

For the quantitation of neutral red in fibroblasts, a spectrophotometric method for determining the release of amines from the lysosomes of cells was developed. Fibroblasts were seeded in 24-well culture plates at a density of 50 x 10^4 cells per well with a 500 µL total well volume. Next, fibroblasts were exposed to 70 µM NR for 6 hrs at 37^{o}C (5% CO_2). NR-containing medium was washed from cell monolayers with warm PBS (3X) and replaced with 500 µL of complete DMEM medium. Measurements were taken at different time-points after replacement with NR-free medium by washing cells again with PBS (3X) and extracting NR from each well with 100 µL of a solution containing 49% methanol and 1% acetic acid. Samples were analyzed by measuring the absorbance at 540 nm using a 96-well plate reader (Multiskan, Thermo Scientific). For normalization of NR amounts to protein, the post-nuclear supernatant protein concentration of 50 x 10^4 cells was determined by the method of Bradford [14].

3.2.5.3. Lysotracker red release

For the comparison of relative amounts of LTR in fibroblasts, a method for determining the release of amines from the lysosomes of cells

was developed using images taken during qualitative evaluations. First, images were scaled for contrast and brightness using MetaMorph software (v. 7.0). Next, images were analyzed using the "Measure Average Intensity" function. Background was subtracted by using this function in a selected area devoid of cells and LTR. Values were converted into percentages by dividing by the initial time point.

3.2.6. Live-cell phase microscopy

Fibroblasts were seeded at 50 x 10^4 cells per well in 4-well culture slides. Cells were kept alive during experimentation using a temperature controlled environmental chamber (Bioscience Tools, San Jose, CA) which was supplemented with CO_2 and water. Cells were kept in focus during experiments using a Prior Pro-scan II x,y,z motorized stage with preset stage positions. Images were acquired at various time points using standard phase contrast optics on an inverted Nikon TE-2000U fluorescence microscope with white light exposure and a Coolsnap-CF color camera (Photometrics, Tuscon, AZ).

3.3. Results

3.3.1. NPC1 is required for the efficient release of lysosome contents

The release of endocytosed fluid phase probes from lysosomes has been shown to be significantly diminished in cells with dysfunctional NPC1 [2; 10]. Since there are many variants of $NPC1^{-/-}$ cell lines available to the research community, we investigated if these observations from cell lines used in previous evaluations extended to the $NPC1^{-/-}$ cells used for our studies. To accomplish this, we employed both qualitative and quantitative evaluations to monitor lysosome secretion using fluorescent and radioactive dextran polymers , respectively. We specifically localized dextran to terminal endocytic compartments using the previously described pulse-chase protocol used for iron dextran (Chapter 2, Section 2.2.8). For qualitative evaluations, fluorescence imaging was performed on dextran containing cells at different wash-out times (Fig. 3.1). A radioactive dextran assay developed previously for determining secretion rates in HL-60 cells was used for quantitative evaluations of dextran release as a function of time in both normal and $NPC1^{-/-}$ fibroblasts (Fig. 3.2) [2]. In both qualitative and quantitative evaluations, $NPC1^{-/-}$ cells experienced inefficient release of dextran from lysosomes when compared to control cells. These results, in agreement with previous research, confirm that NPC1 is required for the efficient egress of lysosome cargo to the cell periphery.

3.3.2. NPC1 is required for the efficient release of amines from lysosomes

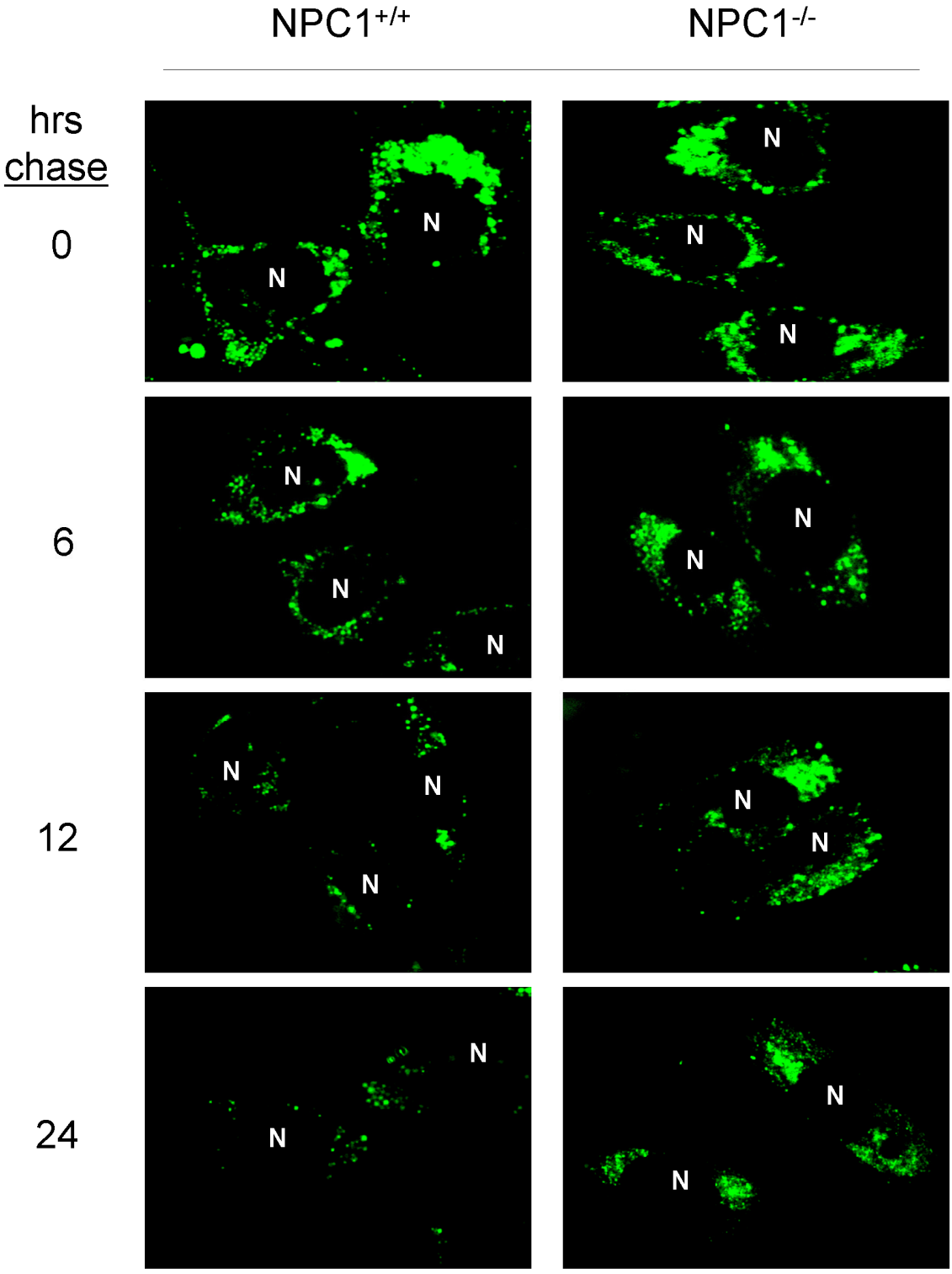

Figure 3.1. Qualitative evaluation of fluorescent dextran exocytosis shows inefficient clearance in NPC1$^{-/-}$ cells. Lysosomes were loaded with Alexa Fluor 488 (green) for 20 hrs. Subsequently, fluorescence micrographs were taken from 0-24 hrs. N = nucleus.

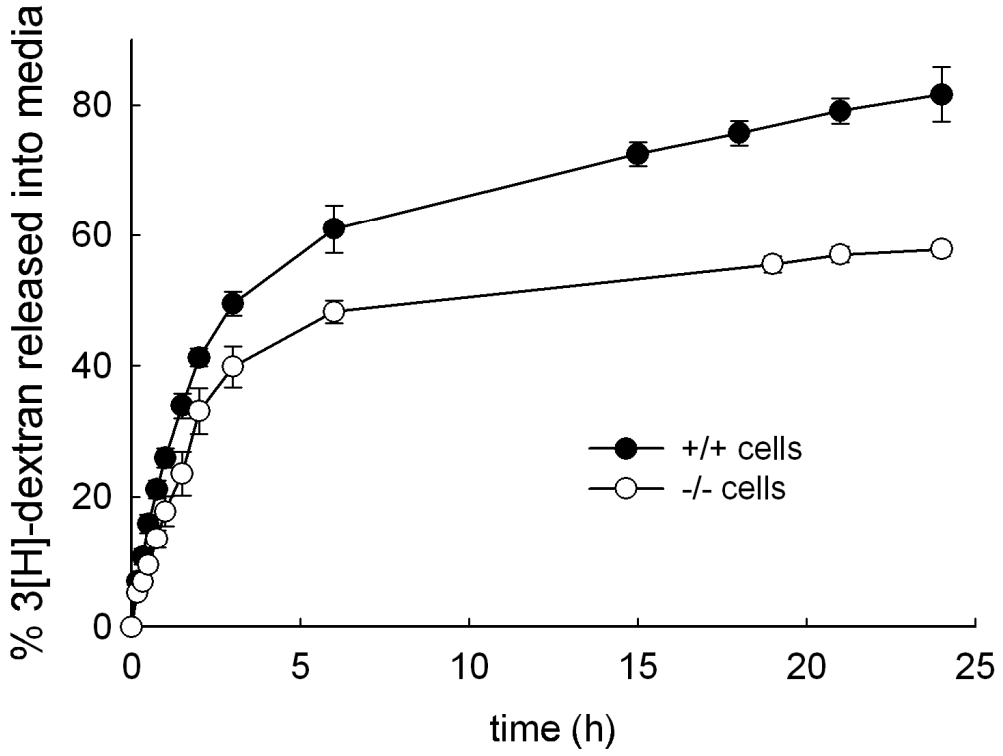

Figure 3.2. Radioactive dextran secretion is impaired in NPC1$^{-/-}$ cells. Full ^{3}[H]-dextran release profiles for both NPC1$^{+/+}$ and NPC1$^{-/-}$ cell lines. Release into the medium was monitored over a period of 24 hrs after localizing the dextran into the lysosomes. Data points represent an average ± SD for the percent dextran released as a function of time.

We have previously shown that the release of protonated amines from lysosomes is significantly impeded in NP-C diseased fibroblasts relative to normal cells [2]. The use of fibroblasts from NP-C patients to study NPC1 function is routinely done but could yield misleading results considering the multiple compensatory pathways that could be established. To more specifically investigate the involvement of NPC1, we evaluated the trafficking of lysosomotropic amines from normal cells treated with siRNA to transiently deplete NPC1. NPC1 siRNA treatment conditions were optimized to enable efficient suppression of NPC1 expression (Chapter 2, Section 2.2.5). The release of two well-known lysosomotropic amines, neutral red (NR) and Lysotracker Red (LTR), was evaluated. Using light microscopy and time-lapse video microscopy, we qualitatively showed that NR release was inefficient in NP-C fibroblasts and normal cells transfected with NPC1 specific siRNA, respectively (Figs. 3.3 and 3.4). This was confirmed using a quantitative NR-release assay. We observed that NR release was efficient in normal fibroblasts compared to NPC1 siRNA-treated normal fibroblasts (Fig. 3.5A). The NR release profile from $NPC1^{-/-}$ fibroblasts was similar to NPC1 siRNA-treated cells as both cells were unable to clear greater than 50% of their initial NR. Furthermore, we demonstrated the release of NR was dependent on a functional microtubule network by evaluating NR-release at $4^{o}C$ (Fig. 3.5B). At this temperature energy dependent processes, such as vesicle trafficking, are inefficient.

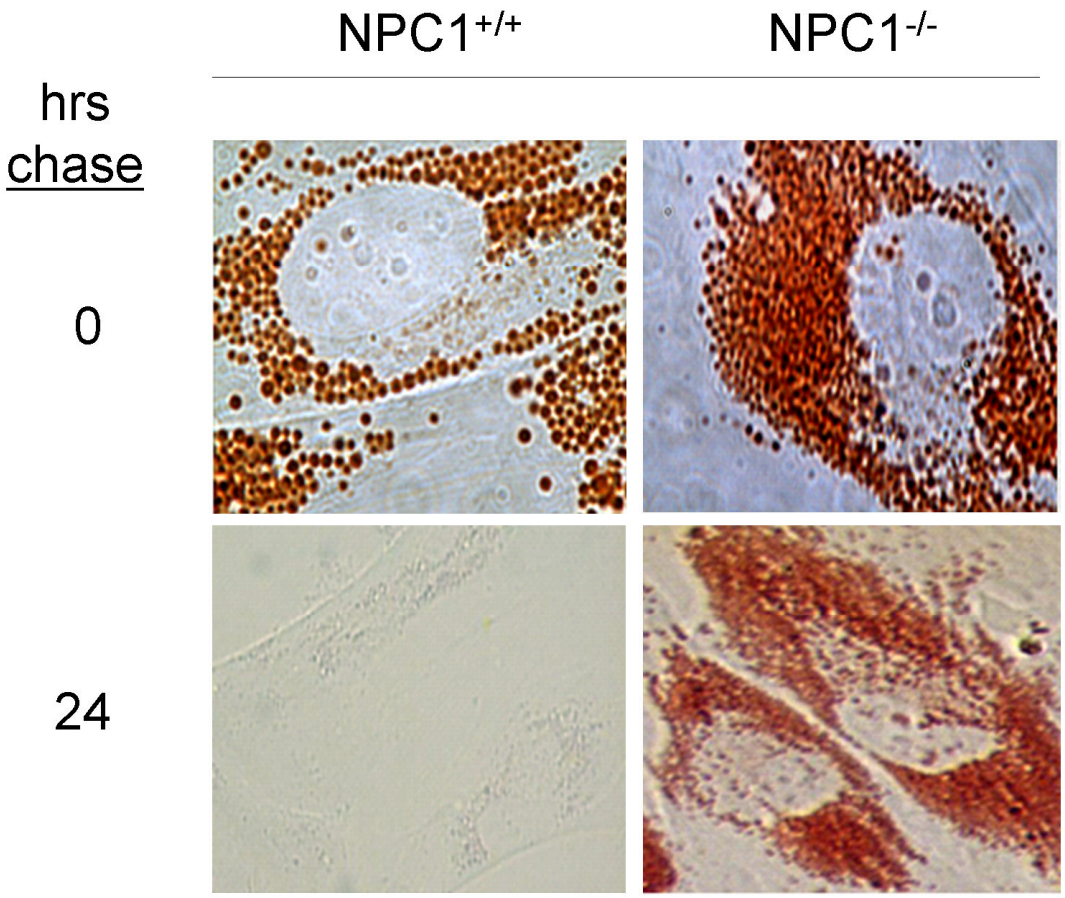

Figure 3.3. Clearance of NR is deficient in NPC1$^{-/-}$ cells. Fibroblasts were exposed to 70 μM NR for 6 hrs and given chase in NR-free medium for 24 hrs. NPC1$^{-/-}$ cells retained most of the initial NR while NPC1$^{+/+}$ cells were able to efficiently traffic NR from lysosomes.

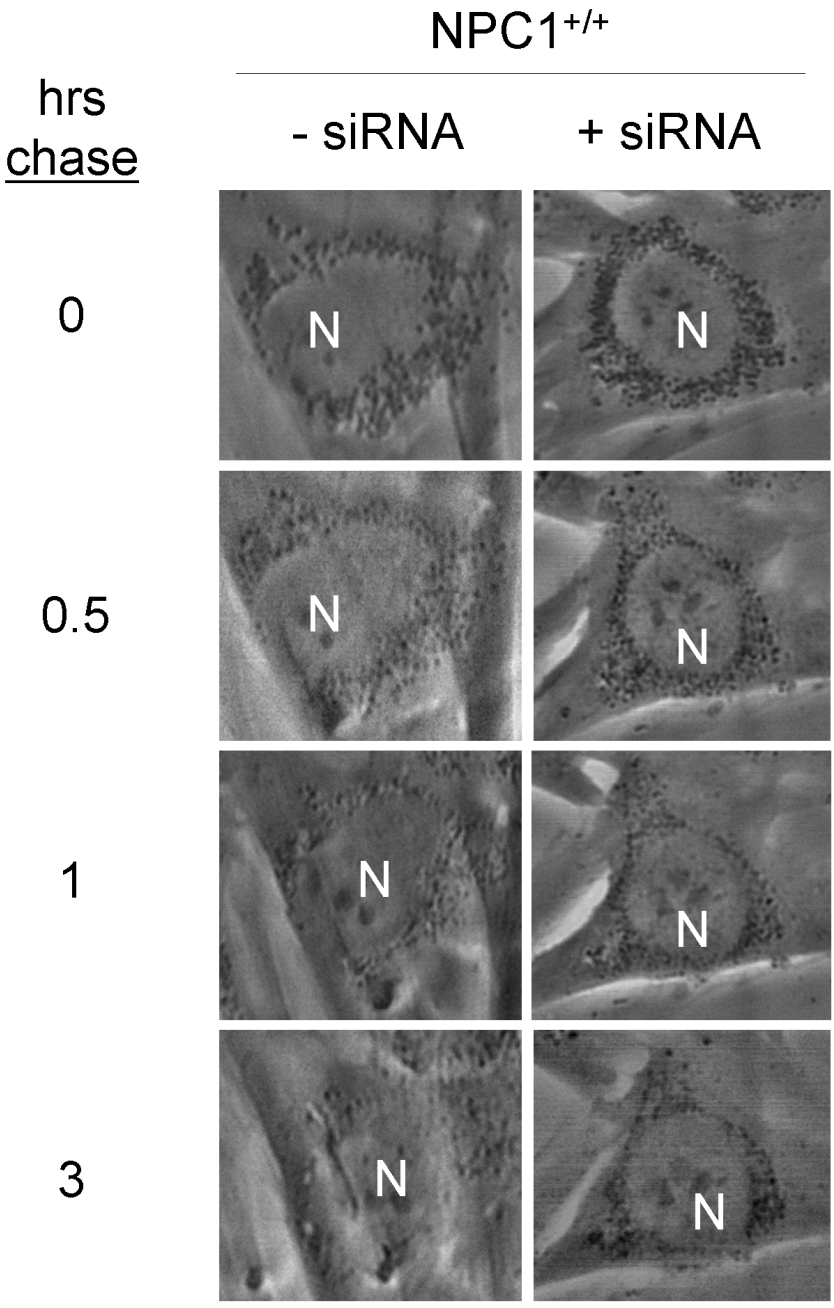

Figure 3.4. Time-lapse microscopy of siRNA treated NPC1$^{+/+}$ cells exposed to NR. Normal fibroblasts were transfected or left untransfected with NPC1-specific siRNA before exposure to 70 μM NR for 6 hrs. Cells were then given chase in NR-free medium and light micrographs of the same cells were acquired over time. siRNA transfected cells were unable to efficiently clear NR (black perinuclear staining) from lysosomes. N = nucleus.

The release of the lysosomal vital stain LTR from $NPC1^{+/+}$ and $NPC1^{-/-}$ cells, evaluated using fluorescence microscopy, provides visual evidence for the differences in release (Fig. 3.6A). To ensure these visual differences in LTR fluorescence were not due to variations in image contrast or brightness, relative amounts of LTR were determined by measuring the pixel intensity, which is independent of contrast/brightness, of LTR images taken at 24 hrs (Fig. 3.6B). It was determined that $NPC1^{+/+}$ cells have little to no LTR present after 24 hrs, whereas, $NPC1^{-/-}$ retain 30-40% of LTR in lysosomes, confirming visual observations.

3.3.3. Lysosomal accumulation of lipids does not affect amine release

It has been previously shown that the hyper-accumulation of lipids in lysosomes can impede organelle motility [15]. Considering this, it is possible that the decreased cellular clearance of amines observed with the NPC1-deficient cell line could be secondary to the lipid accumulation and not directly related to the inactivity of NPC1. To examine this possibility, we visually examined the clearance of LTR and quantitatively determined NR release in two additional fibroblasts obtained from patients with other lysosomal lipid storage disorders, including mucolipidosis IV (MLIV) and Sandhoff's disease. Both of these disorders are characterized by the hyperaccumulation of gangliosides, sphingolipids and cholesterol [16; 17]. The cholesterol accumulation phenotype was confirmed for these cell lines in Chapter 2, Figure 2.4.

LTR clearance from both Sandhoff's and MLIV cell lines using the same conditions was qualitatively evaluated. Both cell lines efficiently cleared LTR from lysosomes as compared to $NPC1^{+/+}$ cells (Fig. 3.7). Quantitative evaluations using NR confirmed these results, as both MLIV and Sandhoff's disease had NR profiles similar to normal fibroblasts (Fig. 3.8). Since both MLIV and Sandhoff's disease cell lines have functional NPC1, these results further support the specific involvement of NPC1 in the efficient efflux of amines from lysosomes.

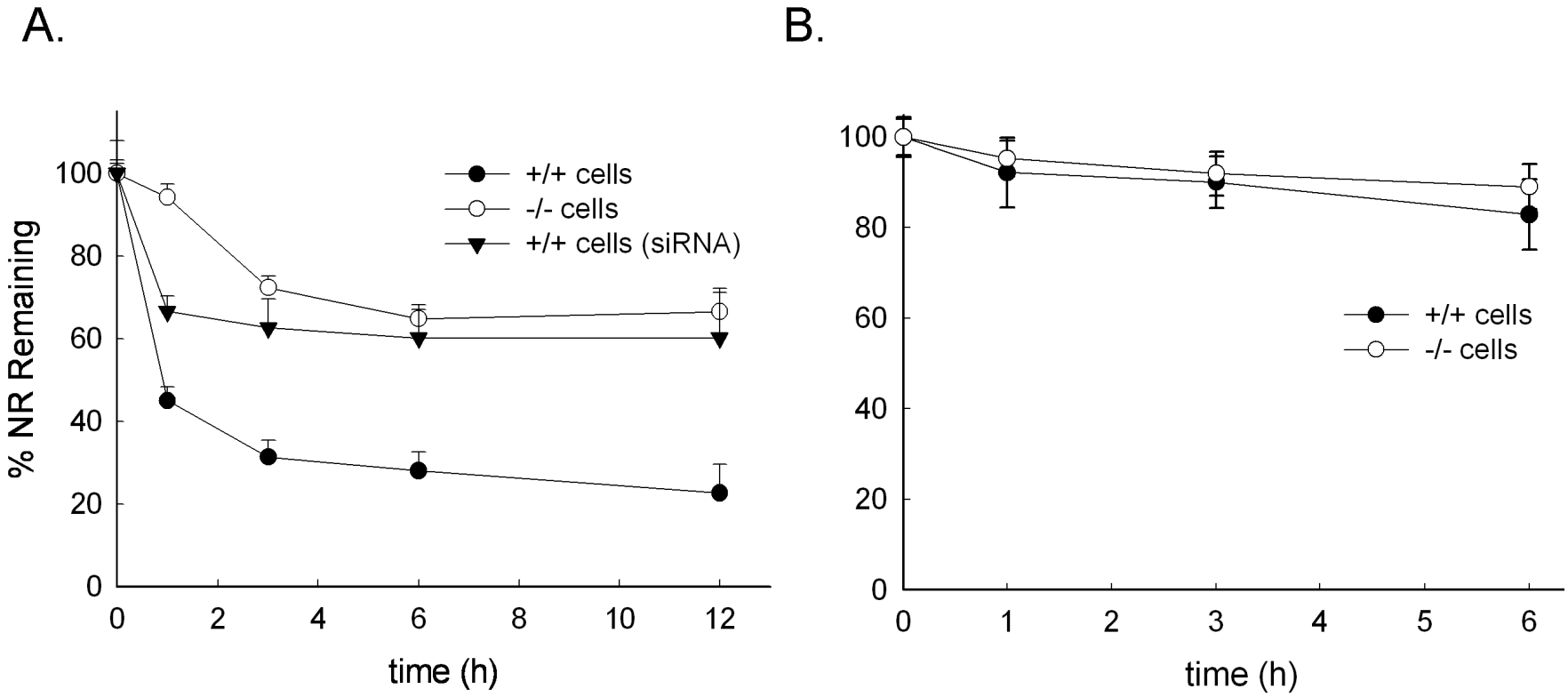

Figure 3.5. Lysosome amine secretion is impaired in NPC1$^{-/-}$ cells. (A) Quantitative evaluation of NR-release shows NPC1$^{+/+}$ fibroblasts clear NR more efficiently than NPC1$^{-/-}$ fibroblasts or NPC1$^{+/+}$ fibroblasts transfected with NPC1 siRNA. Each time point represents the average ± S.D. of 3–10 individual measurements. (B) NR-release experiments at 4°C. Both cell lines show minimal release after 6 hrs. Each time point represents the average ± S.D. of 3 individual measurements.

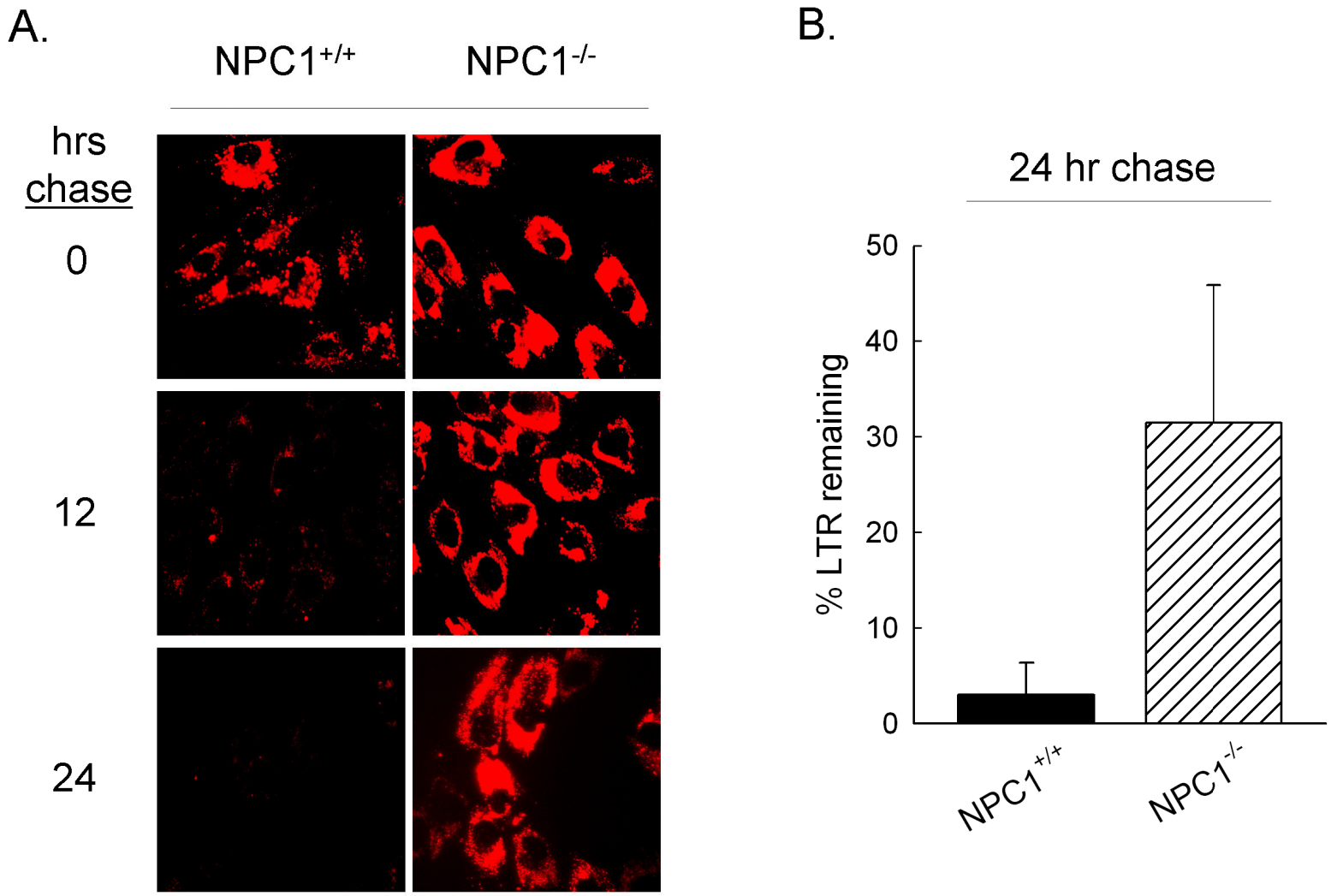

Figure 3.6. Lysosome amine secretion is impaired in NPC1$^{-/-}$ cells. (A) Fluorescence micrographs of LTR-release shows NPC1$^{+/+}$ fibroblasts clear LTR more efficiently than NPC1$^{-/-}$ fibroblasts. All LTR images are representative of data collected from at least 3 independent experiments. (B) Relative LTR remaining after 24 hrs chase as measured by LTR fluorescence intensities. Bars represent the average ± S.D. of 6 individual images.

3.4. Discussion

Contained in this chapter are evaluations that assess the ability of cells to efflux a variety of molecules, including dextran polymers and ion-trapped model amines, from lysosomes by an NPC1-mediated pathway. We have concluded that NPC1 has a functional role in the general trafficking of lysosomal contents to the extracellular space. However, the efflux pathway that NPC1 is mediating remains elusive. Thus the question remains, what specific trafficking step is NPC1 dysfunction negatively affecting?

When considering lysosome secretion, there are two main possibilities for the microtubule-dependent egress of lysosome contents to the cell periphery: 1) direct lysosome fusion with the plasma membrane [18] and 2) lysosome interactions with other sub-cellular organelles that are capable of facilitating secretion to the plasma membrane [19]. The notion of lysosome secretion is relatively new. As mentioned previously, the lysosome has traditionally been considered a terminal compartment that is incapable of interacting in a retrograde fashion with the plasma membrane or other cell organelles. Recently, a significant amount of research has been done in the area of lysosome dynamics that provides evidence for each of these two mechanistic possibilities.

Norma Andrews and colleagues have made significant contributions towards understanding the mechanisms of lysosome fusion with the plasma

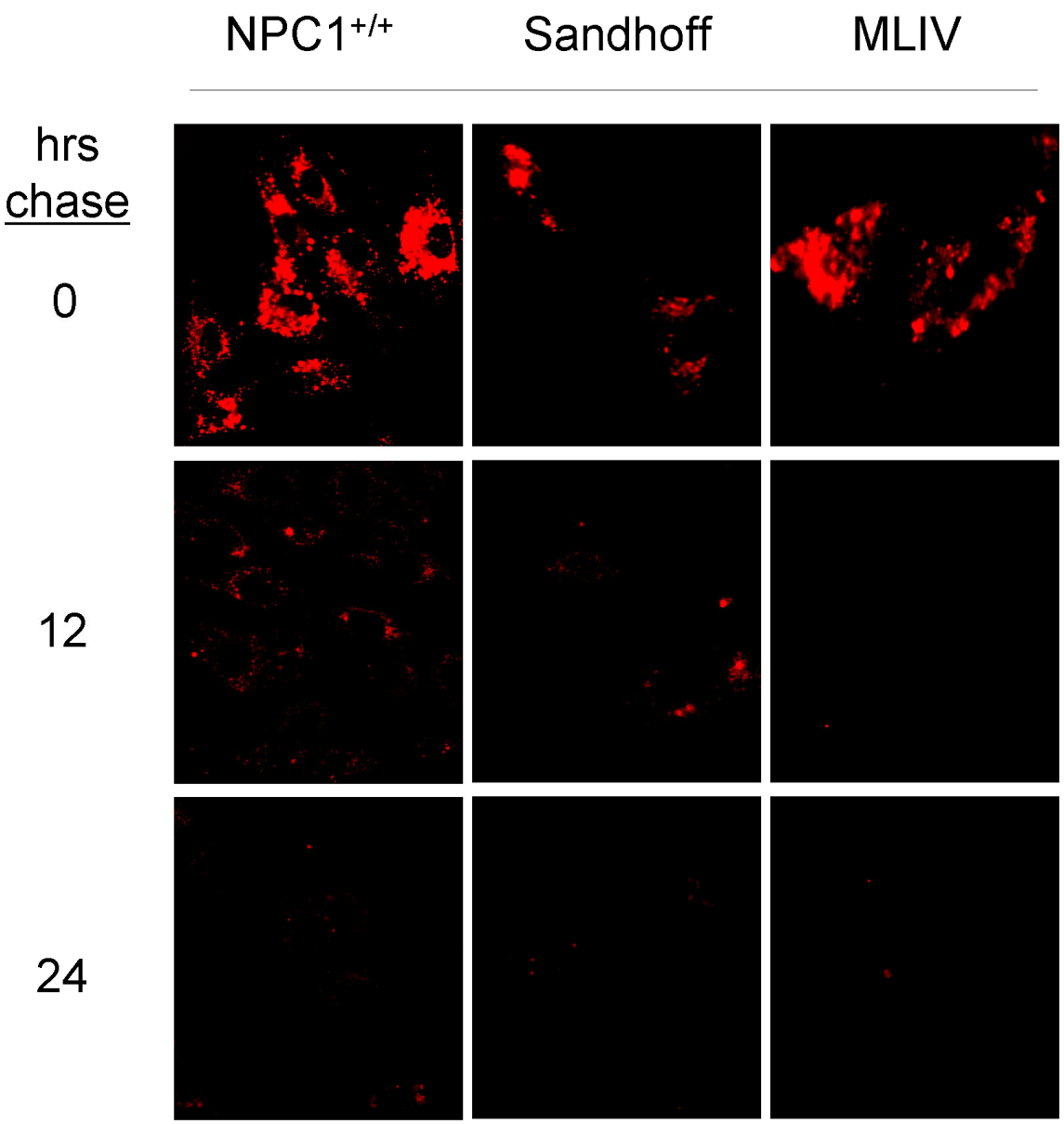

Figure 3.7. Lysosomal clearance of LTR is not impaired in lysosomal storage disorder fibroblasts mucolipidosis type IV (MLIV) and Sandhoff's disease. All cells show efficient clearance of LTR from lysosomes after a 24 h chase. NPC1$^{+/+}$ cells from Fig. 3.6 are included as a reference. All LTR images are representative of data collected from at least 3 independent experiments.

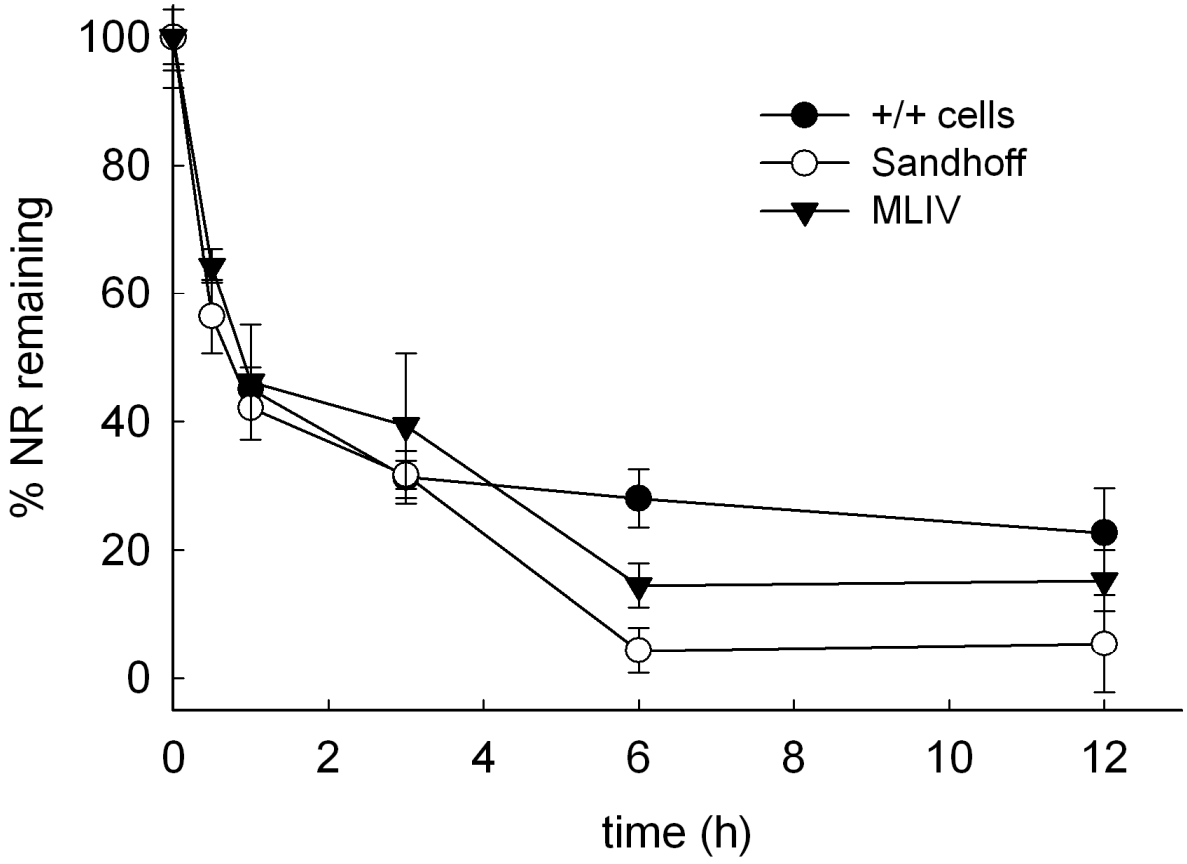

Figure 3.8. NR release is normal in cells with lysosome lipid buildup but functional NPC1 protein. Sandhoff's disease and MLIV had comparable release profiles to normal cells (data from Fig. 3.5A) after 12 hrs of chase in NR-free medium. Each time point represents the average ± S.D. of at least 3 individual measurements.

membrane [18; 20]. They have shown that increases in free intracellular (cytosolic) calcium ion (Ca^{2+}) levels stimulate lysosomal exocytosis [18; 21]. Furthermore, fusion was dependent on synaptotagmin VII, a SNARE protein required for membrane fusion [22]. The extent of fusion was determined by measuring the activity of lysosomal enzymes, such as β-hexosaminidase, that were released into the medium, as well as, the presence of lysosome proteins (lgp120) on the plasma membrane. Although Andrews and others have provided evidence for the existence of this secretory pathway, in the absence of high concentrations of exogenously supplied calcium ions the release of lysosomal enzymes is minimal [23]. If we assume that the lysosome-plasma membrane pathway is the sole contributor for lysosome exocytosis, then we would expect to see minimal radioactive dextran release in Figure 3.2 as demonstrated by the low amounts of lysosomal enzymes observed by Andrews. However, we observe significant exocytosis of dextran into the cell culture medium in normal cells, thus, there must be another contributing mechanism by which dextran and trapped amines can escape lysosomes.

Similar to work done by Andrews, J.P. Luzio and colleagues have described in detail the ability of lysosomes to fuse with other cellular components [24; 25]. In particular, Luzio has demonstrated that lysosomes can interact and fuse with late endosomes resulting in a hybrid organelle of intermediate properties. These content mixing events have been described in cell-free systems, as well as, in living cells [25; 26] The fusion of these organelles has

been shown to be dependent on a number of proteins, which to date include SNAP, SNARE, and Rab proteins, all of which are known to be involved in vesicle fusion [27]. From a trafficking perspective, Jahraus et al. has shown that lysosomes traffic their contents back to late endosomes in a retrograde manner and that this pathway is microtubule dependent [28]. The biological significance of these interactions is currently unknown; however, it has been proposed that this is one way that lysosome cargo can be released to the cell surface [19; 29]. Late endosomes are known to transiently interact with the Golgi apparatus via a vesicle mediated mechanism to return receptors, such as mannose-6-phosphate, which are necessary for the targeting of some proteins to endosome/lysosome compartments [30; 31]. Importantly, the Golgi apparatus is well-known for its functional role in the transport of proteins to the plasma membrane via secretory vesicles [32]. Thus, the interaction of lysosomes with late endosomes may provide an indirect pathway for lysosomal cargo release. In support of this mechanism, we have shown previously that these interactions can occur in normal cells treated with the model amine neutral red (Chapter 2, Section 2.6). A significant amount of late endosome markers were found colocalized with lysosomes in response to amine treatment. Furthermore, we showed that these interactions were NPC1 specific using siRNA and severely diminished in NP-C diseased cells using a FRET-based late endosome-lysosome fusion assay.

3.5. References

[1]I. Mellman, Endocytosis and molecular sorting. Annu Rev Cell Dev Biol 12 (1996) 575-625.

[2]Y. Gong, M. Duvvuri, M.B. Duncan, J. Liu, and J.P. Krise, Niemann-Pick C1 protein facilitates the efflux of the anticancer drug daunorubicin from cells according to a novel vesicle-mediated pathway. J Pharmacol Exp Ther 316 (2006) 242-7.

[3]S. Mukherjee, R.N. Ghosh, and F.R. Maxfield, Endocytosis. Physiol Rev 77 (1997) 759-803.

[4]A.M. Kaufmann, and J.P. Krise, Lysosomal sequestration of amine-containing drugs: Analysis and therapeutic implications. J Pharm Sci 96 (2007) 729-46.

[5]C. de Duve, T. de Barsy, B. Poole, A. Trouet, P. Tulkens, and F. Van Hoof, Commentary. Lysosomotropic agents. Biochem Pharmacol 23 (1974) 2495-531.

[6]H. Tamura, T. Takahashi, N. Ban, H. Torisu, H. Ninomiya, G. Takada, and N. Inagaki, Niemann-Pick type C disease: Novel NPC1 mutations and characterization of the concomitant acid sphingomyelinase deficiency. Mol Genet Metab 87 (2006) 113-21.

[7]X. Sun, D.L. Marks, W.D. Park, C.L. Wheatley, V. Puri, J.F. O'Brien, D.L. Kraft, P.A. Lundquist, M.C. Patterson, R.E. Pagano, and K. Snow, Niemann-Pick C variant detection by altered sphingolipid trafficking and correlation with

mutations within a specific domain of NPC1. Am J Hum Genet 68 (2001) 1361-72.

[8]M. Zhang, N.K. Dwyer, E.B. Neufeld, D.C. Love, A. Cooney, M. Comly, S. Patel, H. Watari, J.F. Strauss, 3rd, P.G. Pentchev, J.A. Hanover, and E.J. Blanchette-Mackie, Sterol-modulated glycolipid sorting occurs in niemann-pick C1 late endosomes. J Biol Chem 276 (2001) 3417-25.

[9]D. te Vruchte, E. Lloyd-Evans, R.J. Veldman, D.C. Neville, R.A. Dwek, F.M. Platt, W.J. van Blitterswijk, and D.J. Sillence, Accumulation of glycosphingolipids in Niemann-Pick C disease disrupts endosomal transport. J Biol Chem 279 (2004) 26167-75.

[10]E.B. Neufeld, M. Wastney, S. Patel, S. Suresh, A.M. Cooney, N.K. Dwyer, C.F. Roff, K. Ohno, J.A. Morris, E.D. Carstea, J.P. Incardona, J.F. Strauss, 3rd, M.T. Vanier, M.C. Patterson, R.O. Brady, P.G. Pentchev, and E.J. Blanchette-Mackie, The Niemann-Pick C1 protein resides in a vesicular compartment linked to retrograde transport of multiple lysosomal cargo. J Biol Chem 274 (1999) 9627-35.

[11]J.P. Davies, F.W. Chen, and Y.A. Ioannou, Transmembrane molecular pump activity of Niemann-Pick C1 protein. Science 290 (2000) 2295-8.

[12]J. Passeggio, and L. Liscum, Flux of fatty acids through NPC1 lysosomes. J Biol Chem 280 (2005) 10333-9.

[13]I.G. Ganley, and S.R. Pfeffer, Cholesterol accumulation sequesters Rab9 and disrupts late endosome function in NPC1-deficient cells. J Biol Chem (2006).

[14]M.M. Bradford, A rapid and sensitive method for the quantitation of microgram quantities of protein utilizing the principle of protein-dye binding. Anal Biochem 72 (1976) 248-54.

[15]D.C. Ko, M.D. Gordon, J.Y. Jin, and M.P. Scott, Dynamic movements of organelles containing Niemann-Pick C1 protein: NPC1 involvement in late endocytic events. Mol Biol Cell 12 (2001) 601-14.

[16]C.S. Chen, G. Bach, and R.E. Pagano, Abnormal transport along the lysosomal pathway in mucolipidosis, type IV disease. Proc Natl Acad Sci U S A 95 (1998) 6373-8.

[17]P.A. Bolhuis, J.G. Oonk, P.E. Kamp, A.J. Ris, J.C. Michalski, B. Overdijk, and A.J. Reuser, Ganglioside storage, hexosaminidase lability, and urinary oligosaccharides in adult Sandhoff's disease. Neurology 37 (1987) 75-81.

[18]A. Rodriguez, P. Webster, J. Ortego, and N.W. Andrews, Lysosomes behave as Ca2+-regulated exocytic vesicles in fibroblasts and epithelial cells. J Cell Biol 137 (1997) 93-104.

[19]T.E. Tjelle, A. Brech, L.K. Juvet, G. Griffiths, and T. Berg, Isolation and characterization of early endosomes, late endosomes and terminal lysosomes: their role in protein degradation. J Cell Sci 109 (Pt 12) (1996) 2905-14.

[20]N.W. Andrews, Regulated secretion of conventional lysosomes. Trends Cell Biol 10 (2000) 316-21.

[21]A. Reddy, E.V. Caler, and N.W. Andrews, Plasma membrane repair is mediated by Ca(2+)-regulated exocytosis of lysosomes. Cell 106 (2001) 157-69.

[22]I. Martinez, S. Chakrabarti, T. Hellevik, J. Morehead, K. Fowler, and N.W. Andrews, Synaptotagmin VII regulates Ca(2+)-dependent exocytosis of lysosomes in fibroblasts. J Cell Biol 148 (2000) 1141-49.

[23]C. Huynh, and N.W. Andrews, The small chemical vacuolin-1 alters the morphology of lysosomes without inhibiting Ca2+-regulated exocytosis. EMBO Rep 6 (2005) 843-7.

[24]J.P. Luzio, P.R. Pryor, and N.A. Bright, Lysosomes: fusion and function. Nat Rev Mol Cell Biol 8 (2007) 622-32.

[25]B.M. Mullock, J.H. Perez, T. Kuwana, S.R. Gray, and J.P. Luzio, Lysosomes can fuse with a late endosomal compartment in a cell-free system from rat liver. J Cell Biol 126 (1994) 1173-82.

[26]N.A. Bright, M.J. Gratian, and J.P. Luzio, Endocytic delivery to lysosomes mediated by concurrent fusion and kissing events in living cells. Curr Biol 15 (2005) 360-5.

[27]B.M. Mullock, C.W. Smith, G. Ihrke, N.A. Bright, M. Lindsay, E.J. Parkinson, D.A. Brooks, R.G. Parton, D.E. James, J.P. Luzio, and R.C. Piper, Syntaxin 7 is localized to late endosome compartments, associates with Vamp 8, and Is required for late endosome-lysosome fusion. Mol Biol Cell 11 (2000) 3137-53.

[28]A. Jahraus, B. Storrie, G. Griffiths, and M. Desjardins, Evidence for retrograde traffic between terminal lysosomes and the prelysosomal/late endosome compartment. J Cell Sci 107 (Pt 1) (1994) 145-57.

[29]E.J. Blott, and G.M. Griffiths, Secretory lysosomes. Nat Rev Mol Cell Biol 3 (2002) 122-31.

[30]W.M. Rohn, Y. Rouille, S. Waguri, and B. Hoflack, Bi-directional trafficking between the trans-Golgi network and the endosomal/lysosomal system. J Cell Sci 113 (Pt 12) (2000) 2093-101.

[31]W.G. Mallet, and F.R. Maxfield, Chimeric forms of furin and TGN38 are transported with the plasma membrane in the trans-Golgi network via distinct endosomal pathways. J Cell Biol 146 (1999) 345-59.

[32]J.E. Rothman, Mechanisms of intracellular protein transport. Nature 372 (1994) 55-63.

Chapter 4

NPC1-dependent regulation of lysosomal amine-content

4.1. Introduction

Our laboratory, as well as many others has shown the clearance of trapped molecules from lysosomes is severely impaired in NP-C disease cells [1; 2; 3; 4]. Considering there are many examples of lysosome secretion pathways that require stimulation by a cargo or signal (see below) we asked: is there a "primary cargo" that regulates this NPC1-mediated lysosomal egress pathway? Thus, the objective of this chapter is to address the hypothesis that NPC1 is responding to lysosomotropic amines and regulating their concentrations in lysosomes. Furthermore, we provide evidence that the clearing of lysosome contents to the extracellular space is accomplished through a novel NPC1-mediated lysosome-late endosome pathway.

There exist specialized cells in which secretion of lysosome contents to the extracellular space can be stimulated [5]. These lysosomes are referred to as secretory lysosomes and differ very little in their properties compared to conventional lysosomes [6]. Cells that possess secretory lysosomes include neutrophils, platelets and mast cells among many others, which secrete chemoattractants, clotting factors and histamine, respectively [5; 7; 8; 9]. The signals and receptors that stimulate the release of these cargos have been identified and well characterized.

For most cells, however, lysosomes are considered the terminal endpoint for endocytosis and are not regarded as secretory organelles. In contrast to this,

we and others have shown that macromolecules (i.e. dextran) which localize to lysosomes, can efficiently escape to the cell periphery (Chapter 3, Figure 3.1 and 3.2) [1; 10; 11]. Griffiths suggested that lysosomes can interact with late endosomes *in vivo* forming hybrid organelles [12]. The physiological relevance for the formation of hybrid organelles, according to Griffiths, is for lysosomes to deliver enzymes to late endosomes for the digestion of endocytosed materials. However, as a consequence of content mixing between the two organelles, other molecules such as dextran are delivered back to late endosomes [13; 14; 15]. Although these results are novel, information concerning the signals or exact molecular stimuli that trigger trafficking events and ultimately the removal of these cargos from conventional lysosomes is lacking.

In this chapter, we utilize a novel FRET assay for late endosome-lysosome fusion to assess the ability of lysosomotropic amines to stimulate hybrid organelle formation in an NPC1-dependent manner. From previous immuofluorescence data taken in the presence of NR, we hypothesize that the administration of lysosomotropic amines will lead to an increased rate of hybrid organelle formation. Furthermore, we hypothesize that as a result of more late endosome-lysosome fusion events, there will be more secretion of lysosome contents to the plasma membrane. To examine this possibility we will utilize a previously described radioactive dextran release assay in the presence of amines in both normal and NP-C cell lines [2].

4.2. Materials and methods

4.2.1. Reagents

[^{3}H]-dextran (70,000MW; 125 μCi/mg) was purchased through American Radiolabeled Chemicals (St. Louis, MO). Scintiverse-BD liquid scintillation cocktail and morpholine were from Fisher Scientific (Pittsburgh, PA). Neutral red, imidazole, spermine, nocodazole and concanamycin A were obtained from Sigma-Aldrich (St. Louis, MO). Imipramine, chlorpromazine and amiodarone were from MP Biomedicals (Solon, OH). U18666A was from Biomol (Plymouth Meeting, PA). Fura2-AM, Fura2 Imaging Calibration Kit, Lysotracker red DND-99, rhodamine 123, biotinylated dextran amine, and Alexa Fluor 555 and 647 succinimidyl esters were obtained from Invitrogen (Eugene, OR). Carboxylate-modified polystyrene beads were purchased from Polysciences (Warrington, PA). All other reagents unless otherwise specified were purchased through Sigma-Aldrich.

4.2.2. Cell culture and conditions

Normal human fibroblasts (CRL-2076, designated NPC1$^{+/+}$) and Niemann-Pick Type C disease fibroblasts (NPC1$^{-/-}$) were cultured as previously described (Chapters 2, Sections 2.2.2). For all experiments, cells were used before passage 5 and plated 24 hrs prior to evaluations to permit adherence. For assays requiring fluorescence measurements, phenol red-free DMEM medium, supplemented the same as regular DMEM, was used to minimize background signal.

4.2.3. Western blotting and densitometry

Western blots were performed as previously described in our laboratory and as described in Chapter 2, Section 2.2.3. β-actin primary antibodies were included to control for protein loading (all primary antibodies were diluted 1:250 in 5% milk-in-TBS). Secondary HRP-conjugated antibodies were used at 1:1000 dilutions. All steps were performed at room temperature unless otherwise stated. Densitometry was performed as previously described in Chapter 2, Section 2.2.3.

4.2.4. Dextran secretion assay

Fibroblasts were plated at 3 x 10^5 cells per well in a 6-well culture plates. Cells were incubated with 50 µCi/mL of [^{3}H]-dextran in addition to 0.9 mg/mL non-radioactive dextran of the same molecular weight in complete medium at 37^{o}C for 3 hrs and subsequently washed with warm media (4X). Cells were then chased in dextran free media and the amount of [^{3}H]-dextran secreted into the media was analyzed at indicated time points. At the end of the assay, the fibroblast monolayer was dissolved using a solution 50 mM Tris, 150 mM NaCl, and 1.0% NP-40 to determine total dextran uptake in each well. To address the non-specific association of radioactive dextran with the cell monolayer on total amounts released, experiments were repeated at 4^{o}C after the initial dextran incubation at 37^{o}C for 4 hrs and curve fit to obtain later data points. These data points were subtracted from the same points from experiments carried out at

37°C. The cumulative amount of dextran released into the media is given as a percentage of the total amount of dextran endocytosed. Quantitation of [^{3}H]-dextran at each time point was performed using a liquid scintillation counter (Beckman LS5000; Beckman Coulter, Fullerton, CA) and Scintiverse-BD liquid scintillation cocktail.

For assays that included treatments with various agents, given concentrations were incubated concomitantly with [^{3}H]-dextran for 3 hrs, washed and chased as described. Analysis and non-specific release correction were performed as described above.

4.2.5. Cytosolic calcium concentration determination

Determination of cytosolic free calcium levels was performed in living cells using a membrane permeable derivative of the fluorescent calcium sensitive dye, FURA2 (FURA2-AM). First, 50 x 10^4 cells were exposed to 2.5 μM FURA2-AM ester for 30 min at 37°C. The uptake of FURA2 was observed to be similar in both normal and NP-C fibroblasts (data not shown). The excitation spectra of FURA2 from 300-425 nm was taken using a Photon Technologies International (Birmingham, NJ) Ratiomaster microscope-mounted spectrofluorimeter with PMT detection. Filters and dichroic mirrors specific to FURA2 (Chroma) were used for selection of FURA2 emission intensities.

The excitation spectrum of FURA2 changes upon binding of free calcium ions in a concentration dependent manner [16; 17]. An example of this is seen in Figure 4.8A. Using pre-made buffers with varying concentrations of free calcium ions in the presence of FURA2, we constructed a standard curve (see Fig. 4.8B). This was accomplished by taking the ratio of FURA2 emission intensities at the 340 and 380 nm excitation wavelengths. The ratio of 340/380 nm was then used to calculate unknown calcium concentrations with or without amine pre-treatments.

4.2.6. Late endosome-lysosome fusion assay

The fusion between late endosomes and lysosomes was evaluated in fibroblasts using a method described by Jahrus *et al.* [13] with modifications to allow quantitative assessments based on fluorescence resonance energy transfer (FRET). Assays were performed exactly as described in Appendix I and Chapter 2, Section 2.2.3. Briefly, biotinylated dextran, fluorescently labeled with Alexa Fluor 647 (FRET acceptor) was incubated with 5 x 10^4 cells and localized to lysosomes using an optimized pulse/chase scheme for dextran. Next, streptavidin-conjugated latex beads (0.792 ± 0.037 μm) fluorescently labeled with Alexa Fluor 555 (FRET donor) were localized to late endosomes per Jahrus *et al.* [13]. To detect fusion, FRET measurements were made using a Photon Technologies International (Birmingham, NJ) Ratiomaster microscope-mounted spectrofluorometer with PMT detection. Experimental details can be found in Appendix I.

For treatments, cells were administered compounds immediately after the localization of the latex bead to the late endosome (after a 2 h pulse) by spiking in a known concentration of compound into the incubation medium. Fluorescence intensity measurements were initiated immediately thereafter.

4.3. Results

4.3.1. Certain lysosomotropic amines stimulate NPC1-mediated release of lysosome cargo

In this chapter we propose that NPC1 plays an important functional role in regulating the concentrations of amines that are sequestered in lysosomes. If this is the case, NPC1 should "sense" the amine accumulation and subsequently facilitate their clearance. To evaluate this we examined the influence of exogenously supplied amines on the release of a membrane-impermeable cargo from lysosomes. Previously, we had shown that the trafficking of dextran was severely impeded by NPC1 malfunction (Fig. 3.2). Here we evaluate the influence of amines on the NPC1-mediated lysosomal egress of 10,000 MW dextran polymers. We specifically localized [^{3}H]-dextran to terminal endocytic compartments and evaluated its release into the cell culture medium as a function of time in both normal and NPC1$^{-/-}$ fibroblasts. The amount of dextran released at the 24 h time point was found to be suitable for representing differences between normal and NP-C cells since this was the time point that showed the greatest difference between the two cell lines. This was also true for NR-treated cells as shown in Figure 4.1, confirming the 24 h time point as suitable for determining secretion differences upon treatments. Therefore, this single time point measurement was obtained for all subsequent experiments evaluating the influence of amines and other molecules on dextran release. For comparison purposes, the amount of dextran released at the 24 h time point for the normal untreated NPC1$^{+/+}$ fibroblasts was set to zero (Fig. 4.2). Accordingly,

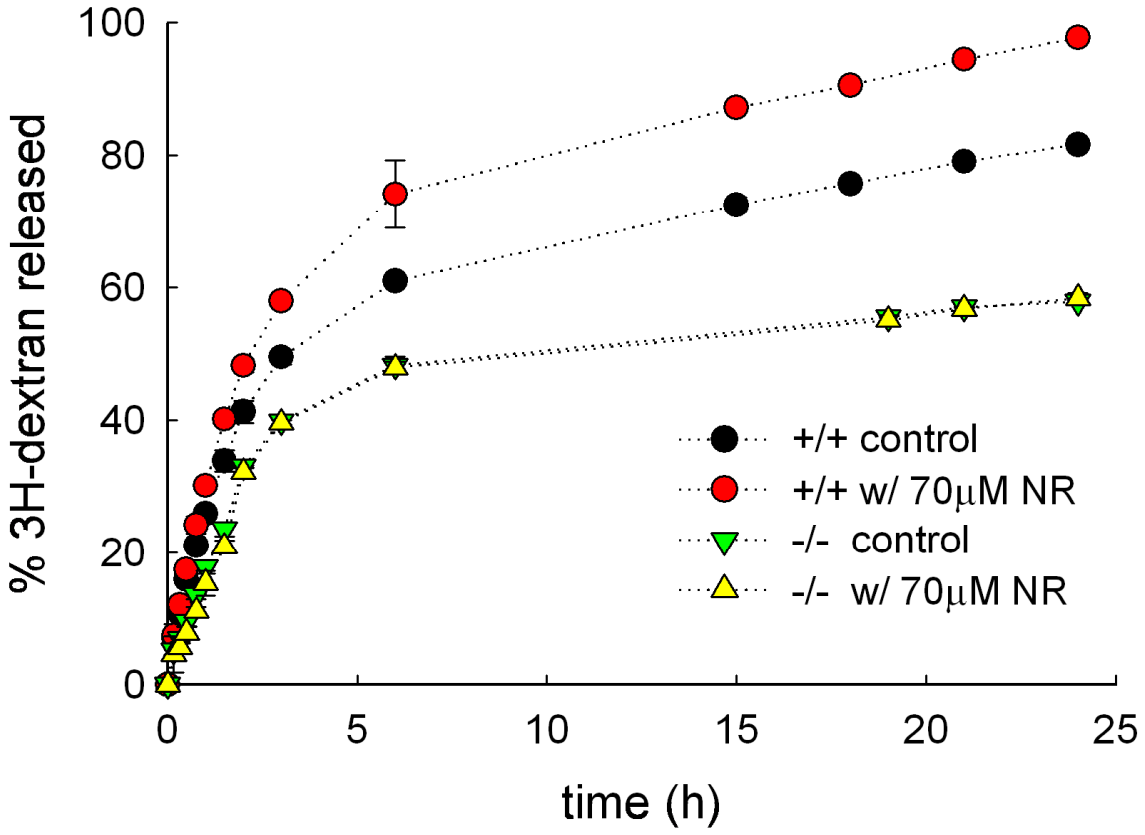

Figure 4.1. ^{3}H-dextran release profiles for cells treated with neutral red (NR). Concominant NR treatments increased the amount of dextran secreted in NPC1$^{+/+}$ cells but not in NPC1$^{-/-}$ cells. Data is the average of at least 6 independent experiments ± S.D.

molecules having a stimulatory effect (resulting in the release of more dextran into the culture medium) will have positive deviations from the control. Alternatively, those treatments that inhibit dextran secretion relative to control cells will have negative deviations.

Three lysosomotropic amines, NR, imidazole (IMDZ), and morpholine (MOR), had the unique ability to significantly stimulate the release of dextran from lysosomes of normal fibroblasts when administered at high concentrations (Fig. 4.2). The reason for the administration of such high concentrations is due to the physicochemical properties of these molecules. Although the molecules are all weakly basic, they have unfavorable logP values for membrane permeability (see Table I). The concentrations used have been shown to sequester enough compound inside the lysosome to cause vacuolization [18].

Since we were observing apparent stimulation of exocytosis of lysosomal contents, we investigated possible reasons for this increase upon amine exposure. Considering the relatively short incubation time with these reagents (6 hrs), up-regulation of NPC1 expression should not have had time to occur. As expected, NPC1 levels similar to untreated cells were observed by Western blot analysis and densitometry (Fig. 4.3). When non-vacuolizing amine concentrations were administered, the same degree of dextran release was not observed. This was observed for low concentrations of NR and MOR (Fig. 4.4) and showed there was a concentration dependency for NPC1 involvement.

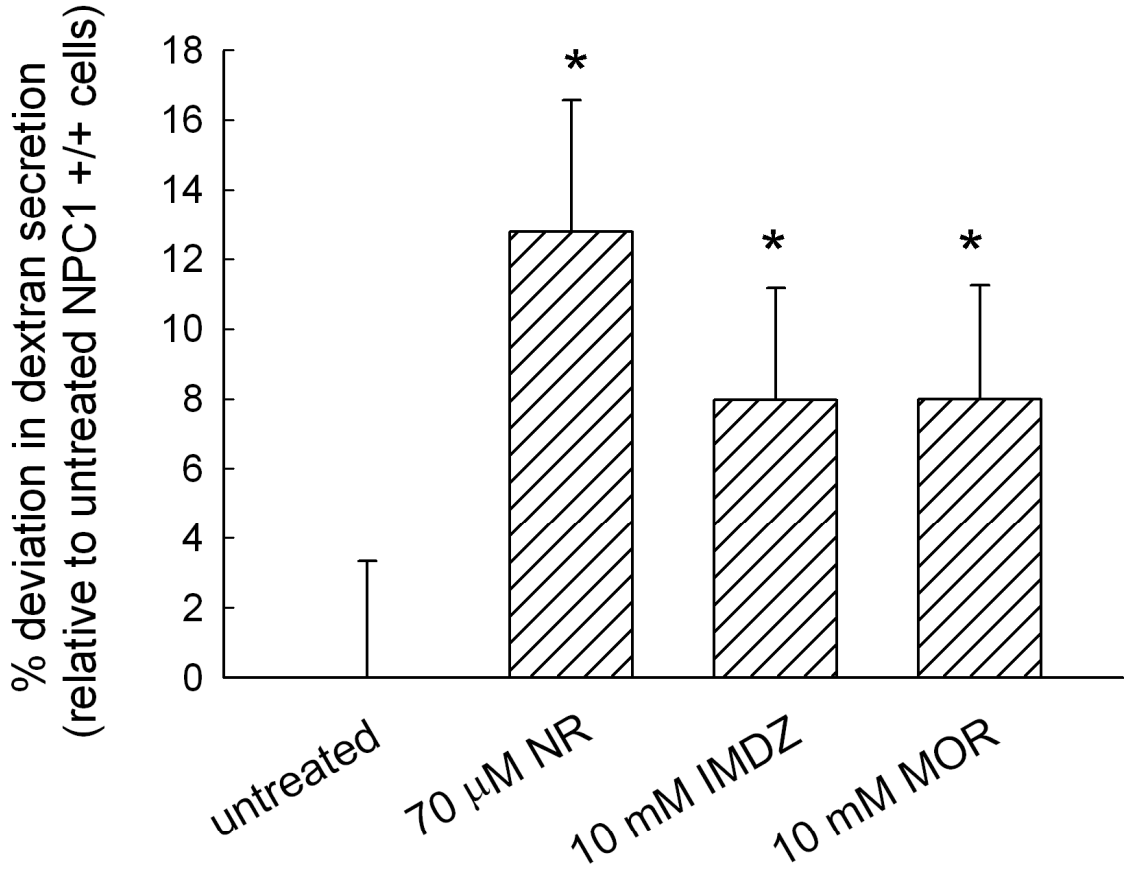

Figure 4.2. Lysosomotropic amines can stimulate the function of NPC1 in the clearance of lysosomal contents. Bars represent average ± S.D. for the percent deviation in dextran amount released relative to untreated $NPC1^{+/+}$ fibroblasts (value set to zero). Stimulation of dextran release was observed for the lysosomotropic amines neutral red (70 μM, NR, n=12), morpholine (10 mM, MOR, n=8) and imidazole (10 mM, IMDZ, n=7) in $NPC1^{+/+}$ fibroblasts relative to the untreated control (*, $p < 0.001$ by unpaired t-test).

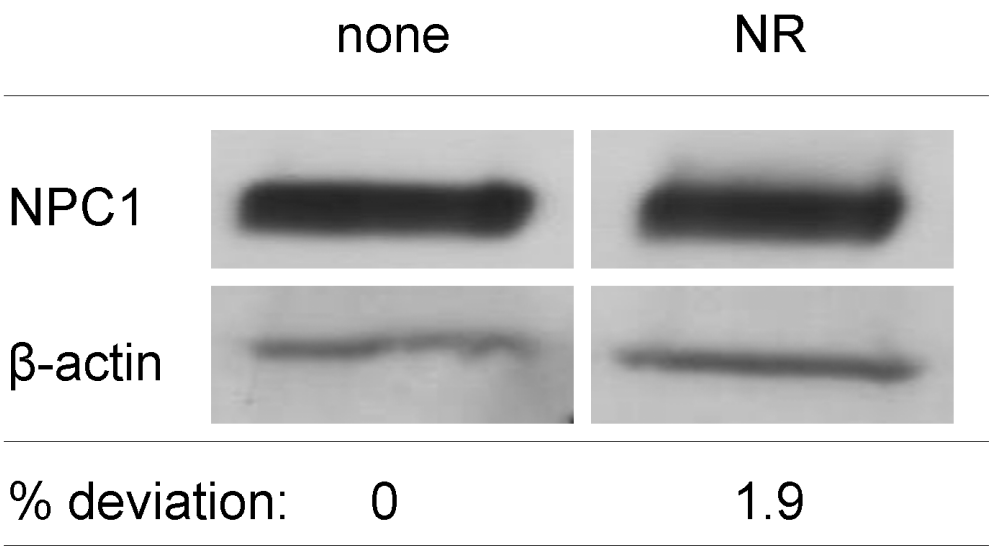

Figure 4.3. NR treatment in NPC1$^{+/+}$ fibroblasts does not dramatically increase NPC1 protein expression. Untreated cells or cells treated with 70 μM NR for 6 hrs were subjected to Western blot and densitometry analysis. NR-treated cells contained only 1.9% more NPC1 protein compared to untreated cells.

It is important to note that not every amine induced secretion. For example, rhodamine 123 (R123), a weakly basic amine that is known to accumulate into mitochondria instead of lysosomes [19], did not induce or inhibit NPC1-mediated secretion (Fig. 4.5). In addition to R123, we examined the effect of vacuole formation by the non-amine sucrose on ^{3}H-dextran secretion and found no statistically significant change (Fig. 4.5).

Somewhat paradoxically, it is well known that certain amphiphilic hydrophobic amines, instead of having a stimulatory role, cause lysosomal trafficking defects [20]. Many of these compounds induce phenotypes similar to NP-C disease (hyperaccumulation of lipids), of which the best known is the weakly basic molecule U18666A (see Figure 4.14) [21; 22]. As anticipated, U18666A had a negative influence on NPC1-mediated dextran secretion in normal NPC1$^{+/+}$ fibroblasts (Fig. 4.6). It is likely that such amines elicit an inhibitory function unrelated to the molecule's propensity for lysosomal sequestration (see Discussion).

As expected, the release of dextran from NPC1$^{-/-}$ fibroblasts was less than that from normal untreated fibroblasts and similar to that from U18666A-treated normal NPC1$^{+/+}$ fibroblasts (Fig. 4.7). Importantly, the amines found to have stimulatory effects on NPC1-mediated secretion in normal cells had no significant impact on dextran release from NPC1$^{-/-}$ cells, which illustrates the specificity of the selected amines for NPC1 (Fig. 4.7).

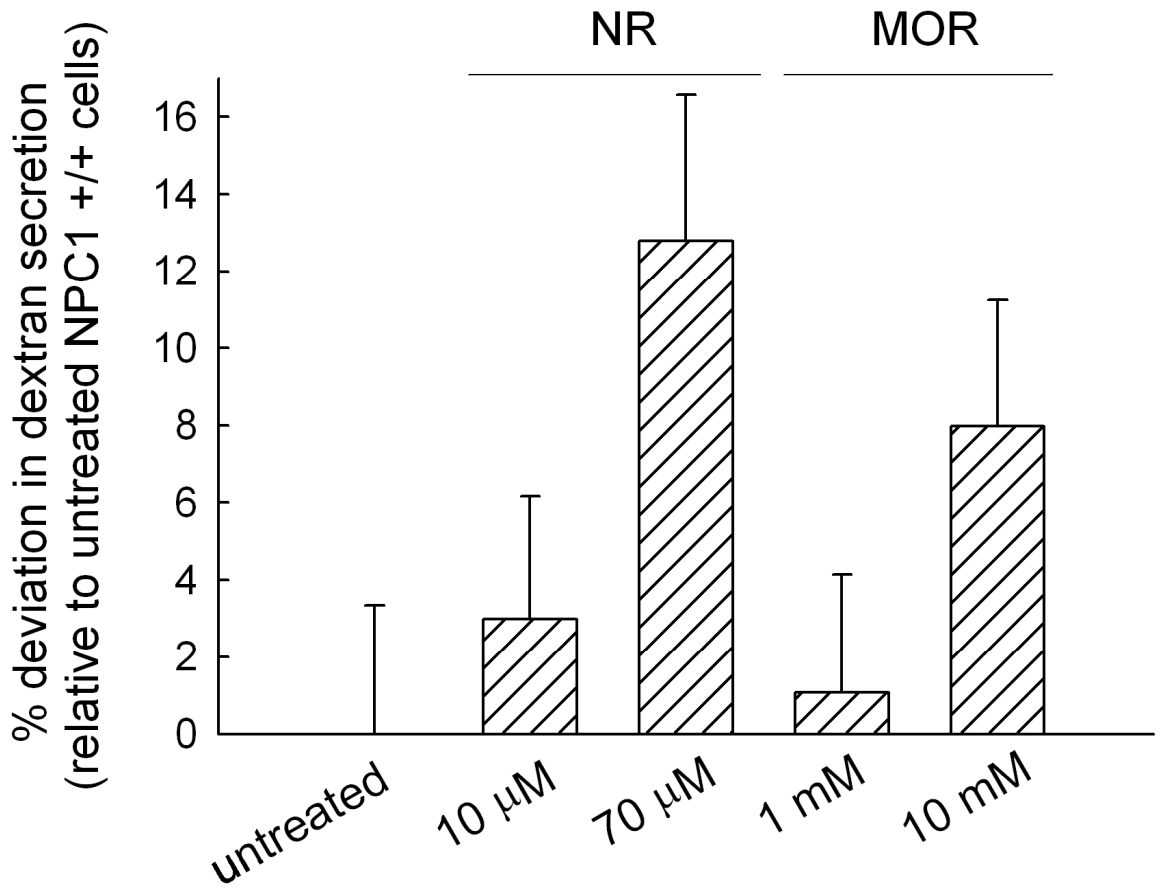

Figure 4.4. Lower concentrations of amine treatments have no effect on dextran secretion. Bars represent average ± S.D. for the percent deviation in dextran amount released relative to untreated NPC1$^{+/+}$ fibroblasts (value set to zero). Stimulation of dextran release was observed for higher concentrations of the amines neutral red (70 μM, NR, n=12) and morpholine (10 mM, MOR, n=8) but not for 10 μM NR (n = 6) and 1 mM MOR (n = 3) relative to the untreated control.

These results demonstrate that select lysosomotropic amines can stimulate NPC1-mediated release of lysosomal cargo to the plasma membrane. There are at least two different pathways that lysosomal contents (i.e., dextran) could be trafficked to the cell surface: direct fusion with the plasma membrane and retrograde transport to other compartments such as late endosomes. Previous studies by Reddy and colleagues had shown that stimulation of lysosome secretion was mediated by elevations in cytosolic Ca^{2+} concentrations and the lysosomal protein synaptotagmin VII [23]. Furthermore, it has been shown that the accumulation of weak bases in lysosomes, such as ammonia and chloroquine, can elevate the lumenal pH [24; 25]. Lysosome pH increases have been linked to increases in cytosolic calcium levels [26]. To determine if the stimulation observed in ^{3}H-dextran release studies was due to increased cytosolic Ca^{2+} concentrations upon amine exposure and subsequent fusion of lysosomes with the plasma membrane we examined if the amines tested caused elevations in cytosolic Ca^{2+} levels. Interestingly, none of the stimulatory amines were able to significantly change cytosolic Ca^{2+} levels. Morpholine treatments are shown as an example in Figure 4.9 for both cell lines.

4.3.2. Certain lysosomotropic amines stimulate NPC1-mediated formation of the hybrid organelle compartment

Ko et al. have suggested that NPC1 may facilitate the release of lysosomal cargo through a late endocytic hybrid organelle [3]. Therefore, we investigated if the stimulatory amines had an impact on the creation of a

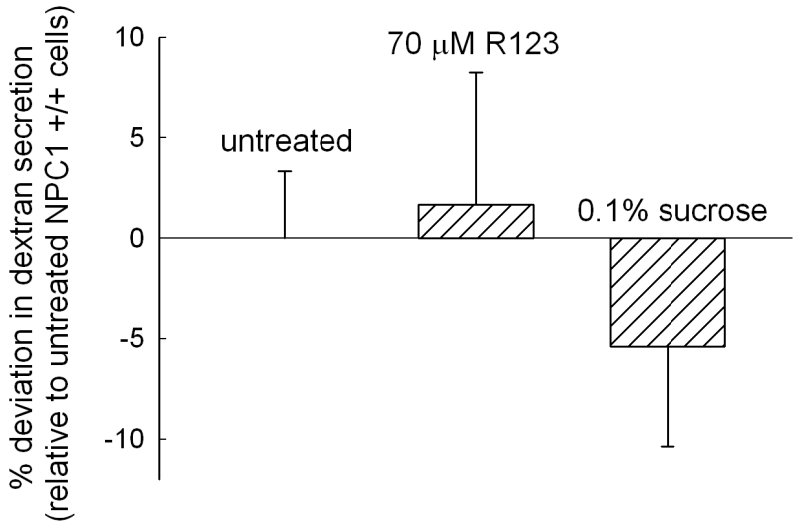

Figure 4.5. Relative dextran release amounts for sucrose and rhodamine-123. Amine-containing molecules that are known not to accumulate in the lysosome, such as rhodamine-123 (R123, 70 μM, n=7), had no effect on dextran release. The formation of vacuoles with sucrose (0.1% w/v, n=4) had no statistically significant influence on dextran secretion. Bars represent average ± S.D. for the percent deviation in dextran amount released relative to untreated NPC1$^{+/+}$ fibroblasts (value set to zero).

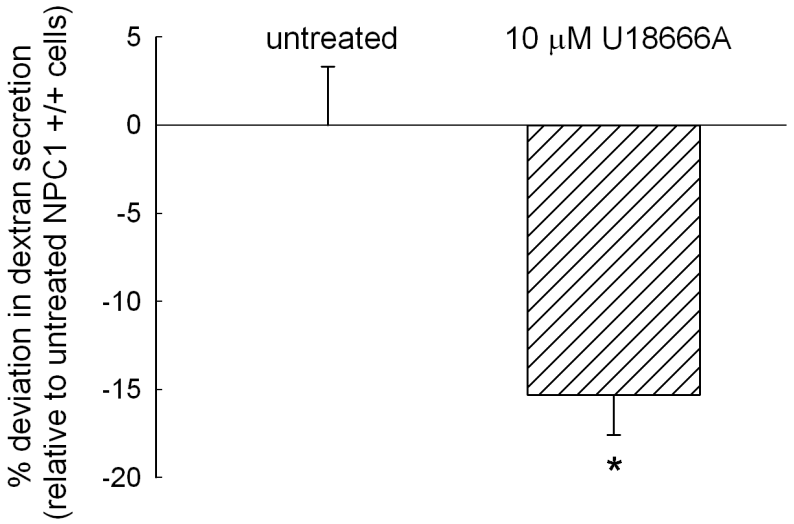

Figure 4.6. Relative dextran release amounts for U18666A. The hydrophobic amine U18666A (10 μM, n=7) inhibited NPC1-mediated dextran secretion in normal cells. Differences were statistically different (*, $p < 0.001$ by unpaired t-test). Bars represent average ± S.D. for the percent deviation in dextran amount released relative to untreated NPC1$^{+/+}$ fibroblasts (value set to zero).

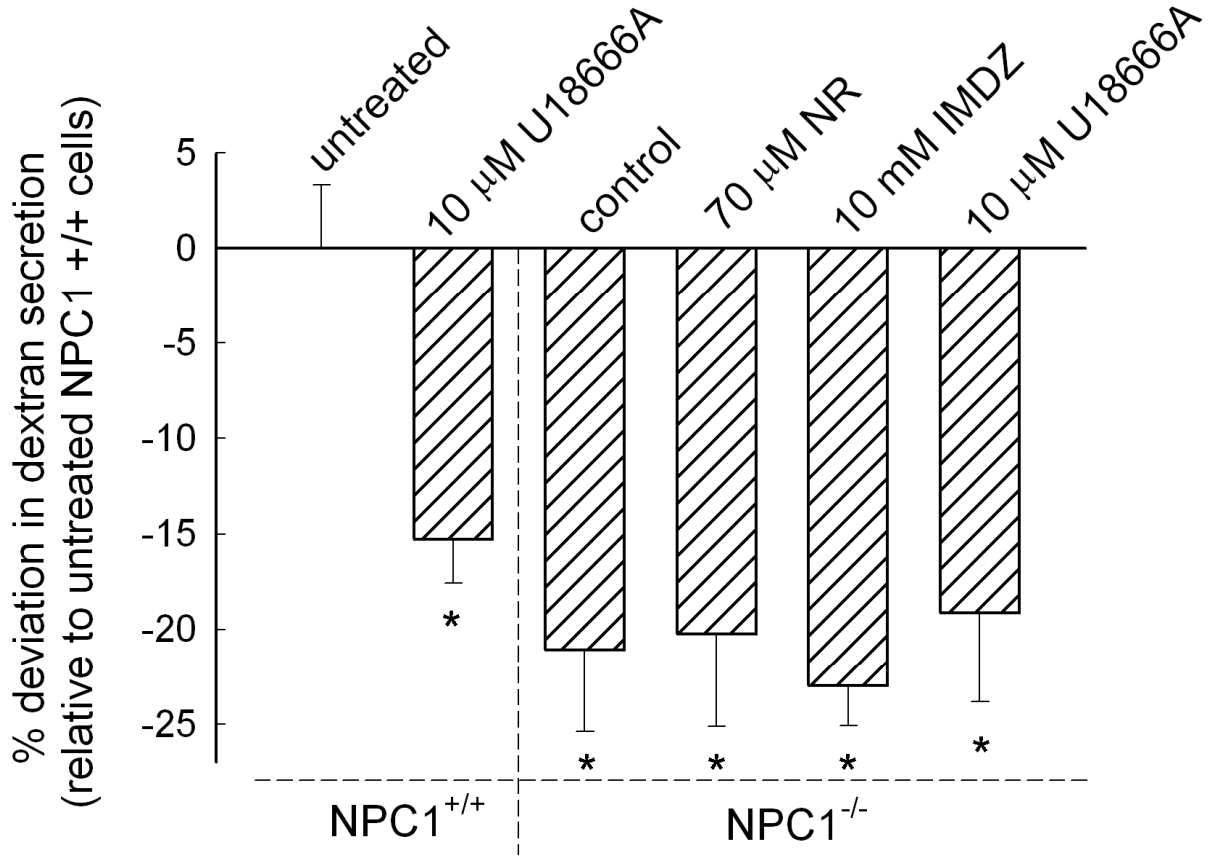

Figure 4.7. Amine treatments have no effect on NPC1$^{-/-}$ impaired dextran secretion. Stimulation of dextran release was not observed for the amines neutral red (70 μM, NR, n=12) and imidazole (10 mM, MOR, n=8) in NPC1$^{-/-}$ cells unlike normal cells in Fig. 4.2. All treatments were statistically different when compared to untreated NPC1$^{+/+}$ control cells (*, $p < 0.001$ by unpaired t-test).

lysosome/late endosome hybrid organelle. To evaluate this fusion event, we utilized a concept for studying late endosome/lysosome fusion originally described by Jahraus et al. [13]. The approach involves the localization of specific tracers to each of these compartments and observation of their interactions. In Jahraus' method, terminal lysosomes were loaded with sucrose to form sucrosomes. Next, late endosomes were specifically populated with endocytosed latex beads (~800 nm diameter) that were covalently coupled to invertase. These beads have been shown not to reach terminal lysosomes due to an apparent size restriction in this transport step [13; 27]. The fusion of late endosomes with lysosomes was observed by the disappearance of sucrosomes as sucrose was enzymatically converted into fructose and glucose, which is subsequently transported out of the lysosome by membrane porters. In our modified method, we utilized fluorescence resonance energy transfer (FRET) to quantitatively evaluate the fusion event in real time. This was accomplished by endocytosing a biotinylated dextran (10,000 MW), covalently labeled with the FRET acceptor Alexa Fluor 647, into lysosomes using the same pulse-chase scheme described previously (Section 3.2.3.1). Subsequently, a streptavidin-conjugated latex bead (~800 nm diameter) tagged with the FRET donor Alexa Fluor 555 was added to cells to label late endosomes. We evaluated the appearance of the FRET signal in untreated normal fibroblasts and cells treated with amines. The lysosomotropic amines IMDZ and MOR stimulated retrograde fusion in normal cells (Fig. 4.10) and had no influence on $NPC1^{-/-}$ fibroblasts (Fig. 4.11). U18666A-treated normal fibroblasts had hybrid organelle formation rates

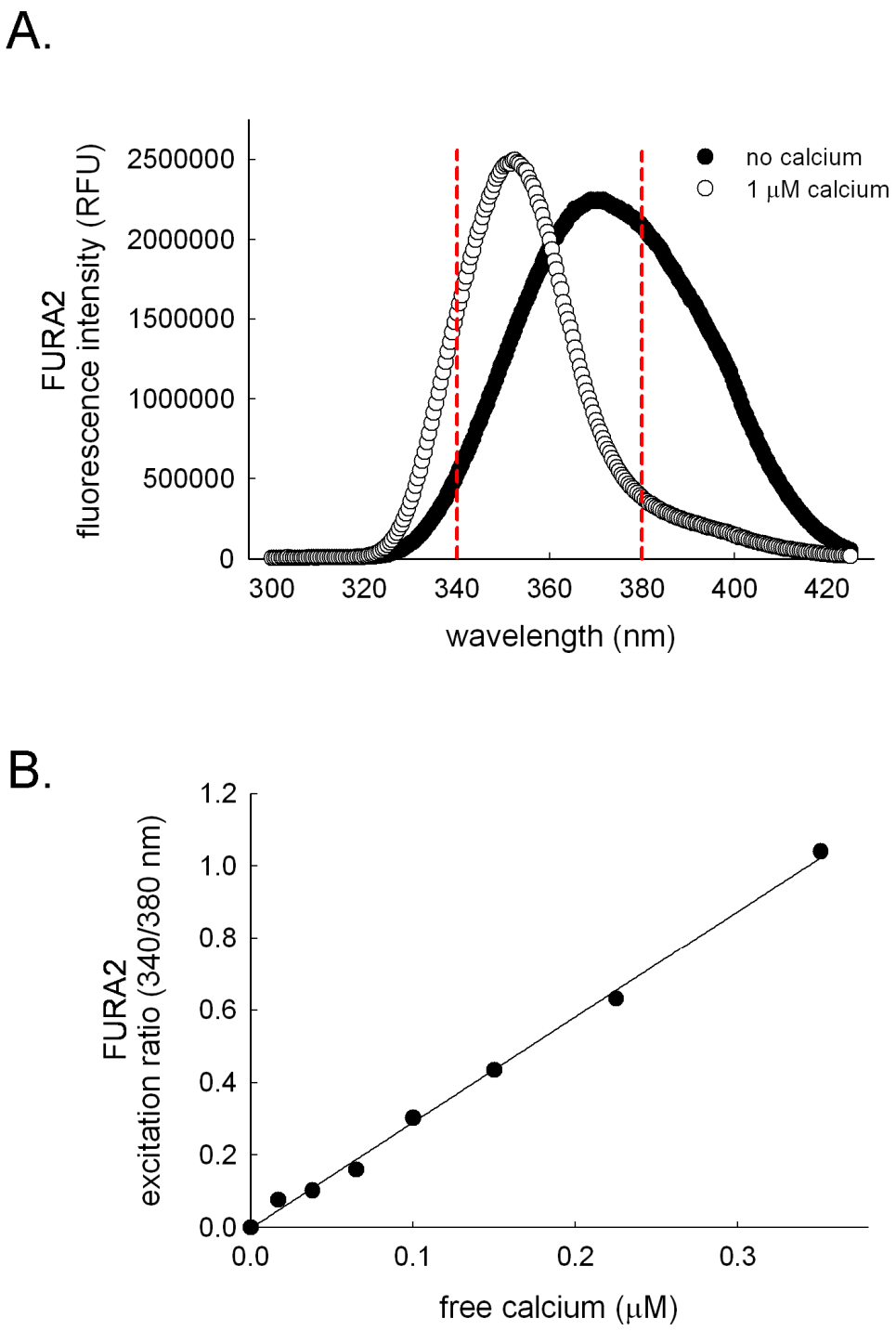

Figure 4.8. Cytosolic calcium determination using FURA2. (A) FURA2 fluorescence properties as a function of increasing calcium concentrations. The ratio of fluorescence intensities at ex. 340 and 380 nm (red) were used to construct a standard curve (B) for determination of unknown calcium levels in cells.

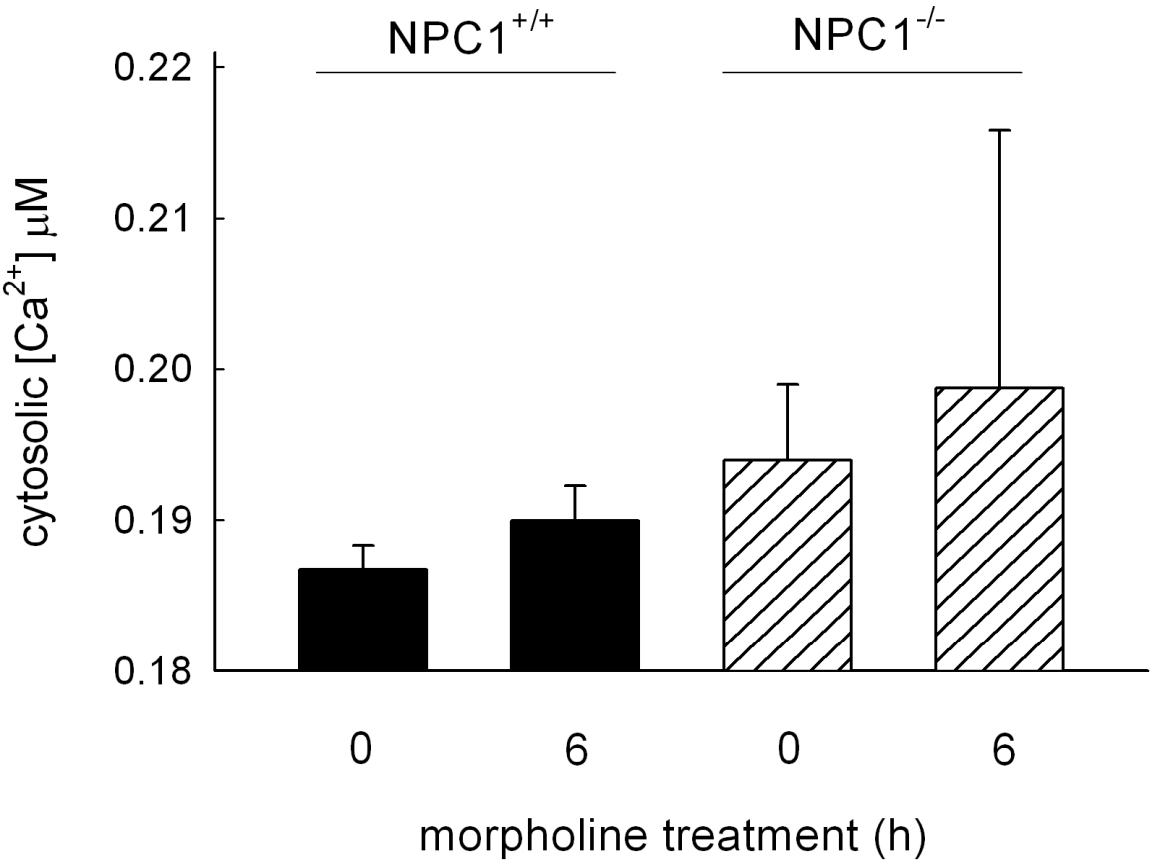

Figure 4.9. Amine treatments do not significantly alter cytosolic calcium levels. The calcium sensitive dye FURA2 was used to evaluate calcium concentrations in amine-treated (n = 6) or untreated (n = 6) cells. $NPC1^{+/+}$ and $NPC1^{-/-}$ cells were exposed to the exocytosis stimulating amine morpholine for 6h and cytosolic calcium levels determined.

that were similar to those of NPC1$^{-/-}$ fibroblasts, which showed minimal hybrid organelle formation regardless of treatment (Fig. 4.12). Furthermore, we investigated other cationic amphiphillic amines similar in structure to U18666A, imipramine, chlorpromazine, and amiodarone, to determine if inhibition of hybrid organelle formation was specific to U18666A. We found that all of these molecules had a negative impact on hybrid organelle formation in normal fibroblasts after 3 h of exposure (Fig. 4.12). The requirement of microtubules in this fusion step was shown by the decrease in FRET signal with nocodazole-treated NPC1$^{+/+}$ fibroblasts and was used as a control (Figs. 4.10 and Appendix I). It was not possible to evaluate the effects of R123 or NR on hybrid organelle formation as was done in dextran release studies (Figs. 4.2 and 4.5), since their intrinsic fluorescence interfered with the spectral properties of Alexa Fluor 555.

4.4. Discussion

Stimulation of direct lysosome exocytosis to the plasma membrane has been shown to occur in the presence of high cytosolic Ca^{2+} concentrations [28; 29; 30; 31]. The cytosolic concentration increase needed for stimulation of lysosome exocytosis is approximately 1 μM above basal levels [28]. Accumulation of weak bases in lysosomes has been shown to increase cytosolic levels of calcium [26]; however, the amine-stimulated release of lysosomal cargo described in this chapter does not appear to involve direct fusion with the plasma membrane since we do not observe elevations in free cytosolic Ca^{2+} upon administration of the weakly basic amine morpholine (Fig. 4.9). The data presented here are consistent with a mechanism whereby amines accumulate into lysosomes and stimulate the NPC1-mediated formation of a hybrid organelle that results from fusion between late endosomes and lysosomes. This statement is supported by several different experimental approaches that all show enhanced colocalization of lysosomal and late endosomal markers in the presence of amines, which was only observed in NPC1-competent cells (Figs. 2.6, 2.8, and 4.10).

Considering the fact that lysosomes are much denser than hybrid organelles, there must be steps involved in hybrid organelle fission that function to reduce membrane content. This follows from the fact that if such reformation never occurred, all of the cell's lysosomes would be "used up" in hybrid organelle formation. In support of this, Mullock et al. have demonstrated

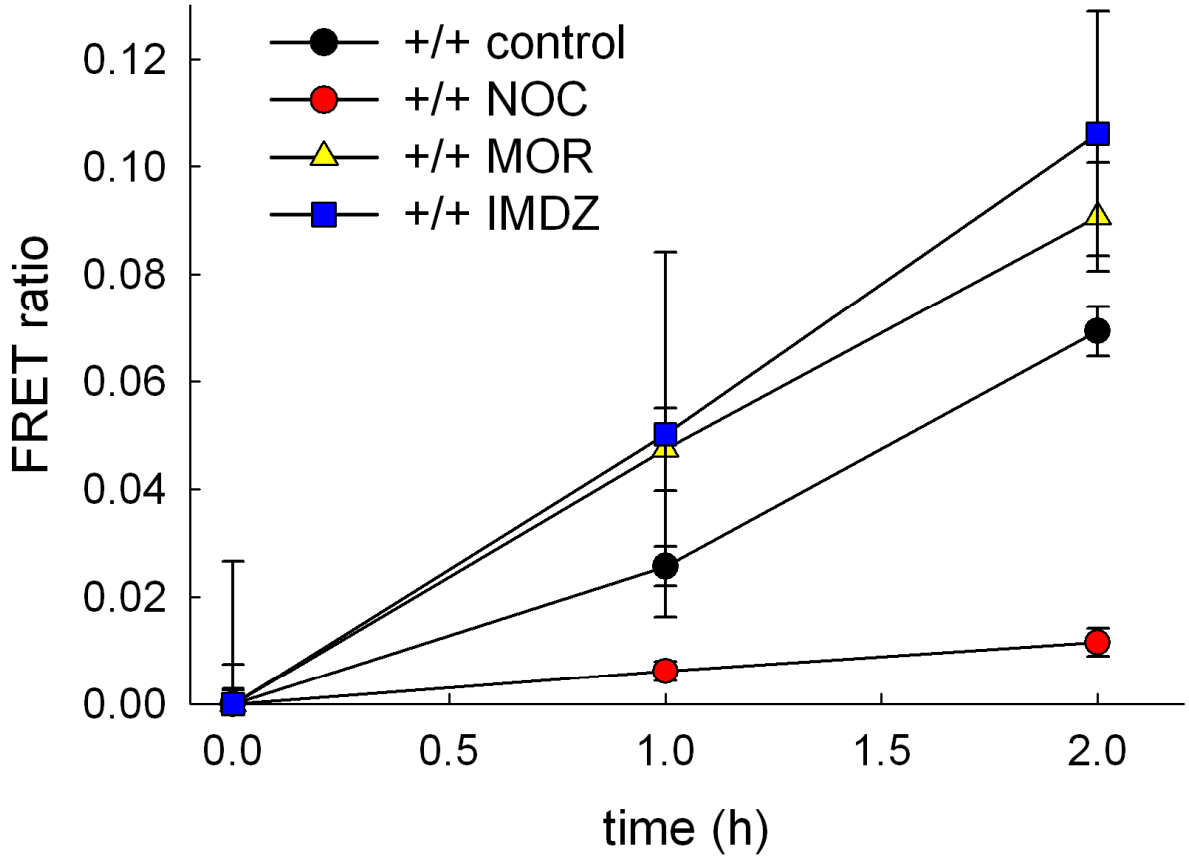

Figure 4.10. Late endosome-lysosome fusion assay in amine-treated NPC1$^{+/+}$ cells. As discussed in Appendix I, a FRET ratio was evaluated over time as a measure of late endosome-lysosome interactions. The degree of late endosome-lysosome hybrid organelle formation in NPC1$^{+/+}$ was enhanced upon exposure to the lysosomotropic amines morpholine (10 mM, MOR, n = 3) and imidazole (10 mM, IMDZ, n = 3) for 2 h. Nocodazole (50 ug/mL, NOC, n = 5) was used as a control to limit late endosome contact with lysosomes.

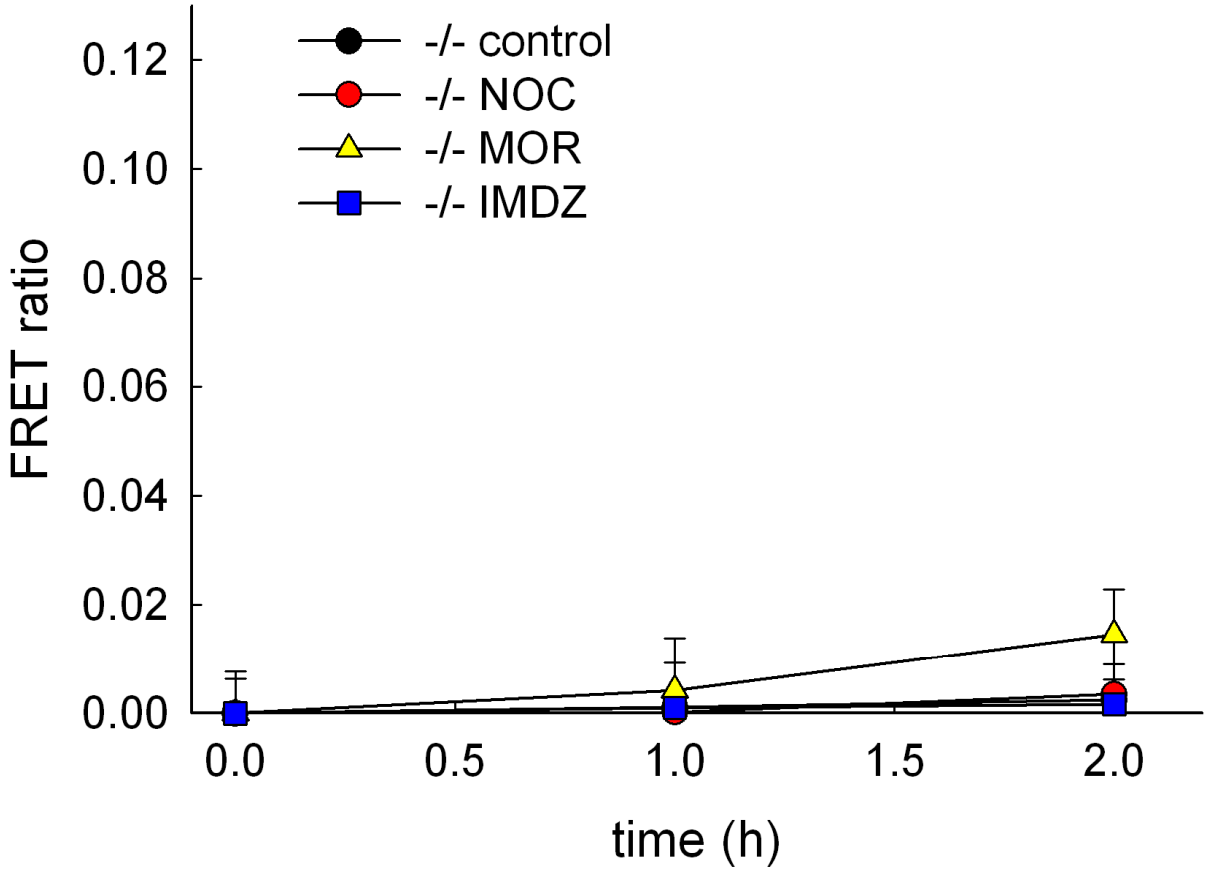

Figure 4.11. Late endosome-lysosome fusion assay in amine-treated NPC1$^{-/-}$ cells. As discussed in Appendix I, a FRET ratio was evaluated over time as a measure of late endosome-lysosome interactions. There was no change in the degree of late endosome-lysosome hybrid organelle formation in NPC1$^{-/-}$ cells upon exposure to the lysosomotropic amines morpholine (10 mM, MOR, n = 3), imidazole (10 mM, IMDZ, n = 3) or nocodazole (50 µg/mL, NOC, n = 3) for 2 h.

that dense core lysosomes are reformed after formation of late endosome-lysosome hybrid organelles [32]. Furthermore, studies in live cells have shown small tubular structures budding off of late endosome/lysosome hybrid organelles [33]. Similarly, Ko et al. have visualized vesicles budding from NPC1-positive hybrid organelles [3]. It is likely that some of these vesicles would transport late endosomal membrane proteins back to their origin. However, it is possible that some of the vesicles may fuse with the plasma membrane or with secretion competent organelles such as the Golgi apparatus. We propose that it is these types of vesicles that traffic lysosomal cargo, such as undigested macromolecules (i.e., dextran), LDL-derived cholesterol, and protonated amines, to the plasma membrane. A model of this hypothesis is described in Figure 4.13.

The formation of hybrid organelles and their subsequent fission to reform lysosomes and late endosomes is a dynamic process [34]. Our data suggest that, at steady state, a relatively small fraction of lysosomes are fused with late endosomes, at any given time, under normal cell culture conditions. This may or may not be relevant to *in vivo* situations. It is possible that the rate of hybrid organelle formation (fusion) is small relative to the rate of reformation of lysosomes (fission) under normal conditions. When cells in culture are exposed to select lysosomotropic amines at high concentrations, we observe nearly 100% colocalization of lysosomes with late endosomes in normal cells after 6 hrs of exposure (Chapter 2, Fig. 2.9). One possible explanation is that the amines

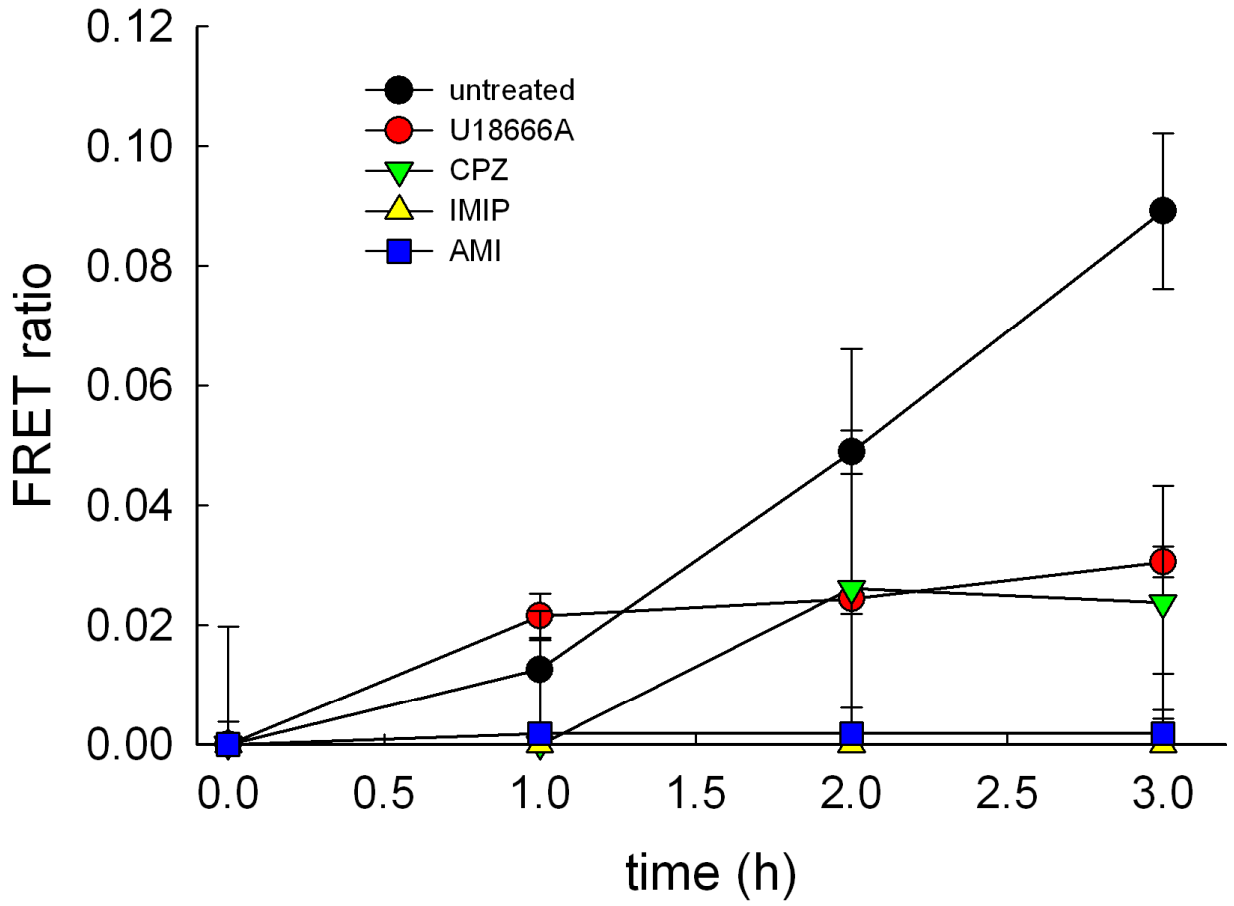

Figure 4.12. Late endosome-lysosome fusion in NPC1$^{+/+}$ cells treated with hydrophobic amine-containing compounds. Appearance of a FRET signal was evaluated 3 h after drug administration. Chlorpromazine (CPZ, n = 3), imipramine (IMIP, n = 3), amiodarone (AMI, n = 3) and U18666A (n = 6) were dosed at 10 μM for 3 h. All compounds had an inhibitory effect on hybrid organelle formation in NPC1$^{+/+}$ cells.

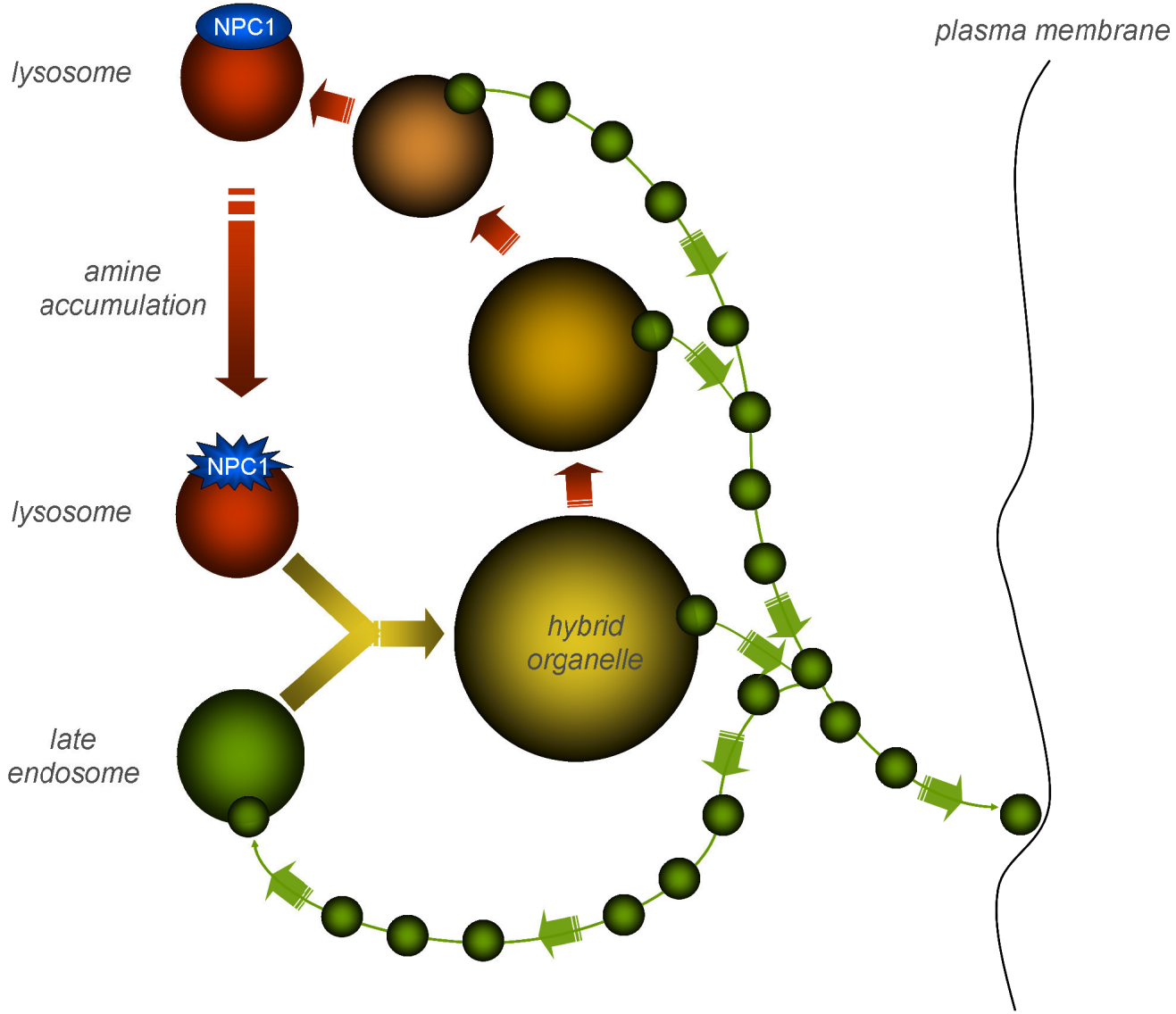

Figure 4.13. Model for NPC1-mediated lysosomal amine regulation. NPC1 (blue) facilitates the fusion of late endosomes and lysosomes in the presence of amines. The release of lysosome contents and amines is proposed to occur through the reformation of lysosomes and late endosomes via the fission of vesicles from the hybrid organelle, which can then traffic to the plasma membrane.

stimulate NPC1-mediated fusion events, leading to the creation of hybrid organelles, yet have no influence on the subsequent fission events that are responsible for the disappearance of the hybrid organelle.

Nearly two decades ago, Liscum and Faust had shown that the weakly basic compound U18666A was able to impair the intracellular transport of LDL-derived cholesterol from lysosomes [22]. This group has since identified a number of other, so-called, class II amphiphilic agents with related activity [35]. The two most studied amines are U18666A and imipramine, and both are used to chemically induce a NP-C disease phenotype. The exact mechanism of action for these agents remains poorly understood, but it is thought that they interfere with some aspect of lysosome to endoplasmic reticulum cholesterol transport. Thus, results showing that some amines had a stimulatory influence on NPC1-mediated lysosome trafficking events would initially appear counterintuitive. However, it is important to consider what might differentiate weakly basic molecules that stimulate NPC1 from those that inhibit it. We have previously evaluated how physicochemical properties of weakly basic molecules influence sequestration in lysosomes. Specifically, we have found that pKa value, membrane permeability and charge delocalization are all important factors (Table I) [19; 36]. According to these parameters, we would predict NPC1 inhibitors (imipramine, chlorpromazine, amiodarone and U18666A) as well as the NPC1 stimulators (neutral red, imidazole and morpholine) all have lysosomotropic properties, which is supported by the literature [18; 21; 37; 38; 39]. The

structures of each of the compounds are shown in Figure 4.14 and highlight distinct differences in the apparent amphiphilic nature of the molecules. Imipramine, chlorpromazine, amiodarone and U18666A all have clear separation between their basic ionizable tertiary amine and hydrophobic moiety. Morpholine, imidazole, and NR all possess an ionizable amine but do not have substantial hydrophobic character, which is apparent in their logP values (Table I). Interestingly, imipramine and chlorpromazine have been shown to insert into lipid bilayers through orientations of their hydrophobic moieties [40; 41]. It could be that the amphiphilic nature of the inhibitory compounds allows them to insert and accumulate in membranes to a greater extent and consequently disrupt the activity of membrane proteins such as NPC1. In support of this, the degree of amphiphilicity of a group of molecules has been shown to correlate well with their propensity to inhibit the activity of the membrane-bound transporter P-glycoprotein [42].

When considering vesicle fusion, lipid asymmetry of the phospholipid membrane has been shown to be crucial for successful fusion events [43; 44]. Ioannou suggests that NPC1 may function as a lipid flippase [45]. This function would allow late endosome-lysosome compartments to maintain the correct degree of lipid asymmetry. This asymmetry, hypothetically, would in turn facilitate the correct membrane curvature required to drive vesicle fusion. The work described in this chapter demonstrates that certain lysosomotropic amines are able to increase NPC1-mediated fusion of late endosomes and lysosomes.

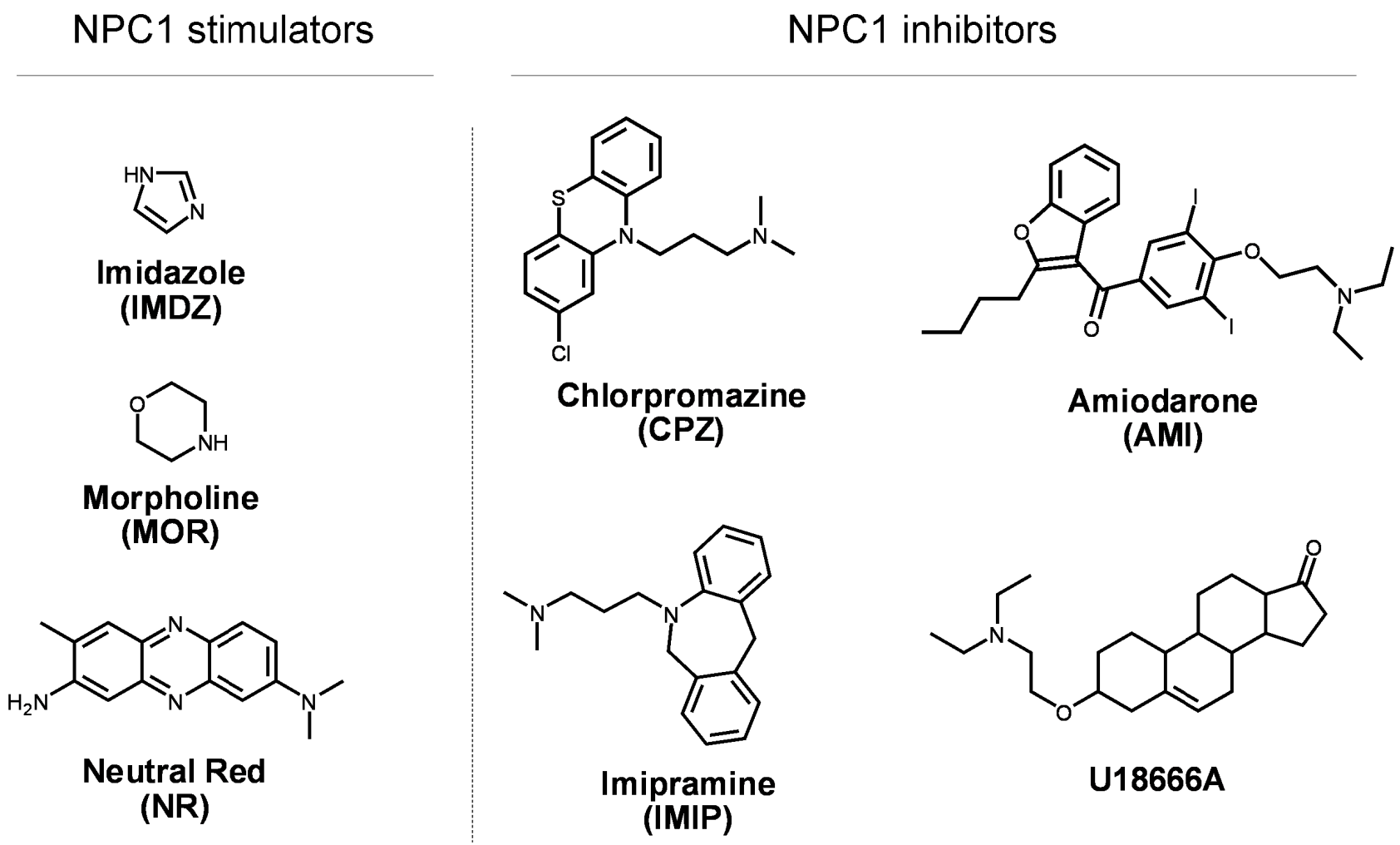

Figure 4.14. Structures of test compounds. All molecules shown are lysosomotropic with respect to their physicochemical properties (Table I). U18666A, IMIP, CPZ and AMI are amphiphilic and have been shown to inhibit NPC1 function. NR, MOR, and IMDZ are not considered to be as amphiphilic and were all found to stimulate NPC1 function.

We believe that this work is consistent with the previously proposed role for NPC1 in vesicle fusion. The accumulation of amines in lysosomal compartments undoubtedly causes increases in both ionic strength and osmotic pressure in the organelle lumen. These changes could potentially favorably influence membrane curvature to facilitate NPC1-mediated membrane fusion, although more work will be needed to address these mechanistic possibilities.

Table 4.1. Physicochemical properties of test compounds.

Compound	*pKa*	logP	MW
NR	6.7	-0.33	288.78
IMDZ	7.0	-0.08	68.08
MOR	8.5	-0.86	87.12
AMI	8.7	7.57	645.32
CPZ	9.2	5.4	318.87
IMIP	9.4	4.8	280.42
U18666A	9.5	4.3	424.10

4.5. References

[1]E.B. Neufeld, M. Wastney, S. Patel, S. Suresh, A.M. Cooney, N.K. Dwyer, C.F. Roff, K. Ohno, J.A. Morris, E.D. Carstea, J.P. Incardona, J.F. Strauss, 3rd, M.T. Vanier, M.C. Patterson, R.O. Brady, P.G. Pentchev, and E.J. Blanchette-Mackie, The Niemann-Pick C1 protein resides in a vesicular compartment linked to retrograde transport of multiple lysosomal cargo. J Biol Chem 274 (1999) 9627-35.

[2]Y. Gong, M. Duvvuri, M.B. Duncan, J. Liu, and J.P. Krise, Niemann-Pick C1 protein facilitates the efflux of the anticancer drug daunorubicin from cells according to a novel vesicle-mediated pathway. J Pharmacol Exp Ther 316 (2006) 242-7.

[3]D.C. Ko, M.D. Gordon, J.Y. Jin, and M.P. Scott, Dynamic movements of organelles containing Niemann-Pick C1 protein: NPC1 involvement in late endocytic events. Mol Biol Cell 12 (2001) 601-14.

[4]L. Liscum, Niemann-Pick type C mutations cause lipid traffic jam. Traffic 1 (2000) 218-25.

[5]E.J. Blott, and G.M. Griffiths, Secretory lysosomes. Nat Rev Mol Cell Biol 3 (2002) 122-31.

[6]G. Griffiths, What's special about secretory lysosomes? Semin Cell Dev Biol 13 (2002) 279-84.

[7]T. Kawakami, and S.J. Galli, Regulation of mast-cell and basophil function and survival by IgE. Nat Rev Immunol 2 (2002) 773-86.

[8]A. McNicol, and S.J. Israels, Platelet dense granules: structure, function and implications for haemostasis. Thromb Res 95 (1999) 1-18.

[9]U. Gullberg, E. Andersson, D. Garwicz, A. Lindmark, and I. Olsson, Biosynthesis, processing and sorting of neutrophil proteins: insight into neutrophil granule development. Eur J Haematol 58 (1997) 137-53.

[10]J.M. Besterman, J.A. Airhart, R.C. Woodworth, and R.B. Low, Exocytosis of pinocytosed fluid in cultured cells: kinetic evidence for rapid turnover and compartmentation. J Cell Biol 91 (1981) 716-27.

[11]A.M. Kaufmann, and J.P. Krise, Niemann-pick c1 functions in regulating lysosomal amine content. J Biol Chem 283 (2008) 24584-93.

[12]G. Griffiths, On vesicles and membrane compartments. Protoplasma 195 (1996) 37-58.

[13]A. Jahraus, B. Storrie, G. Griffiths, and M. Desjardins, Evidence for retrograde traffic between terminal lysosomes and the prelysosomal/late endosome compartment. J Cell Sci 107 (Pt 1) (1994) 145-57.

[14]J.P. Luzio, V. Poupon, M.R. Lindsay, B.M. Mullock, R.C. Piper, and P.R. Pryor, Membrane dynamics and the biogenesis of lysosomes. Mol Membr Biol 20 (2003) 141-54.

[15]B. Storrie, and M. Desjardins, The biogenesis of lysosomes: is it a kiss and run, continuous fusion and fission process? Bioessays 18 (1996) 895-903.

[16]G. Grynkiewicz, M. Poenie, and R.Y. Tsien, A new generation of Ca2+ indicators with greatly improved fluorescence properties. J Biol Chem 260 (1985) 3440-50.

[17]W. Henke, C. Cetinsoy, K. Jung, and S. Loening, Non-hyperbolic calcium calibration curve of Fura-2: implications for the reliability of quantitative Ca2+ measurements. Cell Calcium 20 (1996) 287-92.

[18]S. Ohkuma, and B. Poole, Cytoplasmic vacuolation of mouse peritoneal macrophages and the uptake into lysosomes of weakly basic substances. J Cell Biol 90 (1981) 656-64.

[19]M. Duvvuri, Y. Gong, D. Chatterji, and J.P. Krise, Weak base permeability characteristics influence the intracellular sequestration site in the multidrug-resistant human leukemic cell line HL-60. J Biol Chem 279 (2004) 32367-72.

[20]C.F. Roff, E. Goldin, M.E. Comly, A. Cooney, A. Brown, M.T. Vanier, S.P. Miller, R.O. Brady, and P.G. Pentchev, Type C Niemann-Pick disease: use of hydrophobic amines to study defective cholesterol transport. Dev Neurosci 13 (1991) 315-9.

[21]Y. Lange, J. Ye, M. Rigney, and T. Steck, Cholesterol movement in Niemann-Pick type C cells and in cells treated with amphiphiles. J Biol Chem 275 (2000) 17468-75.

[22]L. Liscum, and J.R. Faust, The intracellular transport of low density lipoprotein-derived cholesterol is inhibited in Chinese hamster ovary cells cultured with 3-beta-[2-(diethylamino)ethoxy]androst-5-en-17-one. J Biol Chem 264 (1989) 11796-806.

[23]N.W. Andrews, Membrane resealing: synaptotagmin VII keeps running the show. Sci STKE 2005 (2005) pe19.

[24]M. Duvvuri, S. Konkar, K.H. Hong, B.S. Blagg, and J.P. Krise, A new approach for enhancing differential selectivity of drugs to cancer cells. ACS Chem Biol 1 (2006) 309-15.

[25]B. Poole, and S. Ohkuma, Effect of weak bases on the intralysosomal pH in mouse peritoneal macrophages. J Cell Biol 90 (1981) 665-9.

[26]K.A. Christensen, J.T. Myers, and J.A. Swanson, pH-dependent regulation of lysosomal calcium in macrophages. J Cell Sci 115 (2002) 599-607.

[27]S. Rabinowitz, H. Horstmann, S. Gordon, and G. Griffiths, Immunocytochemical characterization of the endocytic and phagolysosomal compartments in peritoneal macrophages. J Cell Biol 116 (1992) 95-112.

[28]A. Rodriguez, P. Webster, J. Ortego, and N.W. Andrews, Lysosomes behave as Ca2+-regulated exocytic vesicles in fibroblasts and epithelial cells. J Cell Biol 137 (1997) 93-104.

[29]J.K. Jaiswal, M. Fix, T. Takano, M. Nedergaard, and S.M. Simon, Resolving vesicle fusion from lysis to monitor calcium-triggered lysosomal exocytosis in astrocytes. Proc Natl Acad Sci U S A 104 (2007) 14151-6.

[30]J.K. Jaiswal, N.W. Andrews, and S.M. Simon, Membrane proximal lysosomes are the major vesicles responsible for calcium-dependent exocytosis in nonsecretory cells. J Cell Biol 159 (2002) 625-35.

[31]N.W. Andrews, Regulated secretion of conventional lysosomes. Trends Cell Biol 10 (2000) 316-21.

[32]N.A. Bright, B.J. Reaves, B.M. Mullock, and J.P. Luzio, Dense core lysosomes can fuse with late endosomes and are re-formed from the resultant hybrid organelles. J Cell Sci 110 (Pt 17) (1997) 2027-40.

[33]N.A. Bright, M.J. Gratian, and J.P. Luzio, Endocytic delivery to lysosomes mediated by concurrent fusion and kissing events in living cells. Curr Biol 15 (2005) 360-5.

[34]J.P. Luzio, P.R. Pryor, and N.A. Bright, Lysosomes: fusion and function. Nat Rev Mol Cell Biol 8 (2007) 622-32.

[35]L. Liscum, Pharmacological inhibition of the intracellular transport of low-density lipoprotein-derived cholesterol in Chinese hamster ovary cells. Biochim Biophys Acta 1045 (1990) 40-8.

[36]M. Duvvuri, S. Konkar, R.S. Funk, J.M. Krise, and J.P. Krise, A chemical strategy to manipulate the intracellular localization of drugs in resistant cancer cells. Biochemistry 44 (2005) 15743-9.

[37]J. Ishizaki, K. Yokogawa, F. Ichimura, and S. Ohkuma, Uptake of imipramine in rat liver lysosomes in vitro and its inhibition by basic drugs. J Pharmacol Exp Ther 294 (2000) 1088-98.

[38]I. Scuntaro, U. Kientsch, U.N. Wiesmann, and U.E. Honegger, Inhibition by vitamin E of drug accumulation and of phospholipidosis induced by desipramine and other cationic amphiphilic drugs in human cultured cells. Br J Pharmacol 119 (1996) 829-34.

[39]C. de Duve, T. de Barsy, B. Poole, A. Trouet, P. Tulkens, and F. Van Hoof, Commentary. Lysosomotropic agents. Biochem Pharmacol 23 (1974) 2495-531.

[40]H. Fischer, M. Kansy, and D. Bur, CAFCA: a Novel Tool for the Calculation of Amphiphilic Properties of Charged Drug Molecules. CHIMIA International Journal for Chemistry 54 (2000) 640-645.

[41]G. Gerebtzoff, X. Li-Blatter, H. Fischer, A. Frentzel, and A. Seelig, Halogenation of drugs enhances membrane binding and permeation. Chembiochem 5 (2004) 676-84.

[42]G. Konig, P. Chiba, and G.F. Ecker, Hydrophobic moments as physicochemical descriptors in strucutre-activity relationship studies of P-glycoprotein inhibitors. Monatsh Chem 139 (2008) 401-405.

[43]P.F. Devaux, Static and dynamic lipid asymmetry in cell membranes. Biochemistry 30 (1991) 1163-73.

[44]M.E. Haque, T.J. McIntosh, and B.R. Lentz, Influence of Lipid Composition on Physical Properties and PEG-Mediated Fusion of Curved and Uncurved Model Membrane Vesicles: "Nature's Own" Fusogenic Lipid Bilayer. Biochemistry 40 (2001) 4340-4348.

[45]Y.A. Ioannou, Guilty until proven innocent: the case of NPC1 and cholesterol. Trends Biochem Sci 30 (2005) 498-505.

Chapter 5

Connecting NP-C disease pathology with defects in lysosomal amine regulation

5.1. Introduction

For many decades, NPC1 has been considered a cholesterol transporter due to the presence of a putative sterol sensing domain in the protein and the observed hyperaccumulation of cholesterol in lysosomes of NP-C disease cells. There is little doubt that NPC1 dysfunction affects cholesterol traffic; however, it is clear this is not NPC1's only function. Since NP-C disease research has revolved primarily around cholesterol, the numbers of exploratory studies that are designed to reveal other potential causes of NP-C disease pathology have been limited. As a consequence, the rational development of therapeutic strategies for treating NP-C disease has, for the most part, failed due to the lack of understanding of NPC1's function. In this chapter we suggest a potential cause of the neurodegeneration observed in NP-C disease pathology that is unrelated to lysosomal cholesterol hyperaccumulation.

In previous chapters, we provided evidence that suggests NPC1 plays an important functional role in regulating amine levels in lysosomes. Could such a role be important *in vivo*? First, vast arrays of endogenous small molecular weight amines exist in cells. The most ubiquitous are polyamines (i.e., spermine, spermidine, putrescine, cadaverine), sphingoid bases, ammonia and other biogenic amines. Interestingly, polyamines are found in every cell of our bodies. These molecules have importance with regards to cell proliferation, differentiation and motility as well as stabilizing DNA and RNA structure [1; 2; 3]. The concentrations of polyamines have been shown to be very high in cells,

sometimes reaching millimolar levels [4]. These levels are regulated by enzymes, which have dramatically short half-lives [5; 6], that synthesize and metabolize polyamines. Considering this information, sequestration of polyamines in lysosomes without efficient NPC1-mediated release could cause imbalances in homeostatic levels.

Although polyamine sequestration in lysosomes without release is plausible in NP-C disease, based on their physicochemical properties (highly positively charged at physiological pH), polyamines are not expected to accumulate by pH-partitioning in lysosomes. However, a number of reports have suggested that polyamines and similar molecules can become extensively compartmentalized in lysosomes [7; 8; 9]. Furthermore, Brunk and coworkers have provided evidence concerning the intracellular distribution of polyamine metabolites *in vivo* [10; 11]. They have shown that a particular polyamine metabolite, 3-aminopropanal, localizes to lysosomes and can cause lysosome rupture, which results in apoptosis and cell death [10; 12]. Consistent with NP-C neurodegeneration, the toxic effects of 3-aminopropanal are greatly enhanced in neuronal cell lines although the reasons for this enhanced toxicity is currently unknown [12].

Alterations in endogenous polyamine levels and/or their metabolizing enzymes have been reported to be associated with neurodegenerative disorders similar to NP-C disease [13; 14; 15] including Alzheimer's disease. The

contribution of these alterations to disease pathology is unclear at present. These similarities, however, give cause for investigation of polyamines in the pathology of NP-C disease. In this chapter, we aim to investigate the contribution of polyamines to NP-C disease pathology. Furthermore, we provide a physiologically relevant consequence of NPC1 dysfunction with regard to the regulation of polyamine metabolite accumulation in lysosomes.

5.2. Materials and methods

5.2.1. Antibodies and reagents

Mouse monoclonal anti-glyceraldehyde-3-phosphate dehydrogenase (GAPDH) antibody was from Ambion (Austin, TX). Goat polyclonal anti-polyamine oxidase (PAO) was purchased through Santa Cruz Biotechnology (Santa Cruz, CA). 3-aminopropanal diethyl acetal was obtained from TCI America (Portland, OR). Hyamine hydroxide was purchased through Fisher Scientific (St. Louis, MO). Purpald (4-amino-3-hydrazino-5-mercapto-1,2,4-triazole), propionaldehyde, 2, 4-dinitrophenol, *p*-nitrophenyl-*N*-acetyl-β-D-glucosamidine (PNPG) and Dowex (50 x 2) cation exchange resin were obtained through Sigma-Aldrich (St. Louis, MO). The Quick Cell Proliferation WST-1 assay was purchased from BioVision (Mountain View, CA). All other reagents unless otherwise specified were purchased through Sigma-Aldrich.

5.2.2. Cell culture and conditions

Normal human fibroblasts ($NPC1^{+/+}$) and Niemann-Pick Type C disease fibroblasts ($NPC1^{-/-}$) were cultured as previously described (Chapters 2, Section 2.2.2). For all experiments, cells were used before passage 5 and plated 24 hrs prior to evaluations to allow for adherence. Cells were transfected with NPC1 siRNA as previously described (Chapters 2, Section 2.2.5).

5.2.3. 3-Aminopropanal synthesis

3-Aminopropanal (3-AP) was prepared, as previously described [16], from the hydrolysis of 3-aminopropanal diethyl acetal (145 mM) in 1.5 M HCl for 5 hrs at room temperature. The resulting solution was then applied to a strong cation exchange resin (Dowex 50 x 2, H^+ form) and eluted using a 0-3 M HCl gradient. Fractions were collected and aldehyde content was assayed by the method of Bachrach and Reches [17], and subsequently concentrated using a centrifugal evaporator at room temperature. Aldehydes were spectrophotometrically measured at 530 nm using the aldehyde reactive probe Purpald and quantified using a standard curve constructed of propionaldehyde. Detailed synthesis, purification and characterization of 3-AP is described in Appendix II.

5.2.4. Cytotoxicity evaluations

For cytotoxicity studies, fractions of 3-AP were neutralized to physiological pH using sodium hydroxide before use. For experiments requiring NPC1 depletion, $NPC1^{+/+}$ cells (6×10^3 cells per well) were plated in 96-well plates and transiently transfected with NPC1 or scrambled siRNA. At 72 hrs post transfection cells were exposed to various concentrations of 3-AP or ibuprofen (as a control). Cell death was assessed using the WST-1 assay. The WST-1 assay is an equivalent of the MTT assay, except the formazan-like dye formed in the WST-1 assay is water soluble [18]. To obtain IC_{50} values, data points were curve fit to the 4-parameter Hill equation using the Dynamic Curve Fit function in SigmaPlot (v. 10).

5.2.5. Cytosol purification

To determine the effects on lysosomal membrane integrity after exposure to 3-AP, cellular cytosol was purified as described previously by our laboratory [19]. Briefly, 3-AP was incubated with 50 x 10^6 cells at a previously determined IC-50 concentration. Non-viable cells and debris were removed by washing with PBS (2X). Viable cells were then harvested and homogenized using a dounce homogenizer. Post nuclear supernatant (PNS) was prepared by centrifuging homogenized cells for 5 mins at 1,000 x g. Cytosol was isolated by centrifuging the PNS of 3-AP exposed cells on a layered sucrose gradient (18% top, 86% bottom) in a Beckman Optima TLX centrifuge using a Beckman TLA100.4 fixed angle rotor at 150, 000 x g for 3 hours at 4^{o}C. Fractions of 300 µL were taken from the top and subsequently assayed for β-hexosaminidase activity as described below.

5.2.6. β-hexosaminidase activity assay

β-hexosaminidase activity was assayed as previously described by our laboratory using *p*-nitrophenyl-*N*-acetyl-β-D-glucosamidine (PNPG) as a substrate [20]. First, protein concentrations of purified cytosol fractions were determined by the method of Bradford. 3-AP treated and untreated cytosolic protein solutions were normalized to each other by dilution with 0.1 M citrate buffer (pH = 4.5) so that assay volumes were identical. Next, aliquots of each cytosol fraction (0.1 mg total protein) were exposed to a solution containing 0.5 mM PNPG in 0.1 M citrate buffer at pH 4.5. This mixture was allowed to incubate

for 90 mins at 37^{o}C to allow conversion of PNPG to p-nitrophenol (PNP). After 90 mins, the reaction was stopped with 0.8 mL of 0.1 M sodium bicarbonate buffer at pH 10.0. Next, any precipitated proteins present were removed by centrifugation at 16,000 x g for 2 mins and the supernatant removed. The absorbance at 405 nm of the supernatant was measured for PNP determination and compared to a standard curve constructed using 2, 4-dinitrophenol at the same absorbance. The amount of PNP formed during the reaction was obtained and β-hexosaminidase activity is given as moles of PNP formed per mg of cytosolic protein.

5.2.7. Ornithine decarboxylase activity assay

Ornithine decarboxylase (ODC) activity was assayed as previously described [21]. Briefly, 50 x 10^6 cells were harvested and resuspended in a 50 mM Tris-HCl buffer and 0.1 mM EDTA at pH 7.4 (reaction buffer). Cells were homogenized using 20 strokes in a glass dounce homogenizer at room temperature. Protein levels were obtained using the method of Bradford to normalize protein concentrations between cell lines. On the day of experimentation, 5 mM dithiothreitol and 0.1 mM pyridoxyl-5-phosphate (P5P) were added to 300 µL of reaction buffer. Next, 100 µL of cell homogenate was added to the prepared reaction buffer. To initiate the reaction, 10 µL of ^{14}C-ornithine was added to each protein solution. Samples were allowed to incubate for 2 hrs at 37^{o}C on an incubated shaker. The reaction was stopped by precipitating proteins with trichloroacetic acid. The detection of ODC activity was

accomplished by measuring the liberated radioactive carbon dioxide from ornithine. To capture carbon dioxide, samples were incubated in glass pyrex test tubes with screw-on caps. Inside the cap was a pre-cut square of Whatman filter paper that was soaked with 20 µL of hyamine hydroxide. At the end of the reaction, this filter paper was removed and assayed using liquid scintillation counting. The activity of ODC is expressed as moles of carbon dioxide formed per hour per mg of cellular protein.

5.2.8. Western blot and densitometry analysis

Western blot and densitometry analysis was performed as previously described in Chapter 2, Section 2.2.3. Primary antibodies were used at dilutions of 1:100 for PAO and 1:1000 for GAPDH. Secondary HRP-conjugated antibodies were diluted 1:1000.

5.3. Results

5.3.1. NPC1 deficient cells are more susceptible to 3-aminopropanal-induced toxicity than normal cells

Polyamines have been implicated in neurodegeneration through several possible pathways including metabolism of polyamines forming aldehydes [22; 23; 24]. 3-Aminopropanal is a polyamine metabolite that is formed endogenously from the metabolism of spermidine to putrescine by the enzyme polyamine oxidase (PAO). This compound was selected since it has been shown to be specifically toxic to lysosomes and the numerous reports of its neurotoxic effects [23; 24]. Here, we specifically examined the comparative toxicity of 3-aminopropanal (3-AP) in normal and NPC1-depleted fibroblasts.

In cells with depleted NPC1 levels we reasoned that 3-AP should have more contact time with lysosomes and therefore an increased propensity to exert toxic effects relative to normal cells. To test this hypothesis, 3-AP was synthesized and exposed to normal fibroblasts that were previously transfected with NPC1 siRNA and compared with cells transfected with a non-specific scrambled siRNA (Fig 5.1). As expected, NPC1-depleted cells were more susceptible to 3-AP toxicity than cells expressing NPC1. As a control, NPC1 depletion and transfection conditions had no influence on the IC_{50} of a non-lysosomotropic drug ibuprofen (Fig. 5.2).

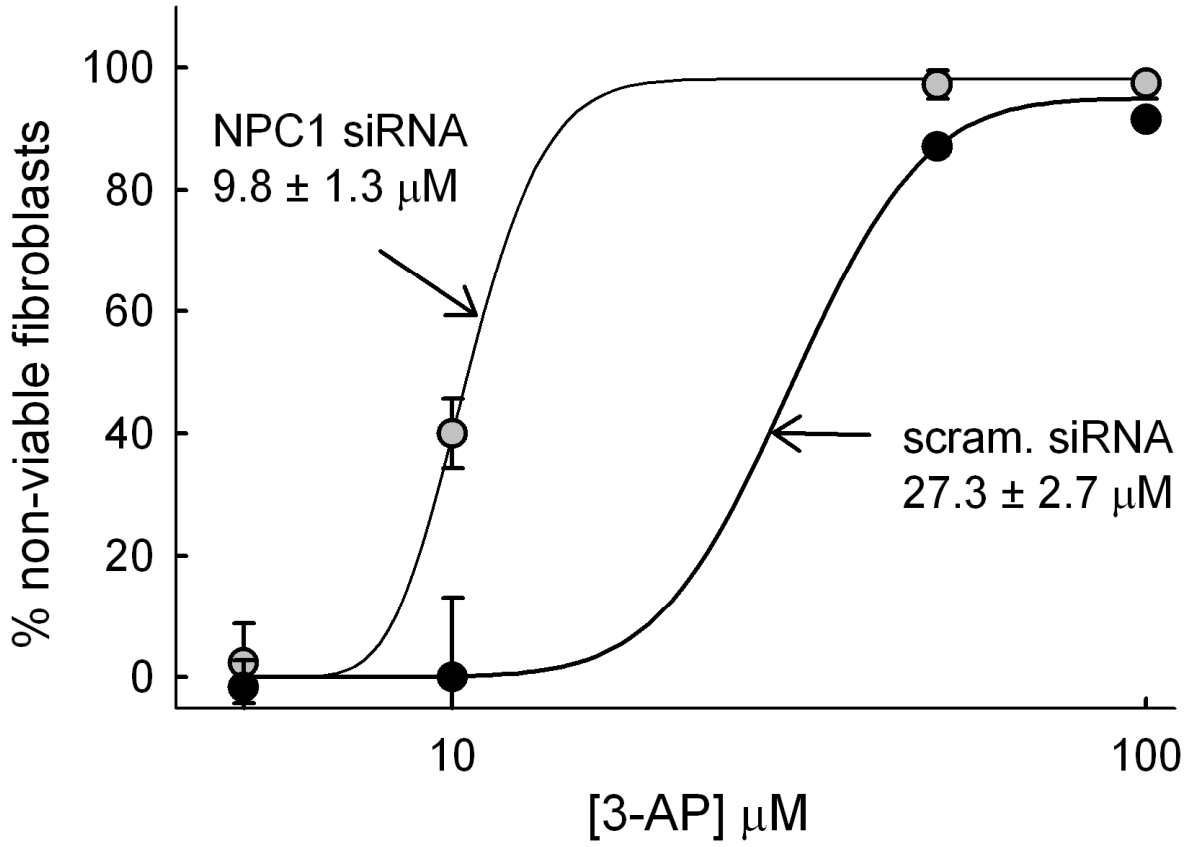

Figure 5.1. NPC1-depleted cells are more susceptible to the toxic effects of 3-aminopropanal (3-AP). siRNA was used to transiently deplete NPC1 in normal cells prior to exposure to 3-AP (grey circles). NPC1-depleted cells had a lower IC_{50} value than cells with NPC1 present (scram. siRNA, closed circles).

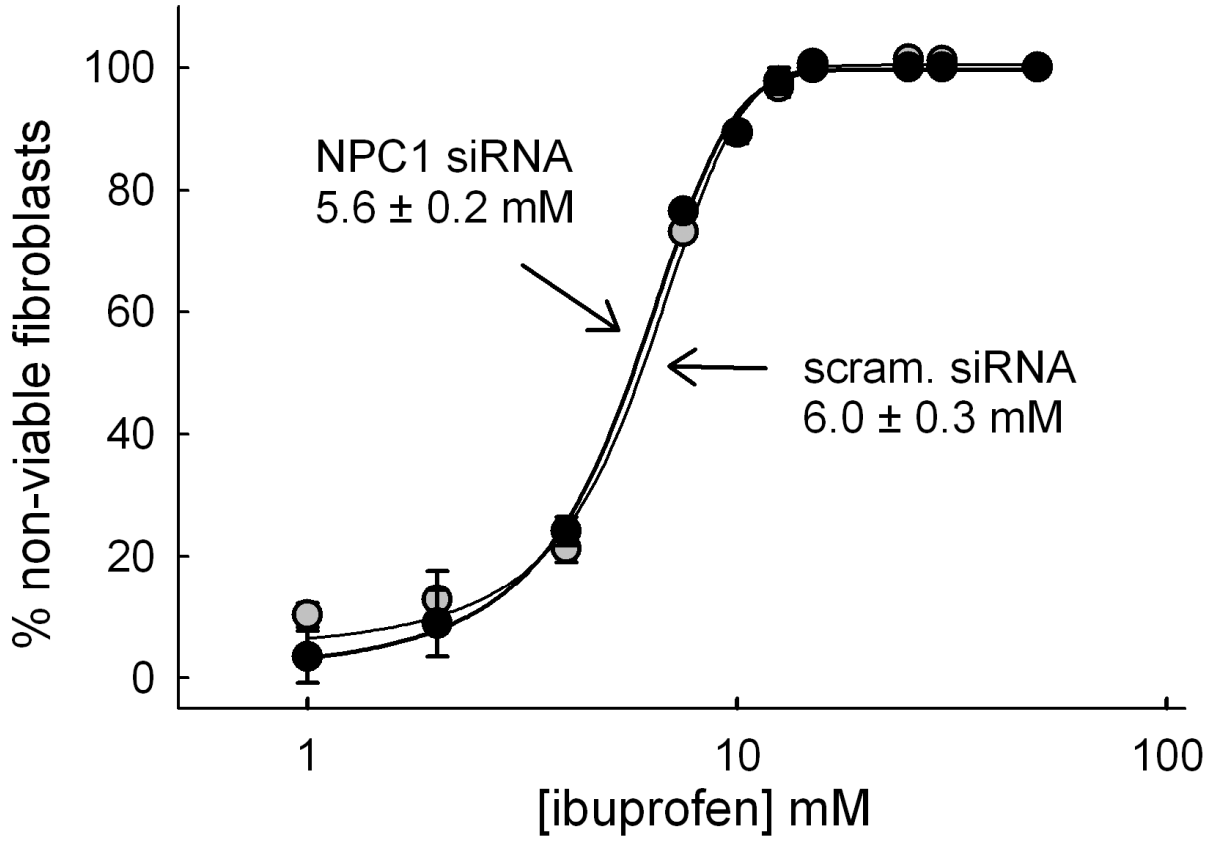

Figure 5.2. Cytotoxicity of ibuprofen, a non-lysosomotropic drug, with or without NPC1 protein expression. NPC1 depleted cells (grey circles) have the same IC_{50} value as cells with normal NPC1 expression (closed circles) when exposed to the acidic drug ibuprofen.

5.3.2. Lysosomes of NPC1 deficient cells are more susceptible to 3-aminopropanal induced rupture

Recent research has shown the main mechanism of 3-AP toxicity in cells is through the specific rupture of lysosomes [10]. From our previous cytotoxicity results, we expected that NPC1 deficient cells would allow 3-AP more residence time within lysosomes leading to more rupture. To assess if NPC1 dysfunction would permit greater lysosome instability in the presence of 3-AP, we assayed lysosomal enzyme activity in purified cytosol. The presence of lysosomal enzymes in the cytosol is indicative of lysosome leakage or complete rupture [25]. To accomplish this, cytosol was purified after 3-AP administration and the presence of β-hexosaminidase, a well-known lysosome hydrolase, was assayed. We found that NPC1$^{-/-}$ lysosomes were more susceptible to rupture than lysosomes from normal cells since higher levels of β-hexosaminidase were observed (Fig. 5.3).

5.3.3. Enzymes responsible for polyamine regulation and 3-aminopropanal synthesis are altered in NP-C disease cells

Differential activities of enzymes that regulate polyamine concentrations *in vivo* have been shown in neurodegenerative disorders similar to NP-C disease [13; 15]. Here, we have evaluated the activity and/or expression of two enzymes responsible for the synthesis and metabolism of polyamines, ornithine decarboxylase and polyamine oxidase [2; 5].

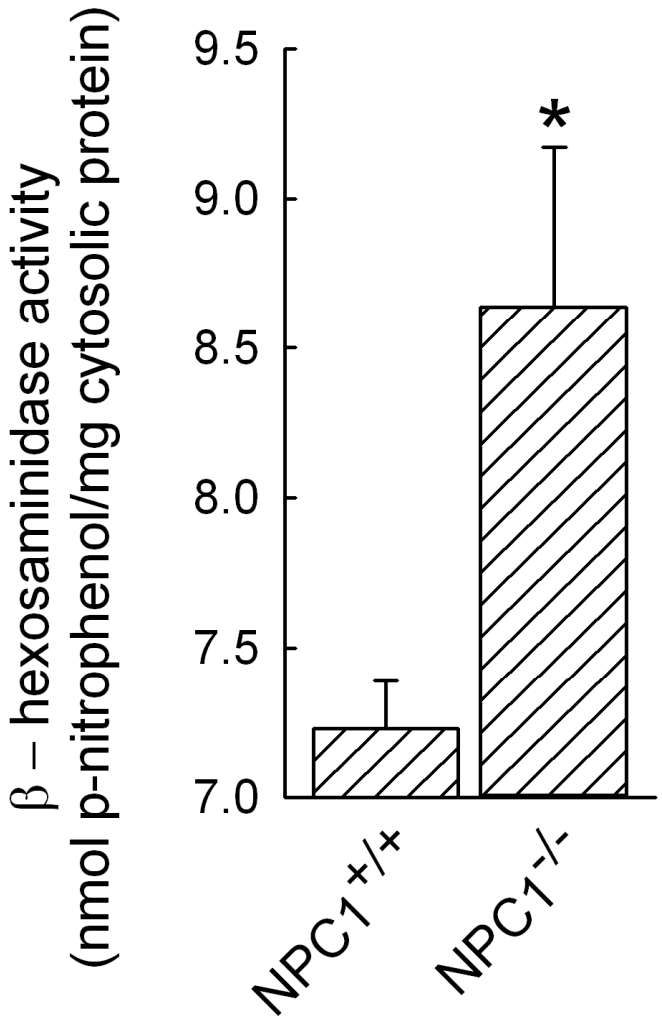

Figure 5.3. Lysosome rupture occurs more readily in NPC1$^{-/-}$ fibroblasts exposed to 3-AP. Cells were exposed to 100 μM 3-AP for 12 hrs and harvested. Cytosol was purified from post-nuclear supernatants and assayed for β-hexosaminidase activity. Results are an average of 3 independent experiments ± S.D. (*, $p < 0.01$)

Ornithine decarboxylase (ODC) is the enzyme responsible for removing the c-terminus from the amino acid L-ornithine to form putrescine, which is the precursor of other polyamines such as spermine and spermidine (Fig. 5.4). To investigate if ODC activity was altered in NP-C cells, we used a previously described assay [21]. Briefly, ODC enzyme activity was assayed by the formation of carbon dioxide that was removed from L-ornithine by ODC. The c-terminus of L-ornithine was radiolabeled such that the liberated CO_2 gas was radioactive. We found that in $NPC1^{-/-}$ cells, the activity of ODC was increased by ~10% and was found to be statistically significant ($p < 0.01$) when compared to normal cells (Fig. 5.5).

Polyamine oxidase (PAO) is the enzyme responsible for the generation of 3-aminopropanal (3-AP) in cells (see Figure 5.6) [24]. Thus, we decided to comparatively examine PAO expression levels in $NPC1^{-/-}$ versus $NPC1^{+/+}$ cells and found it to be significantly elevated in the diseased cell line (Fig. 5.7). Densitometry performed on PAO Western blot bands showed that expression was increased by approximately 300% in $NPC1^{-/-}$ cells when compared to normal cells. Attempts at determining activity of this enzyme by monitoring the amount of polyamine substrate converted to aldehyde were unsuccessful using known methods for aldehyde detection.

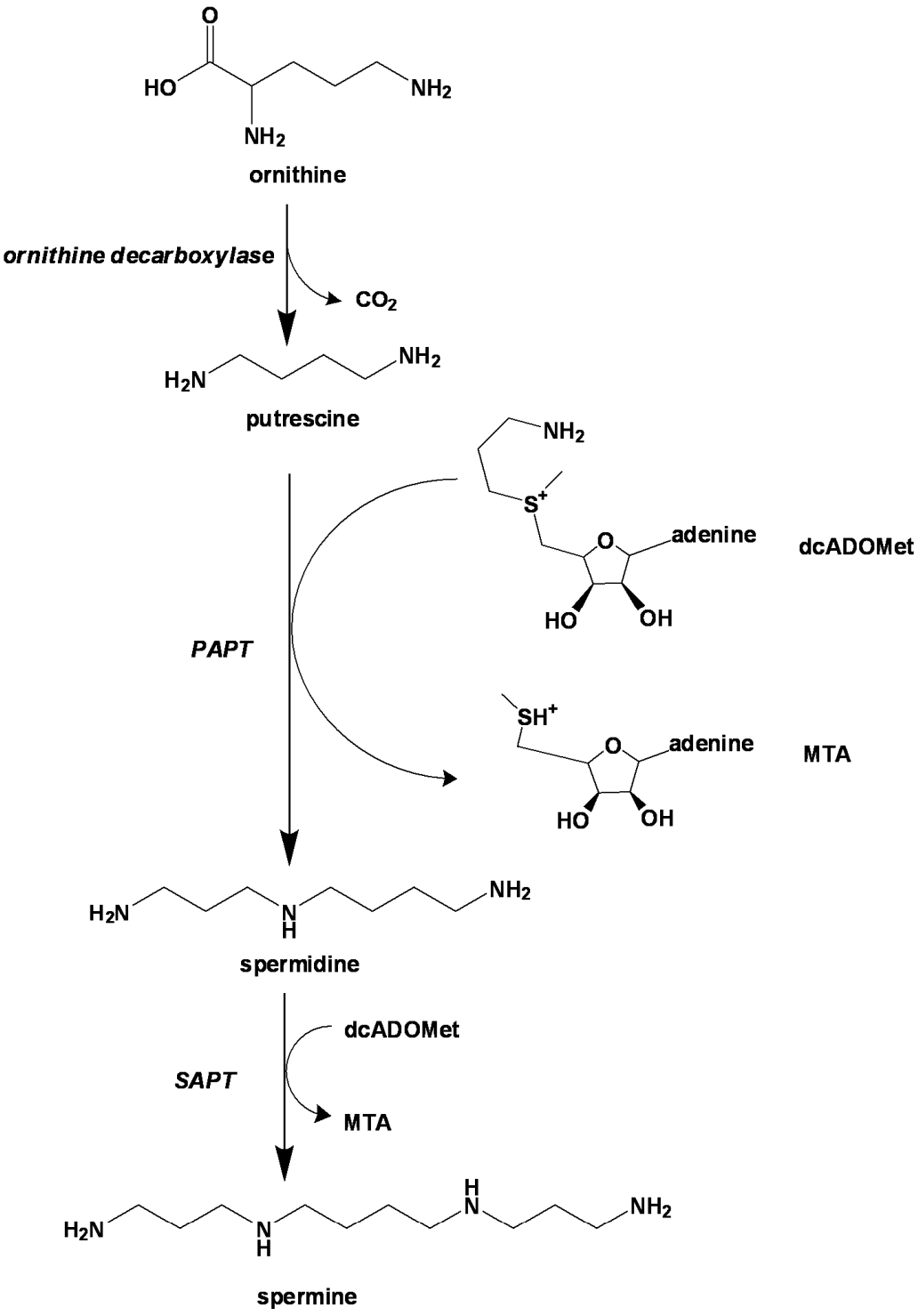

Figure 5.4. Synthesis of polyamines. Ornithine decarboxylase conversion of L-ornithine to putrescine, the precursor molecule of spermidine and spermine, is the rate limiting step in polyamine synthesis.

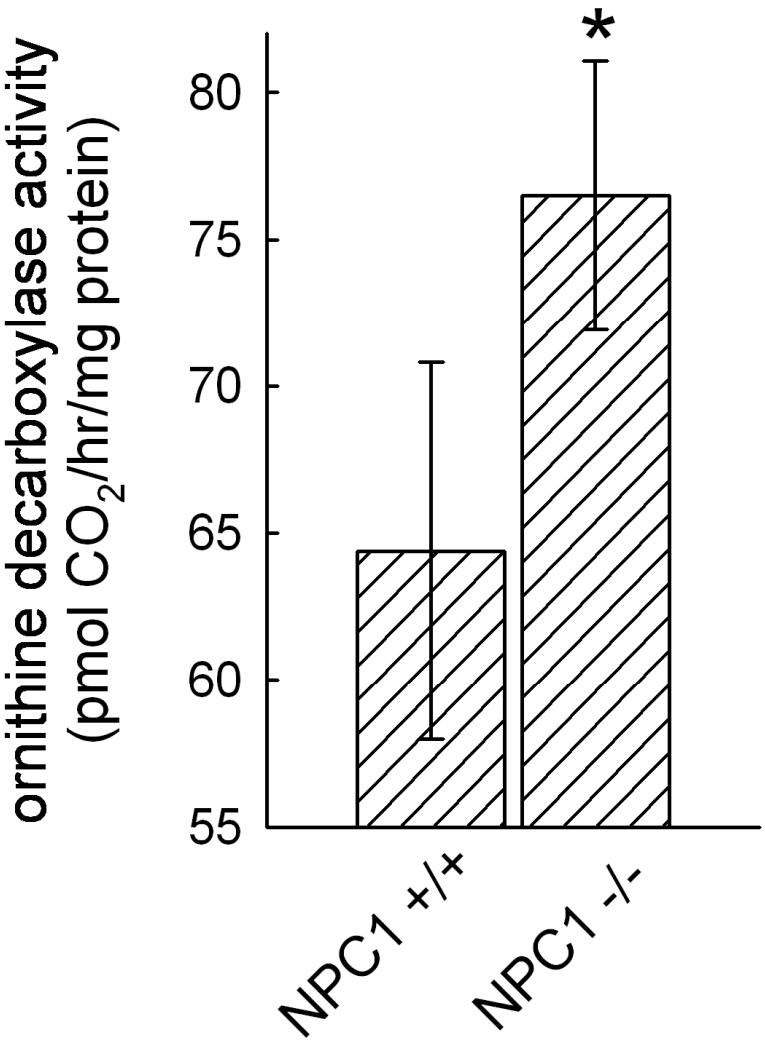

Figure 5.5. Ornithine decarboxylase (ODC) activity is greater in NPC1$^{-/-}$ cells. Post-nuclear supernatants were harvested and assayed for ODC activity using an assay measuring radioactive carbon dioxide formation (see Methods). NPC1$^{-/-}$ supernatants (n = 6) showed a statistically significant increase (*, $p < 0.05$) in ODC activity compared to NPC1$^{+/+}$ cells (n = 6).

5.4. Discussion

In the work presented in this chapter we have focused on polyamines. The precise biological function of polyamines is controversial. It is known, however, that changes in their levels and/or their biosynthetic enzymes have been associated with neurodegenerative-type disorders [13]. Specifically, polyamine levels have been shown to be significantly altered in Alzheimer's disease [15].

Progressive neurodegeneration is the ultimate cause of death in NP-C patients, yet it remains unknown why alterations in lipid homeostasis would lead to such profound neurological deterioration [26]. Alleviation of cholesterol accumulation in late endocytic compartments using pharmacological agents as well as genetic approaches do little to slow the onset of neurodegeneration in murine and feline disease models [27; 28]. Likewise, alleviation of neuronal ganglioside storage had no significant impact on disease progression [29]. Due to these setbacks in NP-C therapy, new avenues for disease treatment must be investigated.

Wood et al. proposed, in a recent report, the theory of "aldehyde loading" as a possible mechanism for neurodegeneration. In this report, they state that similar to oxidative stress, reactive aldehydes can cause modification of proteins and the decrease longevity of neuronal cells [24]. To establish this concept

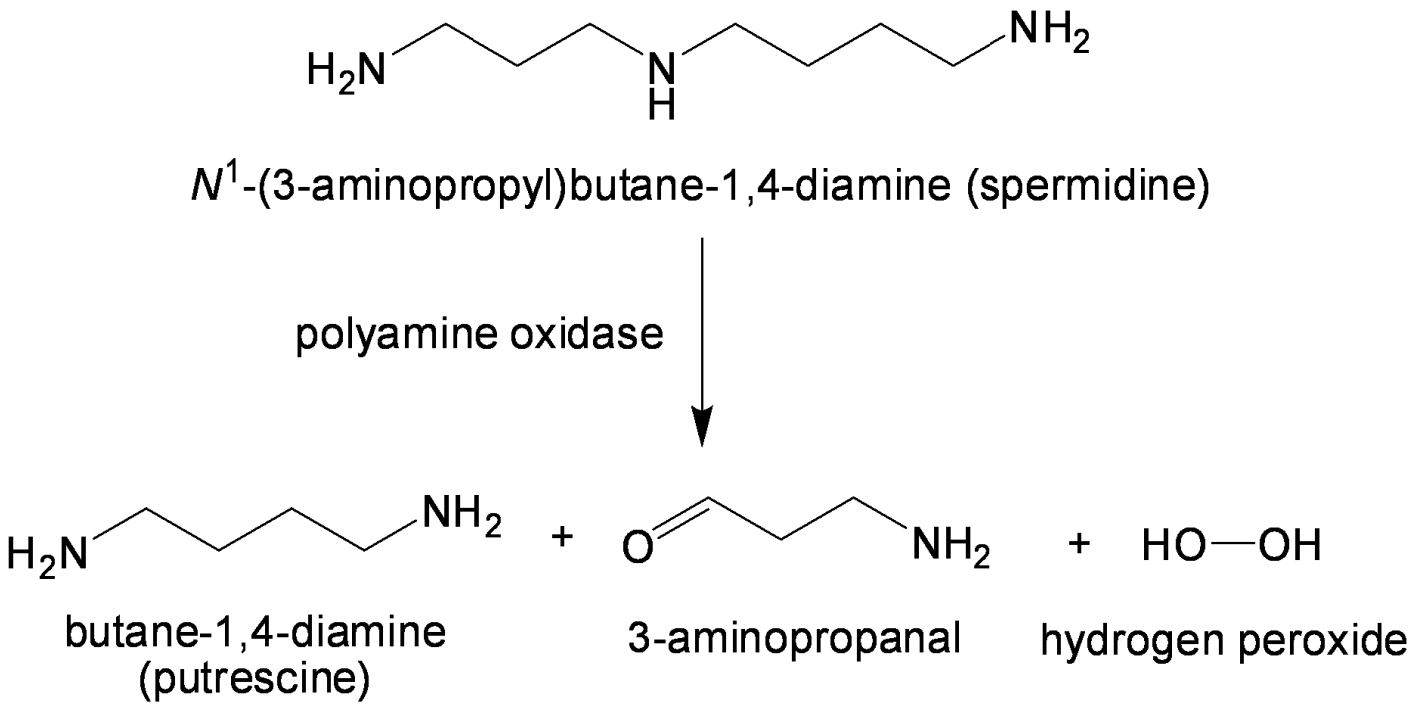

Figure 5.6. Metabolism of polyamines by polyamine oxidase (PAO).

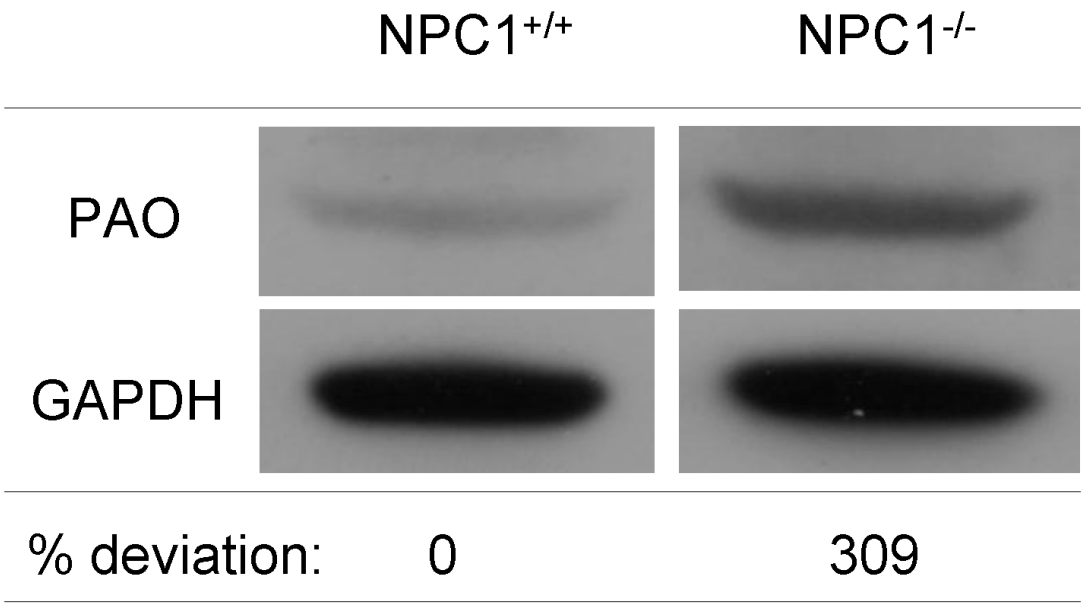

Figure 5.7. Polyamine oxidase (PAO) is overexpressed in NPC1$^{-/-}$ fibroblasts. NPC1$^{+/+}$ and NPC1$^{-/-}$ post-nuclear supernatants were subjected to Western blot analysis for PAO expression. Densitometry analysis revealed that PAO was dramatically overexpressed in NP-C disease fibroblasts.

the authors used a rat model (trimethyltin or TMT) that was previously reported to have alterations in polyamine synthesis/levels. In this model, increased levels of polyamines were confirmed as well as increased levels of the reactive aldehyde 3-AP. Interestingly, the authors went on to alleviate the build-up of 3-AP in rats by neutralizing it with reactive hydroxylamine-containing compounds. These aldehyde scavengers were able to increase the lifespan of TMT rats. Unlike the hydroxylamine compounds, ascorbic acid, an anti-oxidant, did nothing to improve the lifespan of TMT rats. These results suggest that aldehyde-containing molecules like 3-AP may be playing a major role in neurodegeneration and that oxidative stress (from hydrogen peroxide) was a minimal contributor.

In support of 3-AP sequestration contributing to NP-C disease through lysosome toxicity, studies using the anticancer agent tamoxifen have led to increases in the lifespan of an NP-C murine model [30]. Tamoxifen is a weakly basic molecule that has been shown to significantly elevate lysosome pH [31]. If the pH gradient is disrupted between lysosomes and cytosol, then it is expected that 3-AP would not significantly accumulate in lysosomes. Thus, we would expect less 3-AP induced lysosome toxicity and more cell survival (see Figure 5.1).

Similar to the rat TMT model, our studies using NPC1$^{-/-}$ cells found that enzymes necessary for synthesizing and metabolizing polyamines are differentially expressed and/or overactive (Fig. 5.5 and 5.7). Interestingly,

enhanced ODC activity is a common response to various pathological stimuli in the brain, including chemical or metabolic stress [14]. Although our observations concerning ODC activity in NPC1$^{-/-}$ cells are interesting, they do not provide sufficient evidence that 3-AP levels are increased. Further evaluations concerning polyamine levels and reactive aldehyde species in NP-C tissues and cells are needed to be more conclusive.

5.5. References

[1]K. Igarashi, and K. Kashiwagi, Polyamines: mysterious modulators of cellular functions. Biochem Biophys Res Commun 271 (2000) 559-64.

[2]A.E. Pegg, Polyamine metabolism and its importance in neoplastic growth and a target for chemotherapy. Cancer Res 48 (1988) 759-74.

[3]A.U. Khan, P. Di Mascio, M.H. Medeiros, and T. Wilson, Spermine and spermidine protection of plasmid DNA against single-strand breaks induced by singlet oxygen. Proc Natl Acad Sci U S A 89 (1992) 11428-30.

[4]J. Satriano, M. Isome, R.A. Casero, Jr., S.C. Thomson, and R.C. Blantz, Polyamine transport system mediates agmatine transport in mammalian cells. Am J Physiol Cell Physiol 281 (2001) C329-34.

[5]A.E. Pegg, and P.P. McCann, Polyamine metabolism and function. Am J Physiol 243 (1982) C212-21.

[6]A.E. Pegg, Recent advances in the biochemistry of polyamines in eukaryotes. Biochem J 234 (1986) 249-62.

[7]H. Dai, D.L. Kramer, C. Yang, K.G. Murti, C.W. Porter, and J.L. Cleveland, The polyamine oxidase inhibitor MDL-72,527 selectively induces apoptosis of transformed hematopoietic cells through lysosomotropic effects. Cancer Res 59 (1999) 4944-54.

[8]D. Soulet, B. Gagnon, S. Rivest, M. Audette, and R. Poulin, A fluorescent probe of polyamine transport accumulates into intracellular acidic vesicles via a two-step mechanism. J Biol Chem 279 (2004) 49355-66.

[9]P.M. Cullis, R.E. Green, L. Merson-Davies, and N. Travis, Probing the mechanism of transport and compartmentalisation of polyamines in mammalian cells. Chem Biol 6 (1999) 717-29.

[10]Z. Yu, W. Li, and U.T. Brunk, 3-Aminopropanal is a lysosomotropic aldehyde that causes oxidative stress and apoptosis by rupturing lysosomes. Apmis 111 (2003) 643-52.

[11]W. Li, X.M. Yuan, S. Ivanova, K.J. Tracey, J.W. Eaton, and U.T. Brunk, 3-Aminopropanal, formed during cerebral ischaemia, is a potent lysosomotropic neurotoxin. Biochem J 371 (2003) 429-36.

[12]Z. Yu, W. Li, J. Hillman, and U.T. Brunk, Human neuroblastoma (SH-SY5Y) cells are highly sensitive to the lysosomotropic aldehyde 3-aminopropanal. Brain Res 1016 (2004) 163-9.

[13]M. Virgili, C. Crochemore, E. Pena-Altamira, and A. Contestabile, Regional and temporal alterations of ODC/polyamine system during ALS-like neurodegenerative motor syndrome in G93A transgenic mice. Neurochem Int 48 (2006) 201-7.

[14]H.G. Bernstein, and M. Muller, The cellular localization of the L-ornithine decarboxylase/polyamine system in normal and diseased central nervous systems. Prog Neurobiol 57 (1999) 485-505.

[15]L.D. Morrison, and S.J. Kish, Brain polyamine levels are altered in Alzheimer's disease. Neurosci Lett 197 (1995) 5-8.

[16]S. Ivanova, G.I. Botchkina, Y. Al-Abed, M. Meistrell, 3rd, F. Batliwalla, J.M. Dubinsky, C. Iadecola, H. Wang, P.K. Gregersen, J.W. Eaton, and K.J.

Tracey, Cerebral ischemia enhances polyamine oxidation: identification of enzymatically formed 3-aminopropanal as an endogenous mediator of neuronal and glial cell death. J Exp Med 188 (1998) 327-40.

[17]U. Bachrach, and B. Reches, Enzymic assay for spermine and spermidine. Anal Biochem 17 (1966) 38-48.

[18]E. Nissen, G. Pauli, and D. Vollenbroich, WST-1 assay--a simple colorimetric method for virus titration. In Vitro Cell Dev Biol Anim 33 (1997) 28-9.

[19]M. Duvvuri, W. Feng, A. Mathis, and J.P. Krise, A cell fractionation approach for the quantitative analysis of subcellular drug disposition. Pharm Res 21 (2004) 26-32.

[20]M. Duvvuri, and J.P. Krise, A novel assay reveals that weakly basic model compounds concentrate in lysosomes to an extent greater than pH-partitioning theory would predict. Mol Pharm 2 (2005) 440-8.

[21]C.S. Coleman, and A.E. Pegg, Assay of Mammalian Ornithine Decarboxylase Activity Using [14C]Ornithine in: D.M.L. Morgan, (Ed.), Polyamine Protocols, Humana Press, 1998.

[22]W. Paschen, Polyamine metabolism in different pathological states of the brain. Mol Chem Neuropathol 16 (1992) 241-71.

[23]P.L. Wood, M.A. Khan, and J.R. Moskal, The concept of "aldehyde load" in neurodegenerative mechanisms: cytotoxicity of the polyamine degradation products hydrogen peroxide, acrolein, 3-aminopropanal, 3-acetamidopropanal and 4-aminobutanal in a retinal ganglion cell line. Brain Res 1145 (2007) 150-6.

[24]P.L. Wood, M.A. Khan, S.R. Kulow, S.A. Mahmood, and J.R. Moskal, Neurotoxicity of reactive aldehydes: the concept of "aldehyde load" as demonstrated by neuroprotection with hydroxylamines. Brain Res 1095 (2006) 190-9.

[25]K. KÃ¥gedal, M. Zhao, I. Svensson, and U.T. Brunk, Sphingosine-induced apoptosis is dependent on lysosomal proteases. Biochem. J. 359 (2001) 335-343.

[26]I. Vincent, B. Bu, and R.P. Erickson, Understanding Niemann-Pick type C disease: a fat problem. Curr Opin Neurol 16 (2003) 155-61.

[27]R.P. Erickson, W.S. Garver, F. Camargo, G.S. Hossain, and R.A. Heidenreich, Pharmacological and genetic modifications of somatic cholesterol do not substantially alter the course of CNS disease in Niemann-Pick C mice. J Inherit Metab Dis 23 (2000) 54-62.

[28]K.L. Somers, D.E. Brown, R. Fulton, P.C. Schultheiss, D. Hamar, M.O. Smith, R. Allison, H.E. Connally, C. Just, T.W. Mitchell, D.A. Wenger, and M.A. Thrall, Effects of dietary cholesterol restriction in a feline model of Niemann-Pick type C disease. J Inherit Metab Dis 24 (2001) 427-36.

[29]Y. Liu, Y.P. Wu, R. Wada, E.B. Neufeld, K.A. Mullin, A.C. Howard, P.G. Pentchev, M.T. Vanier, K. Suzuki, and R.L. Proia, Alleviation of neuronal ganglioside storage does not improve the clinical course of the Niemann-Pick C disease mouse. Hum Mol Genet 9 (2000) 1087-92.

[30]E.C. Bascunan-Castillo, R.P. Erickson, C.M. Howison, R.J. Hunter, R.H. Heidenreich, C. Hicks, T.P. Trouard, and R.J. Gillies, Tamoxifen and

vitamin E treatments delay symptoms in the mouse model of Niemann-Pick C. J Appl Genet 45 (2004) 461-7.

[31]Y. Chen, M. Schindler, and S.M. Simon, A mechanism for tamoxifen-mediated inhibition of acidification. J Biol Chem 274 (1999) 18364-73.

Appendix I

Development of a method for the quantitative determination of retrograde lysosome traffic to late endosomes

The following is an adaptation of the recently submitted manuscript entitled:

A fluorescence resonance energy transfer-based approach for determining retrograde lysosome traffic to late endosomes

Kaufmann, A.M., Goldman, S.D., Krise, J.P.

A1.0. Summary

Traditionally, lysosomes have been considered to be a terminal endocytic compartment. Recent studies, however, suggest that lysosomes are quite dynamic being able to fuse with other late endocytic compartments as well as with the plasma membrane. Here we describe a quantitative fluorescence energy transfer (FRET)-based method for assessing rates of retrograde fusion between terminal lysosomes and late endosomes in living cells. Late endosomes were specifically labeled with 800 nm latex beads that were conjugated with streptavidin and Alexa Fluor 555 (FRET donor). Terminal lysosomes were specifically labeled with 10,000 MW dextran polymers conjugated with biotin and Alexa Fluor 647 (FRET acceptor). Following late endosome-lysosome fusion, the strong binding affinity between streptavidin and biotin bring the FRET pair donor and acceptor molecules in close proximity, thus facilitating the appearance of a FRET signal. Since apparent size restrictions in the endocytic pathway do not permit endocytosed latex beads from reaching terminal lysosomes in an anterograde fashion, the appearance of the FRET signal is consistent with retrograde transport of lysosomal cargo back to late endosomes. The applicability of this assay is demonstrated using human skin fibroblasts.

A1.1. Introduction

Lysosomes have long been considered as the terminal compartment for fluid phase endocytosis [1]. Recent findings, however, have shown that lysosomes are able to fuse with pre-lysosomal compartments in a retrograde fashion to result in the formation of so-called hybrid organelles [2; 3]. The precise function of such hybrid organelles in cells is not completely understood although Griffiths [4] has proposed a functional role for hybrid organelle formation. It was hypothesized that lysosomes are not terminal degradative compartments for endocytosed materials, but are storage depots for active enzymes. If needed, lysosomes can traffic enzymes in a retrograde fashion back to late endosomes, ultimately forming the primary endocytic site for degradation, the hybrid organelle. Although novel, it still remains unclear the exact molecular stimuli that trigger this interaction to take place.

Jahraus and coworkers [2] were the first to develop a cell-based method that clearly demonstrated the retrograde fusion of terminal lysosomes with pre-lysosomal compartments. Their method utilizes a pulse-chase technique specifically localizing sucrose to terminal lysosomes. Since sucrose is not a substrate for lysosomal nutrient transporters, it can accumulate to an extent that induces the vacuolization of lysosomes. Such vacuoles are referred to as sucrosomes and are clearly visible using conventional light microscopy. Subsequently, cells are incubated with 800 nm latex beads conjugated to the enzyme invertase (sucrase). Latex beads of this size are unique in that they are

endocytosed by cells but, by virtue of their size, fail to progress beyond late endosomes to lysosomes [5]. When in the presence of invertase, sucrose is converted into glucose and fructose, both of which are rapidly transported across lysosomal membranes by specific transporter proteins [6]. Transport of these molecules dissipates the lysosome-cytosol sucrose concentration gradient and results in the shrinking of the sucrosome. Thus, a reduction in sucrosome size is indicative of retrograde fusion of lysosomes with late endosomes. Despite its usefulness in demonstrating retrograde lysosome-late endosome fusion, this method cannot be readily employed to examine rates of hybrid organelle formation.

In this work we examined if the concept developed by Jahraus and colleagues [2] could be redesigned to provide a quantitative measure of retrograde lysosome-late endosome fusion. To accomplish this we investigated the suitability of a fluorescence resonance energy transfer (FRET)-based readout for assessing the extent of these fusion events in living cells.. Specifically, we localized 10,000 MW dextran polymers to lysosomes, instead of sucrose, using previously described pulse-chase protocols [7]. The dextran polymer was coupled with biotin and fluorescently labeled with Alexa Fluor 647 (FRET acceptor). Next, we localized latex beads into late endosomes as previously described [2]. The beads were of the same diameter previously used by Jahraus et. al. but were conjugated with streptavidin, instead of invertase, and fluorescently labeled with Alexa Fluor 555 (FRET donor). If lysosome and late

endosome contents mix, the strong binding affinity of streptavidin for biotin should result in the dextran binding to the latex bead. As a result the FRET fluorophores will be in close proximity to each other and result in the appearance of FRET signal, which is calculated using the fluorescence intensities of the donor and acceptor fluorophores [8; 9]. By monitoring the appearance of new a FRET signal over time, we obtain a quantitative read-out describing the extent of retrograde traffic originating from the lysosome. To assess the specificity of the assay for retrograde lysosome traffic and the appearance of FRET signal, a series of controls were also performed.

A1.2. Materials and methods

A1.2.1. Cell culture

Normal human fibroblasts were purchased from the ATCC and cultured in Dulbecco's modified Eagle's medium (DMEM) supplemented with 1% penicillin/streptomycin and 5% bovine calf serum. Cells were cultured in Corning cell culture flasks at 37^{o}C in a 5% CO_2, humidified atmosphere until monolayers were 80% confluent at which time they were subcultured or seeded for experimentation. All experiments were performed with cells before passage 5. For FRET experiments, a TC-MI temperature controlled, humidified chamber from Bioscience Tools (San Diego, CA) was used for the duration of the experiment.

A1.2.2. Lysosome isolation

Lysosomes were isolated using the methods of Duvvuri et al. [7] with modifications to permit isolations of adherent cells as described in Chapter 2, Section 2.2.8.

A1.2.3. Western blot analysis

Western blot analysis was performed using procedures described previously in Chapter 2, Section 2.2.3 [7]. Primary antibodies were LAMP1 (1:500), CI-MPR (1:50), EEA1 (1:250), and Golgin-84 (1:250). Secondary HRP-conjugated antibodies were diluted 1:1000. Bands were visualized by adding

enhanced chemiluminescence reagents and imaged using Kodak Biomax MR Scientific Imaging Film.

A1.2.4. Fluorescence microscopy

Images were acquired by a Nikon Eclipse 80i microscope equipped for epifluorescence using a Hamamatsu Orca ER camera and MetaMorph software (v. 7.0). Filter sets specific for Cy5 and rhodamine (Cy3, Chroma) were used to detect Alexa Fluor 647 and 555 in cells, respectively. Microscope settings were kept identical for the duration of experiments. Merged images were constructed using the Image Overlay function with original brightness/contrast settings for each image. Immunofluorescence was accomplished as described previously (Chapter 2, Section 2.2.6). Antibodies specific to MPR and LAMP-1 were diluted 1:100 and 1:500 respectively.

A1.2.5. Fluorescent FRET tracer construction

The fusion between late endosomes and lysosomes was evaluated in fibroblasts using a method described by Jahrus *et al.* [2] with modifications to allow for quantitative assessments based on fluorescence resonance energy transfer (FRET) of late endosome/lysosome contents upon fusion. To construct the FRET donor and acceptor, standard labeling strategies were employed as described below:

A1.2.5.1. Lysosome tracer

Biotinylated-dextran-amine (10,000 MW, BDA-10000) was fluorescently labeled with the amine-reactive succinimidyl ester derivative of Alexa Fluor 647 per Invitrogen's instructions. According to the manufacturer, there are two lysine residues per molecule of dextran for Alexa Fluor 647 conjugation. First, the Alexa Fluor 647 was reconstituted in dry DMSO to a concentration of 10 mg/mL. BDA-10000 was reconstituted to 50 mg/mL in 0.1 M sodium bicarbonate buffer (pH 9.0, Buffer A) of which a 100 µL aliquot was added to 75 µL of Buffer A and 25 µL of 10 mg/mL Alexa Fluor 647 stock solution. The reaction was carried out at room temperature for 2 hrs and was quenched with 1 M Tris to a final concentration of 90 mM. The resulting solution was desalted five times using protein desalting columns from Thermo Scientific (Rockford, IL) to remove unconjugated Alexa Fluor 647 and remaining Tris.

A1.2.5.2. Late endosome tracer

For the late endosome tracer, carboxylate-modified mono-disperse polystyrene beads (2.5% solids, 1.08 x 10^{11} beads/ml, 0.792 ± 0.037 µm) were used. First, the beads were activated using N-(3-dimethylaminopropyl)-N′-ethylcarbodiimide (EDAC) to make the carboxylate moiety an amine-reactive center. To accomplish this, 4 mL of the polystyrene beads were washed 3 times with 0.1 M MES buffer (pH 6.0, Buffer B) by centrifuging the beads at 5,000 x g for 20 mins and resuspending with Buffer B. Immediately after the final wash, the beads

were resuspended to a 2% solids mixture in Buffer B and 2 mL of freshly prepared 50 mg/mL EDAC was added drop-wise to the suspension. The EDAC was allowed to activate the carboxylate groups for 15 mins at room temperature followed by three washes with 0.1 M PBS (pH 7.4, Buffer C). Activated beads were then resuspended in 5 mL of Buffer C for subsequent streptavidin conjugation by means of their surface exposed lysine residues. Lyophilized streptavidin, from Invitrogen, was reconstituted in Buffer C at a concentration of 1 mg/mL of which 5 mL was added to the activated beads solution for 3 hrs at room temperature. Unconjugated streptavidin was removed by extensive washing with PBS. The beads were centrifuged and stored at 4^{o}C in a solution of Buffer C containing 0.1% glycine to mask any unreacted sites. Fluorescence labeling of the streptavidin conjugated beads was carried out using the succinimidyl ester derivative of Alexa Fluor 555 per Invitrogen's instructions. First, 1 mL of streptavidin-conjugated beads was washed 2 times with Buffer A to remove the glycine storage buffer and resuspended back to 1 mL. An Alexa Fluor 555 aliquot of 10 µL of a 10 mg/mL solution was added to the freshly washed beads. Labeling was performed at room temperature for 2 hrs and subsequently quenched with Tris. Unreacted Alexa Fluor 555 was removed with extensive washing with PBS. Subsequent dialysis was performed against PBS using a dialysis cassette with a 3.5 kDa cutoff. Beads were centrifuged once more, resuspended in PBS, and stored at 4^{o}C until needed.

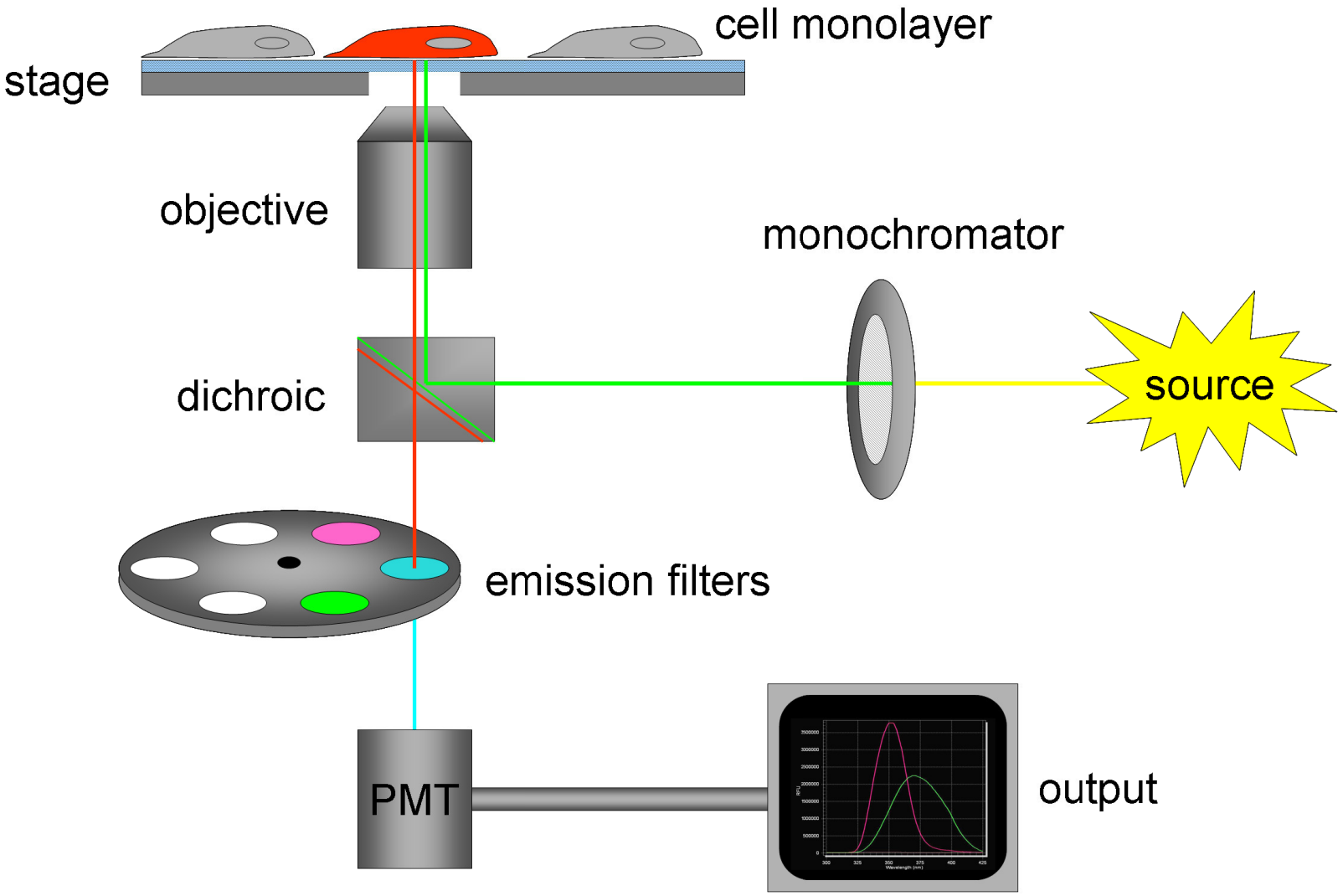

Figure A1.1. Experimental setup for live-cell fluorescence measurements.

A1.2.6. Tracer localization and drug treatments

To evaluate the fusion of late endosomes and lysosomes, cells were seeded in 8-well culture chambers at 75 x 10^4 cells per well. Cells were incubated for 2 hrs with 2.5 mg/mL Alexa Fluor 647 biotinylated dextran in complete phenol red-free DMEM medium, washed once with PBS, and given chase in complete medium for 20 hrs to ensure localization into the lysosome. After 20 hrs post-chase, cells were exposed to 1.28 x 10^7 beads/mL of Alexa Fluor 555 streptavidin-conjugated latex beads for 2 hrs and chased for 1 h to label the late endosomal compartment. FRET measurements were started immediately after the localization of the latex bead to the late endosome compartment. Nocodazole (50 μM), a microtubule depolymerizing agent, was added to respective wells 1 h after the start of FRET measurements. For all other treatments shown in Chapter 4, Section 4.3.2, administration was started immediately after the late endosome tracer chase.

A1.2.7. Fluorescence intensity measurements and analysis

Monolayers were analyzed using a Photon Technologies International (Birmingham, NJ) Ratiomaster microscope-mounted spectrofluorometer. This setup employed a scanning monochromator for precise excitation wavelengths (lamp slit widths set at 2.5 nm). Detection of fluorescence signals was accomplished using a PMT detector attached to one of the microscope camera ports. Dichroic mirrors and emission filters were employed to segregate specific emissions of the two FRET fluorophores (see schematic of experimental setup in

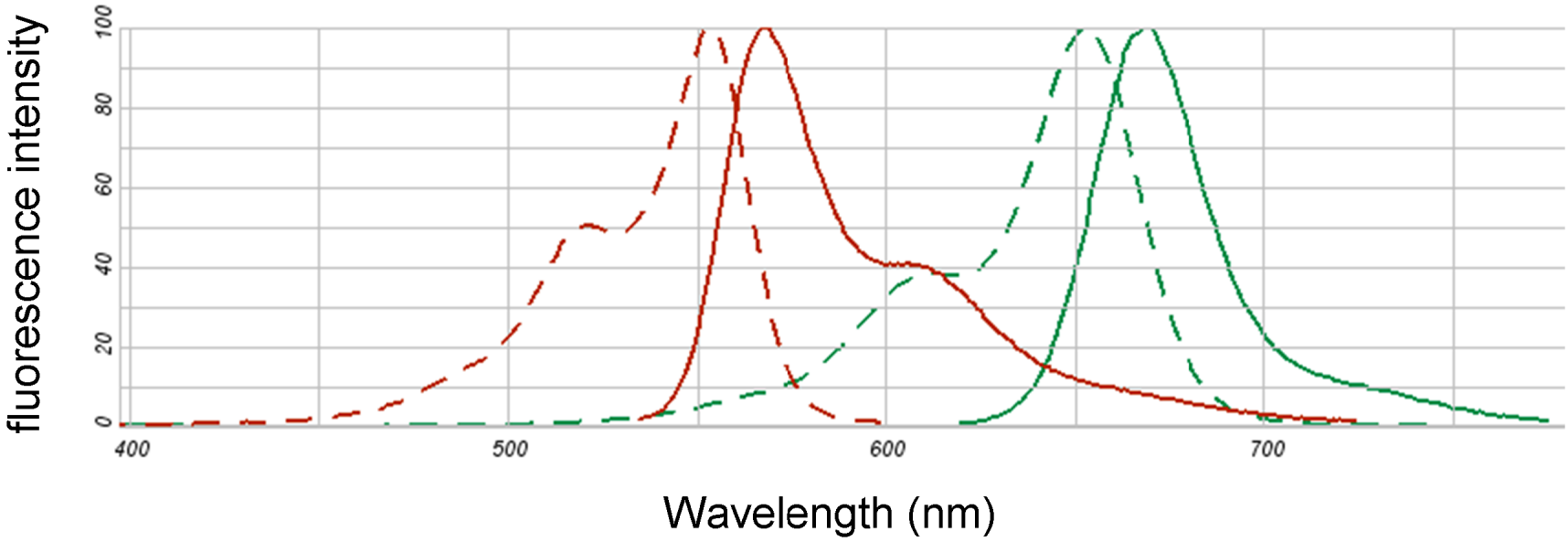

Figure A1.2. Absorption (dotted) and fluorescence emission spectra (solid) for Alexa Fluor 555 (red) and Alexa Fluor 647 (green). Spectra taken from Invitrogen: http://www.invitrogen.com/site/us/en/home/support/Research-Tools/Fluorescence-SpectraViewer.html

Figure A1.1). For each time-point, three measurements were made, corresponding to the Alexa Fluor 555 donor excitation/emission (ex: 550 nm, em: 610/40 nm, dichroic: 565 nm longpass), donor excitation/acceptor emission (FRET, ex: 550 nm, em: 710/60 nm, dichroic: 565 nm longpass), and Alexa Fluor 647 acceptor excitation/emission (ex: 650 nm, em: 670/40 nm, dichroic: 660 longpass). For fluorophore spectra see Figure A1.2. All dichroic and emission filters were from Chroma (Rockingham, VT).

There are many contributing factors that can result in FRET signal artifacts in living cells including cellular autofluorescence [10; 11], spectral cross talk, and differential concentrations of the donor and acceptor present [9; 11; 12]. To account for autofluorescence from our experimental conditions, we measured fluorescence emission intensities of cells without probes, at wavelength intervals corresponding to each of the probes, in the presence of phenol red-free DMEM medium containing fetal bovine serum. Although no significant emission peaks were observed around wavelengths used to measure Alexa Fluor 555 and 647, there was significant background that contributed to the probes apparent signal strength (Fig. A1.3). These scans, without probes, were subsequently subtracted from experimental data before calculating FRET signal.

For fluorescence microscopy evaluations, the donor and acceptor probes did not visually bleed through (detection of donor fluorescence with the acceptor emission filter or detection of acceptor fluorescence with the donor emission filter)

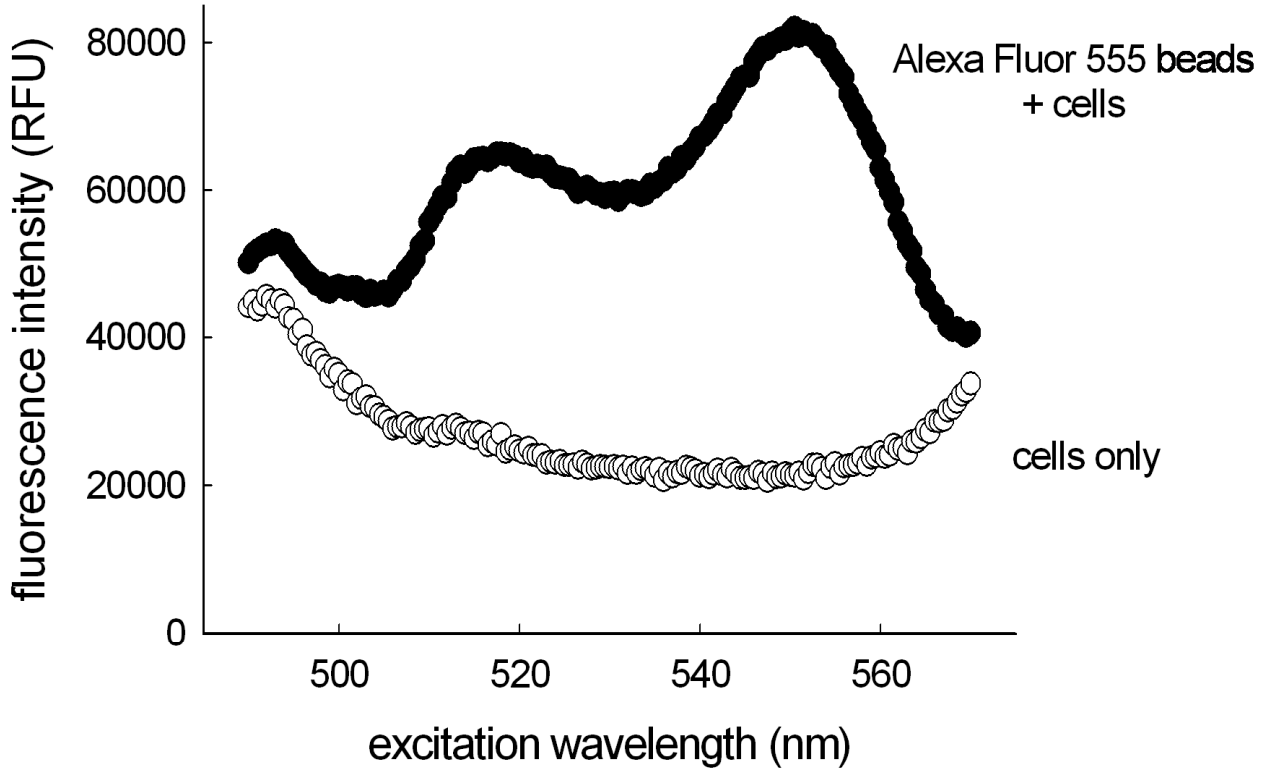

Figure A1.3. Autofluorescence contribution to Alexa Fluor 555 fluorescence in living cells. Living cell monolayers with (black circles) or without (open circles) streptavidin conjugated latex beads labelled with Alexa Fluor 555 were analyzed for background subtraction purposes. The excitation spectrum was analyzed from 490 to 575 nm. Cellular autofluorescence was significant and contributed to Alexa Fluor 555's apparent signal at 550 nm, the wavelength used for subsequent FRET measurements.

their counterparts' filter sets (Fig. A1.4). However, to compensate for both spectral cross talk of the FRET probes and the propensity of cell populations to endocytose differential amounts of the probes (although both sets of cells were similar in the uptake of FRET probes, see Figure A1.5A and B), we applied a widely used equation for the normalization of donor and acceptor intensities for FRET calculation (Eq. 1) [9; 12; 13; 14]. Correction factors α and β were determined to be 0.011 and 0.799, respectively for our experimental setup.

Eqn 1. $$\text{FRET ratio} = \frac{\text{FRET} - \alpha \times \text{AF555} - \beta \times \text{AF647}}{\sqrt{\text{AF555} \times \text{AF647}}}$$

Initial calculated FRET ratio values for each experiment were then normalized to zero and the appearance of new FRET ratio signal was evaluated over time. Each acquisition was no longer than 10 s.

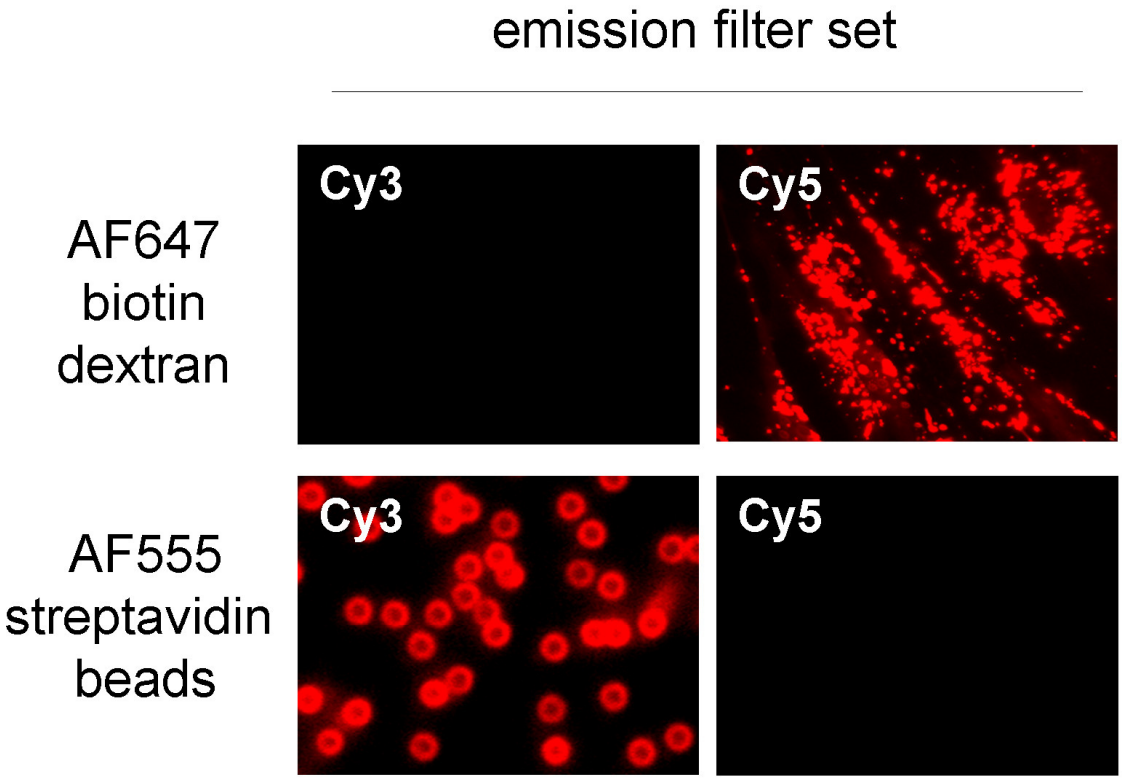

Figure A1.4. Emission filter sets used for FRET determinations show little spectral cross talk between FRET fluorophores. Alexa Fluor 647 (AF647) fluorescence emission was not present in a Cy3 filter set used for Alexa Fluor 555 (AF555) detection. Vice versa for AF555 fluorescence emission in a Cy5 filter set used for AF647 detection.

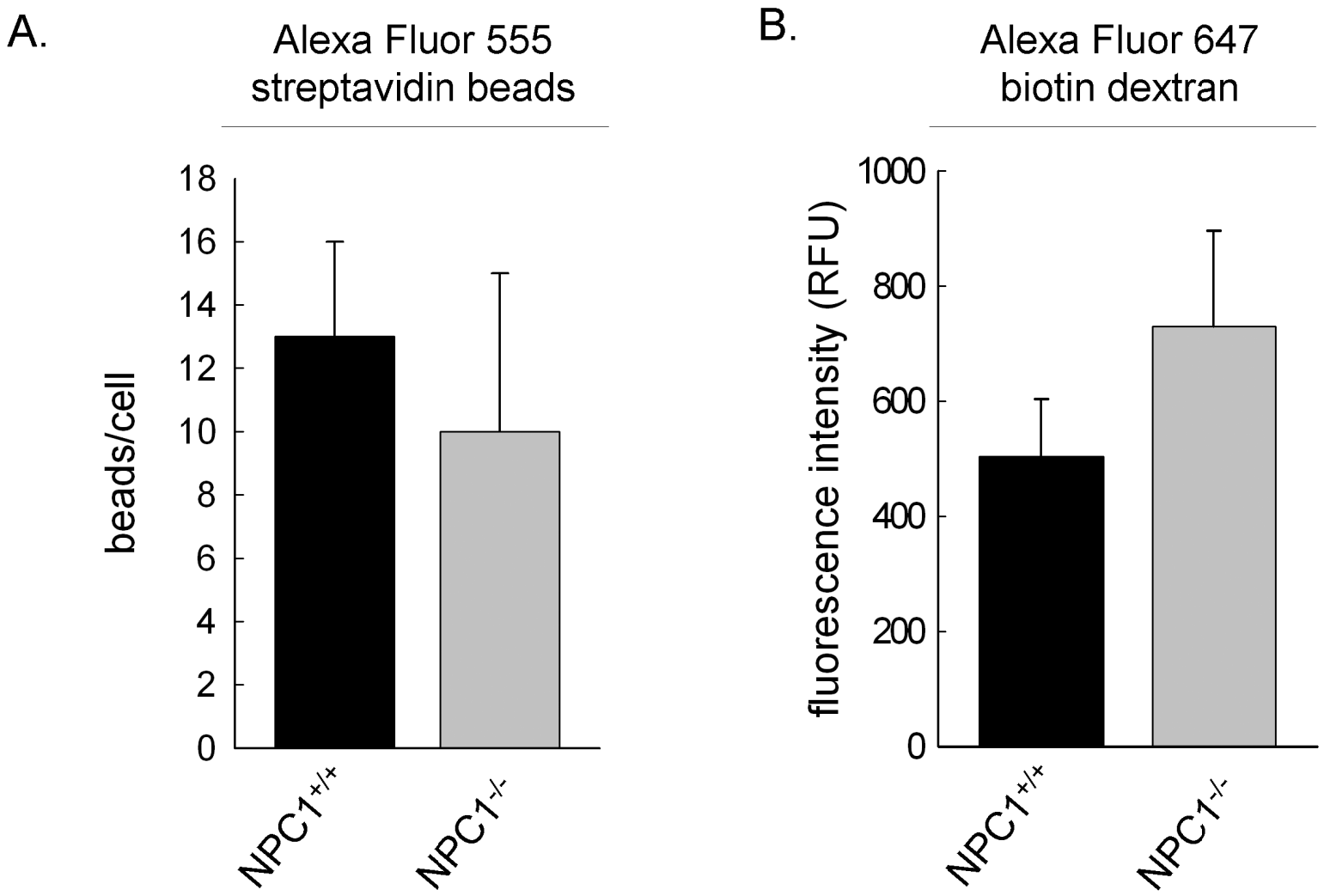

Figure A1.5. FRET probe uptake is similar between NPC1$^{+/+}$ and NPC1$^{-/-}$ cell lines. (A) The average ± S.D. of streptavidin latex beads endocytosed per cell was counted using light microscopy. (B) The average ± S.D. fluorescence intensity of biotin dextran endocytosed per cell was measured using the FRET experimental set-up Fig. A1.1. as described in Materials and Methods.

A1.3. Results

A1.3.1. Synthesis and characterization of FRET probes

Based on previously described methods for specifically localizing probes to lysosomes and late endosomes [2], modified organelle probes were constructed and conjugated with either streptavidin or biotin and a fluorophore that could be utilized for FRET studies. For lysosomes, we utilized a commercially available 10,000 MW dextran polymer that was conjugated with both biotin and lysine groups. For late endosomes, we conjugated carboxylate-modified latex beads, of the same diameter (0.792 μm) used by Jahraus et al., with streptavidin. Fluorescence labeling of the probes was accomplished by using amine-reactive succinimidyl ester derivatives of the known FRET pair Alexa Fluor 555 (AF555, donor) and 647 (AF647, acceptor) against lysine residues present on streptavidin or dextran, respectively. To confirm specific binding of the biotinylated-dextran with streptavidin-coated beads *in vitro*, both probes were mixed, extensively washed, and imaged. The addition of biotinylated-dextran to a solution of streptavidin beads resulted in the appearance of dextran on the perimeter of the beads (FIG A1.6). Binding of the probes allows the FRET fluorophores to come in close proximity to each other, which is required for efficient FRET to occur [8]. Alexa Fluor 488 dextran, without biotin, was used as a negative control and did not bind to the streptavidin beads under the same conditions (Fig. A1.6).

Hoppe et al. has reported that pH-dependent fluorescence intensity fluctuations of FRET fluorophores can result in decreased FRET efficiency between donor and acceptor molecules [13]. To be certain that our FRET probes were suitable for studies in which environmental pH could be manipulated, whether from endogenous factors or exogenously supplied agents, we characterized fluorescence intensities over a broad pH range. We found that fluorescence intensities remained constant for each probe and did not fluctuate significantly at pH values relevant to the endocytic pathway (Fig. A1.7).

A1.3.2. Intracellular localization of the FRET probes

To test the suitability of our pulse-chase protocols, we examined the intracellular localization of both FRET probes in normal human fibroblasts. To accomplish this, subcellular organelle isolations and immunofluorescence microscopy were performed after the probes were endocytosed as described in Materials and Methods. For immunofluorescence, cells were fixed and probed with antibodies specific to the lysosome associated membrane protein-1 (LAMP-1) for lysosomes and the cation-independent mannose-6-phosphate receptor (CI-MPR) for late endosomes. The majority of the biotinylated-dextran was found in LAMP-1 positive, CI-MPR negative organelles (Fig A1.8A) indicative of the lysosome [15]. For lysosome isolations, a super-paramagnetic iron dextran was localized to lysosomes using the same incubation conditions as the biotinylated-dextran. Lysosomes were then purified using a magnetic chromatography approach developed in our laboratory [7]. Western blot analysis revealed the

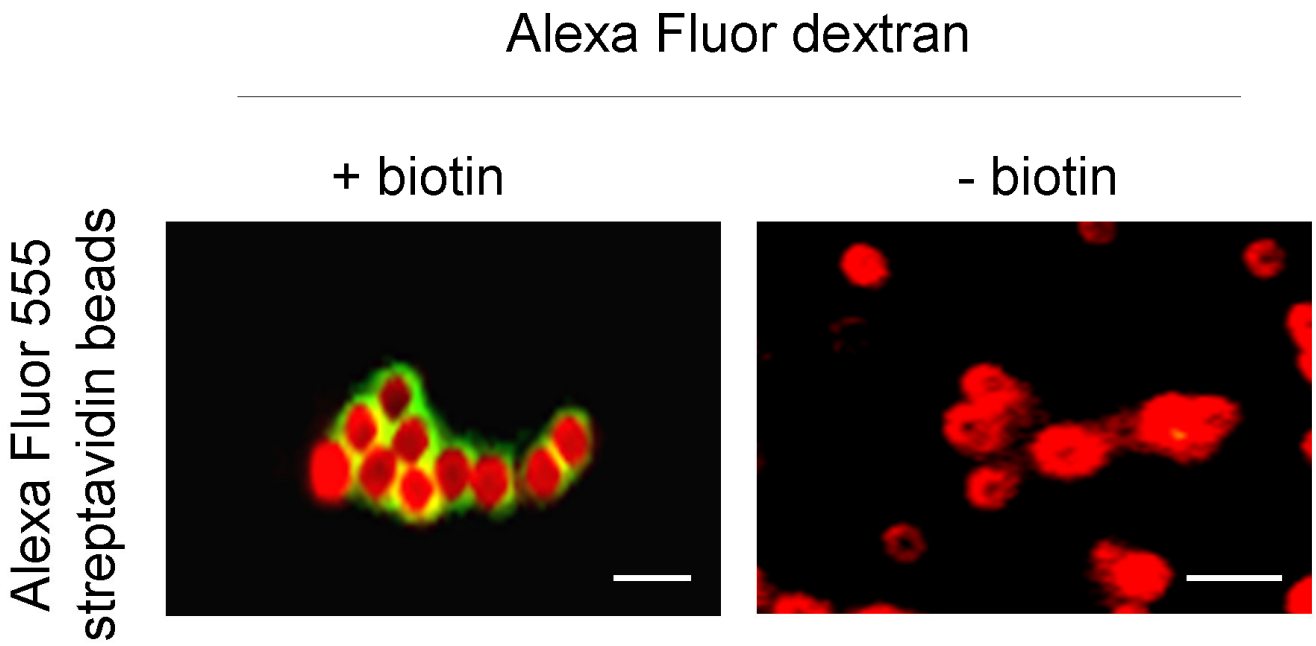

Figure A1.6. FRET probes bind *in vitro*. Fully conjugated probes were incubated together and imaged. Binding of dextran to streptavidin latex beads was dependent on the presence of biotin on the dextran polymer. Scale bar represents 1 μm.

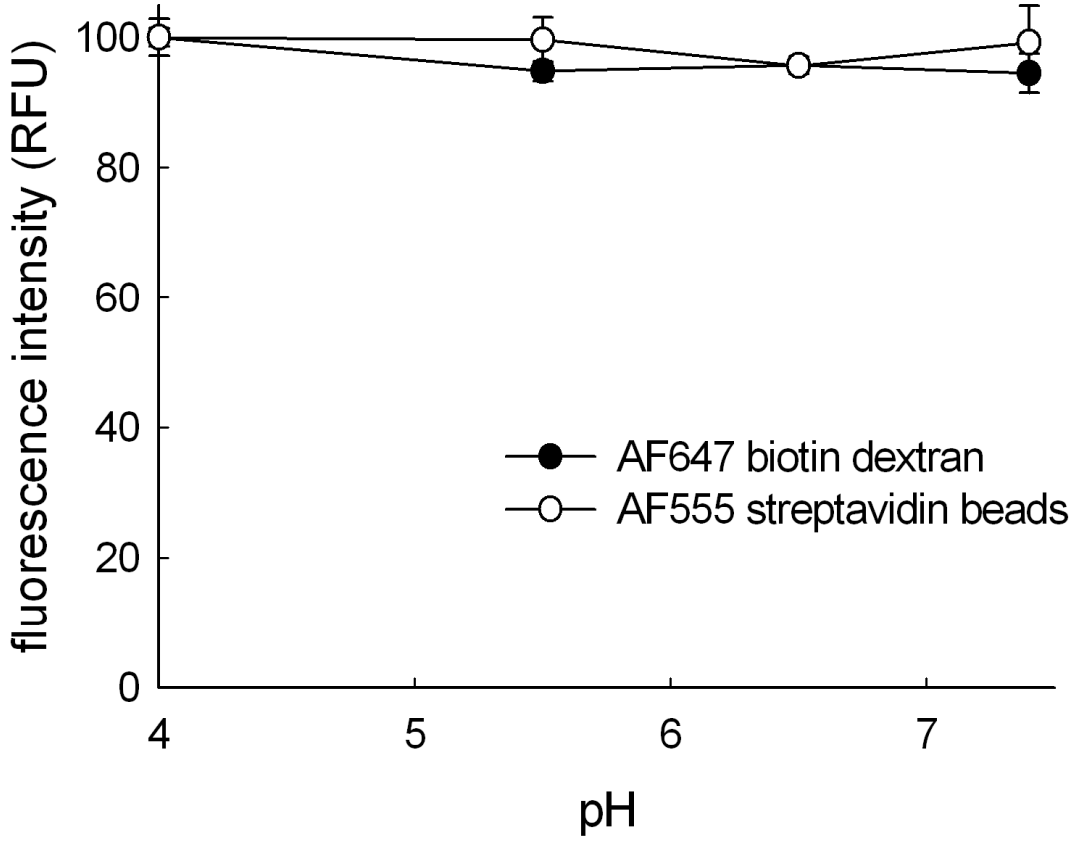

Figure A1.7. Fluorescence intensity of FRET probes as a function of pH. AF647 labeled biotinylated-dextran (closed circles) and AF555 labeled streptavidin beads (open circles) were incubated in buffers of different pH and their fluorescence intensities measured. There was no significant change in intensities of either probe at lower pH values.

presence of CI-MPR in the post nuclear supernatant (PNS) but not in the isolated fraction (Fig. A1.8B). Furthermore, there was no significant localization into either the Golgi apparatus (Golgin-84) or early endosomes (EEA1), suggesting the biotinylated-dextran is almost completely present in lysosomes when using optimized pulse-chase conditions (Fig. A1.8C). Immunofluorescence of cells incubated with streptavidin beads shows localization within CI-MPR positive organelles, indicating that the beads were predominantly in late endosomes (Fig. A1.8D).

A1.3.3. Interactions of FRET probes occur *in vivo*

Previously we had shown that our FRET probes could bind *in vitro* (Fig. A1.6). Considering the lumenal composition of late endosomes and lysosomes is much more complex than PBS, we evaluated if the FRET probes could interact and be colocalized to a significant degree in living cells. To accomplish this, dextran was endocytosed as before and cells were visualized using fluorescence microscopy at the end of the streptavidin bead chase (0 h) and 24 hrs post-chase. Initially, the two probes were visualized in separate compartments. However, at 24 hrs post-chase, dextran signal was observed in bead containing compartments suggesting a significant portion of lysosomal dextran was bound to the streptavidin bead (Fig. A1.9).

In addition to colocalization experiments, we also observed the interaction of lysosomes with late endosomes using time-lapse video microscopy. We found

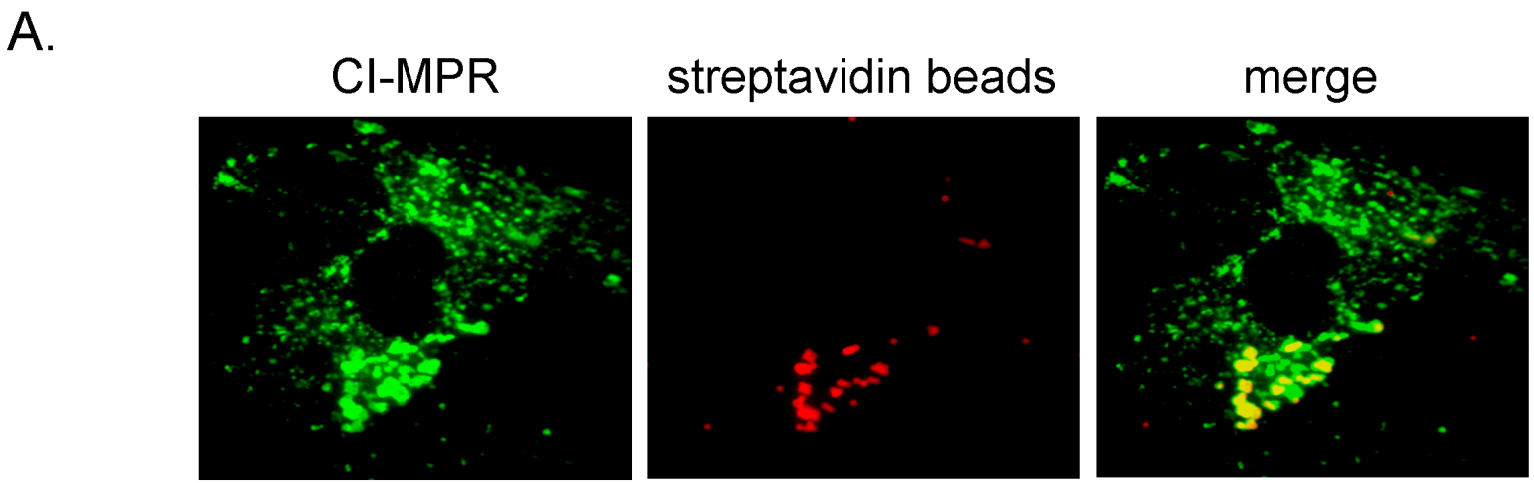

Figure A1.8. Western blot and immunofluorescence analysis shows intracellular localization of the FRET probes in two biochemically distinct compartments. (A) Immunofluorescence was performed after streptavidin beads (red) endocytosis. The beads were found to localize in a CI-MPR positive (green) compartment.

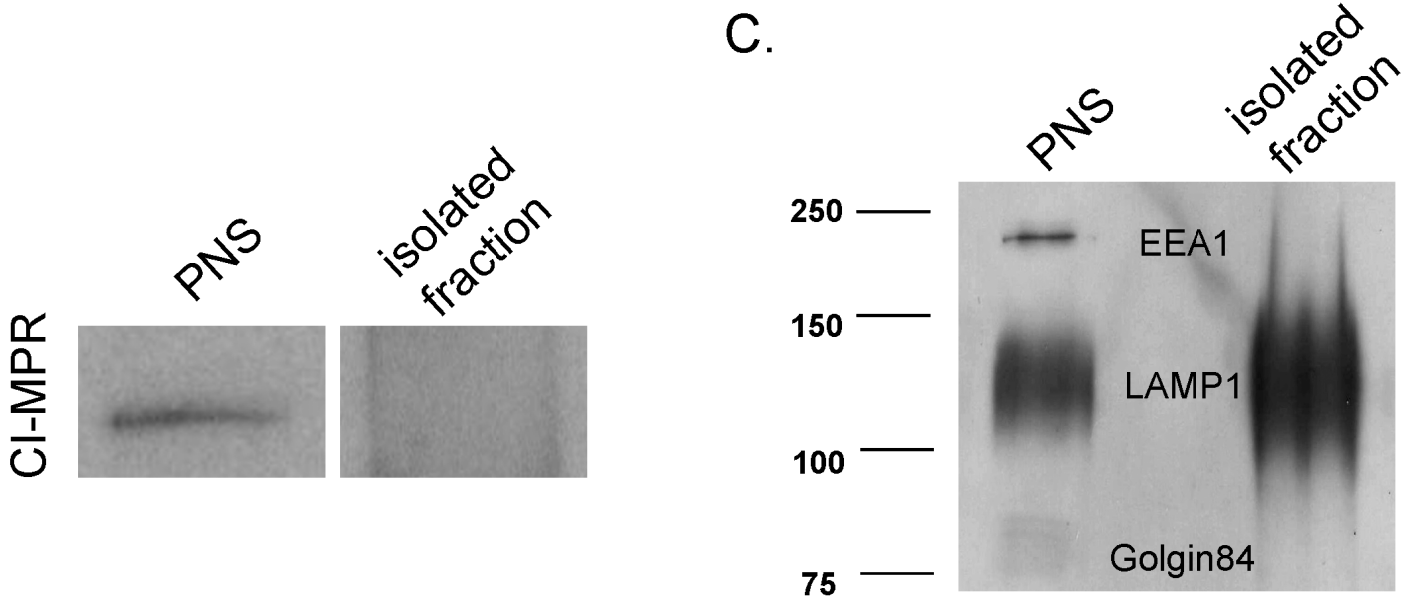

Figure A1.8. ***(cont.)*** (B) Magnetic isolation of lysosomes using iron coated dextran of the same size was performed as described in Materials and Methods. Western blot analysis was performed using antibodies specific to the cation-independent mannose-6-phosphate receptor (CI-MPR), (C) Golgin-84, early endosome antigen-1 (EEA1) and lysosome associated membrane protein-1 (LAMP-1) on fractions of post nuclear supernatant (PNS) and isolated lysosomes. The isolated lysosome fraction was found to be devoid of late endosome, early endosome and Golgi protein markers, and enriched in LAMP-1.

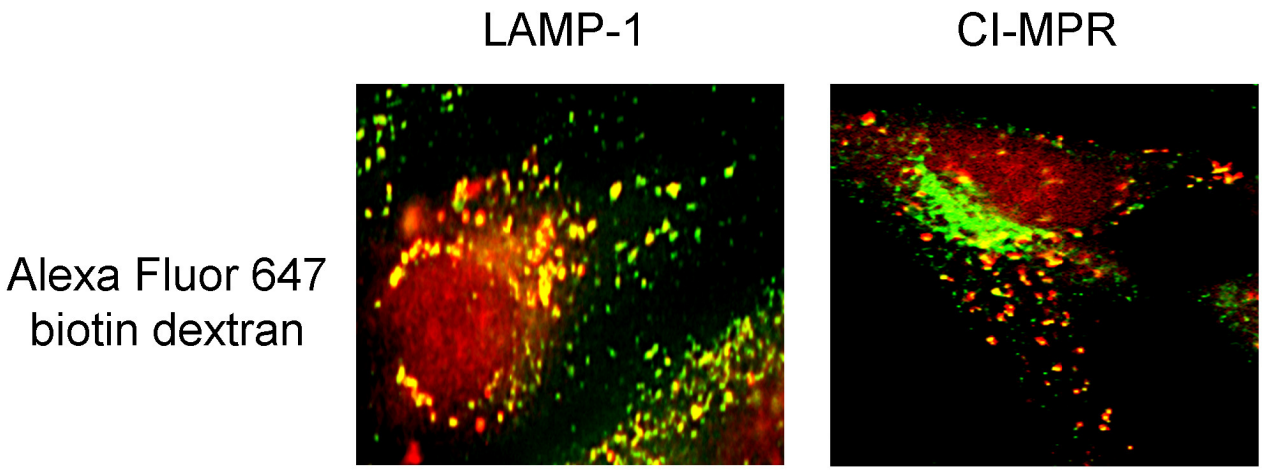

Figure A1.8. ***(cont.)*** (**D**) Immunofluorescence was performed after biotin dextran (green) endocytosis. The dextran was found to localize in a LAMP-1 positive, CI-MPR negative (red) compartment.

that dextran laden lysosomes could interact with bead containing late endosomes through different mechanisms: transient and complete organelle fusion (Figures A1.10 and A1.11). The transient interactions of lysosomes and late endosomes were confirmed by measuring the fluorescence intensity of donor beads before and after acceptor dextran was deposited. As expected, the trafficking of acceptor dextran slightly quenched the emission intensity of the donor latex beads (Fig. A1.11B).

A1.3.4. Detection of a FRET signal is dependent on probe binding affinity

For efficient FRET to occur, donor and acceptor fluorophores are required to be in close proximity to each other (see Figure A1.12) [8]. Streptavidin and biotin facilitate this requirement for FRET when bound together and have been used in previous FRET-based studies [16]. If the appearance of a FRET signal over time in our assay was dependent on probe affinity, then latex bead conjugation to a protein with less affinity for biotin should result in a decreased FRET signal. To evaluate if streptavidin was needed for assay sensitivity, we constructed new beads by conjugating bovine serum albumin (BSA) to latex beads and fluorescently tagging it with AF555. Next, we evaluated each set of latex beads, streptavidin and BSA, in living cells previously incubated with biotinylated-dextran. To use Equation 1, we made 3 separate fluorescence intensity measurements: Alexa Fluor 555 beads, Alexa Fluor 647 dextran and the FRET measurement as described in Materials and Methods.

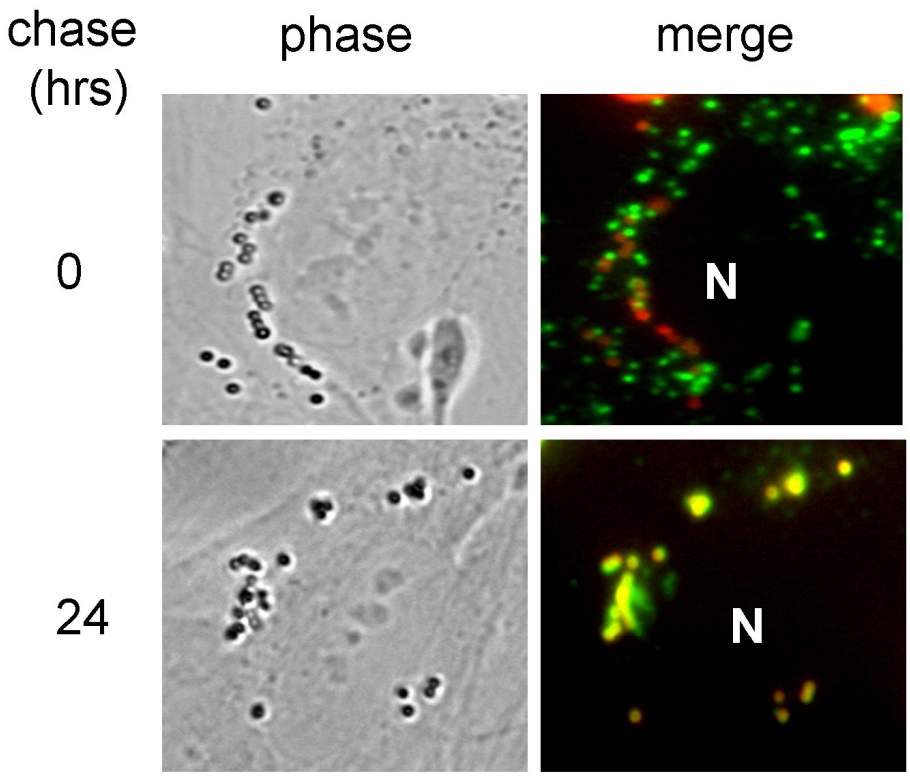

Figure A1.9. Fluorescence microscopy reveals FRET probes interact and colocalize intracellularly in normal fibroblasts. Intracellular interactions were observed between the two probes after sufficient chase times. Initially, the probes are not significantly colocalized with each other. However, after 24hrs chase, the biotinylated-dextran (green) was found bound to the streptavidin beads (red). N = nucleus.

We observed that beads coated with BSA had higher fluorescence emission intensity when excited at the donor excitation of 550 nm than that of the streptavidin coated beads (Fig. A1.13A). In the absence of biotinylated-dextran, BSA-coated beads had a lower fluorescence signal than streptavidin beads (Fig. A1.14). More importantly, the FRET measurement showed streptavidin coated beads had much higher signals when compared to the BSA control beads (Fig. A1.13B). This decrease occurs because the donor emission intensity is efficiently quenched by the presence of an acceptor fluorophore. This does not occur with BSA-conjugated beads. Measurements of the total biotinylated-dextran fluorescence were similar (Fig. A1.13C). This verified that the increased signal for the streptavidin beads in the FRET measurement was not due to differential biotin dextran endocytosis but was from probe interactions. When monitored for a period of 3 hrs, no FRET signal appeared when using BSA-conjugated latex beads. However, experiments with streptavidin show that a significant amount of FRET signal appears over time due to its ability to strongly bind biotin (Fig. A1.15). These results suggest that strong binding between the probes is needed for efficient FRET permitting the sensitive detection of retrograde trafficking from lysosomes in living cells.

A1.3.5. Retrograde Transport of Lysosome Cargo to Late Endosomes is Microtubule Dependent

The movements of lysosomes and late endosomes have been shown to be microtubule dependent [17]. The addition of a reagent that destabilizes

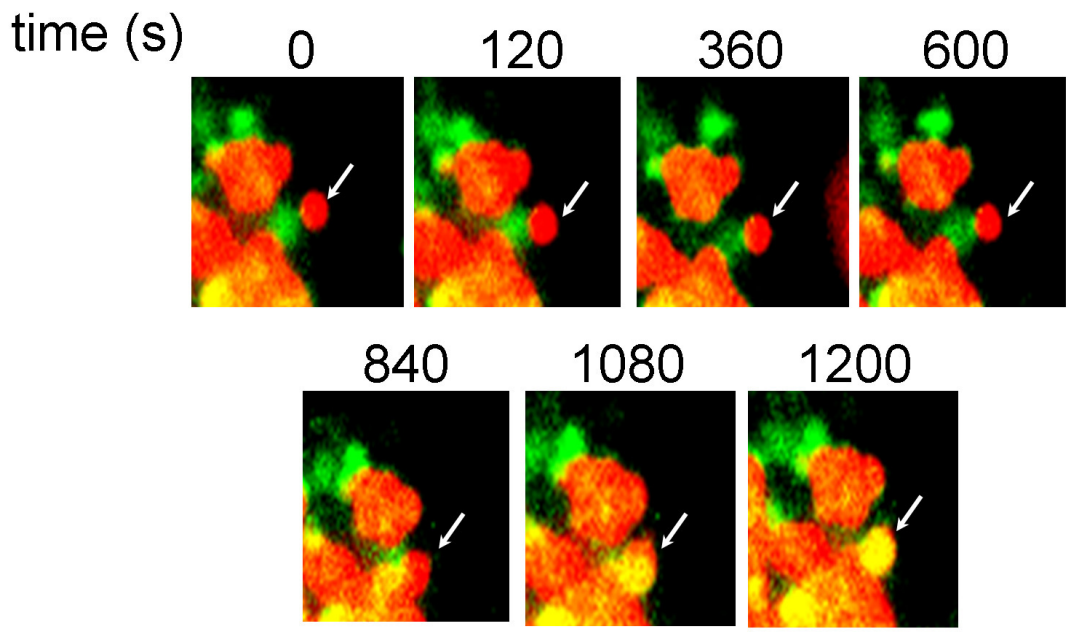

Figure A1.10. Time-lapse fluorescence microscopy reveals FRET probes interacting in normal human fibroblasts. Still images from movies taken of FRET probes over time show lysosomes can completely fuse with late endosomes. The white arrow follows a bead containing late endosome (red) fusing with a dextran laden lysosome (green).

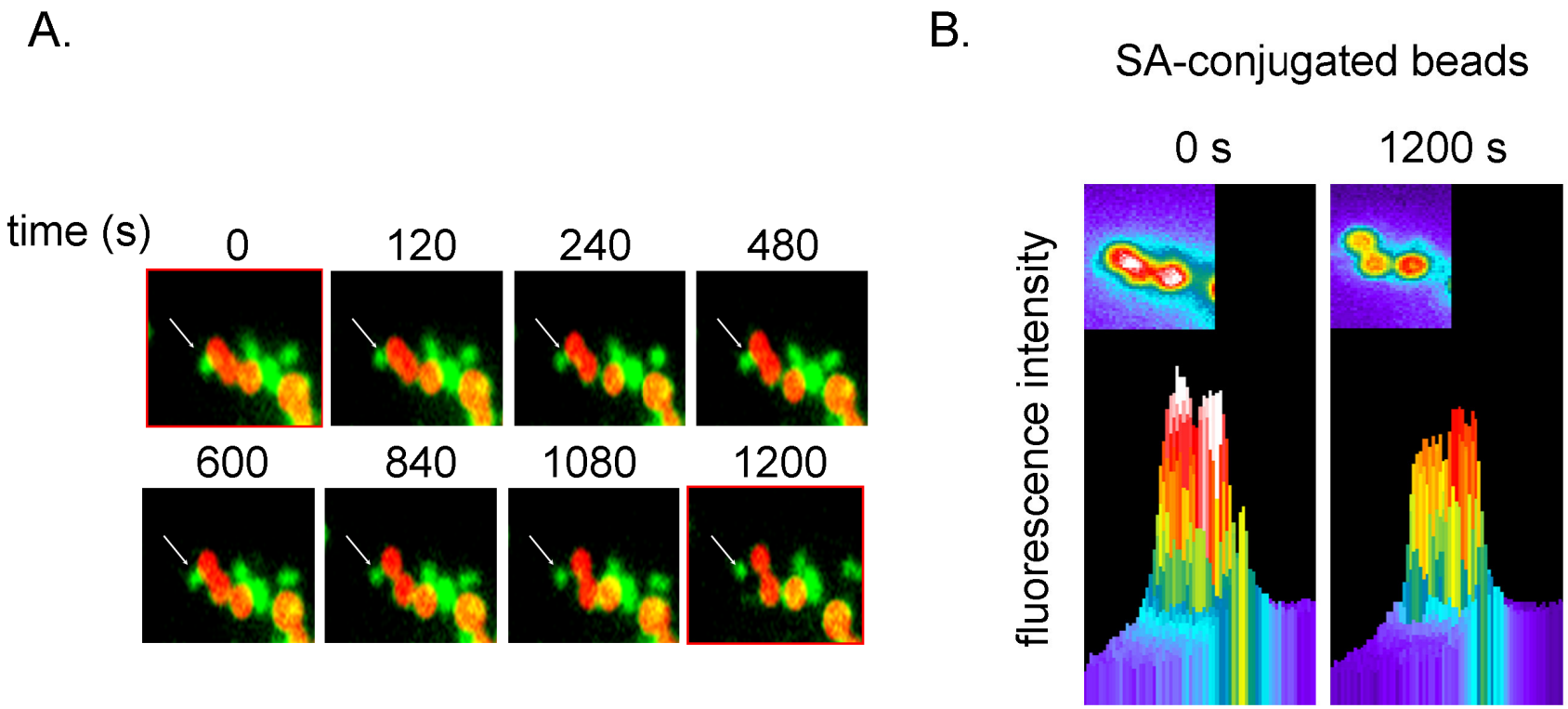

Figure A1.11. Time-lapse fluorescence microscopy reveals FRET probes interacting in normal human fibroblasts. (A) Still images from movies taken of FRET probes over time show lysosomes transiently interact with late endosomes (white arrow). (B) Quenching of Alexa Fluor 555 streptavidin beads by Alexa Fluor 647 biotin dextran over time (white = most intense signal) due to hybrid organelle formation. Red outlined frames from (A) are shown in (B).

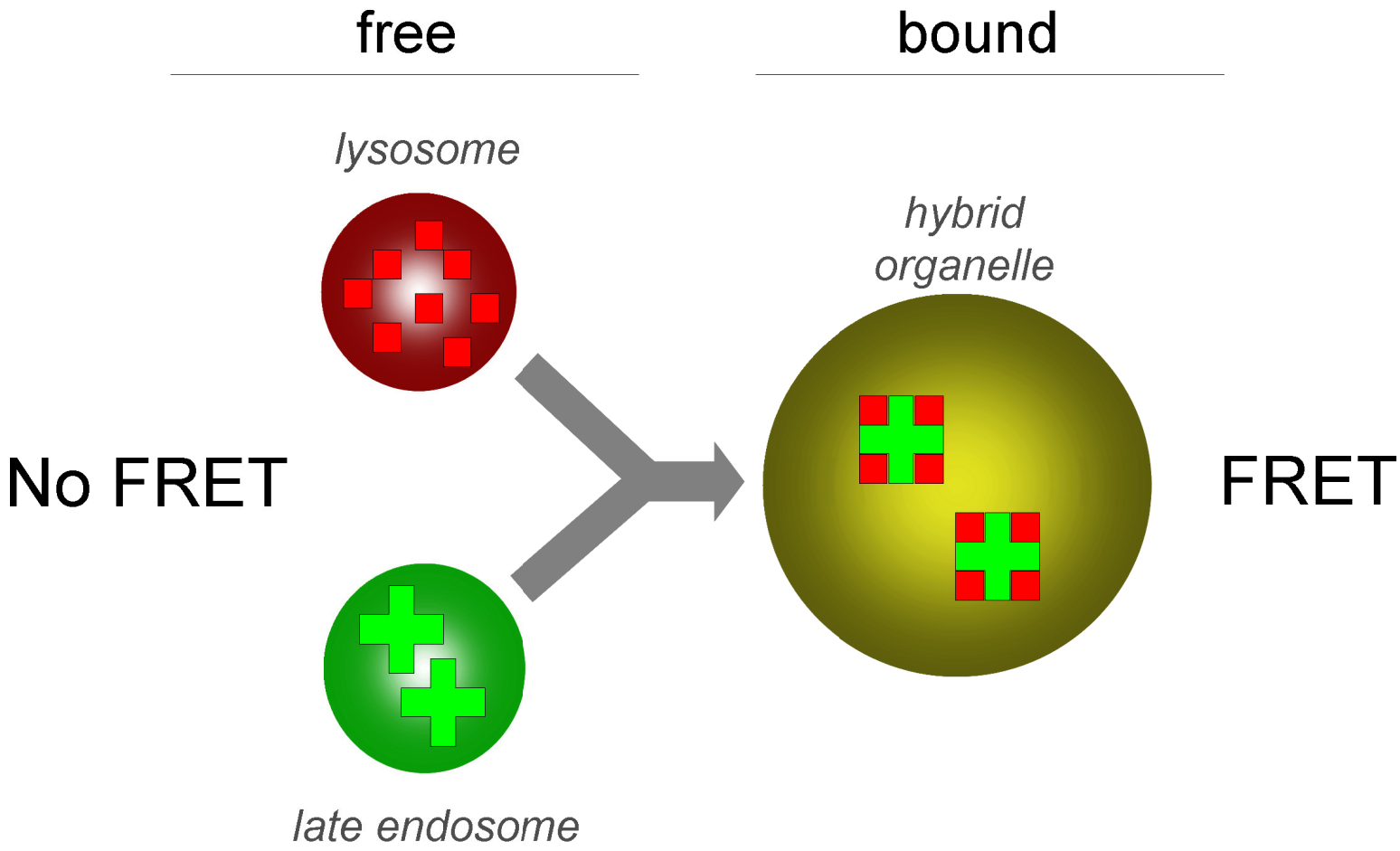

Figure A1.12. For efficient FRET to occur, the FRET probes must be bound to each other. The only way for this to occur is through the fusion of lysosomes with late endosomes.

microtubules and thus inhibits the contact between lysosomes and late endosomes, should diminish retrograde traffic and thus the FRET signal over time. To test this, the microtubule-destabilizing agent nocodazole (NOC) was incubated with cells. First, lysosomes and late endosomes were allowed to interact for 1 h, at which point cells were either treated with 50 μM NOC or left untreated. By not pre-treating cells with NOC prior to FRET measurements, we create the same initial conditions with respect to probe uptake since NOC would affect microtubule dependent endocytosis of the latex beads. Furthermore, allowing lysosomes and late endosomes to interact for 1 h allowed us to evaluate the post-administration effects of NOC in real time. After NOC treatment, the appearance of new FRET signal was minimal compared to that of normal untreated cells (Fig. A1.16). This indicated NOC destabilization of the microtubule network impacted organelle interactions and ultimately the ability of biotinylated-dextran to be delivered to the late endosome via the retrograde lysosome pathway.

A1.4. Discussion

To date, there have been several different approaches developed to investigate the interactions of lysosomes and late endosomes [2; 18; 19]. Mullock et al. described a cell-free content mixing assay based on the mixing of purified late endosomes and lysosomes harvested from rat livers [19]. Briefly, organelle labeling was accomplished by endocytosing avidin-ASF for late endosomes, ^{125}I-biotinylated-IgA for lysosomes and subsequently purified. Each of the purified fractions were separately reconstituted in cytosol containing an ATP-regenerating system and added together. Evidence of late endosome-lysosome fusion was determined by immunoprecipitation of avidin-ASF which bound to ^{125}I-biotinylated-IgA if the two organelles were fused. Use of this assay has identified many components, such as SNARE, SNAP and Rab GTPase proteins, which are necessary for fusion of lysosomes with late endosomes [20; 21]. Although highly elegant and informative, such an assay requires lengthy and complex organelle isolation procedures from animals and radioactive reagents. Jahraus et al. described a cell-based method for observing retrograde lysosome fusion with late endosomes [2]. This method adequately described retrograde lysosome traffic; however, detection of this event was qualitatively accomplished with light microscopy. This detection methodology would not be suitable for evaluating slight changes in the rates of retrograde traffic that could be useful in identifying the molecular mechanisms underlying this trafficking pathway.

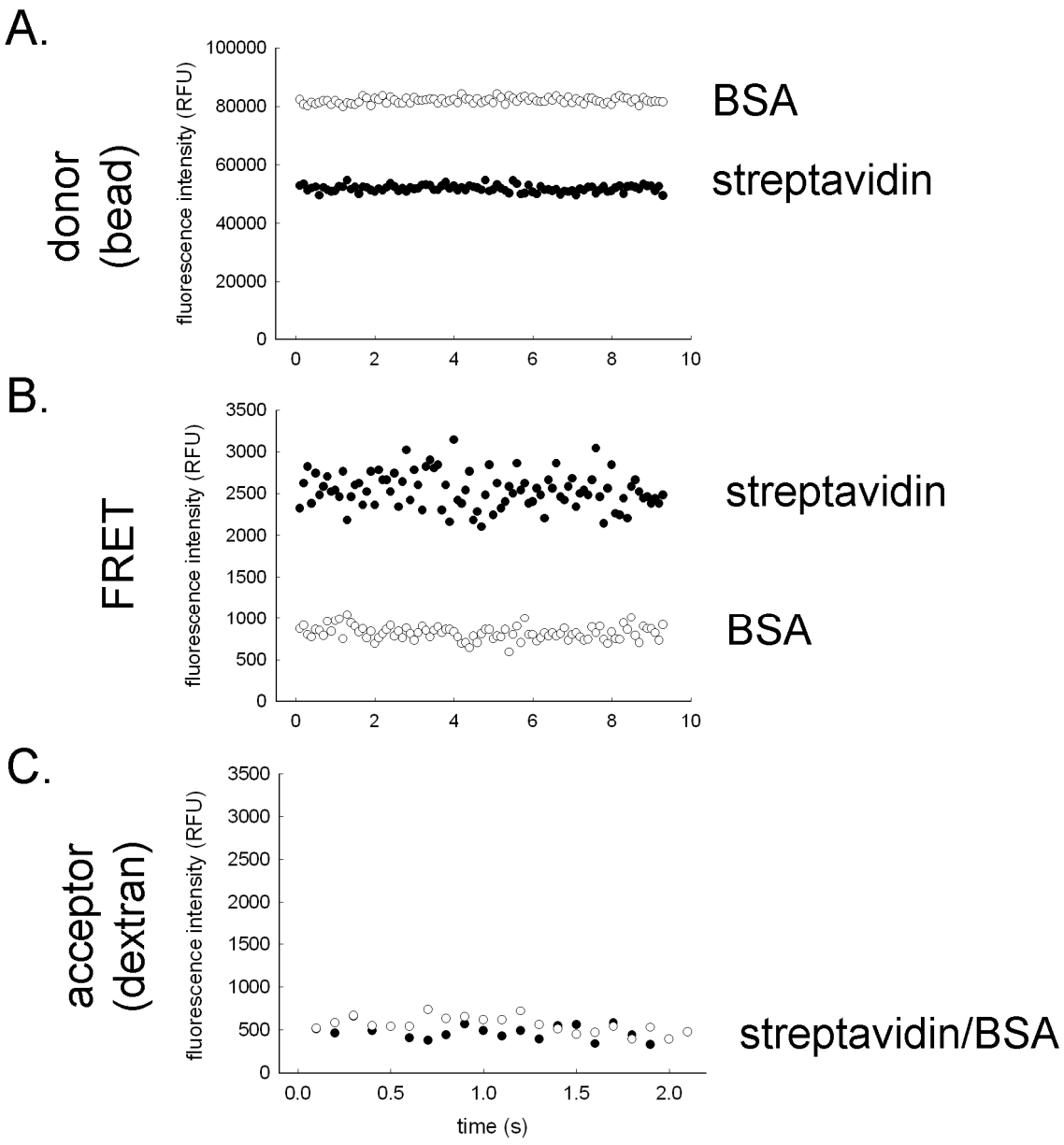

Figure A1.13. Streptavidin coated latex beads experience higher donor quenching and increased signal in the FRET measurement. A comparison between the emission intensities at (A) 570 nm and (B) 670 nm in cells with FRET probes conjugated with either streptavidin (closed circles) or BSA (open circles) when excited at the donor wavelength. Probes conjugated with streptavidin exhibit significant quenching of the donor emission signal and an increased acceptor emission signal at 670 nm indicative of FRET. Beads conjugated with BSA do not specifically bind biotinylated-dextran and thus their 570 nm emission remains high and 670 nm emission signal low. (C) Cellular dextran uptake was similar for both sets of experiments.

In this chapter we describe a method for evaluating late endosome-lysosome fusion that offers significant advancement over previous methods, specifically: 1) quantitative assessment of retrograde lysosome traffic, and 2) its utility for high throughput applications. This approach should permit future studies to elucidate proteins and potential small molecular weight factors that influence this retrograde trafficking step. Furthermore, it is likely that this assay could be used to study lysosomal storage disorders, as has been done in this dissertation with NP-C disease, to identify small molecular weight therapeutic agents that may appropriately modulate this trafficking event and be used in the treatment of such diseases.

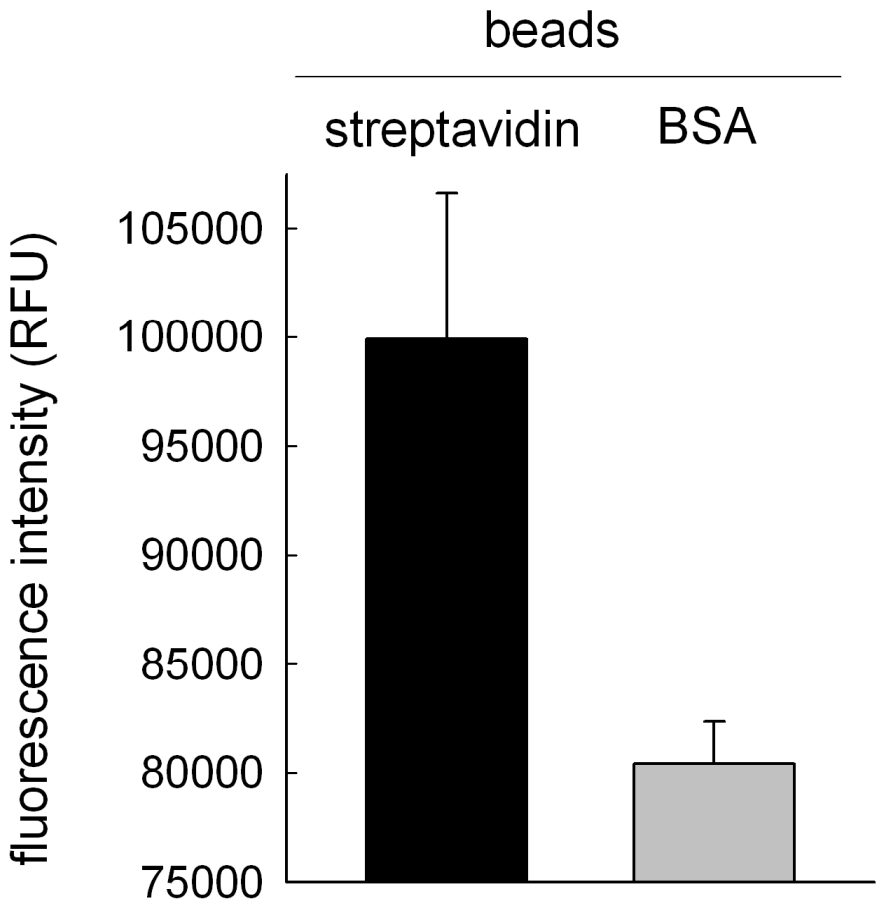

Figure A1.14. Alexa Fluor 555 streptavidin coated latex beads have higher fluorescence emission intensity in the absence of Alexa Fluor 647 biotin dextran. Cells were incubated with either BSA or streptavidin beads and then fluorescence intensities measured by exciting at 550 nm. Data is an average of at least 3 experiments ± S.D.

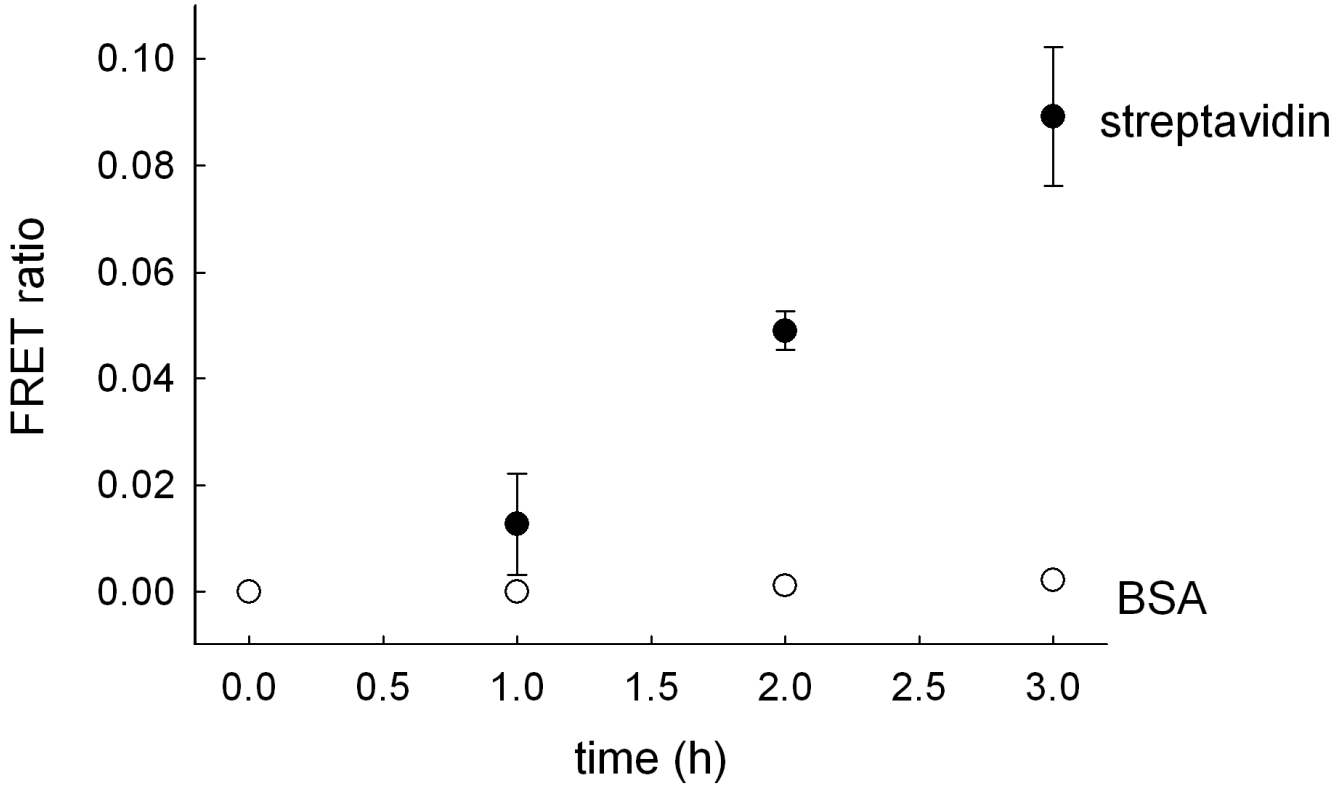

Figure A1.15. The appearance of FRET signal requires the presence of streptavidin on the latex beads. Beads conjugated with bovine serum albumin (BSA) were conjugated to latex beads and used as a control to identify non-specific appearance of FRET signal. Appearance of FRET signal over time was detectable with streptavidin latex beads (closed circles), but not with BSA (open circles) due to its inability to specifically bind the biotinylated-dextran FRET probe. Results are an average of 3 independent experiments ± S.D.

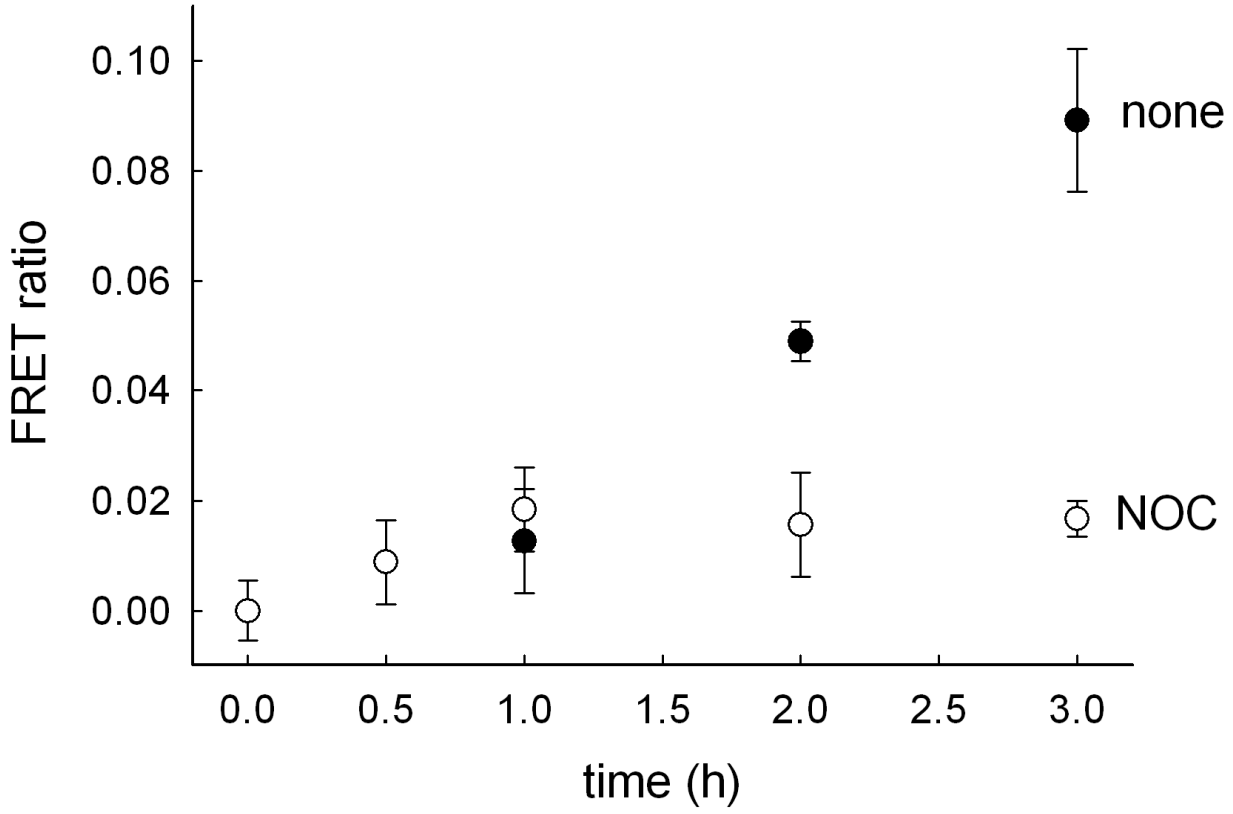

Figure A1.16. FRET profile illustrating retrograde lysosome fusion with late endosomes requires an intact microtubule network. Normalized FRET values for each time point were calculated for cells either treated (open circles) or left untreated (closed circles) with the microtubule depolymerizing agent NOC after 1 h. Results are an average of 3 independent experiments ± S.D.

A1.5. References

[1]I. Mellman, Endocytosis and molecular sorting. Annu Rev Cell Dev Biol 12 (1996) 575-625.

[2]A. Jahraus, B. Storrie, G. Griffiths, and M. Desjardins, Evidence for retrograde traffic between terminal lysosomes and the prelysosomal/late endosome compartment. J Cell Sci 107 (Pt 1) (1994) 145-57.

[3]N.A. Bright, B.J. Reaves, B.M. Mullock, and J.P. Luzio, Dense core lysosomes can fuse with late endosomes and are re-formed from the resultant hybrid organelles. J Cell Sci 110 (Pt 17) (1997) 2027-40.

[4]G. Griffiths, On vesicles and membrane compartments. Protoplasma 195 (1996) 37-58.

[5]S. Rabinowitz, H. Horstmann, S. Gordon, and G. Griffiths, Immunocytochemical characterization of the endocytic and phagolysosomal compartments in peritoneal macrophages. J Cell Biol 116 (1992) 95-112.

[6]G.M. Mancini, C.E. Beerens, and F.W. Verheijen, Glucose transport in lysosomal membrane vesicles. Kinetic demonstration of a carrier for neutral hexoses. J Biol Chem 265 (1990) 12380-7.

[7]M. Duvvuri, and J.P. Krise, A novel assay reveals that weakly basic model compounds concentrate in lysosomes to an extent greater than pH-partitioning theory would predict. Mol Pharm 2 (2005) 440-8.

[8]J.R. Lakowicz, Principles of Fluorescence Spectroscopy, Kluwer Academic/Plenum, New York, 1999.

[9]Z. Xia, and Y. Liu, Reliable and global measurement of fluorescence resonance energy transfer using fluorescence microscopes. Biophys J 81 (2001) 2395-402.

[10]J.E. Aubin, Autofluorescence of viable cultured mammalian cells. J Histochem Cytochem 27 (1979) 36-43.

[11]Z. Sebestyen, P. Nagy, G. Horvath, G. Vamosi, R. Debets, J.W. Gratama, D.R. Alexander, and J. Szollosi, Long wavelength fluorophores and cell-by-cell correction for autofluorescence significantly improves the accuracy of flow cytometric energy transfer measurements on a dual-laser benchtop flow cytometer. Cytometry 48 (2002) 124-35.

[12]G.W. Gordon, G. Berry, X.H. Liang, B. Levine, and B. Herman, Quantitative fluorescence resonance energy transfer measurements using fluorescence microscopy. Biophys J 74 (1998) 2702-13.

[13]A. Hoppe, K. Christensen, and J.A. Swanson, Fluorescence resonance energy transfer-based stoichiometry in living cells. Biophys J 83 (2002) 3652-64.

[14]M. Hillebrand, S.E. Verrier, A. Ohlenbusch, A. Schafer, H.D. Soling, F.S. Wouters, and J. Gartner, Live cell FRET microscopy: homo- and heterodimerization of two human peroxisomal ABC transporters, the adrenoleukodystrophy protein (ALDP, ABCD1) and PMP70 (ABCD3). J Biol Chem 282 (2007) 26997-7005.

[15]S.M. Dintzis, V.E. Velculescu, and S.R. Pfeffer, Receptor extracellular domains may contain trafficking information. Studies of the 300-kDa mannose 6-phosphate receptor. J Biol Chem 269 (1994) 12159-66.

[16]T.T. Nikiforov, and J.M. Beechem, Development of homogeneous binding assays based on fluorescence resonance energy transfer between quantum dots and Alexa Fluor fluorophores. Anal Biochem 357 (2006) 68-76.

[17]Y.P. Deng, and B. Storrie, Animal cell lysosomes rapidly exchange membrane proteins. Proc Natl Acad Sci U S A 85 (1988) 3860-4.

[18]N.A. Bright, M.J. Gratian, and J.P. Luzio, Endocytic delivery to lysosomes mediated by concurrent fusion and kissing events in living cells. Curr Biol 15 (2005) 360-5.

[19]B.M. Mullock, J.H. Perez, T. Kuwana, S.R. Gray, and J.P. Luzio, Lysosomes can fuse with a late endosomal compartment in a cell-free system from rat liver. J Cell Biol 126 (1994) 1173-82.

[20]B.M. Mullock, N.A. Bright, C.W. Fearon, S.R. Gray, and J.P. Luzio, Fusion of lysosomes with late endosomes produces a hybrid organelle of intermediate density and is NSF dependent. J Cell Biol 140 (1998) 591-601.

[21]B.M. Mullock, C.W. Smith, G. Ihrke, N.A. Bright, M. Lindsay, E.J. Parkinson, D.A. Brooks, R.G. Parton, D.E. James, J.P. Luzio, and R.C. Piper, Syntaxin 7 is localized to late endosome compartments, associates with

Vamp 8, and Is required for late endosome-lysosome fusion. Mol Biol Cell 11 (2000) 3137-53.

Appendix II

Synthesis and characterization of the toxic polyamine metabolite 3-aminopropanal

A2.1. Introduction

3-Aminopropanal (3-AP) is an endogenously synthesized amino-aldehyde that has been shown to localize to lysosomes by a pH-partitioning type mechanism [1]. The accumulation of 3-AP has been linked to the rupture of lysosomes in cell culture models [2; 3]. Furthermore, *in vivo*, 3-AP has been implicated as a potent neurotoxin responsible for neurodegeneration [1; 4; 5; 6; 7; 8]. In this dissertation, we have implicated the NPC1 protein functioning as a regulator of amine concentrations in lysosomes. Since 3-AP is an endogenous metabolite of polyamines, we propose that the NPC1 protein plays an important role in regulating concentrations of these molecules in lysosomes to avoid cellular toxicity. Thus, 3-AP gives us an opportunity to evaluate a physiologically relevant amine in NPC1 deficient cells. The synthesis and characterization of 3-AP for use in cell-based evaluations is discussed in this appendix.

A2.2. Materials and methods

A2.2.1. Reagents

3-aminopropanal diethyl acetal (3-APDA) was obtained from TCI America (Portland, OR). Purpald (4-amino-3-hydrazino-5-mercapto-1,2,4-triazole), propionaldehyde, and Dowex (50 x 2) cation exchange resin (H^+ form) were obtained through Sigma-Aldrich (St. Louis, MO). All other reagents unless otherwise specified were purchased through Sigma-Aldrich.

A2.2.2. 3-Aminopropanal synthesis

3-Aminopropanal (3-AP) was prepared, as previously described [8], from the hydrolysis of 3-APDA (see Figure A2.1 for mechanism). 3-APDA was supplied as a solution with a specific gravity of 0.91 g/L. To accomplish hydrolysis of the acetal groups, 1.16 mmol 3-ADPA (0.188 mL of stock 3-APDA solution) was added to 5 mL of 1.5 M HCl for a final concentration of 145 mM 3-ADPA at room temperature. The reaction was carried out for 5 hrs at room temperature in a stirred flask.

To separate amino-aldehydes, the reaction mixture was passed through a freshly prepared cation exchange column. To prepare the column, Dowex (50 x 2) a strong cation exchange resin was rinsed (3X) with water. Washed resin was packed into a thin (1 x 30 cm) glass column with a stopcock and glass wool at the bottom. Next, 50 mL of an aqueous wash solution (pH 4, titrated with HCl) was added to the resin. Once the column was prepared, the reaction mixture

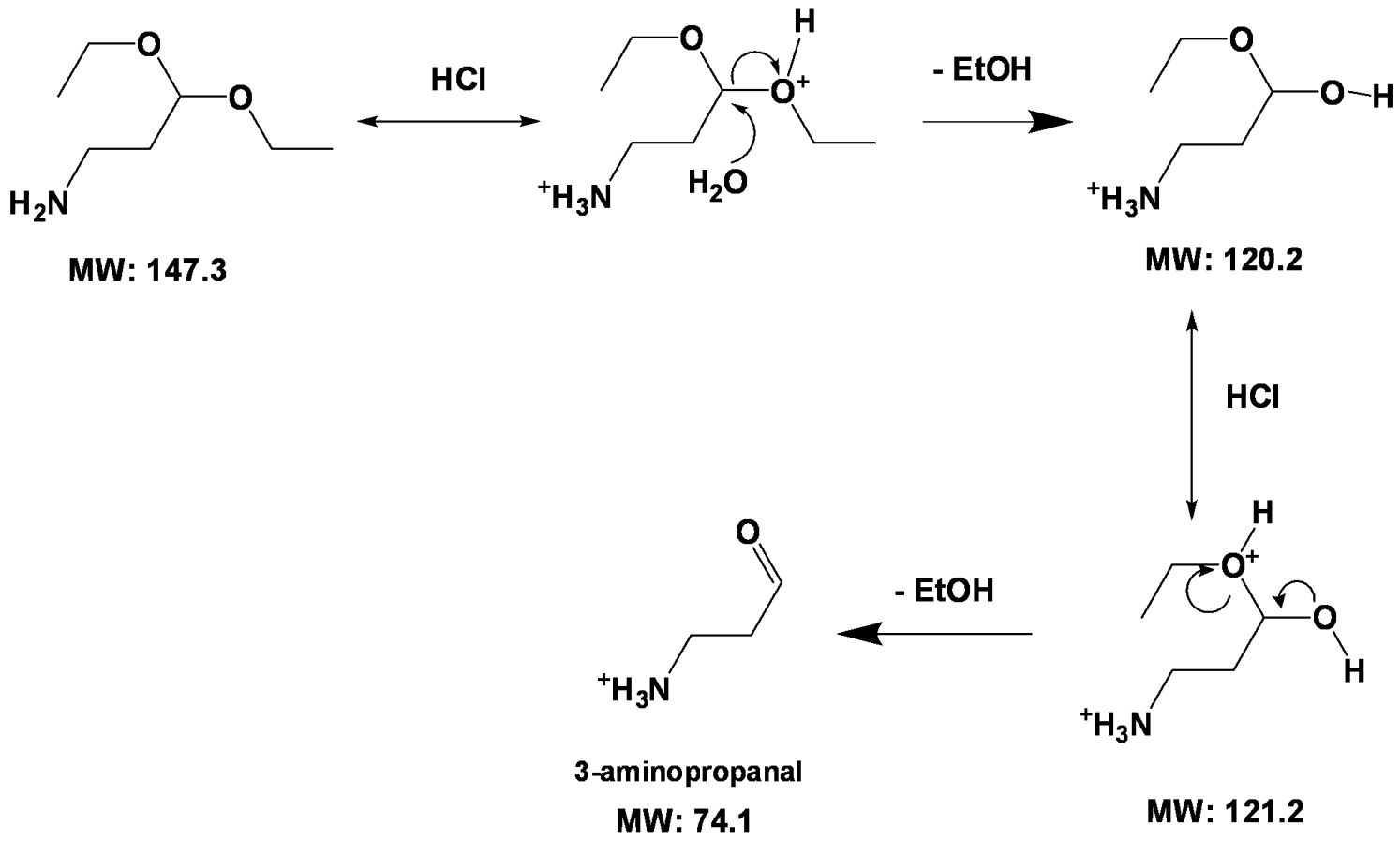

Figure A2.1. Hydrolysis of 3-aminopropanal diethyl acetal to form 3-aminopropanal.

was added and the flow through was collected for later aldehyde analysis. The column was eluted using a linear gradient of HCl (0-3 M) with a total volume of 120 mL being used. Fractions were collected every 10 mL and kept for aldehyde analysis (Fig. A2.2). Fractions were then concentrated (Fig. A2.3) using a centrifugal evaporator at room temperature for 4 hrs prior to mass spectrometry or nuclear magnetic resonance (NMR).

A2.2.3. Aldehyde determination

Aldehyde content was assayed by the method of Bachrach and Reches [9], for each fraction collected. First, the aldehyde reactive probe Purpald was prepared at 50 mg/ml (34 mM) in 2 N HCl. Next, an aldehyde standard curve was constructed using propionaldehyde diluted in PBS (Fig. A2.4). For sample analysis, 100 µL of each standard or unknown (prepared by 1:100 dilution in PBS from collected fraction) was added to a 96-well plate. To start the reaction, 100 µL of 34 mM Purpald solution was added to each well. The reaction was shaken at room temperature for 20 mins before reading absorbance at 530 nm using a plate reader (Multiskan, Thermo Scientific). By determining the presence of aldehydes formed during the reaction we calculated that 89% of the parent compound 3-APDA was converted to 3-AP.

A2.2.4. Mass spectrometry

Mass spectrometry was performed on aldehyde containing fractions post-concentration using an API-2000 ion spray MS/MS (Applied Biosystems).

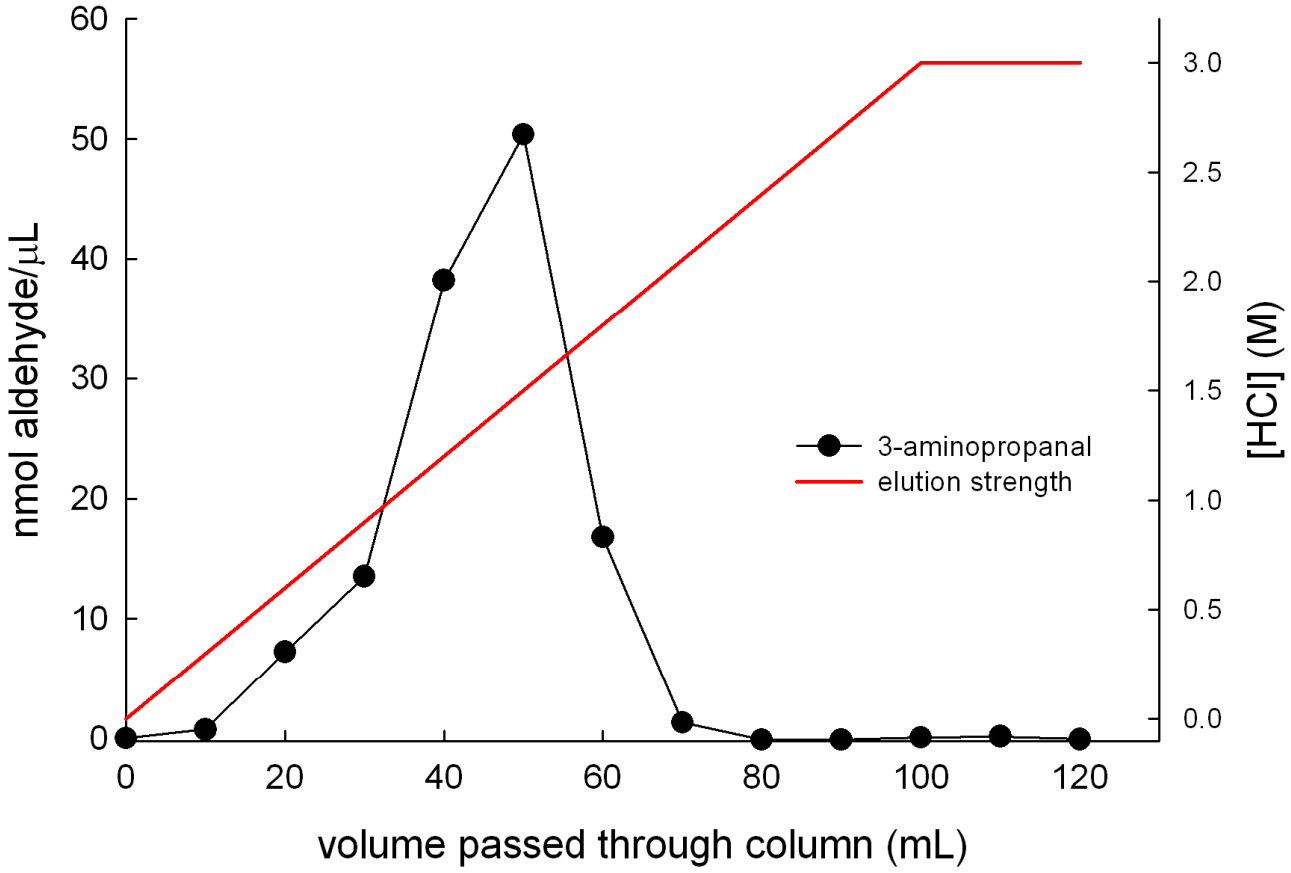

Figure A2.2. Elution of 3-aminopropanal from ion-exchange column. A linear gradient of hydrochloric acid (red line) was used to elute 3-aminopropanal from the Dowex strong cation exchange resin. Fractions were taken every 10 mL. Aldehyde content (closed circles) of each fraction was determined spectrophotometrically as described in Materials and Methods and is reported as nmol aldehyde present per µL of solution (or mM).

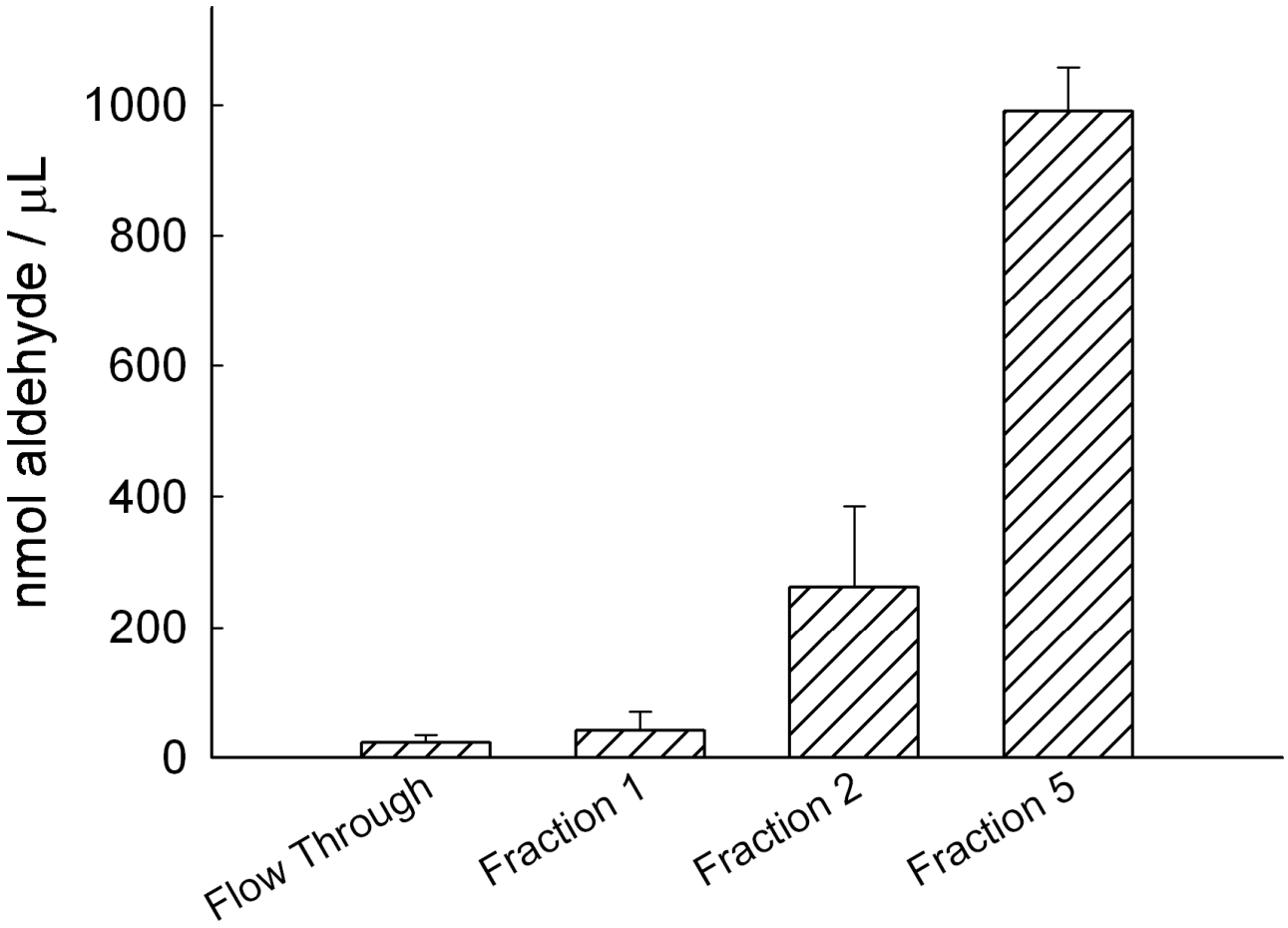

Figure A2.3. Aldehyde content after concentration. Fractions collected from Figure A2.2 were concentrated using a centrifugal evaporator to remove impurities for mass spectrometry and NMR analysis.

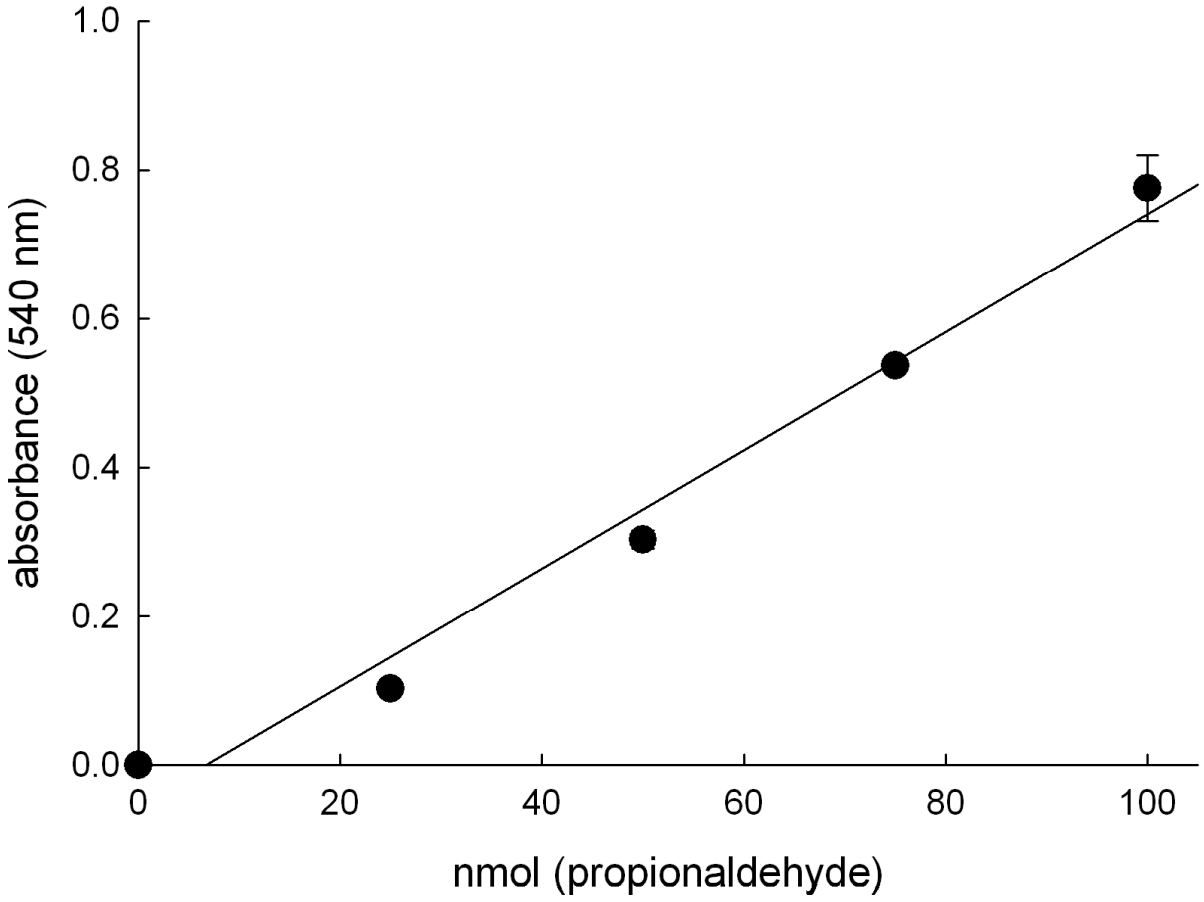

Figure A2.4. Standard curve for aldehyde determination. A standard curve of propionaldehyde was constructed, which contains one aldehyde group like 3-aminopropanal, using the aldehyde reactive dye Purpald.

Aldehyde containing solutions were injected directly into the mass spectrometer in positive ion mode with a Q1 (first quadrapole only) scan type. Parameters were as follows: curtain gas = 15, ion-spray voltage = 5500, temperature = 200, declustering potential = 20, focus potential = 400. Mass peaks were observed from 50 – 500.

A2.2.5. ^{1}H-NMR characterization

NMR characterization was performed by the Molecular Structures Group (Nuclear Magnetic Resonance Laboratory) at the University of Kansas (Lawrence, KS). Concentrated aldehyde-containing samples were reconstituted in D_2O and submitted for routine proton ^{1}H-NMR analysis using an Avance AV-III spectrometer with a 500 MHz magnet.

A2.3. Results

A2.3.1. Mass spectrometry

3-AP has been successfully synthesized by other labs [4; 8] using similar conditions; however, we needed to confirm the presence of 3-AP at the end of the reaction. The purpose of using a mass spectrometer (MS) was to identify the masses of the products present upon completion of the reaction. Simple injections were made into the MS of the retained fraction with the most aldehyde content present (concentrated fraction 5). Although the results revealed other components in the fraction other than 3-AP, we were able to observe the presence of 3-AP (Fig. A2.5). The molecular weight of 3-AP is 73.1. These injections told us only that 3-AP was present in this fraction and were not meant to be quantitative. Thus, the sizes of any contaminating peaks do not translate to concentrations relative to the 3-AP peak.

A2.3.2. Nuclear Magnetic Resonance

To alleviate any concerns about the presence of other compounds in the reaction mixture other than 3-AP observed by MS analysis, we evaluated concentrated aldehyde-containing fractions (fraction 5 from Figure A2.3 is shown in Figure A2.6) by ^{1}H-NMR. We observed the predicted sets of peaks for 3-AP, in addition to peaks for water. Peaks representing the different hydrogen atoms of 3-AP are shown in Fig. A2.6. Note the presence of the upfield aldehyde peak at approximately 9.7 ppm. Significant amounts of contaminating peaks were not observed suggesting we had obtained a pure fraction of 3-AP from the ion

exchange column. This correlates well with our calculation of 89% conversion of 3-APDA to 3-AP.

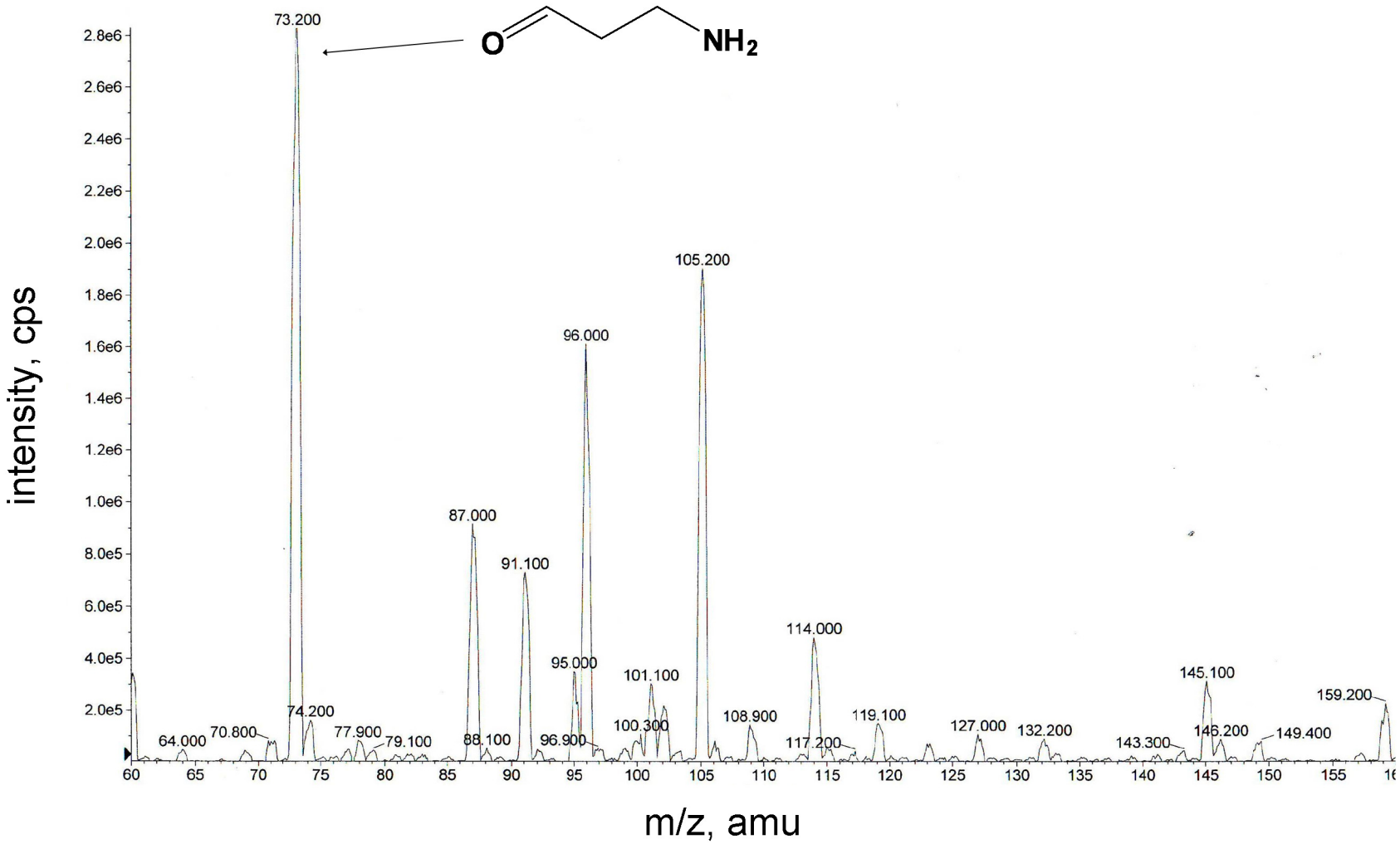

Figure A2.5. Mass analysis on fraction 5 concentrate from Figure A2.3. Mass spectrometry was used to identify 3-AP in isolated aldehyde containing fractions. The presence of a peak at 73.2 amu gives evidence for the presence of 3-AP in eluted fraction 5.

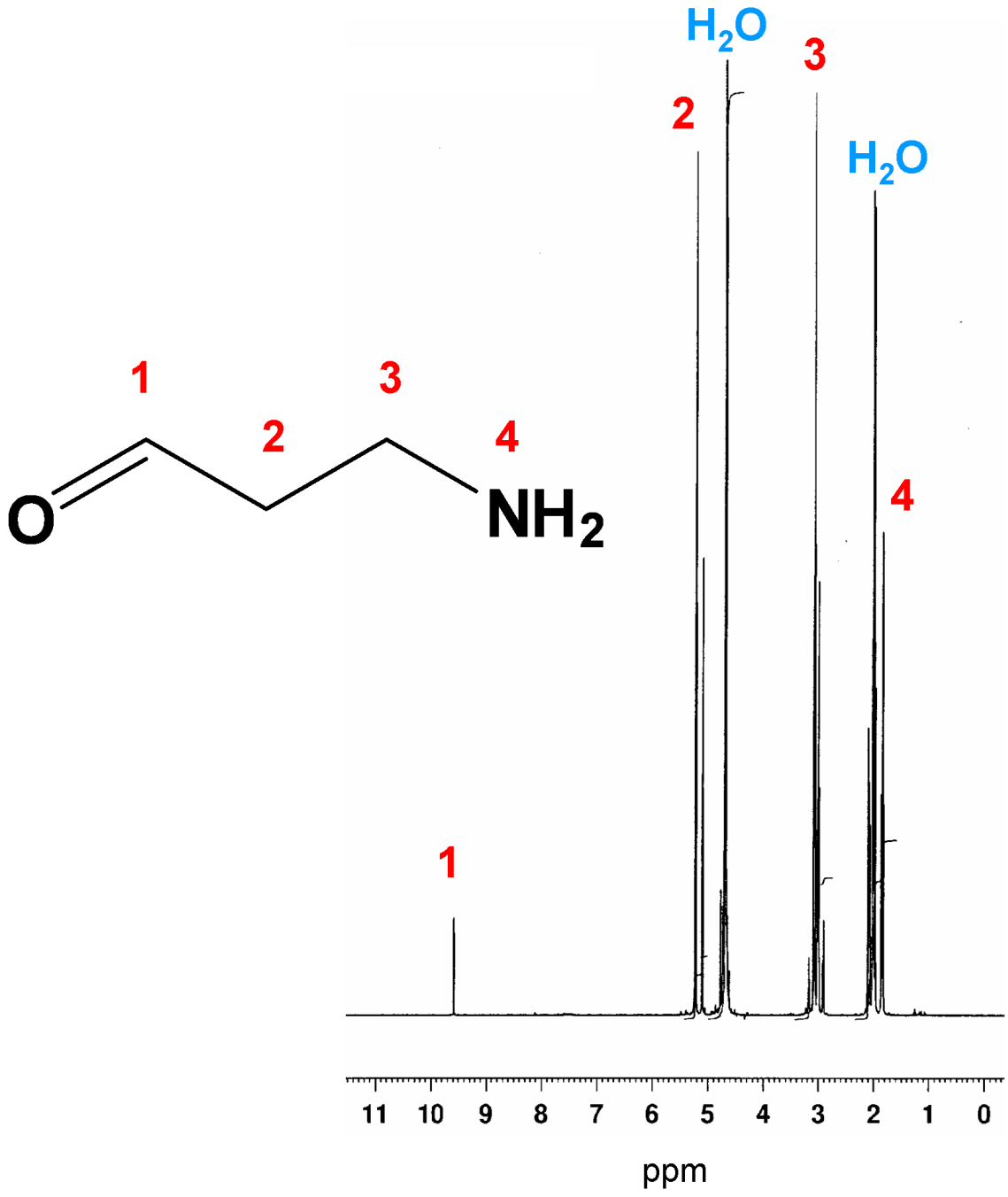

Figure A2.6. ^{1}H-NMR analysis of 3-AP. Purified and concentrated 3-AP was submitted for NMR analysis. 3-AP proton peaks are identified by red numbers and contaminating water peaks are shown in blue.

A2.4. References

[1]W. Li, X.M. Yuan, S. Ivanova, K.J. Tracey, J.W. Eaton, and U.T. Brunk, 3-Aminopropanal, formed during cerebral ischaemia, is a potent lysosomotropic neurotoxin. Biochem J 371 (2003) 429-36.

[2]Z. Yu, W. Li, and U.T. Brunk, 3-Aminopropanal is a lysosomotropic aldehyde that causes oxidative stress and apoptosis by rupturing lysosomes. Apmis 111 (2003) 643-52.

[3]Z. Yu, W. Li, J. Hillman, and U.T. Brunk, Human neuroblastoma (SH-SY5Y) cells are highly sensitive to the lysosomotropic aldehyde 3-aminopropanal. Brain Res 1016 (2004) 163-9.

[4]P.L. Wood, M.A. Khan, S.R. Kulow, S.A. Mahmood, and J.R. Moskal, Neurotoxicity of reactive aldehydes: the concept of "aldehyde load" as demonstrated by neuroprotection with hydroxylamines. Brain Res 1095 (2006) 190-9.

[5]P.L. Wood, M.A. Khan, and J.R. Moskal, The concept of "aldehyde load" in neurodegenerative mechanisms: cytotoxicity of the polyamine degradation products hydrogen peroxide, acrolein, 3-aminopropanal, 3-acetamidopropanal and 4-aminobutanal in a retinal ganglion cell line. Brain Res 1145 (2007) 150-6.

[6]P.L. Wood, M.A. Khan, J.R. Moskal, K.G. Todd, V.A. Tanay, and G. Baker, Aldehyde load in ischemia-reperfusion brain injury: neuroprotection by neutralization of reactive aldehydes with phenelzine. Brain Res 1122 (2006) 184-90.

[7]S. Ivanova, F. Batliwalla, J. Mocco, S. Kiss, J. Huang, W. Mack, A. Coon, J.W. Eaton, Y. Al-Abed, P.K. Gregersen, E. Shohami, E.S. Connolly, Jr., and K.J. Tracey, Neuroprotection in cerebral ischemia by neutralization of 3-aminopropanal. Proc Natl Acad Sci U S A 99 (2002) 5579-84.

[8]S. Ivanova, G.I. Botchkina, Y. Al-Abed, M. Meistrell, 3rd, F. Batliwalla, J.M. Dubinsky, C. Iadecola, H. Wang, P.K. Gregersen, J.W. Eaton, and K.J. Tracey, Cerebral ischemia enhances polyamine oxidation: identification of enzymatically formed 3-aminopropanal as an endogenous mediator of neuronal and glial cell death. J Exp Med 188 (1998) 327-40.

[9]U. Bachrach, and B. Reches, Enzymic assay for spermine and spermidine. Anal Biochem 17 (1966) 38-48.